

## Copyright Undertaking

This thesis is protected by copyright, with all rights reserved.

**By reading and using the thesis, the reader understands and agrees to the following terms:**

1. The reader will abide by the rules and legal ordinances governing copyright regarding the use of the thesis.
2. The reader will use the thesis for the purpose of research or private study only and not for distribution or further reproduction or any other purpose.
3. The reader agrees to indemnify and hold the University harmless from and against any loss, damage, cost, liability or expenses arising from copyright infringement or unauthorized usage.

### IMPORTANT

If you have reasons to believe that any materials in this thesis are deemed not suitable to be distributed in this form, or a copyright owner having difficulty with the material being included in our database, please contact [lbsys@polyu.edu.hk](mailto:lbsys@polyu.edu.hk) providing details. The Library will look into your claim and consider taking remedial action upon receipt of the written requests.

FUNCTIONAL INTIMATE APPAREL FOR ADOLESCENTS WITH  
SCOLIOSIS

FOK LAI HING

PhD

The Hong Kong Polytechnic University

2020

The Hong Kong Polytechnic University  
Institute of Textiles and Clothing

Functional Intimate Apparel for Adolescents with Scoliosis

Fok Lai Hing

A thesis submitted in partial fulfilment of the requirements for the  
degree of Doctor of Philosophy

May 2020

## **CERTIFICATE OF ORIGINALITY**

I hereby declare that this thesis is my own work and that, to the best of my knowledge and belief, it reproduces no material previously published or written, nor material that has been accepted for the award of any other degree or diploma, except where due acknowledgement has been made in the text.

(Signed)

---

Fok Lai Hing

---

(Name of student)



## ABSTRACT

Adolescent idiopathic scoliosis (AIS) is the three-dimensional structural curvature of the spine with unknown etiology which occurs during puberty. Recent survey findings published in 2016 indicate that the prevalence of schoolchildren with AIS in China was 5.14%. Scoliosis not only affects the physical profile such as spinal asymmetry, trunk deformity, shoulder obliquity, scapular asymmetry, and pelvis declination, but also causes spinal pain, restricts physical movement, affects cardiac and pulmonary functions, or even leads to death. Thus, proper treatment for AIS is essential. Rigid bracing is a universal non-invasive treatment for AIS that slows down or stops the progression of the spinal curvature until the bones reach maturity. However, noncompliance with the use of rigid braces is often an issue due to some of the drawbacks of bracing, such as skin irritation, discomfort, loss of aesthetics, and psychological impacts. Therefore, in the last decade, the idea of a flexible brace has been proposed in response to the negative impacts of rigid braces. SpineCor and the posture correction girdle are two examples of flexible braces. Nevertheless, the mechanism and effectiveness of existing flexible braces are still controversial. Therefore, the aim of this study is to develop a novel flexible brace for AIS patients to maximise the performance on spinal correction with the advantage of flexibility and comfort.

This study consists of four components including (a) a clinical study on an existing posture correction girdle which involves radiographic examinations, three-dimensional body scanning and interface pressure measurements of subjects with mild scoliosis, (b) the design and development of a functional intimate apparel to treat scoliosis, (c) a clinical study of the proposed functional intimate apparel to investigate the degree of spinal control, spinal contour changes, psychological impact on patients, and effect of the biomechanics of the brace on the interface pressure, and (d) the formulation of a simulation model to predict the effectiveness of the initial in-brace spinal correction of the proposed functional intimate apparel.

The effectiveness of the existing posture correction girdle was still unclear. To conduct a background study on the existing design and determine the possible design elements for the proposed functional intimate apparel, a 6-month clinical trial of the original posture correction girdle was first carried out. Subjects were required to wear the posture correction girdle for 6 months. Radiographic examinations of the subjects in three conditions, including pre-intervention, after 6 months of brace wear and after 6 months post-brace wear, were carried out through three-dimensional image scanning, and interface pressure measurements were also

done. It was found that the posture correction girdle had a positive effect in controlling the progression of the scoliosis and spinal contour changes. However, the in-brace spinal corrective effect was unsatisfactory. Moreover, the pressure distribution was not even compared to the three-point pressure system, which is the most common system used to exert corrective effects by rigid orthotics.

In response to the unsatisfactory in-brace correction of the original posture correction girdle, a functional intimate apparel for AIS was designed and developed in this study. The proposed design adopted a similar corrective mechanism as rigid braces to control the spinal deformity. A conceptual framework for apparel design that is called the functional, expressive and aesthetic model was applied during the design process. A functional intimate apparel prototype that consisted of a bra top, pants, pelvis belt, hinge bone with a cushioning pad and corrective component was designed and developed to maximise the spinal corrective effect of the proposed flexible brace and minimise the negative impacts, such as mobility restriction and discomfort of rigid braces.

To investigate the efficacy of the proposed functional intimate apparel, a clinical study was conducted to determine the initial effects of this flexible brace in terms of the in-brace correction, posture changes and quality of life and its biomechanics and the short-term effects on spinal deformity, posture and quality of life. It was found that the initial percentage of in-brace correction ranged between 9.7% and 88.7% with the standard deviation of 33.6. Compared to the original posture correction girdle, the in-brace correction of the proposed functional intimate apparel was significantly greater. Moreover, in considering the effect of posture, it was found that 60% of the subjects corrected their initial posture in terms of reducing the shoulder obliquity and shoulder rotation. Surprisingly, there was no correlation between the initial shoulder asymmetry and in-brace correction. In considering the impact on the quality of life, the results of the brace questionnaire shown that the proposed functional intimate apparel almost never had negative impacts with respect to the general health of the user, physical functions, body pain and social aspects. As for the biomechanics, the interface pressure between the corrective pad and body of the user was measured and found to be similar to that of rigid braces. Apart from the initial effect, the initial spinal correction after 3 months of wear was 52.7%. Furthermore, after three months, the shoulder rotation and posterior trunk symmetry index improved by 29.8% and 13.1% respectively. Also, the results showed that the quality of life did not change drastically after three months of wear.

Apart from a clinical study with human subjects, a numerical finite element model was developed to simulate the effectiveness of the in-brace spinal correction of the proposed functional intimate apparel. This model overcame the concerns around human subjects and ethical problems of repeated radiation exposure to examine the scoliotic spine. More importantly, the model could simulate the spinal corrective performance in relation to the position of the pad and loading and material properties of the elastic straps and hinge. The simulation model showed the trend of spinal correction with good accuracy. Moreover, to further investigate the biomechanics of the brace and the effect of the corrective pads on vertebral movement, 15 models with different degrees of thoracic and lumbar loading were constructed. It was found that managing loading from the pads was essential since excessive thoracic loading or insufficient lumbar loading might induce the progression of lumbar curve. The current models showed that a 140% increment in lumbar loading provided the optimum corrective result in both the thoracic and lumbar curves.

The research results in this study provided useful information on the design elements and mechanics of flexible braces to treat scoliosis. The functional intimate apparel was a non-invasive means of controlling spinal deformity. This study showed that the textile materials provided adequate corrective forces and resulted in some in-brace correction. The simulation model could be used to predict the degree of in-brace correction and optimise brace designs. The outputs of this project could be extended to the development of other types of flexible orthotic devices and enhance the comfort and flexibility of textile medical products.

## PUBLICATIONS ARISING FROM THE THESIS

### Journal papers

**Fok, Q.,** Yip J., Yick, K.L., Ng, S.P., and Tse, C.Y. (2018). Effectiveness of posture correction girdle as conservative treatment for adolescent idiopathic scoliosis: a preliminary study. *Orthopedic Research Online Journal*, 1(5).

**Fok, Q.,** Liu, P.Y., Yip J., Cheung, M.C., Yick, K.L., Ng, S.P., and Tse, C.Y. (2020). School scoliosis screening in Hong Kong: trunk asymmetry of girls with scoliosis. *MOJ Orthopedics & Rheumatology*, 12(1):7–10.

**Fok, Q.,** Yip J., Yick, K.L., Ng, S.P., Liu, Z., and Li, X. (2020). Anisotropic Textile Brace for Adolescent Idiopathic Scoliosis: Immediate in-brace effect and biomechanics. (In submission)

### Conference papers

**Fok, L.H.,** Yip J., Yick, K.L., Tse, C.Y., and Ng, S.P. (2016). In-school screening for adolescent idiopathic scoliosis: results of adam's forward bending test and shoulder obliquity in adolescent girls in Hong Kong. *College of Professional and Continuing Education Health Conference*, Hong Kong, 11 Jan.

Cheung M.C., Yip J., **Fok L.H.**, and Kwok, G. (2017). Health-related quality of life in adolescents with mild scoliosis. *31<sup>st</sup> International Academic Conference*, The International Institute of Social and Economic Sciences, London, United Kingdom, 29 May.

**Fok Q.,** Yip J., Yick K.L., and Ng, S.P. (2017). Design and develop functional bra top for adolescent idiopathic scoliosis. *The 14<sup>th</sup> Asian Textile Conference*, Hong Kong, 27-30 June.

**Fok Q.,** Yip J., Yick K.L., and Ng, S.P. (2018). Functional intimate apparel design for scoliotic spine. *Textile Summit*, Shinshu University, Japan, 20-22 Sep.

**Fok Q.,** Yip J., Yick K.L., and Ng, S.P. (2018). A non-invasive method to assess control of body contour for spinal treatment. *11<sup>th</sup> Pan-Pacific Conference on Rehabilitation*, Hong Kong, 17-18 Nov.

**Fok Q.,** Yip J., Yick K.L., and Ng, S.P. (2019). Biomechanical modelling of functional intimate apparel to treat scoliosis. *International Conference on Science and Innovative Engineering*, Rome, Italy, 25-26 May.

### Patent

Yip, Y.W. and **Fok, L.H.** (2018) China Patent Application CN209059579U.

Yip, Y.W. and **Fok, L.H.** (2019) U.S. Patent Application 2020/0032839 A1.

### Awards

Gold Medal at Silicon Valley International Invention Festival in Santa Clara Convention Center, US in June 2019.

Special Award of Association of Polish Inventors and Rationalizers at Silicon Valley International Invention Festival in Santa Clara Convention Center, US in June 2019.

## ACKNOWLEDGEMENTS

I would like to express my most sincere appreciation and gratitude to my Chief Supervisor, Dr. Joanne YIP at the Institute of Textiles and Clothing, The Hong Kong Polytechnic University. Her patient guidance, invaluable advice and profound insight have deeply impressed me. She gave me trust, support, freedom in my works and constructive advice which are all indispensable to the completion of my postgraduate studies. Without her inspiration, mentoring and encouragement, this study would hardly have been completed.

Besides, I would like to express my deepest thanks to my co-supervisors, Dr. Kit-Lun YICK at the Institute of Textiles and Clothing, The Hong Kong Polytechnic University and Dr. Sun-Pui Zerance NG at the Division of Science, Engineering and Health Studies, The Hong Kong Community College, for their constant support, insightful comments and encouragement.

I am greatly indebted to Ms. Nico LIU at the Institute of Textiles and Clothing, The Hong Kong Polytechnic University for sharing her valuable experience with the development of the posture correction girdle. I would also like to send special gratitude to Dr. Shing-Wa LEUNG for the invaluable advices on mechanical and finite element analysis related issues. I am deeply grateful to Mr. Chi-Yung TSE, an experienced prosthetist-orthotist at the Centre for Orthopaedic Surgery in Hong Kong for his professional advices and stimulating discussions on orthopaedic aspect.

I must also acknowledge the help of Prof. Man-Chee Kenneth CHEUNG, Dr. Pui-Yin Jason CHUNG and Dr. Yat-Hong Kenny KWAN at the Department of Orthopedics and Traumatology, the University of Hong Kong for providing professional advice and technical support to the clinical study. I would like to express my appreciation to Dr. Mei-Chun CHENG at the Department of Social Work, the Chinese University of Hong Kong for her valuable experiences on the clinical evaluation and data analysis. I would also express my thanks to Prof. Yong-Ping ZHENG and his team at the Department of Biomedical Engineering, the Hong Kong Polytechnic University for the Scolioscan™ consultation. Thanks are also given to all the subjects who participated in my research for their friendliness, time and help.

I would like to express my appreciation to all the staff members at the Institute of Textiles

and Clothing , the Industrial Center, the University Research Facility in 3D Printing (U3DP) and Pao Yue-Kong Library, The Hong Kong Polytechnic University for their domain and technical support and valuable suggestions.

Thanks are also extended to my research colleagues and teammates, especially Dr. Annie YU, Dr. Lu LU, Dr. Jim LUK, Dr. Fanny TONG, Dr. Frances WAN, Dr. Jess CHAN, Mr. Garcia KWOK, Ms. Olivia FUNG, Ms. Eunice TAM, Ms. Charlotte WONG, Ms. Linda SIT, Ms. Kayla HO, Ms. Claire CHUNG, Ms. Maple LEE, Ms. Lisa WONG and Ms. Hallie CHEUNG for their immeasurable help, continuous encouragement and support.

I must express my very profound gratitude to my family members and friends for their love and unconditional support while I was working on my goals throughout the years of my study and during the process of researching and writing this thesis.

Last but not least, the financial support from the Research Grant Council (PolyU 152061/15E) entitled “Functional Intimate Apparel for Adolescents with Early Scoliosis” and (PolyU 152101/16E) entitled “Anisotropic Textile Braces for Adolescent Idiopathic Scoliosis” and the Department Grant of the Institute of Textiles and Clothing, The Hong Kong Polytechnic University (RULA) for the research project are gratefully acknowledged.

# TABLE OF CONTENTS

<b>Abstract.....</b>	<b>I</b>
<b>Publications arising from the thesis .....</b>	<b>IV</b>
<b>Acknowledgements .....</b>	<b>V</b>
<b>Table of Contents .....</b>	<b>VII</b>
<b>List of Figures.....</b>	<b>XVI</b>
<b>List of Tables.....</b>	<b>XXII</b>
<b>List of Abbreviations.....</b>	<b>XXIII</b>
<b>Chapter 1 Introduction.....</b>	<b>1</b>
<b>1.1 Research Background.....</b>	<b>1</b>
<b>1.2 Problem statement .....</b>	<b>3</b>
<b>1.3 Research Objectives.....</b>	<b>4</b>
<b>1.4 Project originality and significance.....</b>	<b>4</b>
<b>1.5 Outline of thesis.....</b>	<b>6</b>
<b>Chapter 2 Literature review.....</b>	<b>9</b>
<b>2.1 Introduction.....</b>	<b>9</b>
<b>2.2 Background Information on Scoliosis.....</b>	<b>9</b>
2.2.1 Physical examination .....	9
2.2.2 Radiographic examination .....	11
2.2.2.1 Standing AP or PA radiography .....	11
2.2.2.2 Supine AP radiography .....	11

2.2.2.3	Cobb's angle measurement .....	12
2.2.2.4	Nash-Moe method.....	13
2.2.2.5	Risser grade.....	13
2.2.3	Classifications of adolescent idiopathic scoliosis .....	14
2.2.3.1	Lenke classification .....	15
2.2.3.1.1	Curve types .....	16
2.2.3.1.2	Lumbar spine modifiers .....	16
2.2.3.1.3	Thoracic sagittal modifiers.....	17
<b>2.3</b>	<b>Treatment for adolescent idiopathic scoliosis .....</b>	<b>18</b>
2.3.1	Rigid bracing.....	18
2.3.1.1	Milwaukee brace .....	19
2.3.1.2	Boston brace.....	20
2.3.1.3	Chêneau brace .....	22
2.3.1.4	Lyon brace.....	23
2.3.2	Flexible bracing .....	24
2.3.2.1	SpineCor .....	24
2.3.2.2	Posture correction girdle .....	25
2.3.3	Physiotherapy scoliosis specific exercises.....	27
2.3.3.1	Lyon approach (France) .....	27
2.3.3.2	Schroth method (Germany).....	28
2.3.3.3	Barcelona Scoliosis Physical Therapy School (Spain) .....	29
2.3.3.4	Scientific Exercise Approach to Scoliosis (Italy) .....	29
2.3.3.5	Dobosiewicz Method (Poland) .....	30
2.3.3.6	Functional Individual Therapy of Scoliosis (Poland) .....	30
2.3.3.7	Limitations of Physiotherapy scoliosis specific exercises .....	31
2.3.4	Knowledge gap in existing scoliosis treatment.....	31
<b>2.4</b>	<b>Functional intimate apparel.....</b>	<b>32</b>
2.4.1	Intimate apparel that controls posture.....	32
2.4.2	-Functional intimate apparel for medical uses .....	34
2.4.3	Knowledge gap in functional intimate apparel for scoliosis treatment.....	36
<b>2.5</b>	<b>Finite element analysis.....</b>	<b>36</b>



2.5.1	Finite element analysis for AIS braces.....	36
2.5.2	Finite element analysis for pressure garments .....	39
2.5.3	Knowledge gap in finite element analyses: AIS .....	40
<b>2.6</b>	<b>Summary.....</b>	<b>41</b>
<b>Chapter 3</b>	<b>Methodology .....</b>	<b>44</b>
<b>3.1</b>	<b>Introduction.....</b>	<b>44</b>
<b>3.2</b>	<b>Experimental Design.....</b>	<b>44</b>
<b>3.3</b>	<b>Clinical Study of Posture Correction Girdle .....</b>	<b>45</b>
3.3.1	Subject recruitment .....	46
3.3.1.1	Scoliosis screening process in schools.....	46
3.3.2	Clinical study protocols .....	47
3.3.3	Radiographic examination .....	48
3.3.4	3D body scanning .....	49
3.3.5	Interface pressure of posture correction girdle .....	52
3.3.6	Statistical analysis.....	53
<b>3.4</b>	<b>Design and development of functional intimate apparel.....</b>	<b>53</b>
3.4.1	Material selection.....	55
3.4.1.1	Material testing and testing conditions .....	56
3.4.1.2	Stretch and recovery testing.....	58
3.4.1.3	Water vapor permeability .....	59
3.4.1.4	Air permeability .....	59
3.4.1.5	Thermal resistance .....	60
3.4.1.6	Dimensional changes after laundering.....	60
3.4.1.7	Tensile and shear.....	61
3.4.1.8	Bending.....	61
3.4.1.9	Compression .....	61
3.4.1.10	Surface properties .....	61
3.4.1.11	Weight and thickness .....	62
3.4.2	Body measurements .....	62

3.4.2.1	Subject recruitment .....	63
3.4.3	Pattern making .....	64
3.4.4	Garment assembling.....	64
3.4.5	Fitting.....	64
<b>3.5</b>	<b>Clinical study of proposed functional intimate apparel .....</b>	<b>65</b>
3.5.1	Subject inclusion and exclusion criteria .....	65
3.5.2	Two-hour clinical study .....	66
3.5.2.1	Radiographic examination .....	66
3.5.2.2	Three-dimensional body scanning .....	66
3.5.2.3	Wear comfort assessment.....	67
3.5.2.4	Pressure measurement.....	68
3.5.3	Three-month clinical study .....	68
3.5.3.1	Ultrasound imaging of spine.....	68
3.5.3.2	Three-dimensional body scanning .....	69
3.5.3.3	HRQL.....	69
3.5.3.4	Short interview.....	70
3.5.4	Statistical analysis.....	70
<b>3.6</b>	<b>Biomechanical simulation model for functional intimate apparel .....</b>	<b>70</b>
3.6.1	Formulation of finite element model .....	71
3.6.1.1	Geometrical model of torso body, skeleton, and functional intimate apparel .	71
3.6.1.1.1	Construction of model of torso body .....	71
3.6.1.1.2	Construction of skeletal model .....	71
3.6.1.1.3	Construction of model of functional intimate apparel .....	71
3.6.1.2	Defining material properties .....	72
3.6.1.3	Defining mesh element type .....	72
3.6.1.4	Defining boundary conditions.....	73
3.6.1.5	Applying loading in simulation model .....	73
3.6.1.6	Validation .....	73
3.6.2	Modification of hinges.....	74
3.6.2.1	Tensile strength .....	74
3.6.2.2	Torque to failure.....	74
3.6.2.3	Effect of hinge material on vertebral movement .....	74

3.6.3	Optimization of corrective padding .....	74
3.7	Summary.....	75
<b>Chapter 4 Clinical study of posture correction girdle .....</b>		<b>77</b>
4.1	Introduction.....	77
4.2	Subject recruitment .....	77
4.3	Fitting of the girdle .....	79
4.4	Effects on spinal control .....	84
4.4.1	Curvature reduction/increase after 6 months .....	85
4.4.2	In-brace reduction/increase of spinal curvature .....	86
4.5	Effects on standing posture .....	88
4.5.1	Shoulder obliquity.....	88
4.5.2	Shoulder rotation.....	88
4.6	Interface pressure .....	90
4.6.1	Influence of pads on interface pressure .....	91
4.7	Summary.....	94
<b>Chapter 5 Design and development of functional intimate apparel for AIS .....</b>		<b>96</b>
5.1	Introduction.....	96
5.2	Design criteria .....	96
5.3	Preliminary idea.....	97
5.3.1	Preliminary review of first prototype of bra top .....	98
5.3.1.1	Contour changes.....	99
5.3.2	Interface pressure .....	100
5.4	Bra top modifications .....	101
5.4.1	Second prototype of bra top .....	102

5.4.2	Third prototype of bra top.....	102
<b>5.5</b>	<b>Development of pants of prototype .....</b>	<b>104</b>
5.5.1	First prototype of pants .....	104
5.5.2	Second prototype of pants.....	105
<b>5.6</b>	<b>Development of artificial back bone.....</b>	<b>106</b>
5.6.1	First prototype of artificial back bone.....	106
5.6.2	Second prototype of artificial back bone .....	108
5.6.3	Cushioning pad for artificial back bone.....	109
<b>5.7</b>	<b>Development of correction pad.....</b>	<b>110</b>
<b>5.8</b>	<b>Fabric selection.....</b>	<b>111</b>
5.8.1	Stretch and recovery testing .....	113
5.8.2	Water vapor permeability test .....	117
5.8.3	Air permeability test .....	118
5.8.4	Thermal conductivity test .....	119
5.8.5	Tensile test .....	120
5.8.6	Shearing test.....	121
5.8.7	Bending test .....	121
5.8.8	Compression test.....	122
5.8.9	Surface test.....	122
5.8.10	Dimensional changes to laundering test .....	123
5.8.11	Overall evaluation based on test results.....	124
5.8.11.1	Material for corrective component.....	124
5.8.11.2	Main fabric.....	125
5.8.11.3	Material for elastic webbing of bra top and pants.....	127
<b>5.9</b>	<b>Pattern development process .....</b>	<b>127</b>
5.9.1	3D scanning measurements.....	127
5.9.2	Prototype size.....	129
5.9.3	Prototype pattern.....	130
<b>5.10</b>	<b>Prototype for clinical study .....</b>	<b>133</b>

<b>5.11</b>	<b>Summary.....</b>	<b>135</b>
 <b>Chapter 6 Clinical study of functional intimate apparel for AIS .....</b>		
<b>6.1</b>	<b>Introduction.....</b>	<b>136</b>
<b>6.2</b>	<b>Subject recruitment .....</b>	<b>136</b>
<b>6.3</b>	<b>Fitting of the functional intimate apparel for AIS .....</b>	<b>137</b>
<b>6.4</b>	<b>Two-hour clinical study .....</b>	<b>139</b>
6.4.1	Effects on the initial in-brace reduction of spinal curvature.....	139
6.4.2	Effects on initial changes in body contours .....	143
6.4.2.1	Shoulder obliquity.....	143
6.4.2.2	Shoulder rotation.....	143
6.4.2.3	Posterior trunk symmetry index.....	144
6.4.3	Wear comfort.....	146
6.4.3.1	Bad Sobernheim Stress Questionnaire - Brace .....	146
6.4.3.2	Brace questionnaire.....	146
6.4.4	Interface pressure .....	148
<b>6.5</b>	<b>Three-month clinical study .....</b>	<b>150</b>
6.5.1	Effects on spinal curvature progression .....	151
6.5.2	Effects on body contour changes .....	152
6.5.2.1	Shoulder obliquity.....	153
6.5.2.2	Shoulder rotation.....	153
6.5.2.3	Posterior trunk symmetry index.....	153
6.5.3	Effects on quality of life .....	154
6.5.4	Feedback from subject .....	155
<b>6.6</b>	<b>Summary.....</b>	<b>156</b>
 <b>Chapter 7 Biomechanical simulation model for functional intimate apparel to treat AIS</b>		
	<b>158</b>	
<b>7.1</b>	<b>Introduction.....</b>	<b>158</b>

<b>7.2</b>	<b>FE model building.....</b>	<b>158</b>
7.2.1	Geometric modelling of scoliotic torso and FIA to treat AIS .....	158
7.2.1.1	Construction of torso body.....	159
7.2.1.2	Construction of skeletal model .....	161
7.2.1.3	Construction of FIA for AIS .....	165
7.2.2	Defining material properties .....	167
7.2.3	Defining type of mesh element.....	168
7.2.4	Simulating brace wear in model .....	170
7.2.5	Validation .....	173
<b>7.3</b>	<b>Results and discussion .....</b>	<b>173</b>
<b>7.4</b>	<b>Modification of hinge.....</b>	<b>180</b>
7.4.1	Prototypes of modified hinge.....	180
7.4.2	Tensile strength .....	182
7.4.3	Torque to failure.....	185
7.4.4	Effect of hinge materials on vertebral movement.....	188
<b>7.5</b>	<b>Effect of corrective pads on vertebral movement .....</b>	<b>193</b>
7.5.1	Effect of change in thoracic and lumbar loading .....	194
7.5.2	Effect of change of thoracic loading .....	195
7.5.3	Effect of the change of lumbar loading.....	196
<b>7.6</b>	<b>Summary.....</b>	<b>198</b>
<b>Chapter 8</b>	<b>Conclusion and recommendations for future work .....</b>	<b>200</b>
<b>8.1</b>	<b>Conclusion .....</b>	<b>200</b>
<b>8.2</b>	<b>Limitations of the study.....</b>	<b>202</b>
<b>8.3</b>	<b>Recommendations for future work .....</b>	<b>204</b>
<b>Appendix I.</b>	<b>Information sheet for participant in clinical study of posture correction girdle</b>	<b>205</b>

<b>Appendix II. Consent to participant in clinical study of posture correction girdle.....</b>	<b>211</b>
<b>Appendix III. Data sheet for clinical study of posture correction girdle .....</b>	<b>213</b>
<b>Appendix IV. Information sheet for participant in clinical study of functional intimate apparel</b>	<b>215</b>
<b>Appendix V. Consent to participant in clinical study of functional intimate apparel .</b>	<b>218</b>
<b>Appendix VI. Data sheet for clinical study of functional intimate apparel .....</b>	<b>219</b>
<b>Appendix VII. Bad Sobernheim Stress Questionnaire.....</b>	<b>220</b>
<b>Appendix VIII. Brace Questionnaire .....</b>	<b>221</b>
<b>Appendix IX. SRS-22 Questionnaire.....</b>	<b>224</b>
<b>References.....</b>	<b>226</b>

## LIST OF FIGURES

Figure 1-1 Flow diagram of research methodology.....	8
Figure 2-1 Angle of trunk rotation measurement in Adam's forward bending test with scoliometer (Hresko, 2013).....	10
Figure 2-2 Posture during standing radiography (O'Brien et al., 2008) .....	11
Figure 2-3 Measuring Cobb's angle (Rigo, 2011).....	12
Figure 2-4 Nash-Moe method for vertebral rotation assessment (Anitha & Prabhu, 2012)....	13
Figure 2-5 Risser grading.....	14
Figure 2-6 Lenke classification (Lenke et al., 2001) .....	15
Figure 2-7 Three types of lumbar modifiers: A - little to no curve; B - moderate curve; and C - large curve (Lenke et al., 2001). .....	17
Figure 2-8 Three-point pressure from thoracic-lumbo-sacral orthosis to treat scoliosis (Seymour, 2002).....	19
Figure 2-9 Milwaukee brace (Qian et al., 2010).....	20
Figure 2-10 Boston brace for right thoracic curve (Weisz et al., 1989).....	21
Figure 2-11 Three stages in applying corrective forces to spine with Boston brace (Chase et al., 1989) .....	21
Figure 2-12 Dynamic derotation brace (thoracic curve module) (Grivas et al., 2010).....	22
Figure 2-13 Chêneau brace (Pham et al., 2008).....	23
Figure 2-14 Lyon brace (de Mauroy et al., 2011) .....	24
Figure 2-15 SpineCor brace (Coillard et al., 2003) .....	25
Figure 2-16 Posture correction girdle for scoliosis in early stages (Liu et al., 2014).....	26
Figure 2-17 Posture corrector wireless back support bra (Leonisa Inc., 2017) .....	33
Figure 2-18 Posture correcting garment (Wang, 2013).....	33
Figure 2-19 Posture corrective brassiere (Mungo, 1952) .....	34
Figure 2-20 Undergarment for masking scoliosis (Anderson, 2015).....	34
Figure 2-21 Spinomed® active Damen (Medi GmbH & Co. KG, 2015).....	35
Figure 2-22 Postoperative undergarment for sternotomy patients (King et al., 2006) .....	35
Figure 2-23 The 3D geometric modelling of brace with pressure mapping (Delphine Périé et al., 2004) .....	37
Figure 2-24 Design variables for optimization of corrective forces (Gignac et al., 2000) .....	38



Figure 2-25 Finite element model of trunk of patient (D. Périé et al., 2004) .....	38
Figure 2-26 Finite element model of trunk (with omission of intercostal ligaments and abdominal beams for clarity) (Clin, Aubin, Parent, et al., 2010) .....	39
Figure 2-27 Finite element model of bust (Liu et al., 2011) .....	40
Figure 2-28 Estimated hydrostatic pressure in intramuscular and intercompartment model of leg during elastic compression (Rohan et al., 2015) .....	40
Figure 3-1 Flow chart diagram of research plan .....	45
Figure 3-2 OSI scoliometer used for ATR measurement .....	46
Figure 3-3 Screening for scoliosis in school .....	47
Figure 3-4 Prototype of posture correction girdle .....	48
Figure 3-5 Posture correction girdle clinical trial protocols .....	48
Figure 3-6 Anatomic landmarks in this study 1: spinous process of C7. 2,3: acromia angle of shoulders. 4, 5: superior angle of scapulae. 6,7: inferior angle of scapulae. 8: spinous process of L4. 9,10: posterior superior iliac spine. 11,12: iliac crest .....	50
Figure 3-7 Shoulder obliquity measured by angle of acromion in frontal plane .....	51
Figure 3-8 Shoulder rotation measured by angle of acromion in transverse plane .....	52
Figure 3-9 Measured points of interface pressure of posture correction girdle .....	52
Figure 3-10 Apparel design framework (Lamb & Kallal, 1992) .....	55
Figure 3-11 Details of measured body areas .....	63
Figure 3-12 ISO #304 zig zag (Dewellton LLC, 2008) .....	64
Figure 3-13 ISO #301 lockstitch (Dewellton LLC, 2008) .....	64
Figure 3-14 Constructing POSTI as a sum of 6 indices (Patias et al., 2010) .....	67
Figure 3-15 Scolioscan™ .....	69
Figure 4-1 Radiographic images and location of inserted pads: Lenke 1 curve .....	80
Figure 4-2 Radiographic images and location of inserted pads: Lenke 3 curve .....	81
Figure 4-3 Radiographic images and location of inserted pads: Lenke 5 curve .....	82
Figure 4-4 Radiographic images and location of inserted pads: Lenke 6 curve .....	83
Figure 4-5 Shoulder obliquity of subjects: in-brace vs. out-brace .....	88
Figure 4-6 Shoulder rotation of subjects: in-brace vs. out-brace .....	89
Figure 4-7 Interface pressure between under-bust and girdle .....	90
Figure 4-8 Interface pressure between waist and girdle .....	91
Figure 4-9 Interface pressure between pelvis and girdle .....	91
Figure 4-10 Pressure at interface between under-bust and girdle with pad inserted into 3 <sup>rd</sup> .....	

pocket.....	92
Figure 4-11 Pressure at interface between waist and girdle with pad inserted into 4 <sup>th</sup> pocket	93
Figure 4-12 Pressure at interface between pelvis and girdle with pad inserted into 5 <sup>th</sup> pocket .....	94
Figure 5-1 First prototype of bra top for AIS: (a) back, (b) front and (c) side views .....	98
Figure 5-2 First prototype of bra top on Subject R17002: (a) back, (b) front and (c) side views .....	99
Figure 5-3 Shoulder obliquity and shoulder rotation results for in-brace and without brace: Subject R17001 .....	100
Figure 5-4 Symmetry analysis in 3D: (a) prototype not worn, and (b) prototype worn .....	100
Figure 5-5 Interface pressure at thoracic pad and its counter side: Subject R17002 .....	101
Figure 5-6 Second prototype of bra top: (a) front, (b) back, (c) left and (d) right views .....	102
Figure 5-7 Third prototype of frame bra top: (a) front, (b) back and (c) side views, and after attaching corrective component: (d) front, (e) back and (f) side views .....	103
Figure 5-8 First prototype of pants: (a) front, (b) back, (c) right and (d) left views.....	104
Figure 5-9 First prototype of pants on Subject 18001: (a) front and (b) back views.....	105
Figure 5-10 Second prototype of pants on Subject 18001: (a) front and (b) back views .....	106
Figure 5-11 Illustration of first prototype of artificial back bone .....	107
Figure 5-12 Soft resin joints allow 3D movement of body .....	107
Figure 5-13 Broken off resin joint .....	108
Figure 5-14 Schematic of artificial back bone with hinged joint.....	109
Figure 5-15 Second prototype of artificial back bone .....	109
Figure 5-16 Cushioning pad inserted at back of hinge .....	110
Figure 5-17 Schematic of mould of correction pad .....	110
Figure 5-18 Stress-strain curves for 5 <sup>th</sup> cycle of stretching four types of fabric in warp direction .....	114
Figure 5-19 Stress-strain curves at 5 <sup>th</sup> cycle of stretching four types of fabric in weft direction .....	115
Figure 5-20 Stress-strain curves at 5 <sup>th</sup> cycle of stretching five types of elastic bands in warp direction .....	115
Figure 5-21 Bar chart of stretch and recovery test results of four types of fabric and one elastic band.....	117

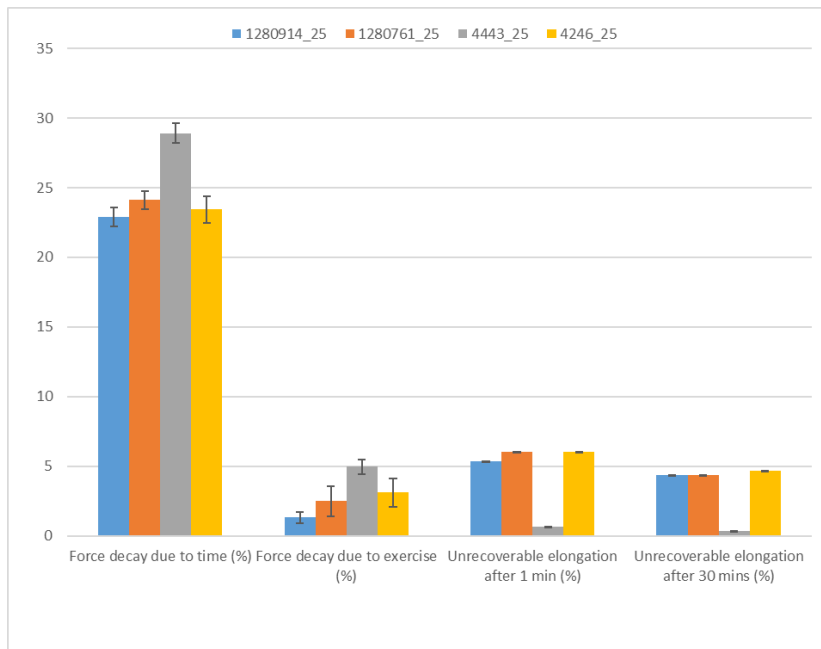


Figure 5-22 Bar chart of

stretch and recovery test results of four types of elastic straps.....	117
Figure 5-23 Bar chart of water vapor permeability test results of four type of fabric .....	118
Figure 5-24 Bar chart of air permeability test results of four types of fabric .....	119
Figure 5-25 Bar chart of thermal conductivity test results of four types of fabric .....	120
Figure 5-26 Bar chart of dimensional changes to laundering results of four types of fabric and one elastic type of band.....	124
Figure 5-27 Bar chart of dimensional changes to laundering results of four types of elastic strap material .....	124
Figure 5-28 Overall sensorial comfort result of four types of fabric .....	126
Figure 5-29 Bra top pattern.....	131
Figure 5-30 Pants pattern.....	131
Figure 5-31 Cushioning pad pattern .....	132
Figure 5-32 Pelvis belt pattern.....	132
Figure 5-33 Thoracic and lumbar corrective component patterns .....	133
Figure 5-34 Prototype for clinical study: (a) front and (b) back views .....	134
Figure 5-35 Prototype worn by subject: (a) front and (b) back views .....	134
Figure 6-1 Radiograph images and placement of corrective components .....	138
Figure 6-2 Radiograph image of Subject 18002: (a) without brace, and (b) in-brace .....	139
Figure 6-3 Relationship between in-brace rate of correction and lumbar-pelvis relationship and in-brace rate of correction and coronal decompensation .....	142
Figure 6-4 Radiograph images of Subject 19002: (a) without brace, and (b) with brace.....	142

Figure 6-5 Shoulder obliquity results .....	143
Figure 6-6 Shoulder rotation results .....	144
Figure 6-7 Posterior trunk symmetry index results.....	145
Figure 6-8 Rate of in-brace reduction/ increase: posterior trunk symmetry index .....	145
Figure 6-9 BSSQ-Brace scores .....	146
Figure 6-10 Scores for individual BrQ questions .....	148
Figure 6-11 Interface pressure of the functional intimate apparel .....	150
Figure 6-12 Ultrasound images of Subject 19002: (a) pre-intervention and (b) 3 <sup>rd</sup> month of intervention .....	152
Figure 6-13 Degree of obliquity (shoulders), degree of rotation (shoulders) and POSTI at pre-intervention and on 3 <sup>rd</sup> month of intervention .....	153
Figure 6-14 Scoring of five domains in SRS-22 Questionnaire at pre-intervention and on 3 <sup>rd</sup> month of intervention.....	155
Figure 6-15 Broken hinge of artificial back bone due to large body movements.....	156
Figure 7-1 Construction of torso body model: (a) point cloud of 3D scanned image, (b) polygon object before processing, (c) polygon object after processing, (d) divided regions to identify contours, (e) polygon object with patch boundary structure, and (f) polygon object with ordered u-v grid in every patch .....	160
Figure 7-2 Final geometric model of torso body .....	161
Figure 7-3 Radiographic images of Subject 18003: (a) frontal plane and (b) sagittal plane .	162
Figure 7-4 Standard skeletal model .....	162
Figure 7-5 Bone tissues of first skeletal model in: (a) frontal plane and (b) sagittal plane ...	163
Figure 7-6 (a) Intervertebral disc built between two successive vertebrae, and (b) intervertebral disc .....	163
Figure 7-7 Bone tissues of second skeletal model in the (a) frontal plane and (b) sagittal plane, and (c) second geometric model of skeletal structure.....	164
Figure 7-8 Bone tissues of final skeletal model in the (a) frontal plane and (b) sagittal plane, and (c) third geometric model of skeletal structure .....	165
Figure 7-9 Segmentation of FIA into 4 components.....	166
Figure 7-10 Final model of FIA which has only one opening .....	166
Figure 7-11 Tensile stress-strain curves for warp direction of FIA material .....	167
Figure 7-12 10-node quadratic tetrahedral element .....	168
Figure 7-13 Meshed model of (a) scoliotic torso, (b) skeletal structure, and (c) intervertebral	

disc .....	169
Figure 7-14 Meshed model of (a) FIA, (b) textile material, and (c) hinge .....	169
Figure 7-15 Tightening corrective components and pelvis belt and adding load on surface of torso under corrective component.....	171
Figure 7-16 (a) Master and (b) slave surface for surface to surface interaction .....	172
Figure 7-17 Boundary conditions of scoliotic torso model .....	173
Figure 7-18 FE model (a) initial stage, (b) - (c) during analysis and (d) after analysis.....	175
Figure 7-19 Stress distribution of torso body: (a) front and (b) back views.....	175
Figure 7-20 Stress distribution on skeletal system after analysis .....	176
Figure 7-21 Displacement of skeletal model .....	177
Figure 7-22 Spinal curves of subject based on radiographic images vs. FE model.....	178
Figure 7-23 Five test specimens .....	181
Figure 7-24 Tensile strength of five hinges .....	183
Figure 7-25 Five specimens after tensile test.....	183
Figure 7-26 Load-displacement curve of Hinge #1 .....	183
Figure 7-27 Load-displacement curve of Hinge #2 .....	184
Figure 7-28 Load-displacement curve of Hinge #3 .....	184
Figure 7-29 Load-displacement curve of Hinge #4 .....	185
Figure 7-30 Load-displacement curve of Hinge #5 .....	185
Figure 7-31 Torsional torque vs. torsional angle for hinges .....	187
Figure 7-32 Five specimens after torsion test.....	188
Figure 7-33 Stress distribution on FIA with different hinges .....	190
Figure 7-34 Stress distribution on scoliotic spine with different hinges .....	191
Figure 7-35 Spinal curves: PMMA, POM, carbon fibre and aluminium hinges .....	192
Figure 7-36 Spinal curves: Models #L0-#L4.....	195
Figure 7-37 Spinal curves: Models #0, #5-9.....	196
Figure 7-38 Spinal curves: Models #0, #10-15.....	198

## LIST OF TABLES

Table 3-1 Functions and criteria of three main textile materials for proposed design.....	56
Table 3-2 Physical tests for material selection of proposed functional intimate apparel.....	57
Table 3-3 Measured body areas .....	62
Table 3-4 Professional bra fitting criteria (McGhee & Steele, 2010) .....	65
Table 4-1 Results of school screening .....	77
Table 4-2 Demographics of recruited subjects.....	78
Table 4-3 Cobb's angle: in-brace and no brace at initial visit vs. six months of girdle wear...	84
Table 4-4 Spinal curvature reduction/increase after 6 months with posture correction girdle	85
Table 4-5 In-brace reduction/increase of spinal curvature after six months of girdle wear.....	87
Table 5-1 Design criteria of the proposed functional intimate apparel.....	96
Table 5-2 Demographics of Subject R17002 .....	99
Table 5-3 Demographics of Subject 18001 .....	105
Table 5-4 Specifications of KE-1310ST .....	111
Table 5-5 Specifications of tested material .....	112
Table 5-6 Results of tensile testing of four types of fabric .....	120
Table 5-7 Results of shearing testing of four types of fabric .....	121
Table 5-8 Results of bending test for four types of fabric .....	122
Table 5-9 Results of compression testing of four types of fabric .....	122
Table 5-10 Results of surface testing of four types of fabric .....	123
Table 5-11 Demographics of 21 scoliotic subjects for 3D scanning measurements.....	128
Table 5-12 Results of body measurements .....	128
Table 5-13 Kendall's Tau-b correlation results .....	129
Table 5-14 Allocation of prototype based on BMI .....	130
Table 6-1 Demographics of clinical study subjects .....	136
Table 6-2 Measured Cobb's angle with different conditions.....	141
Table 7-1 Demographics of scoliotic subject.....	159
Table 7-2 Material properties of models of scoliotic torso and FIA.....	167
Table 7-3 Cobb's angle: with and without brace and FE model .....	179
Table 7-4 Specifications of hinges .....	181
Table 7-5 Material properties of hinges .....	188
Table 7-6 Magnitude of thoracic and lumbar loading in each model. ....	193

## LIST OF ABBREVIATIONS

### A

AATCC	American Association of Textile Chemists and Colorists
AIS	Adolescent Idiopathic Scoliosis
AP	Anterior-Posterior
ASTM	American Society for Testing And Materials
ATR	Angle of Trunk Rotation

### B

B	Bending Rigidity
BMI	Body Mass Index
BrQ	Brace Questionnaire
BS	British Standard
BSI	British Standards Institution
BSPTS	Barcelona Scoliosis Physical Therapy School
BSSQ	Bad Sobernheim Questionnaire

### C

C3D10	10-Node Linear Quadratic Tetrahedral Elements with Three Degrees of Freedom at Each Node
CAT	Catalyst
CD	Coronal Decompensation
CIR	Circumference

CIR	Circumference
CSVL	Center Sacral Vertical Line
CTLSO	Cervical-Thoracic-Lumbo-Sacral Orthosis
<b>E</b>	
EN	European Standard
EVA	Ethylene Vinyl Acetate
<b>F</b>	
FAI-A	Frontal Asymmetry Index Axillar
FAI-C7	Frontal Asymmetry Index C7
FAI-T	Frontal Asymmetry Index Trunk
FE	Finite Element
FEA	Finite Element Analysis
FEM	Finite Element Model
FIA	Functional Intimate Apparel
FITS	Functional Individual Therapy of Scoliosis
<b>G</b>	
G	Shear Rigidity
<b>H</b>	
HDI-A	Height Different Index Axillar
HDI-S	Height Different Index Shoulder
HDI-T	Height Different Index Trunk



HRQL	Health-Related Quality of Life
<b>I</b>	
IBM	International Business Machines
ISO	International Organisation for Standardisation
<b>K</b>	
KES	Kawabata Evaluation System
KES-F	Kawabata Evaluation System of Fabric
<b>L</b>	
LC	Compressional Linearity
LPR	Lumbar-Pelvis Relationship
LT	Tensile Rigidity
<b>M</b>	
MIU	Mean Friction Coefficient
MMD	Fluctuation of Mean Friction Coefficient
MT	Moire Topography
MTS	Bionix Servohydraulic Test System
<b>N</b>	
NURBS	Non-Uniform Rational B-Spline
<b>O</b>	
OSI	Orthopedic System, Inc.
<b>P</b>	

PA	Posterior-Anterior
PMMA	Polymethyl Methacrylate
POM	Polyoxymethylene
POTSI	Posterior Trunk Symmetry Index
PSSE	Physiotherapy Scoliosis Specific Exercises
PU	Polyurethane
<b>R</b>	
RC	Compressional Recoverability
RT	Tensile Recoverability
<b>S</b>	
SD	Standard Deviation
SEAS	Scientific Exercise Approach to Scoliosis
SMD	Surface Roughness
SOSORT	The International Society on Scoliosis Orthopaedic and Rehabilitation Treatment
SRS	Scoliosis Research Society
<b>T</b>	
TLSO	Thoracic-Lumbo-Sacral Orthosis
<b>U</b>	
USA	United States
<b>W</b>	

WC	Compressional Energy
WREST	Women's Recovery from Sternotomy
WT	Tensile Energy
WVT	Rate of Water Vapor Transmission
2D	Two-dimensional
3D	Three-dimensional
2HB	Bending Hysteresis
2HG	Elasticity for Minute Shear
2HG5	Elasticity for Large Shear

# Chapter 1 Introduction

## 1.1 Research Background

The human spine consists of 24 individual bones called vertebrae which interlock with each other to form the spinal column. The vertebrae are made up of 7 cervical, 12 thoracic, and 5 lumbar vertebrae which are labelled as C1-7, T1-12 and L1-5 respectively. The spinal column serves to support the body, protect the spinal cord and spinal nerve roots, and facilitate the movement of the trunk (Cramer, 2014). However, the spine may experience deformity, which is a condition called scoliosis, where there is the abnormal curvature of the spine. This spinal condition in youths is called adolescent idiopathic scoliosis (AIS), and the prevalence in adolescents ranges from 0.47% to 5.2% based on findings of existing studies (Konieczny et al., 2013).

Idiopathic scoliosis is a structural scoliosis and the most common yet clinically important type of spinal deformity. The etiology of idiopathic scoliosis is still unknown. Scholars believe that skeletal immaturity, the female gender and large spinal curvature mainly constitute as the risk factors for further progression of the spinal curvature (Sun et al., 2013; Weiss et al., 2006).

Scoliosis causes the physical deterioration of the body and damage to the internal organs and impacts psychological health. Mild scoliosis affects the physical aesthetics including oblique shoulders, shoulder rotation, asymmetric scapulae, misaligned spinal process, and inclined pelvis while severe scoliosis would cause back pain, limit mobility, and result in cardiac and pulmonary system damage. Due to the fatality of severe scoliosis, surgery is essential after the spinal curvature exceeds 40 degrees with a Risser grade 0-4 (Reamy & Slakey, 2001). Nevertheless, up to 93% of scoliotic surgery is preventable through effective management of AIS (Weinstein et al., 2013b). Thus, investigations on non-operative scoliotic treatment are essential and valuable.

Scholars believe that bracing is the most effective type of non-operative treatment for AIS which slows or stops the progression of scoliosis until the bones mature. There are two types of braces that are prescribed: rigid and flexible braces.

Rigid braces are the traditional means of providing bracing treatment. Most have adopted a convex shape design or a pad which pushes in the perpendicular direction on the body surface against the spinal curvature (Kotwicki & Cheneau, 2008). The three-point pressure system is

the fundamental universal corrective mechanism of such orthotics that provides the corrective forces (Gomez et al., 2016). The system involves exerting lateral external forces onto the apical vertebra and contralateral forces are applied above and below the apical vertebra. In addition to the direct pushing, the free space allowance in the concave part of the brace for expansion purposes is also an important feature of contemporary brace designs. The space for free expansion of the body allows the tissues to effectively shift from the convex to the concave parts of the brace (Kotwicki & Cheneau, 2008). The high efficacy of rigid braces has been well studied. However, non-compliance with rigid bracing is often an issue due to some of the drawbacks such as skin irritation, discomfort, reduced physical aesthetics, and negative psychological impacts (Bunge et al., 2010; Danielsson et al., 2001).

In response, flexible braces have been developed which remedy the negative impacts of rigid braces. As a result, there have been major changes in scoliotic orthoses throughout the 2000s. SpineCor is a typical example of a flexible brace. Apart from using thermoplastic materials, SpineCor uses adjustable straps to control the spinal deformity based on a corrective movement principle. The process of using straps to realign the orientation of the thoracic, thoracolumbar, and lumbar segments is based on dynamic movement of clockwise and counter-clockwise rotations and tilts, lateral shifts, and inclinations and bends (Coillard et al., 2008; Smith, 2002). In addition to SpineCor, Liu et al. (2014) developed a posture correction girdle for AIS. The main corrective principle of the girdle is to use a waist band to create compressive forces in the circumferential direction and strengthen the scoliotic spine. However, there has been few empirical studies on the effectiveness of spinal correction with the posture correction girdle in Liu et al. (2014).

Functional intimate apparel such as shapewear and undergarment that aims to correct posture apply large corrective forces onto the torso through elastic material and supporting resin bones. These features allow diverse applications of function intimate apparel. For instance, functional intimate apparel can have medical purposes, such as postoperative bras. However, few functional intimate apparels have been designed in the orthopaedic field, especially for scoliosis.

In view of the above, this study set out to examine the performance of the posture correction girdle in Liu et al. (2014) to reduce the spinal curvature of scoliotic patients. The aim of this study is to explore the mechanisms and effectiveness of functional garments for scoliosis control. Aside from an evaluation of the existing functional garments available to treat AIS,

this study also elaborated on the design and development of a novel functional intimate apparel for AIS which is intended to control spinal deformity but also offers good wear comfort and flexibility.

## **1.2 Problem statement**

### **1. Discomfort and lack of flexibility of rigid braces**

Bracing is an effective way to control the progression of AIS. However, wear discomfort and the lack of flexibility are usually the shortcomings of rigid braces. One of the possible reasons for the wear discomfort and lack of flexibility is the use of thermoplastic rigid material, which does not accommodate body movement and is not breathable. As such, rigid braces likely reduce the quality of life which results in a low compliance rate with the treatment. Therefore, in this study, textile material which has the advantages of breathability and conformability was taken into consideration in the design and development of a novel functional intimate apparel for AIS.

### **2. Ambiguity around efficacy of posture correction girdle**

Liu et al. (2014) developed a posture correction girdle for AIS patients and conducted a clinical study with 9 subjects to investigate its efficacy. However, in her study (Liu, 2015), the Cobb's angle of some of the subjects is less than  $10^\circ$  and thus her results cannot truly reflect the efficacy of the girdle on scoliosis patients. In fact, scoliosis is defined as the lateral curvature of the spine with a Cobb's angle that is equal or greater than  $10^\circ$  (Hresko, 2013). Therefore, a clinical study with scoliosis subjects who have a Cobb's angle that is equal or greater than  $10^\circ$  was conducted to investigate the efficacy of this posture correction girdle.

### **3. Risk of progression of spinal curvature of patients with moderate scoliosis**

The posture correction girdle in Liu et al. (2014) was designed for patients in the early stages of scoliosis whose Cobb's angle is less than  $20^\circ$ . However, the literature suggests that the benchmark for bracing or physiotherapy treatment should be  $\geq 20^\circ$  since patients with moderate scoliosis and skeletal immaturity face a high risk of spinal curvature progression (Aulisa et al., 2015; Weinstein et al., 2013b; Weiss et al., 2006). Therefore, in this study, a novel flexible brace was developed for patients with moderate scoliosis.

### **4. Ambiguity of biomechanics of flexible braces**

The biomechanics of existing flexible braces such as SpineCor (Coillard et al., 2008) and the

posture correction girdle (Liu et al., 2014) has not been reported pressure. They have only observed the changes in the spinal curvature by using radiography. Therefore, the amount of corrective forces applied by the posture correction girdle and novel functional intimate apparel were studied and compared. Moreover, a finite element model was developed to investigate the biomechanics of the proposed functional intimate apparel.

### **1.3 Research Objectives**

The aim of the study is to design and develop a functional intimate apparel that offers wear comfort and is flexible but also effectively controls the spinal deformity of AIS patients. The research objectives of this study are as follows.

1. To conduct background research on AIS and the different treatment methods and review the different corrective mechanisms of functional intimate apparel in order to design and develop a suitable functional intimate apparel for adolescents with scoliosis.
2. To further investigate the performance of an existing posture correction girdle developed by Liu et al. (2014) and study the biomechanics and spinal correction process of the girdle.
3. To design an innovative functional intimate apparel which will: a) offer compression and pulling forces through a tightly fitting garment pattern, b) prevent lumbar flexion with a supporting belt, c) exert transverse forces through a 3-point pressure system, d) prevent axial rotation or address simultaneous movement of the body regions due to uneven pressure distribution from the use of different types of straps, and e) provide corrective forces that shift the trunk away from areas of pressure to reduce the spinal curvature and enhance the posture of individuals with AIS.
4. To conduct wear trials of the proposed innovative functional intimate apparel, evaluate its effectiveness in terms of the degree of spinal curvature reduction through radiography and measure the amount of pressure exerted onto the torso.
5. To formulate a model that simulates the biomechanical effects of the proposed functional intimate apparel for AIS.

### **1.4 Project originality and significance**

Bracing is a conservative universal method to treat moderate scoliosis. The fundamental objectives of this conservative treatment for AIS are to halt the progression of spinal curvature at puberty, prevent or treat respiratory dysfunctions, prevent or treat spinal pain, and improve

aesthetics of the wearer through postural correction. Traditional rigid braces are made of thermoplastic material which restricts movement, causes physical and psychological discomfort, results in skin irritation, and are also aesthetically unpleasing. These shortcomings might result in a low compliance rate and reduce the quality of life of patients. To address these limitations, Coillard et al. (2008) developed a flexible brace called SpineCor. However, the literature continues to debate on its corrective mechanisms and efficacy. Aside from SpineCor, there is also a posture correction girdle for AIS which was developed by Liu et al. (2014). However, they did not systematically investigate its effectiveness in reducing spinal curvature and the biomechanics of the brace. Therefore, a clinical study was conducted in this study to investigate the performance of the girdle in Liu et al. (2014) on controlling the spinal curvature of AIS patients.

On the other hand, the proposed novel functional intimate apparel intends to provide effective spinal control and maximise wear comfort and mobility. The aim of this study is to therefore provide a bracing treatment option for AIS patients. To optimise the reduction of spinal curvature, the biomechanics of the posture correction girdle and proposed functional intimate apparel were studied. Moreover, a biomechanical model was developed to predict the effectiveness of the proposed functional intimate apparel on reducing the spinal curvature and optimising the loading of corrective forces.

The scope of this project includes: (1) a study of the effectiveness and biomechanics of the posture correction girdle in Liu et al. (2014), (2) an investigation of the critical design criteria and features for the novel posture correction girdle, (3) an evaluation of the physical properties of textile materials for the novel functional intimate apparel, (4) an assessment of the effectiveness of the functional intimate apparel, and (5) the development of a biomechanical model that simulates vertebral movement after donning the novel flexible brace. These provided relatively useful information for related product development, especially in terms of the problem identification and application of corrective forces.

The output of this study contributed to the development of other functional garments or flexible braces and advance existing knowledge by providing the possibility of using textile materials in the medical field. Above all, the ability of currently available flexible braces such as the posture correction girdle in Liu et al. (2014) to control spinal curvature could be enhanced by applying the principles of the novel functional intimate apparel. Also, the functional intimate apparel enhanced quality of life due to flexible and comfortable to wear textile material. In



addition, the formulated biomechanical model provided a radiation-free method to assess the effectiveness of bracing treatment for design optimisation.

## **1.5 Outline of thesis**

There is a total of eight chapters in this thesis as shown in Figure 1-1. Chapter 1 provides the background information, problem statement, objectives, project originality and significance and outline of the study.

Chapter 2 is the literature review which includes a review of the background information on scoliosis, some of the non-invasive treatments for AIS, some of the designs used for medical functional intimate apparel, and biomechanical models for AIS braces and pressure garments.

Chapter 3 is a summary of the overall research plan and methodology. The objectives of each method and experiment are reported. The methods and standards adopted, and the software and equipment used in this study are also listed and explained in detail.

Chapter 4 reports the evaluation results of the effectiveness of the posture correction girdle in Liu et al. (2014). The results of a 6-month quasi-experimental pre-test-post-test clinical study which focuses on the effects of the brace on spinal deformity, shoulder orientation, and interface pressure are reported.

Chapter 5 presents the design and development process of the novel functional intimate apparel for AIS. The chapter provides the design criteria based on the findings in Chapters 2 and 4, the preliminary idea, and the design of the bra top, pants, artificial hinges, and corrective pads in detail. Suitable textile materials with good mechanical, thermal, sensorial, and durability properties are determined through physical testing. The pattern development process is also elaborated in detail.

Chapter 6 reports on the evaluation results of the efficacy of the proposed functional intimate apparel for AIS which is discussed in Chapter 5. The results of a 2-hour clinical study and a 3-month clinical study including the effects on spinal correction, body contour changes, quality of life and interface pressure are reported.

Chapter 7 presents a biomechanical predictive model of the novel functional intimate apparel with the aim to determine the effectiveness of the initial in-brace spinal correction. The model is developed based on the mechanical properties of the fabric used, hinges, geometries of the spine and torso and the interaction between the body and brace by using the finite element method. A validation of this model is conducted by comparing the results from the in-brace

radiographic image. Based on the limitations discussed in Chapter 6, modification of the hinge is discussed and finalized through physical testing results as well as the in-brace changes to the curvature of the spine estimated by this predictive model. The optimum loading of the corrective pad is also determined by using this predictive model to optimise the spinal corrective effect.

Chapter 8 is the last chapter, which provides a general conclusion on the thesis work. The limitations of this study and recommendations for future works are also discussed in this chapter.

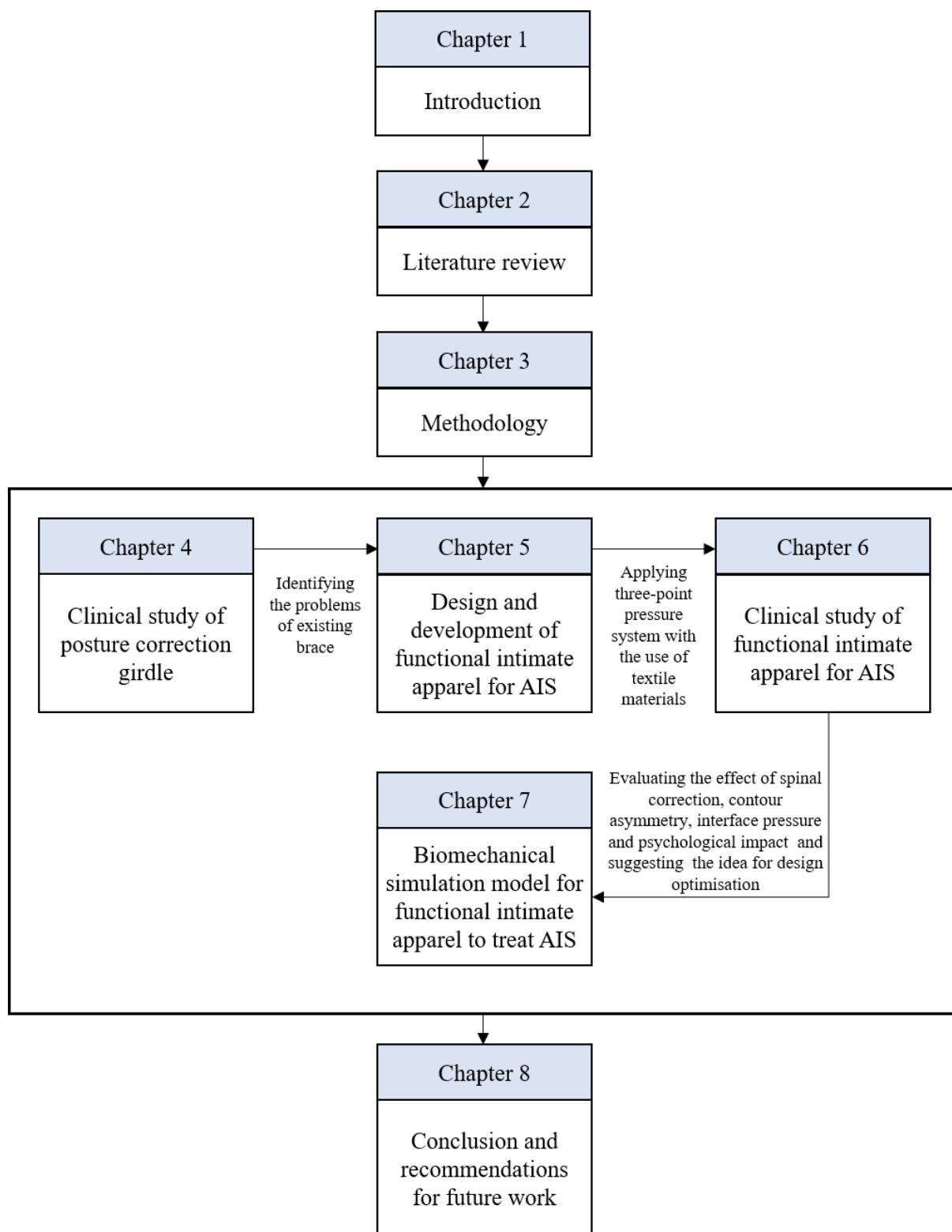


Figure 1-1 Flow diagram of research methodology

## **Chapter 2 Literature review**

### **2.1 Introduction**

This chapter reviewed some of the background information of scoliosis to provide a better understanding about this medical condition. A review of the physical and radiographic examination methods, as well as the classification of scoliosis based on the Lenke classification system provided basic clinical knowledge on diagnosing this condition and as a means of preparing for screening and wear trial programs. In addition, this chapter also reviewed some of the current conservative treatments for AIS which would provide a better understanding of the principles, advantages, and limitations of such treatments. Moreover, the third section reviewed functional intimate apparel items including shapewear, posture corrective intimates, and medical-use undergarments for managing AIS, and discussed some of the technical knowledge behind these garments. The last section of this chapter elaborated on numerical models to offer some background information for the development of a biomechanical model for the proposed design in this study.

### **2.2 Background Information on Scoliosis**

Scoliosis is defined as a lateral spinal deformity with a spinal curvature that is equal to or more than  $10^\circ$  in a standing radiography. The aetiology of most scoliosis cases is idiopathic, which means that the cause is unknown. The prevalence rate of adolescent idiopathic scoliosis is about 2% (Hresko, 2013).

Scoliosis causes many complications to the patients. They experience disfiguration of their torso with imbalanced shoulders or waist line, asymmetrical trunk or rib rotation. These are usually the major concerns of scoliosis patients as they mature into adults. Moreover, pain is common among patients who have a significant curvature of the spine. More importantly, severe scoliosis may cause respiratory and pulmonary diseases (Hresko, 2013). Thus, proper diagnosis is essential to scoliosis patients so that they can receive treatment in the early stages. The following sections discuss the different ways of diagnosing scoliosis through physical and radiographic examinations.

#### **2.2.1 Physical examination**

Physical examination is a fundamental part of diagnosing scoliosis. When scoliosis is suspected in a physical examination, radiographic imaging is essential for a formal diagnosis of scoliosis

(Horne et al., 2014).

Physical examination of an individual who appears to have scoliosis includes height measurement, gait check, skin inspection, assessment of pubertal development, a neurological examination, examination of the symmetry of the shoulders and iliac crest, and evaluation of the contours of the back (Janicki & Alman, 2007).

During the physical examination, the individual may need to undergo the Adam's forward bending test, which is the classic scoliosis screening method (Figure 2-1) to check the symmetry of the shoulders, scapulae, waist and trunk (Adobor et al., 2011; Horne et al., 2014; Hresko, 2013). The patient is required to bend forward with his/her knees in extension and arms towards the ground. The examiner would assess the angle of trunk rotation (ATR) at three areas of the spine: the proximal thoracic, main thoracic, and thoracolumbar or lumbar region (Horne et al., 2014; Hresko, 2013). When the patient bends forward, a rib hump may be produced, which is usually considered to be a sign of scoliosis (Horne et al., 2014). The ATR is used to quantify the degree of the rib hump with the use of a scoliometer (Horne et al., 2014; Kotwicki, 2008).

In Hong Kong, there is a standardized screening protocol managed by the Department of Health. Students in Grade 5 or 10 years or older are eligible for screening in the annual health program carried out by their student health service center. Students in Grades 5, 7, and 9 are invited to undergo the Adam's forward bending test to screen for scoliosis. Students with  $5^{\circ} \leq \text{ATR} < 15^{\circ}$  are subjected to a Moiré topography (MT) and students with  $\text{ATR} \geq 15^{\circ}$  or  $\text{MT} \geq 2$  Moiré lines are required to undergo a radiographic examination (Luk et al., 2010).

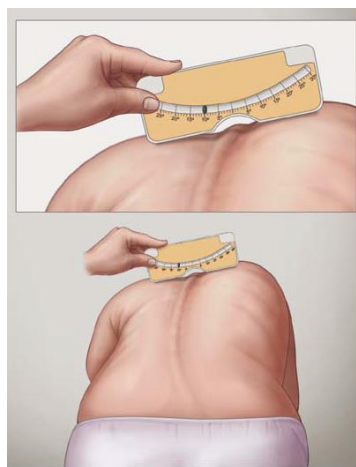


Figure 2-1 Angle of trunk rotation measurement in Adam's forward bending test with scoliometer (Hresko, 2013)

### **2.2.2 Radiographic examination**

Radiography is the standard imaging method for diagnosing scoliosis (Hresko, 2013). A good scoliosis radiographic image should include the vertebrae from the seventh cervical vertebra (C7) to the iliac crest (Hresko, 2013). In clinical practices, a posterior-anterior (PA) radiograph is preferred as opposed to an anterior-posterior (AP) radiograph so that the thyroid and breast tissue are exposed to less radiation (Hresko, 2013; Kotwicki, 2008). Aside from the anterior view, a lateral radiograph image is also important to assess the deformity of the sagittal plane (Hresko, 2013).

#### **2.2.2.1 Standing AP or PA radiography**

Standing plain radiography is universally used in radiographic examinations (Lee et al., 2013). The patient is required to stand with locked knees, feet are spaced a shoulder width apart, look straight ahead, bend her elbows and place her knuckles over the clavicles (Figure 2-2) (Malfair et al., 2010; O'Brien et al., 2008). If the patient has leg length discrepancy, a block should be placed under the shorter leg to obtain symmetry (Bernau, 1983).



Figure 2-2 Posture during standing radiography (O'Brien et al., 2008)

#### **2.2.2.2 Supine AP radiography**

Supine radiography is useful for evaluating spinal flexibility which is also important for pain treatment (Klepps et al., 2001). Even though side bending radiography is the common method used to assess spinal flexibility, it requires effort and a technician to carry out the work, and cannot be replicated (Cheh et al., 2006). On the other hand, supine radiography is more reliable and reproducible compared to side bending radiography (Cheh et al., 2006). As well, previous studies (Cecen et al., 2016; Keenan et al., 2014; Torell et al., 1985; Yazici et al., 2001) have pointed out that compared to the standing position, spinal lateral curvature is spontaneously corrected in the supine position when the effect of gravity is eliminated and muscles are

activated.

More importantly, Cheung et al. (2017) conducted a study about the correlation between the flexibility of scoliosis as revealed by the supine radiograph and the in-brace correction. They suggested that using the Supine radiograph as a guideline to determine the amount of correction achievable with brace-wear.

After radiography is carried out, the spinal curvature is measured based on the radiographic images. The spinal curvature is determined by measuring the Cobb's angle, using the Nash-Moe method and Risser grading.

### **2.2.2.3 Cobb's angle measurement**

Measurement of the Cobb's angle is a universal quantitative means of assessing the spinal curvature (Wills et al., 2007). The Cobb's angle (Figure 2-3) is the maximal angle between the inclination of the superior end plate of the superior end vertebra and the inclination of the inferior end plate of the inferior end vertebra (Malfair et al., 2010). If it is difficult to identify the end plates, the borders of the pedicles might have superseded them (Malfair et al., 2010). Generally, the total error in measuring the Cobb's angle ranges from  $2^{\circ}$  to  $7^{\circ}$  depending on the selected end plate, whether protractor and pencil are used on radiographic films, or a digital method is used (Malfair et al., 2010).

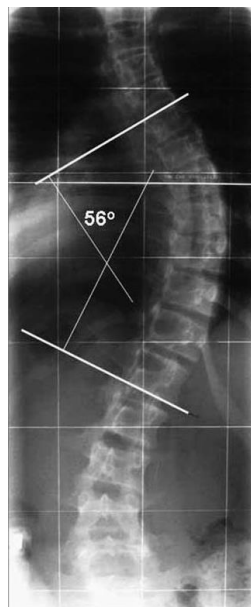


Figure 2-3 Measuring Cobb's angle (Rigo, 2011)

#### 2.2.2.4 Nash-Moe method

The Nash-Moe method (Figure 2-4) is used to measure the vertebral rotation which is graded as five grades according to the position of the vertebral pedicles at the apex of the curve (Anitha & Prabhu, 2012) as follows.

- Natural (0): The pedicles are symmetric which means that there is no rotation.
- Grade I: The pedicle at the concave side is located at the edge of the vertebral body and the pedicle at the convex side slightly migrates to the midline of the spine.
- Grade II: The pedicle at the concave side is barely visible and the pedicle at the convex side is closer to the midline of the spine.
- Grade III: The pedicle at the concave side is not visible and the pedicle at the convex side is on the midline of the spine.
- Grade IV: The pedicle at the concave side is not visible and the pedicle at the convex side has migrated beyond the midline towards the concave side of the vertebral body (Anitha & Prabhu, 2012).

Upadhyay et al. (1995) stated that vertebral rotation is one of the risk factors in lateral curvature progression. Their study concluded that an increase in vertebral rotation increases the chances of treatment failure. They stated that in addition to lateral curvature control, vertebral rotation control is also necessary.

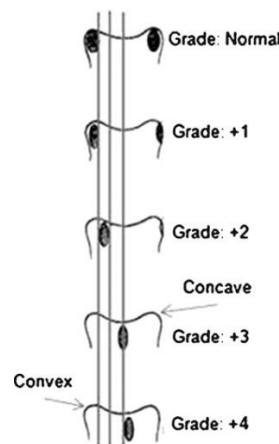


Figure 2-4 Nash-Moe method for vertebral rotation assessment (Anitha & Prabhu, 2012)

#### 2.2.2.5 Risser grade

Skeletal maturity is used as an index of growth potential. Skeletal immaturity is one of the major risk factors for the progression of scoliosis (Horne et al., 2014). To assess skeletal



maturity, the Risser classification is widely used (Malfair et al., 2010) which involves 6 different stages (Figure 2-5) based on the degree of ossification of the iliac crest apophysis as follows.

- Risser Stage 0: The apophysis is not visible. This stage corresponds to the pre-puberty stage.
- Risser Stage I: The apophysis covers 25% of the iliac crest. This stage is the beginning of the decline of the pubertal growth spurt.
- Risser Stage II: The apophysis covers 50% of the iliac crest. This stage corresponds to 14 years of bone age for a girl or 16 years of bone age for a boy.
- Risser Stage III: The apophysis covers 75% of the iliac crest. This stage corresponds to a 14.5 years of bone age for a girl or 16.6 years of bone age for a boy, and both of their remaining growth time is one year.
- Risser Stage VI: The apophysis covers 100% of the iliac crest. This stage corresponds to 15 years of bone age for a girl or 17 years of bone age for a boy.
- Risser Stage V: The iliac apophysis is fused to the iliac crest, which indicates that growth has ended (Dimeglio, 2001).

Sun et al. (2013) conducted a study to predict the curve progression of AIS patients. They pointed out that patients with Risser grades of 0 to 1 have a higher progression rate of scoliosis than those with Risser grades of 2 to 4. Their finding indicated that patients with Risser grades of 0 to 1 should receive treatment to control scoliosis such as wearing a hard brace.

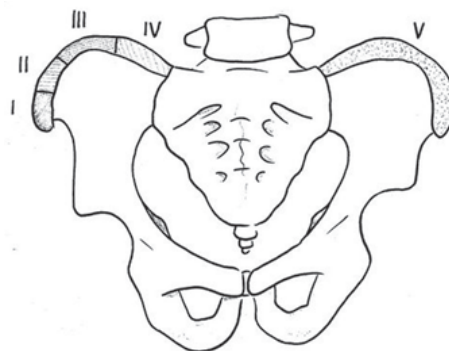


Figure 2-5 Risser grading

### 2.2.3 Classifications of adolescent idiopathic scoliosis

The classification of AIS is essential for planning the treatment of AIS and conducting clinical research on AIS. It also plays an important role in assessing patterns in similar spinal deformities and categorizing them, thus providing a common language to compare various

treatment methods and results (Alam et al., 2013). An ideal classification of AIS should be reproducible which enables the same treatment to be concluded when assessing the same type of curve (Alam et al., 2013). The King and Lenke classifications are widely used systems to classify AIS (Zhang et al., 2013). Several studies (Alam et al., 2013; Edgar, 2002; Lenke et al., 2001; Rigo et al., 2010; Zhang et al., 2013) have concluded that the Lenke classification is a more comprehensive, reliable and reproducible system as curves in the coronal plane are primarily classified and then in the sagittal plane which includes the triple curve (three curves in the thoracic, thoracolumbar and lumbar regions). As such, the Lenke classification system will be discussed in more detail and used to classify the curve type in this study.

### 2.2.3.1 Lenke classification

The Lenke classification system (Figure 2-6) consists of six types of curves (Types 1 to 6), a lumbar spine modifier (A, B and C) and a sagittal thoracic modifier (-, N and +). Lenke et al. (2001) defined six curve types based on the magnitude and location of the curvature with information on three levels of lumbar and thoracic sagittal deformities respectively.

Curve Type				
Type	Proximal Thoracic	Main Thoracic	Thoracolumbar / Lumbar	Curve Type
1	Non-Structural	Structural (Major*)	Non-Structural	Main Thoracic (MT)
2	Structural	Structural (Major*)	Non-Structural	Double Thoracic (DT)
3	Non-Structural	Structural (Major*)	Structural	Double Major (DM)
4	Structural	Structural (Major*)	Structural	Triple Major (TM)
5	Non-Structural	Non-Structural	Structural (Major*)	Thoracolumbar / Lumbar (TL/L)
6	Non-Structural	Structural	Structural (Major*)	Thoracolumbar / Lumbar - Main Thoracic (TL/L - MT)

**STRUCTURAL CRITERIA**  
(Minor Curves)

**Proximal Thoracic:** - Side Bending Cobb  $\geq 25^\circ$   
- T2 - T5 Kyphosis  $\geq +20^\circ$

**Main Thoracic:** - Side Bending Cobb  $\geq 25^\circ$   
- T10 - L2 Kyphosis  $\geq +20^\circ$

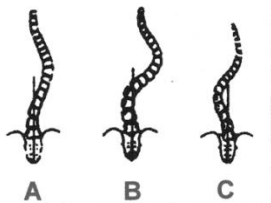
**Thoracolumbar / Lumbar:** - Side Bending Cobb  $\geq 25^\circ$   
- T10 - L2 Kyphosis  $\geq +20^\circ$

\*Major = Largest Cobb Measurement, always structural  
Minor = all other curves with structural criteria applied

**LOCATION OF APEX**  
(SRS definition)

<b>CURVE</b>	<b>APEX</b>
THORACIC	T2 - T11-12 DISC
THORACOLUMBAR	T12 - L1
LUMBAR	L1-2 DISC - L4

Modifiers		
<b>Lumbar Spine Modifier</b>	<b>CSVL to Lumbar Apex</b>	
<b>A</b>	CSVL Between Pedicles	
<b>B</b>	CSVL Touches Apical Body(ies)	
<b>C</b>	CSVL Completely Medial	

Thoracic Sagittal Profile T5 - T12	
-	(Hypo) < 10°
N	(Normal) 10°- 40°
+	(Hyper) > 40°

Curve Type (1-6) + Lumbar Spine Modifier (A, B, or C) + Thoracic Sagittal Modifier ( -, N, or +)  
**Classification (e.g. 1B+):** \_\_\_\_\_

Figure 2-6 Lenke classification (Lenke et al., 2001)

Notes: SRS=Scoliosis Research Society. CSVL= center sacral vertical line.

### **2.2.3.1.1 Curve types**

In the Lenke classification (Figure 2-6), there are primarily 6 curve types with regard to spinal lateral deformity.

- Lenke 1 Main thoracic: The primary structural curve is in the main thoracic region and there are minor non-structural (secondary) curves that are in the proximal thoracic and thoracolumbar/lumbar regions.
- Lenke 2 Double thoracic: The major structural curve is in the main thoracic region and there is a minor structural curve in the proximal thoracic region while a minor non-structural curve is in the thoracolumbar/lumbar region.
- Lenke 3 Double major: The major structural curve is in the main thoracic region and there is a minor structural curve in the thoracolumbar/lumbar region with a non-structural curve in the proximal thoracic area.
- Lenke 4 Triple major: The structural curves are in the proximal thoracic, main thoracic and thoracolumbar/lumbar regions. The major curve can be either the thoracic or the thoracolumbar/lumbar curve.
- Lenke 5 Single thoracolumbar/lumbar: The primary structural curve is in the thoracolumbar/lumbar region while the non-structural curves are in the proximal thoracic and main thoracic areas.
- Lenke 6 Double thoracolumbar/lumbar: The major structural curve is in the thoracolumbar/lumbar region and 5 degrees more than the main thoracic curve. The non-structural curve is in the proximal thoracic area (Lenke et al., 2001).

### **2.2.3.1.2 Lumbar spine modifiers**

Assessing the degree of lumbar deformity is essential as the lumbar spine is related to spinal balance and affects the proximal curves. There are three types of lumbar deformities (Figure 2-7), which are determined by the position of the lumbar pedicles and the stable vertebra is compared with the CSVL on an upright coronal radiograph image. The CSVL is drawn as a vertical line that bisects the proximal sacrum and parallel to the lateral edge of a radiograph. The stable vertebra is defined as the lowest proximal thoracic or lumbar vertebra that is most closely bisected by the CSVL (Lenke et al., 2001).

- Lumbar modifier A: The CSVL falls between the lumbar pedicles and stable vertebra and there is little to no lateral deformity and rotation in the lumbar region.

- Lumbar modifier B: The CSVL falls between the medial border of the lumbar concave pedicle and the lateral margin of the apical vertebral body or bodies. There must be a thoracic apex with minimal to moderate rotation in the lumbar region. The CSVL touches the medial or lateral aspect of the lumbar apical pedicle or lateral margin of the apical vertebral body.
- Lumbar modifier C: The CSVL does not touch the apical vertebral body or bodies right above and below the apical disc (Lenke et al., 2001).

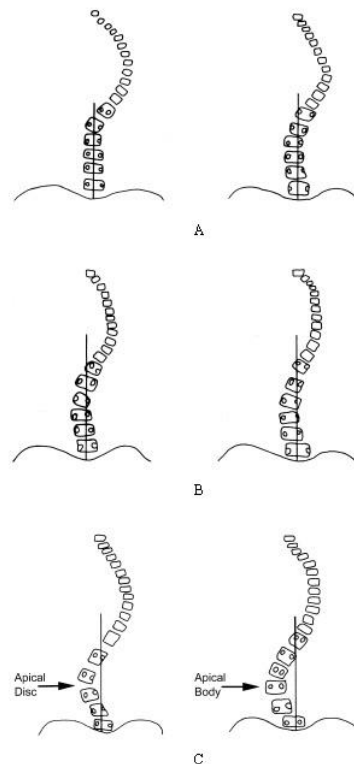


Figure 2-7 Three types of lumbar modifiers: A - little to no curve; B - moderate curve; and C - large curve (Lenke et al., 2001).

### 2.2.3.1.3 Thoracic sagittal modifiers

The thoracic sagittal modifiers are discussed here to further elaborate on the six curve types in terms of the alignment of the thoracic spine which would complete the classification of the scoliotic spine. A normal sagittal thoracic alignment from T5 to T12 is in the range of  $+10^\circ$  to  $+40^\circ$  in a standing lateral radiograph (Lenke et al., 2001).

- A minus sign (-): The sagittal thoracic curvature is less than  $+10^\circ$  which is also defined as hypokyphosis.
- Normal (N): The sagittal thoracic curvature is between  $+10^\circ$  and  $+40^\circ$  which is also defined

as normal kyphosis.

- A plus sign (+): The sagittal thoracic curvature is more than  $+40^\circ$  which is also defined as hyperkyphosis (Lenke et al., 2001).

### **2.3 Treatment for adolescent idiopathic scoliosis**

In general, patients with a Cobb's angle between  $10^\circ$  -  $20^\circ$  are asked to undergo periodic assessments during their period of rapid growth (adolescence). If the Cobb's angle increases to more than  $20^\circ$  and the spinal deformity is considered to be progressive, conservative treatment which includes bracing and physiotherapy is recommended. If the Cobb's angle is greater than  $50^\circ$  and the patient experiences pain or appreciable progression in spinal deformity, surgery may be prescribed (Hresko, 2013).

The basic objectives of using conservative treatment for AIS are to: 1) stop curvature progression or possibly even reduce the curvature, 2) prevent or treat respiratory dysfunction, 3) prevent or treat spinal pain symptoms, and 4) improve the physical aesthetics through postural correction (Negrini et al., 2012).

In the following, the different types of conservative treatment will be discussed, including rigid bracing and the different types of rigid braces that are available, flexible bracing and the different types of flexible braces, and physiotherapy scoliosis specific exercises (PSSEs).

#### **2.3.1 Rigid bracing**

Rigid bracing is an effective conservative treatment that has been traditionally prescribed for AIS patients. The majority of rigid braces including the Milwaukee, Boston, Chêneau and Lyon braces adopt a three-point pressure system to correct the scoliotic spine. The three-point pressure system (Figure 2-8) is a universal system for orthotics in treating scoliosis. Studies have been carried out that conclude the three-point pressure system is the most effective mechanism for orthotic correction. The process involves exerting a lateral external force on the apical vertebra and contralateral forces above and below the apical vertebra (Qian et al., 2010).

Weinstein et al. (2013b) conducted both randomized and cohort preference studies of bracing in an AIS trial to investigate the effectiveness of bracing compared to observation in preventing surgery. Their results found that the rate of treatment success is 72% after bracing and 48% after observation. More importantly, they pointed out that the success of treatment is significantly and positively correlated with the hours of brace wear.

Katz et al. (2010) conducted a prospective study on the efficacy of bracing treatment to determine the relationship between the hours of brace wear and control of curve progression in 100 AIS patients. They found that 82% of the patients who wore the brace for more than 12 hours each day have less than 6° of curve progression while this is true for only 31% of those who wore the brace for less than 7 hours each day. Thus, patient compliance with bracing is a critical factor for enhancing the success rate of bracing treatment.

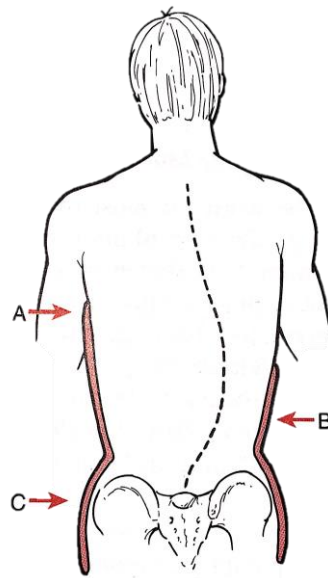


Figure 2-8 Three-point pressure from thoracic-lumbo-sacral orthosis to treat scoliosis (Seymour, 2002)

In the following, four different types of rigid braces will be discussed: the Milwaukee, Boston, Chêneau and Lyon braces.

### 2.3.1.1 Milwaukee brace

The Milwaukee brace (Figure 2-9), which is also known as a cervical-thoracic-lumbo-sacral orthosis (CTLSSO), is a full torso brace that covers the body from the pelvis to the base of the skull (Federico & André, 2011). This brace consists of one anterior and two posterior bars, a pelvic section, a neck ring, axillary sling, and thoracic and lumbar pads (Maruyama et al., 2008). The pelvic section and neck ring provide end point control which aligns the position of the upper thoracic spine relative to that of the pelvis (Lusardi, 2012). The thoracic and lumbar pads provide external forces to the subcutaneous skeletal structures such as the rib cage and vertebra to correct the scoliotic spine through the three-point pressure system (Qian et al., 2010).

The advantages of the Milwaukee brace are minimal restriction of respiration due to an open

design and adjustability to manage the physical growth and spinal curvature changes of the patient while its limitations are lack of aesthetics due to the visible extended neck ring and the bulkiness of the brace itself (Seymour, 2002).



Figure 2-9 Milwaukee brace (Qian et al., 2010)

#### 2.3.1.2 Boston brace

The Boston brace is also known as a thoracic-lumbo-sacral orthosis (TLSO) which incorporates the three-point pressure system. Unlike CTLSOs, TLSOs do not have a neck ring and can be easily concealed under clothing. Normally, TLSOs are primarily effective for applying pressure onto the thoracic curve at T7 or below (Laurnen et al., 1983). The advantages of TLSOs are their low profile and quick fabrication compared to CTLSOs. However, their limitations are that they cannot be adjusted to accommodate vertical growth, and retain heat due to the closed design which restricts respiration (Seymour, 2002).

The Boston brace (

Figure 2-10) was developed in 1972 at the Boston Children's Hospital in Massachusetts, USA by M.E. Bill Miller and Dr. John Hall (Seymour, 2002). The brace is constructed with two layers which are the outermost and inner layers. The outermost layer is a prefabricated polypropylene pelvic module with an anatomic configuration that provides 15° lumbar of flexion with strap fixations at the waist, high magnitude of force to the abdominal front and lateral support to the torso. The inner layer is composed of pads which are usually made of polyethylene foam and fitted inside the module to change the symmetry of the inner surface of the orthosis based on the degree of rotation and the apex of the spinal curves (Chase et al., 1989). The dynamic alignment of the spine is controlled by applying lateral and derotation forces (Figure 2-11). However, some studies have pointed out that the Boston brace can only

prevent the progression of vertebral rotation, degree of vertebral translation, severity of the rib hump and increase in the Cobb's angle in idiopathic scoliosis patients instead of correcting these issues (Federico & André, 2011; Seymour, 2002).

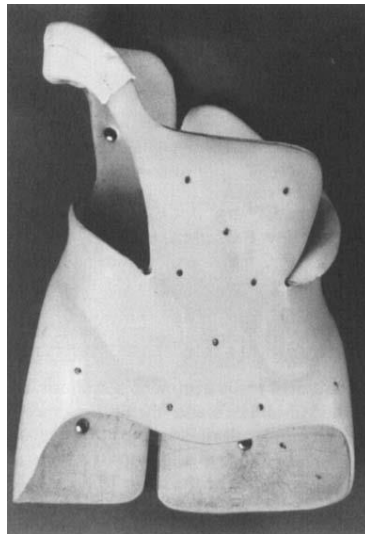


Figure 2-10 Boston brace for right thoracic curve (Weisz et al., 1989)

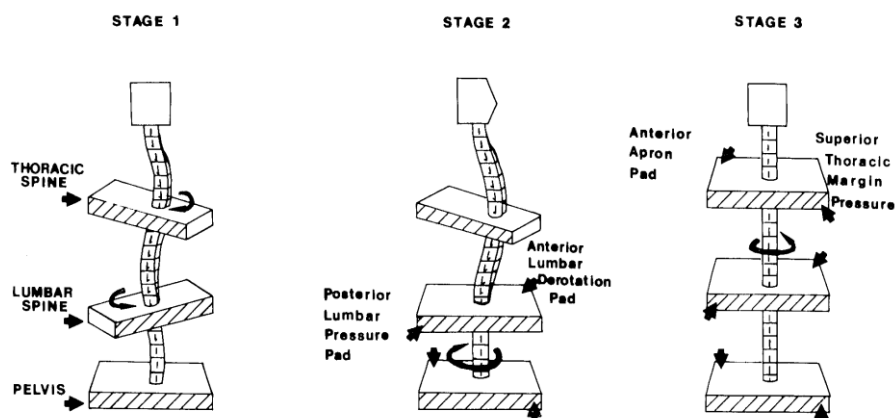


Figure 2-11 Three stages in applying corrective forces to spine with Boston brace (Chase et al., 1989)

The Boston brace has also been modified for scoliosis patients who suffer from vertebral rotation which has resulted in the dynamic derotation brace (Figure 2-12). The key feature of the dynamic derotation braces are posterior anti-rotatory aluminium blades which provide anteriorly-directed force at the attached side and posteriorly-directed force under the opposite half of the brace and thus push the two halves of the brace to shift horizontally in opposite directions to each other (Grivas et al., 2010). Similar to most scoliosis orthoses, the dynamic derotation brace applies both passive and active corrective forces. The brace provides



mechanical support to the wearer, which is a passive type of correction, and the wearer pulls away from the pressure sites which is an active type of correction (Grivas et al., 2010).



Figure 2-12 Dynamic derotation brace (thoracic curve module) (Grivas et al., 2010)

### **2.3.1.3 Chêneau brace**

The Chêneau brace (Figure 2-13) was developed in 1979 by Jacques Chêneau (Federico & André, 2011) and is also a TLSO that applies the three-point pressure system. Spinal correction is achieved through a system of multipoint pressure zones and expansion chambers (Giorgi et al., 2013). The brace creates a pushing force on the convex prominence of the posterior ribs and simultaneously on the concave prominence of the anterior ribs. Pressure is applied to convex side directly which migrates centripetally while the concave side migrates centrifugally as a result of the natural movement of tissue. The convex anterior and concave posterior free spaces create rib cage displacement passively which allows rib cage expansion resultant of squeezing the convex parts. The free spaces also allow active movement of the rib cage which guides the rib cage towards the concavities. Also, the free-space design allows deep breathing, and provides room for asymmetrical respiration during exercise when wearing the brace (Kotwicki & Cheneau, 2008). The Chêneau brace is usually used along with the PSSEs (Federico & André, 2011).

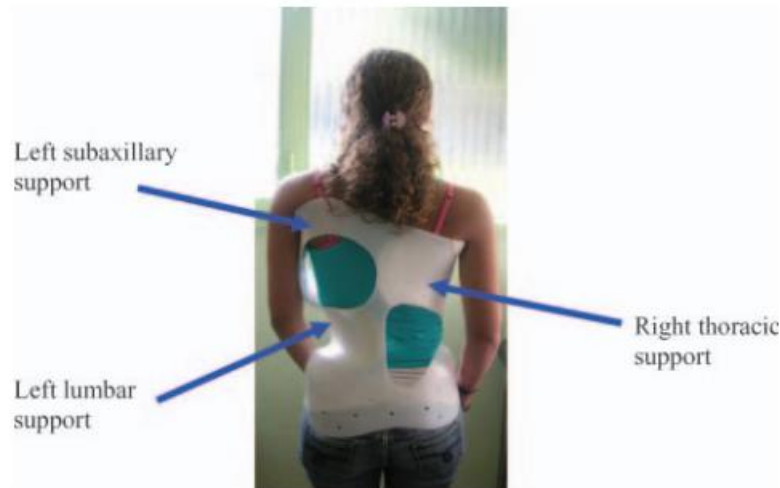


Figure 2-13 Chêneau brace (Pham et al., 2008)

#### 2.3.1.4 Lyon brace

The Lyon brace (Figure 2-14) was first created by Pierre Stagnara in 1947 and is a hard brace that is commonly prescribed to patients with thoracic curves in Europe (Aulisa et al., 2015). It is also a TLSO based on the three-point pressure system. The Lyon brace consists of vertical posterior and vertical anterior bars made of metal. There are shells made of polymetacrylate of methyl (PMM; also known as Plexidur) that are attached to the structure from top to bottom: a shell to balance the shoulders on the side with thoracic convexity, a thoracic shell at the level of the thoracic convexity and one that is placed at the opposite side to provide counter force, a lumbar shell at the abdominal ribs, and a pelvic girdle made up of two hemi-shells. The PMM shells play an important role in directly pushing the convex side while the free space (concave side) allows expansion. More importantly, unlike other TLSOs such as the Boston and Chêneau braces, the Lyon brace can be casted under continuous traction so that it allows elongation of the scoliotic spine with the aim to reduce the constraints of the spinal discs and enhance spinal correction (de Mauroy et al., 2011).



Figure 2-14 Lyon brace (de Mauroy et al., 2011)

## 2.3.2 Flexible bracing

Aside from hard braces, there are flexible braces to treat scoliosis. These braces are fabricated from textile materials to control spinal curvature. The use of textile materials allows the wearer to feel more comfortable as the brace is light in weight and fits the body more closely. Some designs also effectively limit movement of the spine and encourage the wearer to maintain a proper posture (Coillard et al., 2008; Liu et al., 2015).

### 2.3.2.1 SpineCor

The SpineCor (Figure 2-15) dynamic corrective brace is the most representative flexible brace, and consists of two components. The first component is a pelvic base which has a fastening system that comprises three soft thermo-deformable plastic pieces. The pelvic base is stabilised with two belts on the thighs and two bands at the crotch, thus providing trunk support. The second component is a bolero of corrective bands of elastic material that wraps around the torso to induce corrective forces.

The SpineCor brace was initially produced in 1993 by Drs. Christine Colliard and Charles Rivard of St. Justine Hospital in Montreal, Canada. Subsequently, the brace was evaluated by Smith (2002) who reported that the brace reduced the Cobb's angle through clinical observations. The original SpineCor researcher Coillard et al. (2003) and her team further elaborated on the mechanism behind the brace which they called The Corrective Movement principle. They stated the corrective mechanism behind the Spinecor system is mainly derived from physical therapy which uses straps to realign the orientation of the thoracic,

thoracolumbar, and lumbar segments through dynamic movement in the form of clockwise and counter-clockwise rotations and tilts, postural shifts, bending and lateral inclinations. This corrective approach is premised upon “the unique kinematics of the thoracic, thoracolumbar and lumbar segments of the spine. The amplitude and direction of these kinematics is defined by the shape of the vertebra, the geometry of its articular facets, the spinous processes and the presence or absence of rib articulations” (Coillard et al., 2008, p 113). The Corrective Movement principle allows neuromuscular control of the spine to be maintained and re-educate through active bio-feedback.

Coillard et al. (2008) also conducted a prospective study in the effectiveness of SpineCor and their results showed that 93.2% patients stabilized or corrected their curves up to 2 years after bracing. However, the success rate of SpineCor was found to be significantly lower than rigid bracing (Guo et al., 2014; Wong et al., 2008). Moreover, the SpineCor brace has some drawbacks which include being difficult to wear, inconvenient to don and doff when the wearer needs to use the toilet and causing high levels of pain due to the concentrated force from the straps.



Figure 2-15 SpineCor brace (Coillard et al., 2003)

### **2.3.2.2 Posture correction girdle**

Liu et al. (2014) developed a posture correction girdle in the form of a flexible tightly fitting garment with the aim to reduce further advancement of scoliosis by exerting corrective forces and improving the posture of the wearer.

This posture correction girdle is composed of 3 main parts: the shoulder straps, main torso, and waist band, as shown in Figure 2-16. The shoulder straps are attached to the back panel and

wrapped around the shoulders of the wearer with a front Velcro opening. The material of the shoulder straps is elastane with a high elastic modulus. The straps pull the shoulders backwards so that the upper thoracic spine is pushed into the appropriate posture. The main torso panel is a vest-like corset that has a front zipper-opening. The garment also features a crotch with a Velcro opening to facilitate ease of going to the toilet. The entire girdle consists of 3 layers. The shell layer is the basic frame of the girdle and designed with aesthetics and comfort taken into consideration. The mid layer contains supporting resin bones that are inserted in the back and side panels. The resin bones provide vertical support to the body and control the lateral movement of the wearer. The inner layer contains pocket lining that are fabricated from powernet. The pocket linings allow insertion of semi-rigid ethylene vinyl acetate (EVA) foam pads. The EVA pads are inserted in the apex region based on the radiograph taken of the wearer to provide corrective forces against the convexity of the spine. The waist band is elastic with a high modulus that covers the thoracolumbar to lumbar regions with a front Velcro opening. The waist band creates a compressive circumferential corrective force onto the body with the use of the EVA pads.

Liu et al. (2015) also evaluated the effectiveness of their posture correction girdle on posture control and their findings showed a trend of improvement in posture and motion control. However, their study did not mention the performance of the girdle in controlling spinal deformity and the biomechanics behind the application. Also, their study has some limitations including a small sample size and incomprehensive classification of the curve type. Thus, this study will further evaluate the performance of their posture correction girdle especially in determining the magnitude of correcting spinal deformities and the related biomechanics.

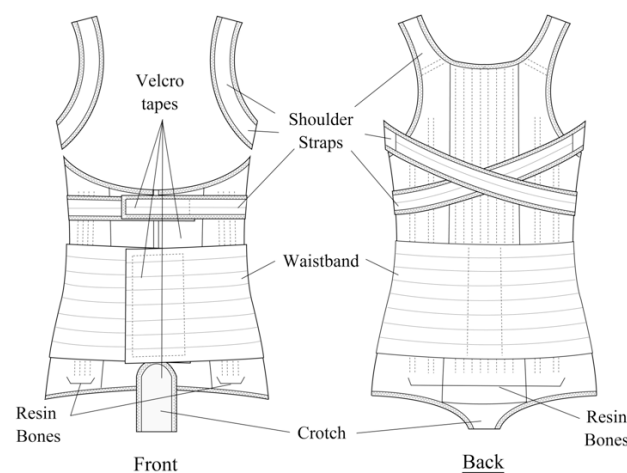


Figure 2-16 Posture correction girdle for scoliosis in early stages (Liu et al., 2014)

### **2.3.3 Physiotherapy scoliosis specific exercises**

PSSEs are a therapeutic intervention to treat scoliosis that can be applied alone or in combination with bracing or surgery (Berdishevsky et al., 2016; Bettany-Saltikov et al., 2012). The standard characteristics of these exercises are 3-dimensional self-correction, training activities that are incorporated in daily life activities and stabilization of corrected posture (Berdishevsky et al., 2016).

Scoliosis progression usually starts in a triggering event of vertebrae wedging and the wedged vertebrae cause the spinal curvature which is an asymmetric load on the spine. This unbalanced load results in the asymmetric growth of the spine which increases the wedging of the vertebrae. This entire process is cyclic until the bones mature and stabilize, thus causing a vicious cycle for the scoliotic patient (Burwell et al., 2006).

The general goals of PSSEs are to prevent this vicious cycle through patient education, and enhance spinal and trunk alignment by reducing asymmetric loads and thus halt the progression of the scoliosis (Berdishevsky et al., 2016). Several PSSE approaches are discussed in the following.

#### **2.3.3.1 Lyon approach (France)**

The Lyon method was developed by Dr. Pierre Stagnara in 1947. This method is traditionally a supplementary treatment with the use of the Lyonnaise (Lyon) brace and casting. This method aims to improve the motivation of the wearer to comply with bracing and heighten his/her awareness of postural deficiencies. The Lyon method also aims to increase the range of motion of the user, increase his/her control over the spinal nerve muscles, improve spinal coordination, increase trunk stabilization, add to muscle strength, and improve respiration based on ergonomics (Berdishevsky et al., 2016).

The principle behind this method involves 5 stages. The first stage is the Lyon approach to assessment. This stage is planning the therapy regimen in accordance with the age and the Cobb's angle of the patient and his/her level of postural imbalance. The second stage is the awareness of trunk deformity. The patient starts to develop a sense of awareness of his/her posture deficiencies with visual aids, such as mirrors and real-time video feedback. The third stage is carrying out the exercises themselves. Sample exercises are provided which are related to the correction of the frontal plane, as well as "segmental mobilization, core stabilization, proprioception, balance, and stabilization" (Berdishevsky et al., 2016). The intention of the

Lyon approach is to avoid spinal extension during exercise and increase thoracic kyphosis and lumbar lordosis to counter the flat back problem. The fourth stage is understanding what should not be done, and the reasons for not doing such activities, which include avoiding extreme movement of the sagittal plane and any activities that cause shortness of breath or a flat back and strengthening muscles through superficial body building. The fifth stage is understanding which sports are ideal for scoliosis patients and whether physiotherapy is enough. Patients are taught to properly play sports and the most ideal types of sports for them, which include biking, rock climbing, and track and field while some that require excessive extension of the spine is not recommended, such as gymnastics and dancing (Berdishevsky et al., 2016; Bettany-Saltikov et al., 2012).

Negrini et al. (2008) conducted a systematic literature review on the reduction of the rate of progression of AIS in patients who received PSSEs. They stated that about 42-44% of the AIS patients treated with the Lyon method experienced an increase in their spinal curvature while 75-77% of the AIS patients who did not receive any treatment had a larger curvature.

### **2.3.3.2 Schroth method (Germany)**

The Schroth method was developed by Katharina Schroth in 1920. She was a teacher who had scoliosis and eventually established a clinic in Germany to teach her techniques to other patients. The Schroth system divides the body into blocks: shoulder, thoracic, lumbar and hip-pelvic blocks. Scoliosis causes the deformation of these blocks. The geometric shape of the body blocks is changed from a rectangular to a trapezium shape. The Schroth system shows the direction of the side deviation and the rotation of the body blocks, thus providing a clear orientation for therapy. This method aims for a proactive way to correct spinal deformities to avoid surgery and improve posture to reduce or halt the progression of the spinal curvature.

The Schroth method involves five principles of correction for the position of the pelvis. The first correction is auto-elongation which is also called self-elongation is extending the spine for a detorsional correction effect which reduces the lateral deviation and rotation of the spine and flattens the sagittal spinal curve. The second correction is deflection which is related to postural correction in the frontal plane. The third principle is derotation which is also called asymmetric sagittal straightening, which is achieved by correcting only one side of the body. The fourth principle is rotational angular breathing which is also considered as orthopaedic breathing. This involves rotating the spine to mobilize the spine and trunk and give them more flexibility through breathing. In doing so, the muscles are activated which increases the corrective effect

and re-shapes the deformed trunk. The last principle is stabilization which improves the correction of the scoliotic spine through muscle activation (Berdishevsky et al., 2016; Bettany-Saltikov et al., 2012).

Otman et al. (2005) carried out a study with 50 AIS patients to investigate the efficacy of the Schroth exercises. Their results showed that the Cobb's angle is reduced by 8.25° on average after one year of exercising. Also, the vital capacity and muscle strength of the subjects significantly improve after one year of exercising.

Moreover, Park et al. (2018) conducted a meta-analysis on the effect of Schroth exercises on idiopathic scoliosis patients. They found that the Schroth exercises have a significant influence on idiopathic scoliosis. Also, they pointed out that mild to moderate scoliosis patients whose Cobb's angle is between 10° and 30° may benefit more than moderate to severe scoliosis patients whose Cobb's angle is greater than 30°.

#### **2.3.3.3 Barcelona Scoliosis Physical Therapy School (Spain)**

The Barcelona Scoliosis Physical Therapy School (BSPTS) treatment was founded by Dr. Manuel Rigo in 2009. Dr. Manuel Rigo modified the Chêneau brace and developed the Rigo classification system for determining curve type. The principles of the approach of this school are based on the Schroth method which originated in Germany in the 1920s. The approach of the school involves trunk reshaping through isometric muscle activation of the convexities and rotational breathing into the concavities (Berdishevsky et al., 2016).

Zapata et al. (2016) conducted a single case study to investigate its effects. Their results showed that after one year of exercising, the Cobb's angle of the dominant curve is reduced by 8° while that of the secondary curve is increased by 5°. Their data also showed that after one year of exercising, the Cobb's angle of the secondary curve is larger with exercising than relaxed standing by 6°. This could imply that the corrective exercises have a negative effect on the secondary curve despite its positive effect on the dominant curve.

#### **2.3.3.4 Scientific Exercise Approach to Scoliosis (Italy)**

The Scientific Exercise Approach to Scoliosis (SEAS) is based on the Lyon approach. There are two main treatment objectives. The main objective of SEAS is to improve spinal stability through active self-correction. The scoliosis patient needs to have the best possible alignment in the 3D spatial planes autonomously without any external aids and movement of other body parts. The approach trains the neuro-motor systems to activate reflexes for posture self-



correcting during daily activities. This results in regaining postural control and improving spinal stability (Berdishevsky et al., 2016; Bettany-Saltikov et al., 2012).

Zaina et al. (2009) conducted a retrospective controlled study with 68 AIS bracing patients to investigate the efficacy of exercise in reducing the corrective loss during brace wear. They found that the Cobb's angle of patients who only underwent bracing treatment without performing the exercises regularly is significantly increased after the end of the bracing treatment. The Cobb's angle of the SEAS group who was receiving bracing treatment but also incorporated the SEAS routine regularly did not change. Their study shows that the combination of bracing and SEAS can contribute to reducing the correction loss in brace wear for those with AIS.

#### **2.3.3.5 Dobosiewicz Method (Poland)**

The Dobosiewicz method (DoboMed) was developed by Professor Krystyna Dobosiewicz, a physiotherapist and doctor, in 1979. The primary aim of this method is to prevent the progression of the spinal curvature or reduce the curvature by the asymmetric trunk mobilisation in strictly symmetric position. This method is a biodynamic approach in 3D self-correction and involves the mobilization of the primary curve. The method consists of three components: 3D self-correction of the spinal curvature and rib cage with forward bending, promoting thoracic kyphosis and lumbar lordosis with simultaneous 3D self-correction, and 3D self-correction in the upright position against gravity (Berdishevsky et al., 2016).

Dobosiewicz et al. (2002) conducted a study with 208 AIS patients who were treated with DoboMed. They reported that the regression rate of the Cobb's angle is 33.6% for those with a single curve and 22.8 and 26.1% for those with double curves in the thoracic and lumbar regions respectively. They claimed that DoboMed has a positive influence on inhibiting the progression of spinal curvature as well as improving respiratory functions. However, some researchers, such as (Mordecai & Dabke, 2012) questioned their methodology and the reliability of their results.

#### **2.3.3.6 Functional Individual Therapy of Scoliosis (Poland)**

The Functional Individual Therapy of Scoliosis (FITS) concept was developed by Polish scoliosis experts Marianna Bialek and Andrzej M'hango in 2003. This therapy is based on several therapeutic approaches and consists of three stages. The first stage is an examination of the patient. The second stage is the detection and elimination of the myofascial retraction by

using myofascial relaxation techniques. In doing so, the restriction of 3D corrective movement is eliminated which will help to prepare the patient for 3D self-correction. The last stage is the building and stabilization of new corrective posture patterns. The patient needs to perform correct foot loading, do stabilization exercises and build corrective posture patterns sequentially (Berdishevsky et al., 2016).

Bettany-Saltikov et al. (2012) reported that 8.9% of mild scoliosis patients (Cobb's angle between 10° and 25°) who underwent the FITS method without bracing increased their spinal curvature by more than 5° or 21.6% (Cobb's angle between 26° and 40°) whereas those who underwent the FITS method combined with bracing increased their spinal curvature by more than 5° at the 2.8 year follow-up.

#### **2.3.3.7 Limitations of Physiotherapy scoliosis specific exercises**

To sum up, PSSEs seem to be a good additional treatment to stop the progression of scoliosis. However, a combination of bracing may be required especially for moderate scoliosis patients. Mordecai and Dabke (2012) also stated that there are no randomised control trials conducted to prove the effectiveness of PSSEs on scoliosis control in the current literature. Thus, PSSEs cannot be used to replace bracing treatment. Moreover, the long duration of therapy is another shortcoming of PSSEs. Unlike bracing, PSSEs do not provide an immediate effect after the initial training (Park et al., 2018; Zapata et al., 2016). In addition, some PSSE methods such as FITS are complex and require utmost accuracy and thus absolute cooperation of the therapists and parents in the therapeutic process of the patient might be required (Bettany-Saltikov et al., 2012).

#### **2.3.4 Knowledge gap in existing scoliosis treatment**

Undoubtedly, rigid braces have proven to be more effective in controlling the progression of AIS. However, they induce a high level of compression forces, have a bulky profile, and are constructed from material that has low air permeability, so that they cause low compliance with treatment and reduce the quality of life of AIS patients. To address the shortcomings of the rigid braces, flexible braces such as SpineCor and a posture correction girdle have been developed to improve the comfort and movement of patients. Nevertheless, the effectiveness of these flexible braces is still being questioned and there still are some limitations such as the difficulty of donning and doffing the brace, as well as inconvenience when the patient needs to use the toilet.

Therefore, the following knowledge gaps are acknowledged.

Knowledge Gap 1: Rigid braces provide effective spinal correction but lack comfort and does not allow freedom of mobility. Flexible braces such as the SpineCor brace are more comfortable to wear and allow more mobility but are not proven to be effective in controlling scoliosis. There are therefore limited options which provide effective spinal correction, comfort and flexibility at the same time.

Knowledge Gap 2: The intention of the posture correction girdle design is to control the progression of scoliosis in AIS patients. However, little evidence-based research has been done on the effects of the girdle and its ability to control the progression of scoliosis as opposed to controlling the posture of the wearer.

## **2.4 Functional intimate apparel**

While intimate apparel such as bras, panties, pantyhose, corsets, and girdles have often been depicted as the ‘second skin’ since they serve to protect the skin of the wearer and support the different body components (Yu, 2006), functional intimate apparel is fast becoming an emerging demand. Conventional functional intimate apparel includes girdles, corsets and functional bras which mainly focus on providing shape and posture control. However, functional intimate apparel is now being used to offer medical related therapy. That is, functional intimate apparel items have also been used to manage conditions like AIS. In the following, some of the functional intimate apparel items will be discussed and how they can be used to manage medical conditions will be elaborated.

### **2.4.1 Intimate apparel that controls posture**

There has been some work done in the literature on intimate apparel that controls posture. For example, Leonisa Inc. (2017), a lingerie company, offers a posture corrector wireless back support bra (Figure 2-17). The bra is a vest type of apparel with a front hook and eye opening. This design is novel in its X reinforcement back which provides back support and helps wearers maintain a good posture.



Figure 2-17 Posture corrector wireless back support bra (Leonisa Inc., 2017)

Wang (2013) designed a posture correcting garment (Figure 2-18) which mainly focuses on kyphosis correction. The design features include padded shoulder straps attached to a back/lumbar panel in a double cross pattern, with a wide waist band and two constructed back straps. The shoulder straps provide a back pulling force onto the shoulders which is similar in concept to the design in Mungo (1952).

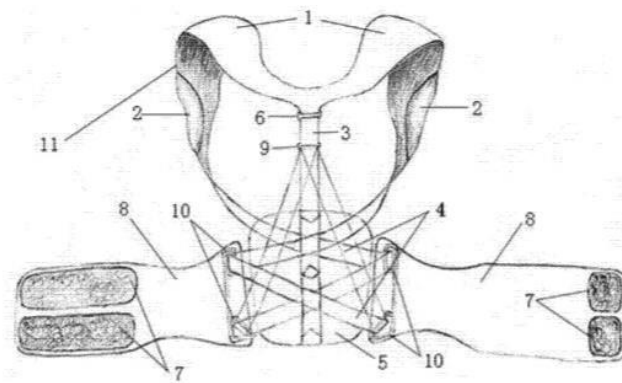


Figure 2-18 Posture correcting garment (Wang, 2013)

Mungo (1952) patented a posture corrective brassiere (Figure 2-19) which provides adjustable support for the breasts and back. The apparel is a vest bra with a belt attached to the rear portion of the bra over the waist. This belt design creates a downward pulling force on the back panel and backwards pull of the shoulder straps. These forces help the body maintain a good posture.

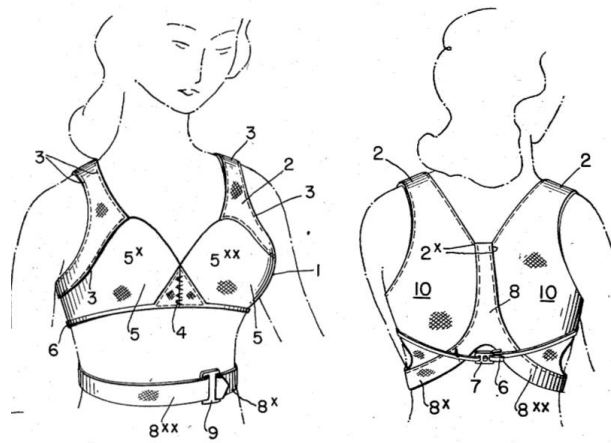


Figure 2-19 Posture corrective brassiere (Mungo, 1952)

#### 2.4.2 -Functional intimate apparel for medical uses

Anderson (2015) developed an undergarment for masking scoliosis (Figure 2-20). This is an elastic undergarment with attached inside pockets which help to conceal, hide and mask the visible deformity. Thus, the garment improves the self confidence and self-esteem of scoliosis patients.

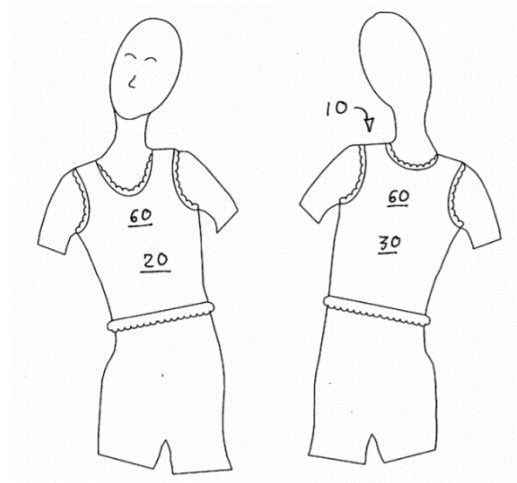


Figure 2-20 Undergarment for masking scoliosis (Anderson, 2015)

Medi GmbH & Co. KG (2015), a manufacturer of medical aids, offers a back brace called Spinomed® active Damen (Figure 2-21) for treating kyphosis from osteoporosis. The main treatment principle is that the back muscles are strengthened through a biofeedback mechanism. The custom-made pre-moulded splint provides support and elevates the trunk of the body. Spinomed® active Damen activates the trunk muscles and reduces the likelihood of a humpback. After a long period of training, the muscles will increase in strength which then

increase body mobility and reduce spinal pain (Meccariello et al., 2016).



Figure 2-21 Spinomed® active Damen (Medi GmbH & Co. KG, 2015)

King et al. (2006) conducted a study that focused on women's recovery from sternotomy (WREST) by designing an undergarment for postoperative use as part of the early care of such patients (Figure 2-22). The supportive undergarment is a vest-type bra top with a front zipper opening that provides compressive support to reduce breast pain and discomfort after a sternotomy procedure.



Figure 2-22 Postoperative undergarment for sternotomy patients (King et al., 2006)

Naismith and Street (2005) designed the Cardibra which is a bra worn post-cardiac surgery. Similar to the WREST undergarment, the Cardibra is a non-wire vest-type bra with a front zipper opening that can be opened and laid flatly during the sternum operation. This bra is adjustable with simple Velcro shoulder straps. Besides, the Cardibra can promote sternal wound healing and reduce chest wall pain after cardiac surgery.

### **2.4.3 Knowledge gap in functional intimate apparel for scoliosis treatment**

Functional intimate apparel is now available to support different body parts, exert compressive pressure to facilitate healing after surgical procedures, produce pulling forces on the shoulders for posture control and re-shape the torso with the use of elastic materials, straps and supporting bones. There is great potential of using these designs in the medical field for therapy. However, few studies have been done on how functional intimate apparel can be used to control the progression of scoliosis and correct spinal deformity. In view of the paucity of work in this area, this study aims to investigate the use of functional intimate apparel for treating and/or preventing scoliosis. The following knowledge gap will be addressed accordingly.

#### **Knowledge Gap 3:**

Functional intimate apparel provides support to the body, exerts compressive pressure to facilitate healing after surgical procedures, produces pulling forces on the shoulders for posture control and re-shapes the torso with the use of elastic materials, straps and supporting bones. However, specific designs for controlling spinal deformity have been largely absent.

To investigate the use of functional intimate apparel for treating and/or preventing scoliosis, one of the most cost effective and efficient ways is to carry out numerical modelling through finite element analyses.

## **2.5 Finite element analysis**

Finite element analysis (FEA) is a common numerical method used to solve problems in engineering and mathematical physics. Here, the method will be used to design the most effective textile brace.

### **2.5.1 Finite element analysis for AIS braces**

FEA has been widely used in the medical field especially to simulate the effectiveness of scoliosis braces and optimize brace designs. The main advantage of FEA is that it overcomes the experimental limitation of repeated exposure to radioactive waves through radiography when images are taken to examine the effect of different brace designs on the same patient. It has been a common and useful tool to simulate in-brace correction (Clin, Aubin, Parent, et al., 2010).

Delphine Périé et al. (2004) developed a finite element model to analyse patient-specific bracing biomechanics for scoliosis. The 3D geometry of spine and ribcage was modelled by the Multiview radiographic reconstruction technique. The brace-patient interface was constructed by two orthogonal sets of bi-cubic spline curve by the use of detection on the radiographs and 3D reconstruction of electric wires connecting the pressure sensor. The pressure measured at the brace-torso interface on patient were calculate and applied to the personalised FE model (Figure 2-23). They validated their FE model by comparing the deformed FE model and in-brace radiograph by using several computed geometric parameters. The Cobb's angle, orientation of the plane of the maximum deformation, and the Pearson's product moment correlation coefficients were analysed.

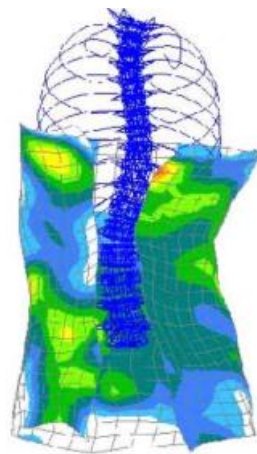


Figure 2-23 The 3D geometric modelling of brace with pressure mapping (Delphine Périé et al., 2004)

Gignac et al. (2000) utilised the finite element model developed by Delphine Périé et al. (2004) and investigated the optimum load that provides the best corrective force in both the frontal and sagittal planes (Figure 2-24). In their study, the angles of maximum deformity in the frontal, sagittal, and transverse planes were measured to evaluate the corrective effects. Their results suggested that the optimal forces are the thoracic corrective forces mostly found exerted on the anterior convex side of the fifth rib with an amplitude of 63 N while the lumbar corrective forces act postero-laterally on the convex side of the ninth rib with an average amplitude of 34 N.



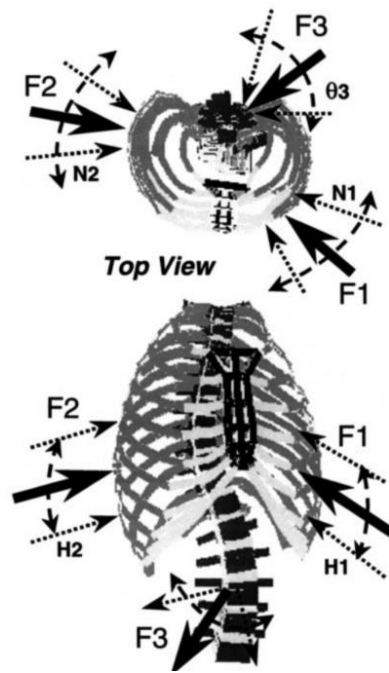


Figure 2-24 Design variables for optimization of corrective forces (Gignac et al., 2000)

D. Périé et al. (2004) developed a finite element model of the trunk, and a Boston brace and its interface with the torso (Figure 2-25) to demonstrate the load transfer from the brace to the spine rather than a direct application of force to the spinal model. In their study, the means of vertebrae positioning and the angle of maximum deformity in both the frontal and sagittal planes were adopted to evaluate the results. More importantly, they validated their model by comparing the estimated and actual geometries of the brace and the estimated contact reaction forces at the brace-torso interface and equivalent forces which were calculated from pressure measurements made on the patient while the brace was worn.

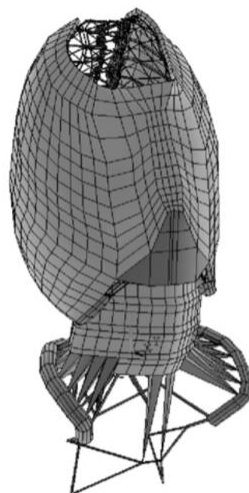


Figure 2-25 Finite element model of trunk of patient (D. Périé et al., 2004)

Clin, Aubin, Parent, et al. (2010) investigated the immediate correction by using 15 design factors of a rigid brace. They used a patient-specific finite element model (Figure 2-26) to generate a total of 12,288 different virtual braces. Their results found that the position of the brace opening, strap tension, trochanter extension side, lordosis design and shape of the rigid shell are the 5 most influential design factors. In this study, they compared the estimated spinal shape, correction of several clinical indices such as the Cobb's angle, kyphosis level, lordosis curvature, rib hump severity and axial rotation of the spine with the interface pressure with actual in-brace experimental data to validate the FE model.

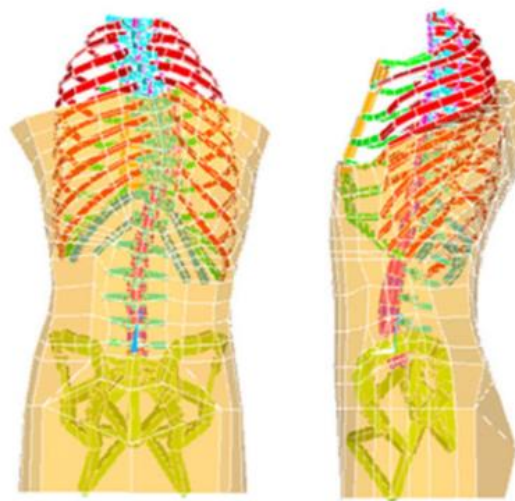


Figure 2-26 Finite element model of trunk (with omission of intercostal ligaments and abdominal beams for clarity) (Clin, Aubin, Parent, et al., 2010)

Pea et al. (2018) developed a modelling method by using a single frontal radiograph and surface topography which enabled them to investigate the effectiveness of different braces. They used 3D body scanned images to estimate the sagittal plane of the spine. In their study, the Cobb's angle, thoracic kyphosis and lumbar lordosis were used for evaluation.

### **2.5.2 Finite element analysis for pressure garments**

Apart from using FEA to model scoliotic braces, researchers (Chassagne et al., 2016; Liu et al., 2011; Rohan et al., 2015; Yinglei et al., 2011) also used FEA to investigate the contact pressure of sportswear .

Liu et al. (2011) developed a bust model (Figure 2-27) which includes the skin, soft tissues and bones, and simulated the clothing pressure exerted onto the bust. They used 3D scanned images and a photo of the body cavity of a female to develop the bust model. Then, the estimated

clothing pressure and measured pressure were compared to verify their model. Their study found that the point that is closest to the nipple has a higher pressure since clothing pressure is positively related to the curvature of the body.



Figure 2-27 Finite element model of bust (Liu et al., 2011)

Rohan et al. (2015) developed a finite element model of a slice of the lower leg (Figure 2-28) from a magnetic resonance image to study the biomechanical response of the deep veins of the lower leg to elastic compression and muscle contraction when the patient is wearing medical compression stocking. Unlike previous models, their lower leg model which includes fat, muscle, skin muscle aponeurosis, veins and arteries is considered as a hyper-elastic material instead of a linear elastic material.

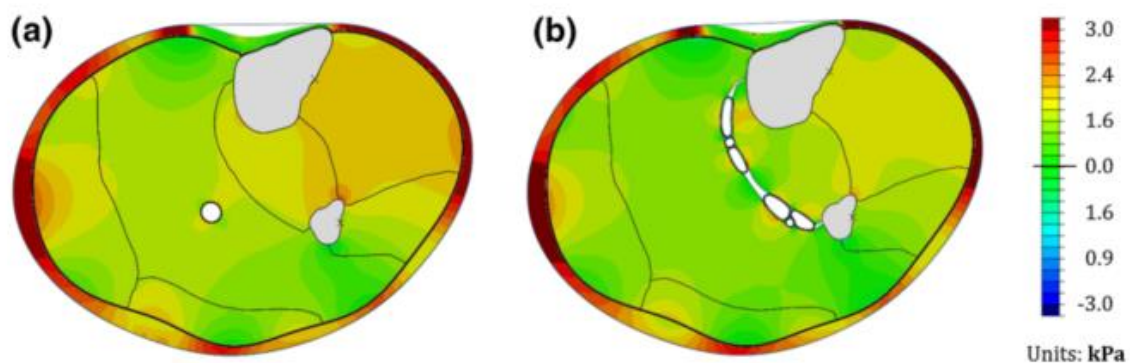


Figure 2-28 Estimated hydrostatic pressure in intramuscular and intercompartment model of leg during elastic compression (Rohan et al., 2015)

### 2.5.3 Knowledge gap in finite element analyses: AIS

Several studies have used an FEA to simulate the effectiveness of bracing to treat AIS. No human subjects need to be involved for design optimisation with the use of FEA. However,

most existing studies have mostly focused on the effectiveness of rigid braces. There are few studies that use FEA to examine the effectiveness of flexible braces for AIS patients.

In addition to rigid bracing intervention, some researchers have recently started to use FEAs to investigate the garment pressure and the internal body pressure. However, such models have focused on the pressure only instead of the displacement of the bones and tissues. As such, the following knowledge gap is acknowledged.

**Knowledge Gap 4:**

While the FEA is an effective tool to investigate the biomechanics, effectiveness and optimisation of bracing treatment, few studies have used FEAs to investigate the effectiveness of flexible braces in reducing spinal curvature as most have only examined rigid braces.

## **2.6 Summary**

This chapter has provided background information through a literature review on scoliosis from its symptoms, diagnosis to treatment methods.

Scoliosis is a medical condition in which the lateral curvature of the spine is greater than or equal to 10 degrees. The Adam's forward bending test is used as a quick means of screening for scoliosis while radiographic examination is the standard method for diagnosing scoliosis. An AP/PA radiograph of the full spine provides fundamental clinical information on the angles of the lateral curvature, levels of axial vertebral rotation, and degree of skeletal maturity. The information presents the conditions of the spinal deformity and the risk of the progression of the curvature. The posture and position from the radiographic images have effects on the measurement of the spinal curvature. Standing AP or PA radiography is common in routine practices while supine AP radiography is usually considered to determine treatment that controls the progression of the condition. Several studies have used the Lenke classification as a comprehensive, reliable, and reproducible system based on the curve type, lumbar spine modifier and sagittal thoracic modifier. Since the treatment method usually depends on the curve type, the clinical trial in this study will use the Lenke classification to determine the suitability of the treatment.

There are mainly two types of non-operative treatment for AIS which are bracing and PSSEs. The three-point pressure system is a universal system for orthotics in treating scoliosis. Most

hard braces apply this system for scoliosis correction. Nevertheless, most hard braces have some drawbacks due to their high compressive forces, bulkiness, and use of material with low air permeability, which all lead to low compliance with the treatment. On the other hand, flexible braces have been used to address spinal curvature and the corrective movement principle is one of the alternative approaches used along with a flexible brace called the Spinecor brace to inhibit the progression of the curvature. However, there are some limitations with the use of flexible braces including difficulty of going to the toilet and high pain scores resultant of the strap tension. There is also a posture correction girdle which is an innovative functional garment used to control spinal deformity with induced direct corrective forces and maintenance of the proper posture. Nevertheless, few studies have evaluated the effectiveness of the posture correction girdle for spinal correction or explored its biomechanics as it is mostly used as a means of posture correction. Therefore, this study will further investigate the performance of the posture correction girdle especially in terms of spinal correction and its biomechanics. More importantly, a flexible textile brace that uses the corrective mechanism of hard braces will be developed to maximize comfort and mobility of the wearer yet provide effective scoliotic control.

PSSEs are a supplementary approach to reducing the curvature of the spine. The main objectives of PSSEs are to improve the spinal and trunk alignment in the frontal plane, to reduce the asymmetric load on the spine, and thus halt the progression of scoliosis. Some of the basic principles of PSSEs are reviewed, including the Lyon approach, the Schroth method, BSPTS approach, SEAS approach, Dobomed method, and FITS approach. Three-dimensional self-correction, training activities that are incorporated in daily life activities and stabilization of corrected posture are the common features of these exercises. These exercises can be performed alone or in combination with bracing. In the PPSEs, the importance of spinal and trunk alignment and balance loading of the spine is discussed.

While functional intimate apparel for medical use has been developing in recent years, few empirical research work has been done on functional intimate apparel for controlling and inhibiting the progression of scoliosis. As such, this study sets out to investigate the capacity of functional intimate apparel for scoliosis correction and/ or prevention.

To do so, finite element analysis which is a common numerical method used to solve problems in engineering and mathematical physics will be carried out. Traditionally, in-brace radiography is carried out to evaluate the performance of a brace in controlling spinal curvature.

Due to the concerns of repeated exposure to radiation, researchers are now using FEA to determine the effectiveness of bracing treatment and investigate the biomechanics of braces. More importantly, FEAs can be used to optimise brace designs and determine which design factors influence the effectiveness of the treatment. To build a finite element model, x-rays of the multiple body planes and 3D scanned images of the body are usually required. The Cobb's angle, kyphosis and lordosis angles and vertebrae position are usually used to evaluate the changes in the spinal curvature. However, the majority of existing finite element models focus on rigid braces instead of flexible braces. Indeed, some researchers have used FEA to estimate clothing pressure and internal body pressure with the use of pressure garments. Nevertheless, such finite element models neglect the displacement of the bones and tissues. After reviewing various studies on FEA, a methodology to build and evaluate a finite element model for a brace to treat AIS is determined. Moreover, due to the lack of finite element models for flexible braces to treat AIS in the existing literature, a finite element model of a flexible textile brace for AIS will be developed to investigate its biomechanics and effectiveness.

## **Chapter 3 Methodology**

### **3.1 Introduction**

This chapter described the research methodology used in this study to develop a functional intimate apparel for AIS. The methodology includes: a) a clinical study of the posture correction girdle fabricated in Liu et al. (2014), b) the design and development of a novel functional intimate apparel for AIS, c) a clinical study of the proposed design, and d) the formulation of a numerical simulation model to investigate the biomechanical performance of the novel functional intimate apparel.

### **3.2 Experimental Design**

Figure 3-1 shows the research plan of this study in a flow chart diagram. A clinical study of the posture correction girdle in Liu et al. (2014) was conducted to better understand its mechanisms and limitations as a flexible brace for AIS. The findings would serve as the background study of functional garments for controlling scoliosis. The background study and information provided the means for the design and development of the functional intimate apparel for AIS and thus a clinical study of the proposed design was subsequently conducted to evaluate its performance. Moreover, a biomechanical simulation model of the functional intimate apparel was developed to evaluate the proposed design and optimize its design elements.

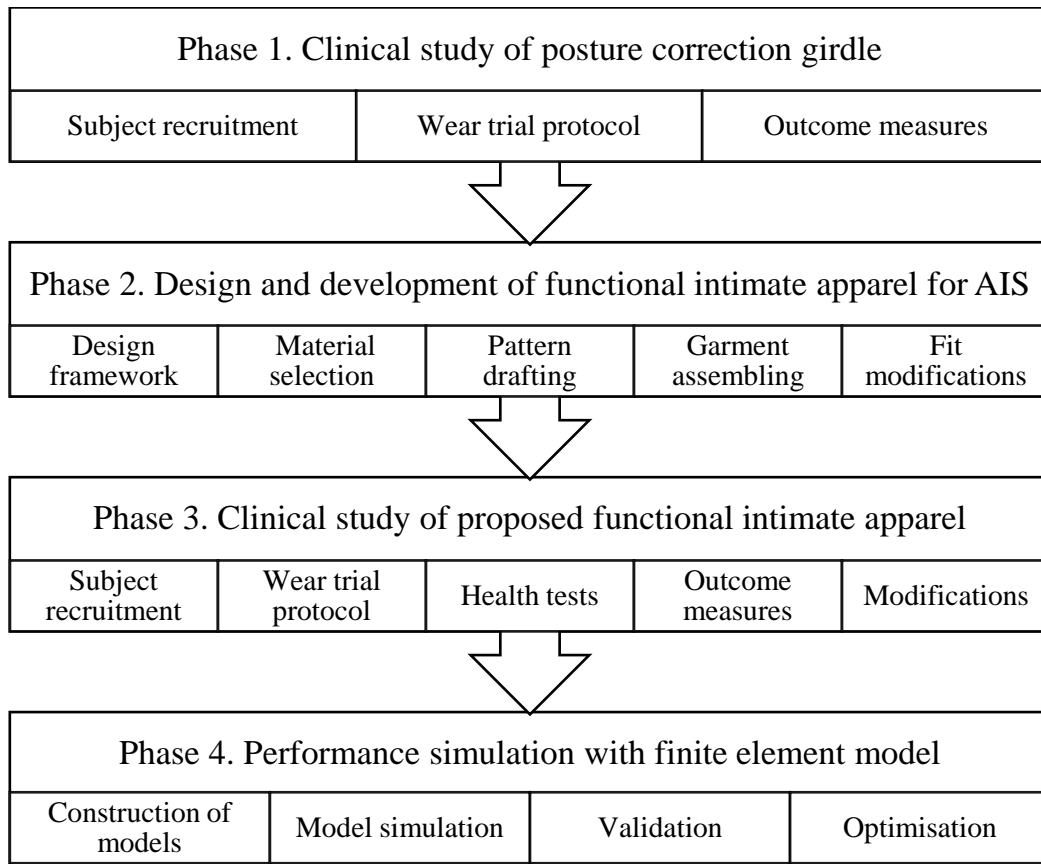


Figure 3-1 Flow chart diagram of research plan

### 3.3 Clinical Study of Posture Correction Girdle

In the previous literature on newly developed soft braces, in particular, the posture correction girdle developed by Liu et al. (2014), it was found that their clinical study (Liu et al., 2015) has some limitations such as subjects with a small spinal curvature, lack of a comprehensive classification of the type of spinal curvature of the subjects, and the absence of an investigation on the reduction of the spinal deformity with the use of the girdle. Thus, a clinical study has been conducted in this study to further evaluate the performance of their posture correction girdle. The purpose is to address the knowledge gap, and the clinical study is important as it provides a systematic evaluation in terms of the amount of control of the spinal curvature and asymmetric areas of the body, as well as the pressure distribution of the girdle. Finally, detailed information on this girdle will be provided in this chapter.

The clinical study is a quasi-experimental pretest-posttest process. The study design is based on that in Liu et al. (2015). The goal of this clinical study is to further assess the performance of the posture correction girdle in Liu et al. (2014). The recruited participants received six to nine-months of intervention with the posture correction girdle.



### 3.3.1 Subject recruitment

A total of 16 subjects who have mild AIS without cessation of growth were recruited in Hong Kong during October 2015 to December 2016. The criteria for participation were: 1) 12-15 years old; 2) a Cobb's angle between 10 and 25 degrees; 3) a Risser grade of the iliac crest of 0-4; 4) has the ability to adhere to the study protocols both physically and psychologically; and 5) literate in either English or Chinese for communication purposes. Those who have a history of previous surgical or orthotic treatment for AIS, contraindication towards radiography exposure or pulmonary tests, recent trauma, mental disorder, skin allergies, or failure to comply with the protocols were excluded from the study. All of the participants and their parents/guardian signed a consent form prior to engaging in the clinical study.

#### 3.3.1.1 Scoliosis screening process in schools

A screening process for scoliosis was carried out in Hong Kong schools to recruit subjects for the clinical trial. The screening involved the Adam's forward bending test to identify whether the students showed characteristics of scoliosis. During the Adam's forward bending test, the students were required to stand with their feet together and palms clasped together. Then, they were asked to slowly bend forward at the waist until their back was parallel to the horizontal plane with arms hanging down their sides and knees extended. A professional prosthetist-orthotist (P&O) then examined the students from behind along the horizontal plane of the column vertebrae and measured the angle of trunk rotation (ATR) in the thoracic and lumbar regions by using a scoliometer (OSI, Orthopaedic Systems Inc., Hayward, California, USA) (Figure 3-2). Moreover, the P&O observed and rated the level of their head tilt, spinal asymmetry, and shoulder and hip balance by referring to The Standards for Scoliosis Screening in California Public Schools by California Department of Education (2007). An ATR of 3° was chosen as the cut-off point for follow up. Figure 3-3 shows the setup of the screening process at a school.



Figure 3-2 OSI scoliometer used for ATR measurement



Figure 3-3 Screening for scoliosis in school

### 3.3.2 Clinical study protocols

The scoliosis screening participants with an  $ATR \geq 3^\circ$  and some potential subjects referred by orthopedic surgeons underwent radiographic examination at a medical diagnostic center to examine the amount of spinal deformity and the bone maturity. If the participants met the inclusion criteria, they would be invited to partake in the wear trial study. During the first visit, the subjects underwent a girdle fitting session at the Hong Kong Polytechnic University. During the fitting, the P&O inserted pads in the girdle based on their spinal deformity. The position of the pad(s) was recorded. The posture correction girdle is available in standard sizes of small, medium, and large based on the torso length and the subjects were provided their correct size accordingly. After the fitting and examination by the P&O, the interface pressure of the posture correction girdle along the middle axillary line was measured. Then, the subjects underwent 3D body scanning to assess the asymmetry of their body contours.

After the fitting session, the subjects were required to wear the girdle at least 8 hours every day for 6 months (Liu et al., 2015). After 6 months, the subjects were required to undergo a radiographic examination both in-brace and without wearing the brace. Figure 3-4 shows the prototype of the posture correction girdle. A flow chart for the wear protocol is shown in Figure 3-5.



Figure 3-4 Prototype of posture correction girdle

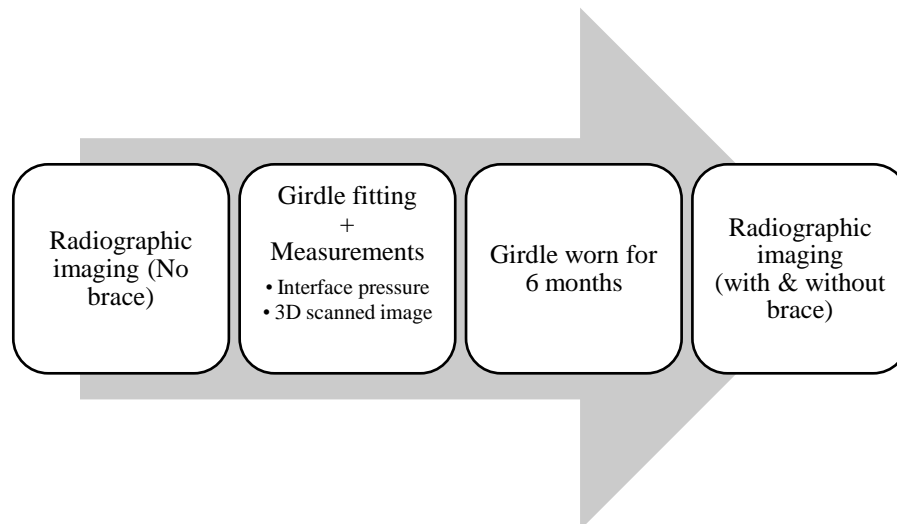


Figure 3-5 Posture correction girdle clinical trial protocols

### 3.3.3 Radiographic examination

Radiography was the primary means of determining the effectiveness of the girdle on controlling spinal deformity. The subjects were required to take a radiographic image without the brace at the onset of the study and two additional radiographic images with the brace donned and doffed on the sixth month of the study.

The participants were required to undergo a standing full spine anterior-posterior radiography at the Irad Medical Diagnostic Centre in Mong Kok, Hong Kong or The Duchess of Kent Children's Hospital at Sandy Bay, Hong Kong. The location to take the radiographic images depended on the follow up advice by the Student Health Service. During the radiography

process, the subjects were required to stand with locked knees, place their feet at a shoulder's width apart, look straight ahead, bend their elbows and place their knuckles over their clavicles (O'Brien et al., 2008).

The Cobb's angle was also measured to assess the lateral deformity. The Cobb's angle is the largest angle between the obliquity of the endplate of the superior end vertebra and that of the endplate of the inferior end vertebra (Malfair et al., 2010). In addition, the skeleton maturity of the subjects was measured through their Risser grade, which denotes the degree of ossification of the iliac crest apophysis.

To reduce conscious and unconscious bias, blind experiments are usually carried out in clinical studies which use independent outcome measurements (Lusini et al., 2014; van Loon Piet et al., 2012; Weinstein et al., 2013a). Thus, all of the radiographic measurements were conducted by two independent orthopedic surgeons who were not involved in this project. Moreover, these two independent doctors were blind to all of the information of the participants and their intervention.

The rate of reduction/increase of spinal curvature was calculated by using Equation 3.1. The rate of reduction/increase of spinal curvature in-brace on the sixth month was calculated by using Equation 3.2. The negative value indicates the reduction of spinal curvature while the positive value indicates the increase of spinal curvature.

Rate of reduction/increase of the spinal curvature =

$$\frac{Cobb's\ angle_{post-intervention} - Cobb's\ angle_{pre-intervention}}{Cobb's\ angle_{pre-intervention}} \times 100\% \quad (3.1)$$

$$In - brace\ reduction/increase\ rate = \frac{Cobb's\ angle_{In-brace} - Cobb's\ angle_{Out-brace}}{Cobb's\ angle_{Out-brace}} \times 100\% \quad (3.2)$$

### 3.3.4 3D body scanning

Three-dimensional imaging of the body was used as the secondary outcome measure to assess the asymmetry of the body contours. The subjects were required to undergo two 3D body scans with and without the brace during their first visit.

The external geometry of the trunk is useful for monitoring the changes during treatment intervention (Duong et al., 2009). Three-dimensional scanning is an advanced technology to obtain comprehensive data of the external geometry and hence can help to explore more in-depth the effectiveness of the posture correction girdle in controlling the asymmetry of the body contours. The 3D body scanning was conducted by using the Vitus Smart XXL 3D body

scanner (Human Solutions GmbH, Germany), which was available at the Hong Kong Polytechnic University. The scanner captured the body measurements in 3D space with an error of 1 mm at a measurement range of 2100 mm in height, 1000 mm in width, and 1200 mm in depth and the uses optical triangulation with a laser light, which is safe for the eyes (Human Solutions GmbH, 2015).

With reference to the guidelines and recommendations provided by the Society on Scoliosis Orthopaedic and Rehabilitation Treatment (SOSORT), the spinous process, posterior iliac spines, neck, shoulders, scapulae, waist and coccyx (tailbone) were used as anatomic surface landmarks in the surface topographic assessment (Kotwicki et al., 2009). Duong et al. (2009) validated the use of 10 landmarks for the trunk geometry to correlate with the external body shape of patients and provide feedback on spinal correction. Hence, 12 landmarks including the spinous process of C7, acromial angle of the shoulders, superior angle of the scapulae, inferior angle of the scapulae, spinous process of L4, posterior superior iliac spine, and iliac crest, were used as the anatomic surface landmarks (Figure 3-6). These twelve landmarks were placed when the patient did not have the brace donned. when the patient was wearing the brace, only the spinous process of C7 and acromial angle of the shoulders were used.

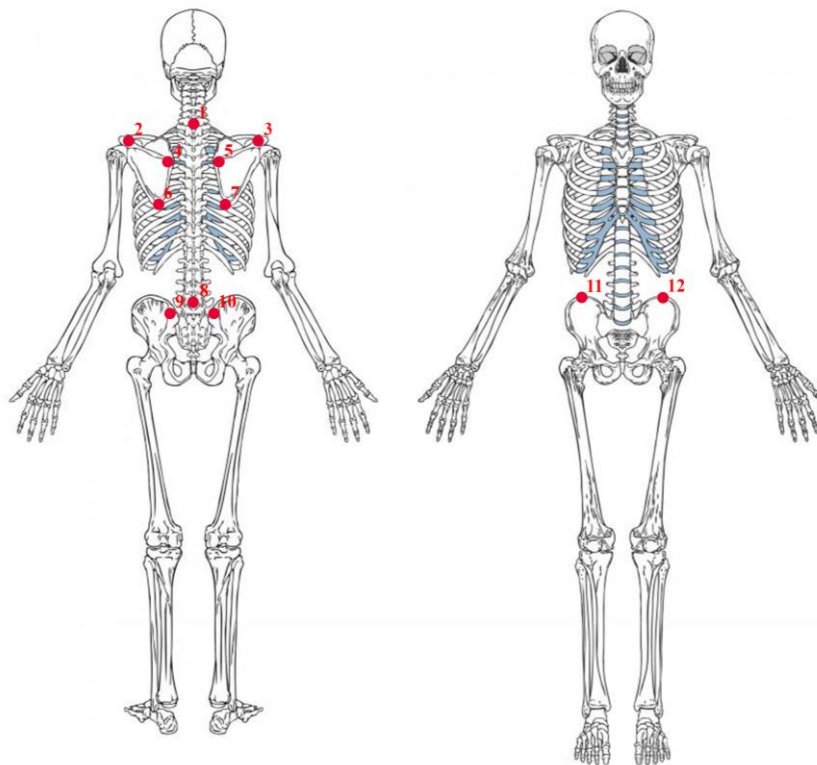


Figure 3-6 Anatomic landmarks in this study

1: spinous process of C7. 2,3: acromia angle of shoulders. 4, 5: superior angle of scapulae.

6,7: inferior angle of scapulae. 8: spinous process of L4. 9,10: posterior superior iliac spine.

11,12: iliac crest.

To avoid the problems of scanning interference and error, the participants were required to wear a white-color tightly fitting undergarment, tie up their hair and place their feet on a footprint image on the floor. During scanning, the participants were asked to perform their habitual standing posture with slightly open arms.

The 3D images captured from the 3D scanning process were processed as point clouds. The information on the external geometry was extracted from these 3D images. The data were then processed by using Solidwork 2016 software. Duong et al. (2009) measured the angles that define the external geometry of the trunk which provide information on the shoulder orientation, trunk balance, spine length, and thoracic and lumbar humps. In this study, the effectiveness of the girdle on maintaining a balanced shoulder orientation was examined by measuring the angle of the acromion. Figure 3-7 and Figure 3-8 show that the shoulder obliquity and shoulder rotation were measured by the angle of the acromion in the frontal and transverse planes, respectively.

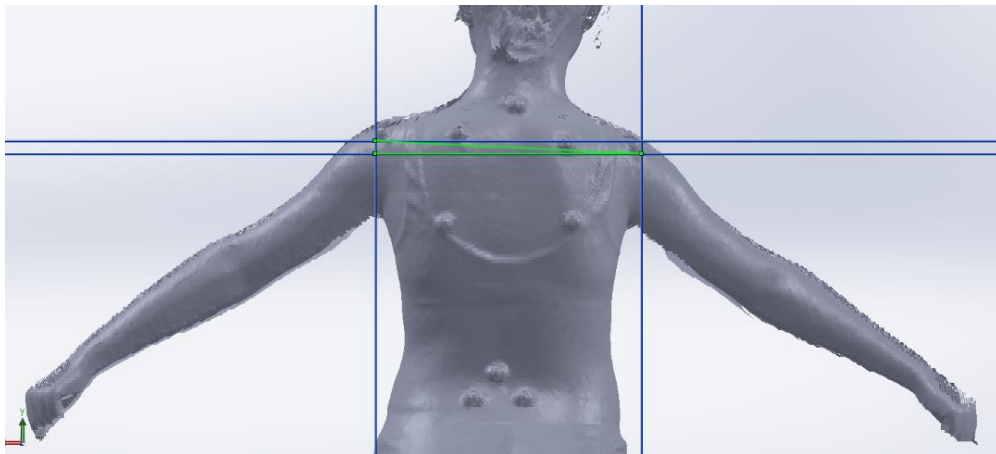


Figure 3-7 Shoulder obliquity measured by angle of acromion in frontal plane



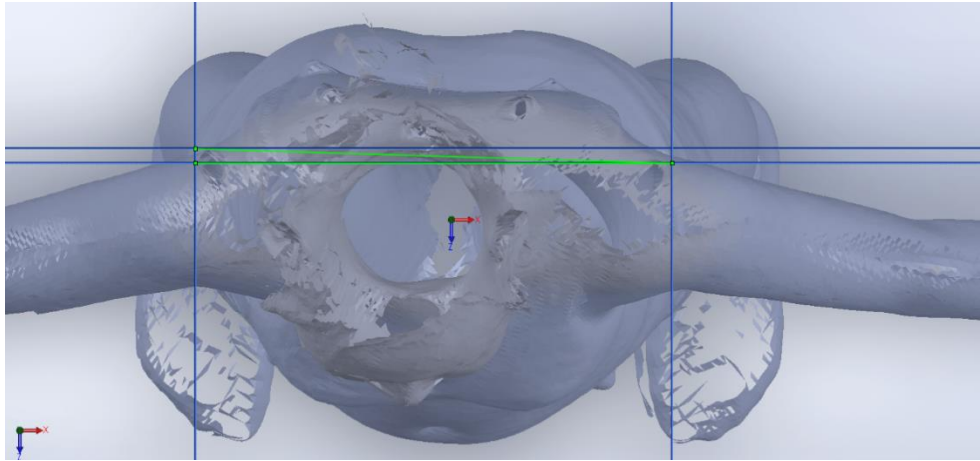


Figure 3-8 Shoulder rotation measured by angle of acromion in transverse plane

### 3.3.5 Interface pressure of posture correction girdle

The interface pressure was used as a secondary outcome measure to investigate the biomechanics of the girdle. The interface pressure was measured during the first visit.

The Pliance®-xf-16 (-32) system with 3x3 Socket Sensor XL was used to measure the interface pressure of the posture correction girdle. The sensing area was 30 x 30 mm<sup>2</sup> and the typical pressure range was between 3 and 200 kPa. Points were measured along the middle axillary line in at the under-bust, waist and pelvis levels (Figure 3-9). During measurement, the participants were required to perform their habitual standing posture and the interface pressure was recorded at least once every minute.

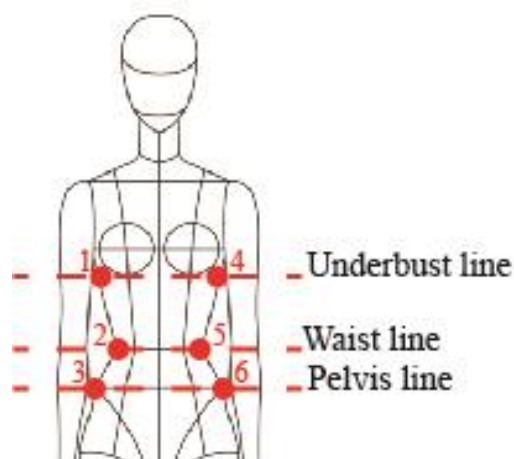


Figure 3-9 Measured points of interface pressure of posture correction girdle

1: right side of underbust. 2: right side of waist. 3: right side of pelvis. 4: left side of underbust. 5: left side of waist. 6: left side of pelvis.

### **3.3.6 Statistical analysis**

Wilcoxon signed rank tests were carried out to investigate the differences in the Cobb's angle, shoulder obliquity and shoulder rotation when the girdle was donned or doffed, and/or pre-intervention versus post-intervention. Moreover, the interface pressure at the side of the girdle with a pad and its counter side was compared by using a Wilcoxon signed ranked test. The Statistical Package for Social Science Version 25 (IBM, New York, United States) was used, and the confidence interval was set at 95% ( $p < 0.05$ ).

### **3.4 Design and development of functional intimate apparel**

The functional intimate apparel would be designed according to the conceptual framework for apparel design (Figure 3-10) in Lamb and Kallal (1992), which is called the functional, expressive and aesthetic model. The design process consists of 6 stages including identifying the problem, generating the preliminary ideas, refining the design, developing the prototype, evaluating the results, and implementing the concept. This design model combines functional, expressive, and aesthetic considerations with a creative problem-solving process for the development of apparel design and thus this model is appropriate for use in this study.

The design process started with identifying the problem. The identified problem would then be used to define the design criteria, which takes the functional, expressive, and aesthetic considerations into account.

After the literature review and the clinical study of the posture correction girdle, problems with the brace in Liu et al. (2014) were identified. The effectiveness of this posture correction girdle on spinal control was discussed and the mobility restriction and discomfort of rigid braces as functional problems were also elaborated.

As for the explicit problems, bracing patients usually suffer from pain due to the rigid cast and high compression forces from the brace. They may also experience difficulties in physically participating in social activities, have fear of injury, or feel self-conscious about their appearance (Law et al., 2016). More importantly, bracing treatment may lead to psychological damage of the patients and approximately 25% of the bracing patients in a study by Danielsson et al. (2001) stated that their teenager years were "ruined".

Regarding the aesthetic problems, patients usually have a negative first impression of their rigid brace and the nude colour of the brace also arouses negative emotions in them. The colour and aesthetics of braces might cause psychological discomfort and therefore a negative



perception towards the brace (Law et al., 2016).

This is followed by generating the preliminary ideas, which requires the most creativity as design solutions are produced which would solve the problems identified in the first stage. To respond to these functional, expressive and aesthetic problems, some design criteria were listed. The preliminary idea and the initial prototype which is a long bra top with a derotation strap were then developed. The initial prototype was then evaluated. Due to ethical concerns, a radiographic examination was not conducted in the initial stage. Three-dimensional body scanning, interface pressure measurement, and a fitting session were instead conducted. Refinement of the design was also carried out to meet the design criteria.

The third stage is refining the design which enhances the preliminary design elements. During this stage, some preliminary ideas were adopted, some were modified, while others were eliminated based on the functional, expressive and aesthetics criteria. In this stage, the designs of the bra top, pants, artificial back bone, cushioning pad for the artificial back bone and corrective pad were developed and refined.

The fourth stage is developing the prototype which includes material selection, stitch selection, pattern drafting, and garment assembling. The method for fabric section, pattern making and garment assembling is discussed in the following section.

The fifth stage is evaluating the prototype, on whether the product meets the functional, expressive and aesthetic needs that were determined during the identification of the problem by using subjective and objective measurements. If the prototype does not meet the requirements, then the designer needs to retract his/her steps and return back to the previous stage and modify the design. After modifications have been made and the final design is obtained, the last stage, or implementation of the concept, will take place, which includes manufacturing and distribution.

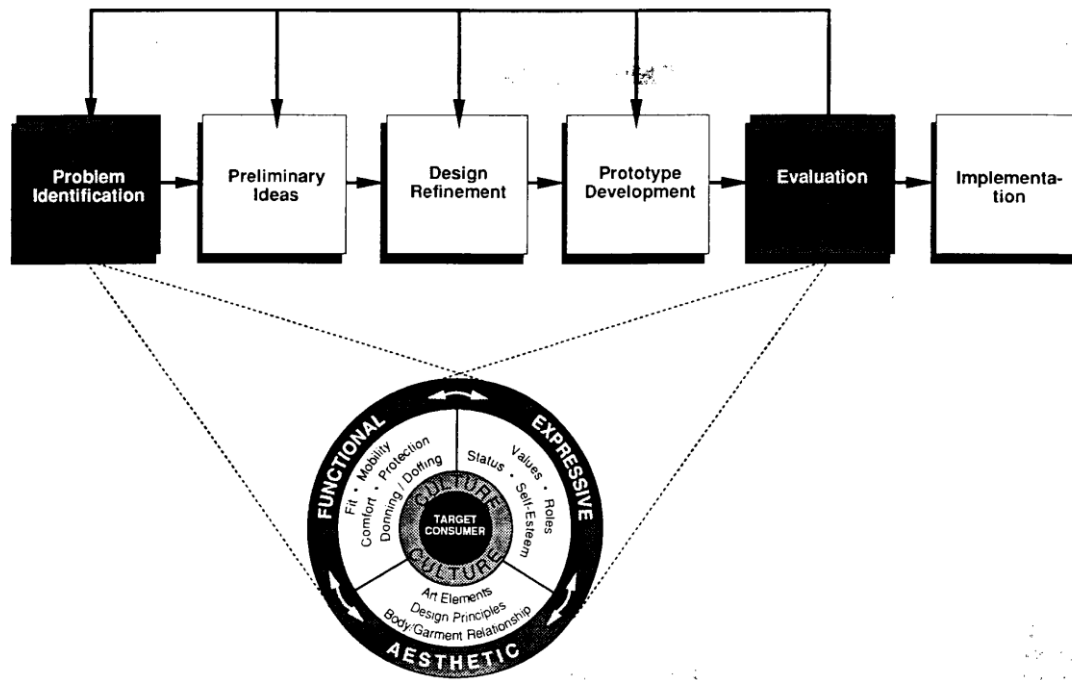


Figure 3-10 Apparel design framework (Lamb & Kallal, 1992)

### 3.4.1 Material selection

Material selection is essential as the physical properties of the textile materials used impact the performance of the product. This section discussed the selection of appropriate textile materials for the proposed functional intimate apparel through various material tests. The proposed design uses three key textile materials, which are the main fabric, elastic bands and elastic straps. Table 3-1 lists the functions and description of these three textile materials in the proposed design.

The main fabric forms the basic framework of the garment shape. The fabric should be elastic with a high modulus which stabilizes the corrective component and provides a good fit. Moreover, the functional intimate apparel has a tight fit and is expected to be worn for 6-9 months, so the fabric should feel comfortable but is also durable.

The elastic bands provide the compressive forces to exert corrective effects onto the torso. Since they are used in the corrective component, they need to be more than 4 inches in width. Also, the elastic bands need to have a high modulus to provide the compressive forces and have durability.

The elastic straps are used for the shoulder straps and bra underband. The main function of these straps is to stabilize the garment on the torso and assist with the placement of the

corrective component. Thus, the straps should have a high modulus and durability.

Table 3-1 Functions and criteria of three main textile materials for proposed design

<b>Component</b>	<b>Function</b>	<b>Application</b>	<b>Examined criteria</b>
<b>Main fabric</b>	Provides frame of garment	Shell fabric for bra cups and pants, and lining fabric for corrective component	Stretch and recovery behavior; Thermal and sensorial comfort; Dimensional changes
<b>Elastic bands</b>	Provide corrective forces	Corrective component	Stretch and recovery behavior; Dimensional changes
<b>Elastic straps</b>	Fix garment onto body	Shoulder straps and bra underband	Stretch and recovery behavior; Thermal and sensorial comfort; Dimensional changes

#### 3.4.1.1 Material testing and testing conditions

The following elaborates on the selection process of the optimum textile material for the proposed functional intimate apparel. Physical tests were conducted in respect of the mechanical performance, comfort and durability of the material. The testing details are provided in Table 3-2.

In terms of the mechanical performance, the stretch and recovery of the elastic material were essential considerations which are highly impactful on the biomechanics, fit and durability of the garment (Xiong & Tao, 2018). During the material selection process, the material had to be high in modulus, low in force decay with time and due to exercise, as well as offer a high recoverability.

Comfort was a secondary functional consideration for the design criteria. Rahman et al. (2012) stated that the comfort properties of textiles comprise three factors, which are thermos-

physiological comfort, sensorial comfort, and body movement comfort. Water vapor and air permeabilities, and thermal resistance were tested for thermos-physiological comfort as these are the key thermal parameters of intimate apparel. The sensorial comfort was objectively measured by using the Kawabata Evaluation System of Fabric (KES-F). In this objective measurement method of sensorial comfort, the characteristic values of the tensile and shear strengths, bending, compression, surface properties, weight and thickness were measured (Kawabata et al., 2002). As for body movement comfort, since the supportive artificial backbone restricts the primary movements of the trunk, the flexibility of other textile materials is only a minor factor in body movement comfort. Thus, the body movement comfort of the textile material was not examined.

Durability was also one of the essential criteria in fabric selection. The criteria for the durability of textile material referred to the standard performance specifications for bras, slips, lingerie, and underwear fabric which were established by American Society for Testing and Materials International (2014), otherwise known as ASTM D7019-14. ASTM D7019-14 provides the testing method and specification requirements of undergarment fabric including the breaking, bursting and tearing strengths, yarn distortion, strength, dimensional changes, colorfastness, fabric appearance, and flammability. In considering that the primary material was a white-colored weft knit, and that this was an intimate apparel, the dimensional changes during laundering were assessed to determine the durability of the garment based on AATCC 135.

All of the physical tests were performed in a conditioned laboratory. The standard atmosphere was a temperature of 20.0°C and a relative humidity of 65% based on EN ISO 139:2005 Textiles — Standard atmospheres for conditioning and testing. All of the samples underwent conditioning for 24 hours prior to testing.

Table 3-2 Physical tests for material selection of proposed functional intimate apparel

Material	Usage	Mechanical performance	Thermal comfort			Durability
		Stretch and recovery (BSI BS EN 14704-1)	Water vapor permeability (ASTM E96)	Air permeability (KES air-permeability tester)	Thermal resistance (KES thermos Labo II tester)	Dimensional Changes of Fabrics after Home Laundering (AATCC 135)

Weft knit	Shell fabric, lining	✓	✓	✓	✓	✓	
Elastic bands	Corrective component	✓					✓
Elastic straps	Shoulder straps, upper bra band, bra underband	✓					✓
		Sensorial comfort					
		Tensile (KES-FB1-A tensile and shear tester)	Shearing (KES-FB1-A tensile and shear tester)	Bending (KES-FB2-A pure bending tester)	Compression (KES-FB3-A compression tester)	Surface (KES-FB4-A surface tester)	Weight and thickness (KES-FB3-A compression tester)
Weft knit	Shell fabric, lining	✓	✓	✓	✓	✓	✓

### 3.4.1.2 Stretch and recovery testing

A stretch and recovery test was conducted on the strip structure of the elastic fabric based on BS EN 14704-1:2005 and EN 14704-3:2006 to determine the elasticity of the fabric. BS EN 14704-1 was used to test the elastic fabrics while EN 14704-3 was used to test the narrow elastic fabric; that is, the shoulder straps. A constant rate of extension was used with an Instron 4411 tensile tester to perform the testing. The test dimension of strip specimen was 100 mm in length and for weft knitted fabrics 75 mm in width, and for elastic strap materials 25 mm (full width) in width. Reference marks were made on the samples to determine the unrecovered elongation. The weft knit sample was extended to a fixed elongation 100% and the strip sample to a fixed load of 61 N at a constant rate of 500 mm/min for 5 cycles and the strip sample was held for 1 minute at the maximum force. The modulus, force decays due to exercise and with time, the immediate unrecovered elongation, and the unrecovered elongation after 30 minutes were measured, calculated and recorded. In each case, 3 samples were measured, and the average value was recorded. The force decay and unrecovered elongation were calculated by using Equations 3.3 and 3.4 respectively.

$$A = \frac{V-W}{V} \times 100 \quad (3.3)$$

where:

$A$ = force decay with time/due to exercise, %

$V$ = the maximum force after the final cycle, N

$W$ = the maximum force after the final cycle after a specific holding period, N

$$C = \frac{Q-P}{P} \times 100 \quad (3.4)$$

where:

$C$ = unrecovered elongation, %

$Q$ = distance between applied reference marks after a specific recovery period, mm

$P$ = initial distance between applied reference marks, mm.

#### 3.4.1.3 Water vapor permeability

The water vapor permeability denotes the amount of moisture or water vapor transmitted from the skin to the environment. ASTM E96 Standard Test Methods for Water Vapor Transmission of Materials was used to evaluate the amount of water vapor permeability. The test area was 0.003117 m<sup>2</sup>. In each case, 2 samples were tested, and the average value was recorded before and after 24 hours. Through periodic weighting of the test dishes, the water vapor transmission was calculated by using Equation 3.5:

$$WVT = \frac{G}{tA} \quad (3.5)$$

where:

$WVT$ = rate of water vapor transmission, g/h·m<sup>2</sup>

$G$ = weight change (from the straight line), g

$t$ = time, h

$A$ = test area (cup mouth area), m<sup>2</sup>.

#### 3.4.1.4 Air permeability

The KES-F8 air-permeability tester was used to measure the breathability and permeability of the materials. The constant ventilation method was used to determine ventilation resistance.

The piston speed applied was 2 cm/sec, the ventilation was 2 cc/cm<sup>2</sup>/sec and the vented area was 2π cm<sup>2</sup>. The sample size was 100 mm x 100 mm. The airflow resistance was measured and recorded as kPa · s/m. In each case, 5 samples were tested, and the average value was recorded.

#### 3.4.1.5 Thermal resistance

The KES Thermo Labo II tester was used to measure the perceived heat or cold to the skin. The heat plate was set to 30°C while the water box was set to 20°C. The sample size was 5 cm x 5 cm. In each case, 5 samples were tested, and the average value was recorded. The amount of heat that passed through the sample from heat transmitted through the heat plate was measured and the thermal conductivity value was calculated by using Equation 3.6.

$$\text{thermal conductivity} = \frac{\text{heat flow rate} \times \text{distance}}{\text{area} \times \text{temperature difference}} \quad (3.6)$$

$$k = \frac{W \times D}{A \times \Delta T}$$

where:

$k$ = thermal conductivity, Wm<sup>-1</sup>K<sup>-1</sup>

$W$ = rate of heat transferred, watt

$D$ = thickness of sample, m

$A$ = area of the heat plate of the BT-box, m<sup>2</sup>

$\Delta T$ = temperature difference between the heat plate and water box, K.

#### 3.4.1.6 Dimensional changes after laundering

The dimensional changes of the samples after laundering were evaluated based on AATCC Test Method 135. The sample size was 50 cm x 50 cm with a benchmark of 25 cm. In each case, 3 samples were tested, and the average value was recorded. The samples underwent a normal wash cycle at 41°C with a rinse cycle that did not exceed 29°C and then tumble dried for 2 hours. The AATCC standard amount of detergent was used (60 g) and the weight of the samples and dummy load was 1.8 kg in total. The length of the benchmark was measured, and the dimensional changes were calculated by using Equation 3.7.

$$\% \text{ dimensional changes} = \frac{(B-A)}{A} \times 100\% \quad (3.7)$$

where:

$A$ = original dimensions of the benchmark

$B$ = dimensional changes of benchmark after laundering.

#### **3.4.1.7 Tensile and shear**

The KES-FB1-A tensile and shear tester was used to perform the tensile and shear tests. The load control method was used to test the tensile strength while the deformation control method was used to test the shear strength. The tensile rigidity, tensile energy and tensile recoverability were obtained during the tensile strength testing and shear rigidity, elasticity for minute shear and elasticity for large shear were obtained during the shear strength testing. The sample size was 20 cm x 20 cm with a maximum thickness of 2 mm. In each case, 3 samples were tested, and the average value was recorded.

#### **3.4.1.8 Bending**

Sensorial comfort through bending was evaluated by using the KES-FB2-A pure bending tester. The bending properties are useful for determining the stiffness and fullness, softness, and anti-drape stiffness. The bending rigidity and bending hysteresis were obtained during the testing. The bending tester was operated by using the controlled maximum curvature system with load detection of the torsional moment of a steel wire and detection of the curvature with a potentiometer. The rate of the bending was 0.5 cm<sup>-1</sup>/sec. The sample size was 20 cm x 20 cm with a maximum thickness of 1 mm. In each case, 3 samples were tested, and the average value was recorded.

#### **3.4.1.9 Compression**

The KES-FB3-A compression tester was used to evaluate the compression of the material and has been used to determine “the softness of disposable diapers and the hardness of mousse” (Kato Tech Co. Ltd.). During the experiment, the linearity, work and recoverability of the compression were obtained. The circular surface area of the compression sensor was 2 cm<sup>2</sup> and the compressional deformation rate was 0.02 mm/sec. The sample size was 10 cm x 10 cm. In each case, 3 samples were tested, and the average value was recorded.

#### **3.4.1.10 Surface properties**

The KES-FB4-A surface tester was used to evaluate the surface friction of the material. The mean frictional coefficient, fluctuation of the mean frictional coefficient, and surface roughness were measured during the testing. The amount of surface friction and surface roughness, and



direction of the movement of the surface tester were identified by using a ring-type detector with a differential transformer, differential transformer, and potentiometer respectively. The dimensions of the friction contactor of the sensor were 10 mm x 10 mm while the roughness contactor was a single wire with a diameter of 0.5 mm. The surface tester velocity used was 1 mm/sec, and the sample size was 20 cm x 20 cm with a maximum thickness of 2 mm. In each case, 3 samples were tested, and the average value was recorded.

#### 3.4.1.11 Weight and thickness

The weight of material was measured by using a scale and the thickness of material was measured by using the KES-FB3-A compression tester. The testing details of KES-FB3-A compression tester are provided in Section 3.4.1.9. In each case, 3 samples were tested, and the average value was recorded.

### 3.4.2 Body measurements

Precise measurements of the body are essential for the development of a well fitting functional intimate apparel. In total, 37 variables as shown in Figure 3-11 were used to identify the body shape which includes the height, width, depth, surface distance and girth (Table 3-3). Three-dimensional scanning technology was applied to obtain the body profile of the participants by using the Vitus Smart XXL 3D body scanner (Human Solutions GmbH, Germany) which was available at the Hong Kong Polytechnic University. The measurements were then processed by using Rapidform XOR3 Version 3.0.0.4 (INUS Technology Inc., USA).

Table 3-3 Measured body areas

Type of measurement	Measurement point	Measured area	Description
Girth	a	Upper bust girth	Circumference of the upper bust
	b	Under bust girth	Circumference of the under bust level
	c	Waist girth	Circumference of the waist
	d	Pelvis girth	Circumference of the pelvis

	e	Hip girth	Circumference of the hips
	f	Upper thigh girth	Circumference of the upper thigh
Vertical	g	Waist to gusset	Vertical distance between waist and gusset
	h	Under bust to waist	Vertical distance between the under bust and waist
	i	Upper bust to pelvis	Vertical distance between the upper bust and pelvis
Surface area	j	Shoulder	Length across one side of shoulder between bust and center back at the upper bust

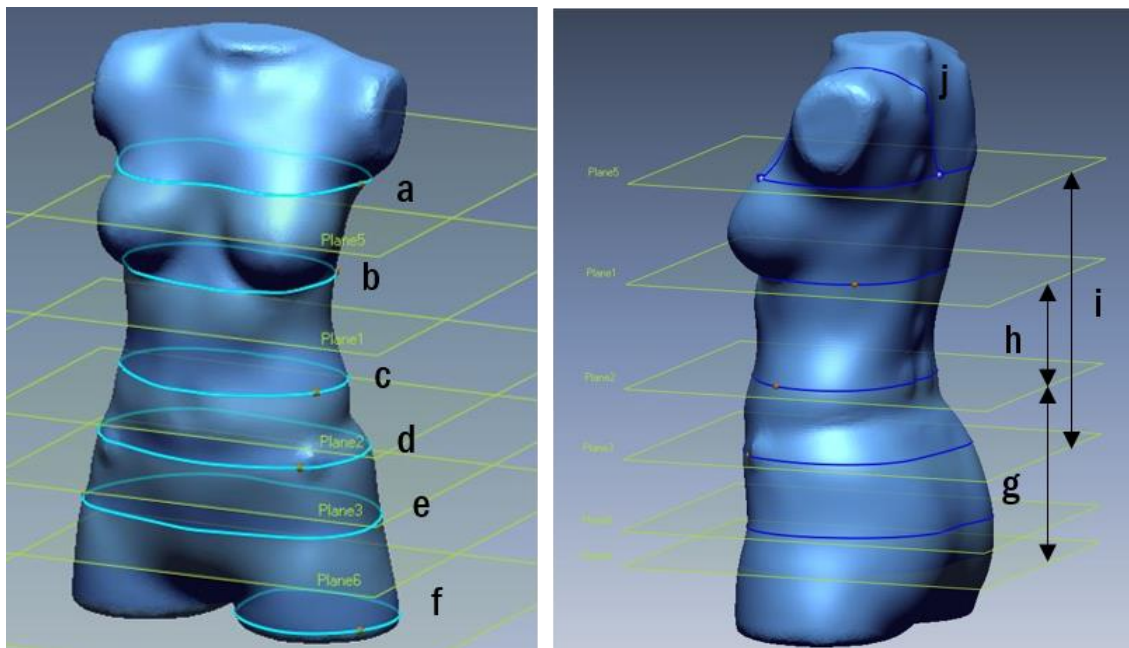


Figure 3-11 Details of measured body areas

#### 3.4.2.1 Subject recruitment

A total of 21 subjects in Hong Kong who have AIS were recruited during March 2018 to January 2019. They underwent 3D body scanning in the standing position in order to obtain

measurements to construct the pattern of the proposed brace design. Since the proposed brace was designed for mild to moderate AIS patients, subjects with a high degree of Cobb's angle were also included in this section. The inclusion criteria of the participants were: 1) between 12-14 years old; 2) female; and 3) to have a Cobb's angle between 10-30 degrees. All of the participants and their parents/guardian signed a consent form to take part in the study.

### 3.4.3 Pattern making

The pattern of the proposed functional intimate apparel was constructed from the basic block pattern in Shin (2010), which consists of three main panels including the bra top, pants, and corrective component. The pattern was drafted with a 25% shrinkage to achieve a better fit with the use of elastic material. The location of the artificial backbone, notches, gridlines, and 6 mm seam allowance were added to the pattern.

### 3.4.4 Garment assembling

As the functional intimate apparel has a tightly fitting bra top, a seam allowance of 6 cm was adopted to minimize the bulkiness and weight of the garment. As for the stitch application, the ISO #304 zigzag (Figure 3-12) was used as the horizontal seam, which provides adequate room for stretching and avoids breaks in the seams. The ISO #301 lockstitch (Figure 3-13) was used as the vertical seam to promote vertical support and secure the trunk. Moreover, a bar-tag stitch was used for the seam edge for reinforcement purposes.

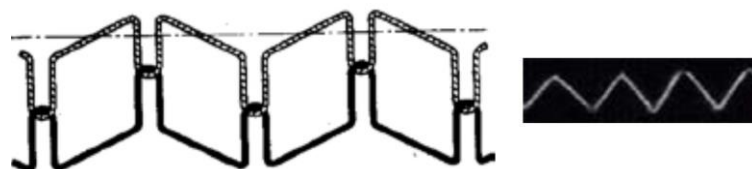


Figure 3-12 ISO #304 zig zag (Dewellton LLC, 2008)

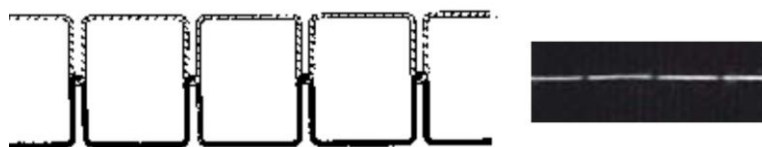


Figure 3-13 ISO #301 lockstitch (Dewellton LLC, 2008)

### 3.4.5 Fitting

The objectives of doing a fitting are to: 1) examine the fit of the proposed functional intimate apparel and 2) place the corrective component or straps to optimize scoliotic control. The fitting

criteria were based on the professional bra fitting criteria developed in McGhee and Steele (2010) which are also listed in Table 3-4. The corrective component was inserted at the convex side of the scoliotic spine in accordance with the three-point pressure system (Gomez et al., 2016),

Table 3-4 Professional bra fitting criteria (McGhee & Steele, 2010)

<b>Bra component</b>	<b>Fit criterion</b>
<b>Bra Band</b>	No flesh bulging over the top of band, no subjective discomfort of feeling overly tight
	No lifting of band when arms are placed above head, posterior band should level with inframammary fold
<b>Bra Cup</b>	No wrinkles in bra cup
	No breast tissue bulging above, below, or at the sides
<b>Underwire</b>	Should not sit on breast tissue laterally (under armpit) or anterior midline. No subjective complaints of discomfort
<b>Shoulder Straps</b>	No digging in. No subjective complaints of discomfort. Carries appropriate weight of breast.
	Should not slide off shoulders without need to adjust the length
<b>Front bra band</b>	Should be in contact with the sternum

### 3.5 Clinical study of proposed functional intimate apparel

In order to evaluate the efficacy of the proposed functional intimate apparel, a preliminary clinical study was carried out. This clinical study includes two phases. The first phase is a 2-hour clinical study to investigate the initial performance of the garment and the second phase is a 3 month-clinical study to investigate the short-term effects of the proposed design.

#### 3.5.1 Subject inclusion and exclusion criteria

Since the objective of this clinical study is to evaluate the effectiveness of proposed functional intimate apparel in moderate AIS patients, the subject criteria of this section were different

from the section 3.3.1. The subject selection criteria were females diagnosed with AIS who have a Cobb's angle between 20 to 30 degrees, between 10 and 13 years old, at a high risk of further progression in their spinal curve, and a Risser grade  $\leq 2$ . The exclusion criteria were patients with contraindications of x-ray exposure, diagnosis of other musculoskeletal or developmental illness that might be responsible for the spinal curvature, contraindications for pulmonary or exercise tests, and psychiatric disorders. All of the participants and their parents/guardian signed a consent form prior to engaging in the study.

### **3.5.2 Two-hour clinical study**

The objective of the 2-hour clinical study is to investigate the initial in-brace performance, initial changes in the asymmetry of the body contours, psychological comfort of the brace on the subjects, and biomechanical performance of the proposed garment.

#### **3.5.2.1 Radiographic examination**

Radiography was the primary means of determining the effectiveness of the girdle on controlling spinal deformity in the first phase of the clinical trials. The participants were required to undergo a standing full spine anterior-posterior radiography in the beginning without the brace donned, and after wearing the brace for 2 hours at the Irad Medical Diagnostic Centre or The Duchess of Kent Children's Hospital at Sandy Bay. The location to take the radiographic images depended on the follow up advice by the Student Health Service. The radiographic imaging method was the same as that described in Section 3.3.3.

The Cobb's angle, Risser grade, lumbar-pelvis relationship (LPR) and the coronal decompensation (CD) were measured on the radiographic images. The definitions of the Cobb's angle and Risser grade were provided in Section 3.3.3. The LPR is the angle of the line drawn on the inferior endplate of the 5th lumbar vertebra to the iliac crest line. The CD is the distance between the plumb line which is parallel to the centre sacral vertical line that passes through the 7th cervical vertebra and bisects the body (Katz & Durrani, 2001). The amount of in-brace reduction was then calculated by using Equation 3.2.

#### **3.5.2.2 Three-dimensional body scanning**

Three-dimensional imaging of the body was used as the secondary outcome measure to assess the asymmetry of the body contours. The subjects were required to undergo two 3D body scans with and without the brace during their first visit. The 3D body scanning was conducted by using the Vitus Smart XXL 3D body scanner (Human Solutions GmbH, Germany), which was

available at the Hong Kong Polytechnic University.

The shoulder obliquity, shoulder rotation and posterior trunk symmetry index (POTSI) were measured on the 3D body images. The methods for measuring the shoulder obliquity and shoulder rotation were the same as those in Section 3.3.44. The POTSI is a simplified means of analyzing the deformation in the dorsal part of the trunk. The POTSI value is positively correlated with the trunk asymmetry in the frontal plane. It was calculated by summing the indices of the differences in height between particular markers on the right and left sides of the body, as well as the points of asymmetry in their distance from the central line (Durmala et al., 2015). Figure 3-14 shows the measurements as well as the construction of the POTSI.

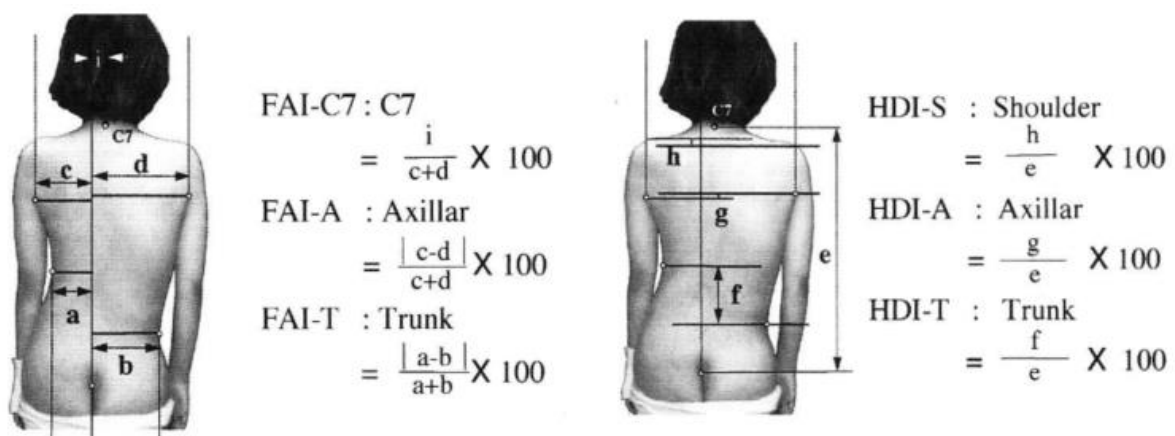


Figure 3-14 Constructing POSTI as a sum of 6 indices (Patias et al., 2010)

### 3.5.2.3 Wear comfort assessment

The subjects completed two questionnaires on the psychological and physiological comfort of the functional intimate apparel which reflect their acceptance of the garment and compliance with the treatment (Chan, 2014). The psychological and physiological instruments were the Chinese version of the Brace Questionnaire (BrQ) (Vasiliadis et al., 2006), and the Chinese version of the Bad Sobernheim Stress Questionnaire (BSSQ) - Brace. The patients completed the BrQ and BSSQ-Brace after donning the proposed functional intimate apparel for 2 hours.

The BSSQ-Brace questionnaire contained 8 questions and each question had 4 levels. The maximum score for each question was 3 and minimum score was 0. The total BSSQ-Brace score ranged between 0 and 24. The total score of all the questions should be negatively correlated with the stress level.

The BrQ contained 24 questions and each question had 5 levels. These questions measured quality of life across 7 domains which are perceived general health, physical and emotional

functioning, self-esteem and aesthetics, vitality, body pain and social functioning. Since the experiment was only 2 hours, some of the questions in the BSSQ-Brace related to school activity and social functioning were omitted. The maximum score in each domain was 5 and minimum score was 1 with a higher score representing higher quality of life. The total score was calculated by multiplying each item by 20 and subsequently dividing the total score by 24. The total score ranged from 20 to 100.

#### **3.5.2.4 Pressure measurement**

The interface pressure of the functional intimate apparel was measured to investigate its biomechanics. The Pliance®-xf-16 system (Novel, Munich, Germany) with 6 single sensors was used to measure the interface pressure. Each sensor could sense an area of 78 mm<sup>2</sup>, and the pressure measured ranged from 0 kPa to 60 kPa. The sensors were placed onto the apex of the corrective pad and the middle of the pelvis belt. During measurement, the participants were required to perform their habitual standing posture and the interface pressure was recorded at least once every minute.

#### **3.5.3 Three-month clinical study**

After the initial 2-hour clinical study, the subject who showed an in-brace reduction of the spinal curvature of 80% was invited to participate in the 3-month clinical study. During the 3-month clinical study, she wore the functional intimate apparel for at least 8 hours every day for three months. Subsequently, she underwent an ultrasound assessment and 3D body scanning, answered questions to determine her health-related quality of life (HRQL) and participated in a short interview to provide feedback.

##### **3.5.3.1 Ultrasound imaging of spine**

The changes in the spinal curvature before and after wearing the functional intimate apparel for 3 months would show the effectiveness of the brace in controlling the spinal deformity of AIS patients. Due to concerns of repeated radiation exposure, a radiation-free ultrasound assessment (Scolioscan™) was conducted to monitor the spinal deformity instead of a radiographic examination. The Scolioscan angle measurement showed a high intra-rater and intra-operator reliability (both ICC>0.87) (Zheng et al., 2016).

The subject underwent ultrasound imaging at pre-intervention and on the 3<sup>rd</sup> month of intervention at the Jockey Club Rehabilitation Engineering Clinic at The Hong Kong Polytechnic University. Scolioscan™ (Figure 3-15) was used to extract the ultrasound images

of the spine in the coronal plane (Zheng et al., 2018). The Cobb's angle was measured on the ultrasound image and the initial rate of reduction in the spinal curvature was calculated by using Equation 3.1.



Figure 3-15 Scolioscan™

### 3.5.3.2 Three-dimensional body scanning

Three-dimensional body scanning was conducted to examine the changes in the asymmetry of the body contours after wearing the functional intimate apparel for 3 months. The scanning was conducted at pre-intervention and on the 3<sup>rd</sup> month of intervention by using the Vitus Smart XXL 3D body scanner (Human Solutions GmbH, Germany). The shoulder obliquity, shoulder rotation and POTSI were measured on the 3D body images. The methods for measuring the shoulder obliquity, shoulder rotation and POTSI were the same as those in Section 3.5.2.2.

### 3.5.3.3 HRQL

Determining the HRQL was done by examining how patients with spinal deformities perceive their quality of life and using the validated Chinese version of the SRS-22 Questionnaire (Cheung et al., 2007). The SRS-22 Questionnaire was a simple, practical, disease-specific assessment for scoliosis patients. The subject completed the SRS-22 questionnaire at pre-intervention and on the 3<sup>rd</sup> month of intervention.



The SRS-22 Questionnaire consisted of 22 questions and each question had 5 levels. The questionnaire measured the quality of life in 5 domains including function (5 questions), pain (5 questions), self-image (5 questions), mental health (5 questions), and satisfaction/dissatisfaction (2 questions). The maximum score in each domain was 5 and minimum score was 1, with higher scores representing a higher quality of life. The scores of each question were summed to calculate the total score, which ranged from 22 to 110. Higher values represent a better outcome.

#### **3.5.3.4 Short interview**

After the wear trial, an interview was conducted with the subject to understand her wear experience and views around the functional intimate apparel. The questions are listed below.

1. Please share your feelings and experience during the trial wear period.
2. Was there anything about the functional intimate apparel that caused you to feel uncomfortable?
3. Did the functional intimate apparel affect your daily life?
4. Between the rigid brace and functional intimate apparel, which one would you prefer to wear?

#### **3.5.4 Statistical analysis**

A Kendall's tau test which is a nonparametric rank correlation test was carried out to investigate the correlation between the rate of reduction of the spinal curvature when the brace is worn, and variables such as the LPR, CD, Cobb's angle, POTSI and interface pressure. A Mann-Whitney U test which is a nonparametric independent test was carried out to compare the interface pressure between the thoracic pads and lumbar pads and to compare the amount of reduction of the spinal curvature with the functional intimate apparel vs. the posture correction girdle. The Statistical Package for Social Science Version 25 (IBM, New York, United States) was used, and the confidence interval was set at 95% ( $p < 0.05$ ).

### **3.6 Biomechanical simulation model for functional intimate apparel**

A finite element model (FEM) was used to conduct numerical simulation to predict the biomechanical performance of the functional intimate apparel and simulate the effect on the scoliotic spine. Three-dimensional virtual models were widely used to predict the effect of scoliosis treatment. By changing the material properties or design of the functional intimate apparel, the effect of the amount of in-brace reduction and the pressure distribution on the

spinal skeleton could be predicted.

### **3.6.1 Formulation of finite element model**

The simulation was carried out by using a commercial finite element analysis software, Abaqus/CAE 6.14-4 (Dassault Systèmes Simulia Corp., USA). The simulation model mainly consisted of three parts: the torso body, skeleton and functional intimate apparel, with 6 steps carried out: 1) creating the geometrical models, 2) defining the element type and material properties, 3) meshing of the models, 4) defining the initial and boundary conditions, 5) numerical processing of the setting displacement and loading of the functional intimate apparel, and 6) post processing and validating the results.

#### **3.6.1.1 Geometrical model of torso body, skeleton, and functional intimate apparel**

##### **3.6.1.1.1 Construction of model of torso body**

A 3D geometrical model of the torso body was constructed to predict the biomechanical behavior of the proposed functional intimate apparel. A teenage girl (13 years old, Lenke type 3, T5-T11: 25°, and T11-L3: 22°) with AIS participated in the development of the FEM. To extract the geometry of her torso body, she underwent 3D body scanning with the Vitus Smart XXL 3D body scanner.

##### **3.6.1.1.2 Construction of skeletal model**

To obtain the geometry of the scoliotic spine, the subject underwent frontal and lateral standing radiographies at The Duchess of Kent Children's Hospital at Sandy Bay. Based on the radiographic images, the skeletal model including the vertebrae, ribcage, and intervertebral disc was built by using SolidWorks 2012 x64 Edition (Dassault Systèmes SolidWorks Corp., USA).

##### **3.6.1.1.3 Construction of model of functional intimate apparel**

The model of the functional intimate apparel included the shoulder straps, bra top, thoracic panel, lumbar panel, artificial hinges, and pelvis belt. In order to ensure that the functional intimate apparel could be fitted onto the model of the torso, the geometry of the functional intimate apparel was extracted from the model of the torso by using SolidWorks 2012 x64 Edition (Dassault Systèmes SolidWorks Corp., USA). The thickness of the model was 2 mm based on the thickness of the functional intimate apparel.

### 3.6.1.2 Defining material properties

There were five different material properties in the FEM, including the torso body, bones, intervertebral disc, textile material of the functional intimate apparel, and material of the hinges in the functional intimate apparel. All of the materials were assumed to be homogeneous, isotropic and linearly elastic. The material properties of the torso body, bones, intervertebral disc, and hinge material had been defined in previous studies (Cahill et al., 2012; Cheng et al., 2010; D. Périé et al., 2004). The tensile strength of the textile material was examined by using the Instron 4411 tensile tester. The elasticity of the textile material was measured in accordance with BS EN 14704-1:2005. The Young's modulus of the textile material was defined based on the stress-strain curve which was plotted by using Equation 3.8 while its Poisson's ratio was already determined in a previous study (Zhou et al., 2010).

$$E = \frac{\sigma}{\varepsilon} = \frac{s(1+e)}{\ln(1+e)} = \frac{s(1+\frac{l_i-l_f}{l_i})}{\ln(\frac{l_i-l_f}{l_i})} \quad (3.8)$$

where:

$E$ = Young's Modulus, MPa

$\sigma$ = true stress, N/mm<sup>2</sup>

$\varepsilon$ = true strain

$s$ = engineered stress

$e$ = engineered strain

$l_i$ = initial length, mm

$l_f$ = elongated length, mm.

### 3.6.1.3 Defining mesh element type

It is important to define the correct mesh element since there is a trade-off among the mesh density, required time for analysis, and accuracy of the results (Shivanna et al., 2010). A fine mesh could provide more accurate results; however, more computational resources are required along with a long processing time. On the other hand, a coarse mesh or a simple model might lead to less accurate results but it reduces computational time and resources. Thus, reaching a compromise between the desired quality and computational time with an appropriate element size is important.

In general, triangular and quadrilateral elements are usually used for 2D models while tetrahedron and hexahedron elements are commonly used for 3D models (Srirekha & Bashetty, 2010).

### 3.6.1.4 Defining boundary conditions

The boundary conditions are essential in simulation work and related to the movement of the elements. In a mechanical model, there are several boundary conditions which are displacement, velocity, and acceleration. In this study, displacement boundary conditions were used to simulate the wear process. During the wear process, surface-to-surface contact was applied to simulate the inter-surface interaction between the functional intimate apparel and torso.

### 3.6.1.5 Applying loading in simulation model

Apart from the boundary conditions, loading is also important to simulate the pressure from the padding in the functional intimate apparel. To do so, measurements of the pressure exerted by the pads were conducted. The method was the same as that in Section 3.5.2.4.

### 3.6.1.6 Validation

Validation work was conducted by comparing the results between the FEM and the clinical result with the human subject. The same subject who underwent body scanning, radiographic examination and pressure measurement also participated in the in-brace radiographic imaging. Her spinal conditions and demographics were provided in Section 3.6.1.1.1. The simulated geometry of the spine was compared with that with the brace donned. The spinal curvature was analyzed by examining the vertebrae position and angles between the curvature (inflexion points) equivalent to the Cobb's angle (D. Périé et al., 2004).

The correlation coefficient of the vertebral body from the measured in-brace radiographic images versus the FE estimations was calculated by using Equation 3.9 (Chou et al., 2012):

$$\text{Correlation coefficient} = \frac{\sum_{i=1}^{17} [(T_i - \bar{T}) \times (E_i - \bar{E})]}{\sqrt{\sum_{i=1}^{17} (T_i - \bar{T})^2} \times \sqrt{\sum_{i=1}^{17} (E_i - \bar{E})^2}} \quad (3.9)$$

where:

$T$  = vertebral displacement measured from the radiographic image

$E$  = vertebral displacement estimated from the FEM

$\bar{T}$  = average vertebral displacement measured from the radiographic image

$\bar{E}$ = average vertebral displacement estimated from the FEM

$i$ = vertebral body in the scoliotic spine.

### **3.6.2 Modification of hinges**

Since the original 3D printed hinges broke easily, there was the need to improve the durability of the hinges by using a higher strength material. Different materials such as cast acrylic, polyoxy-methylene, carbon fiber reinforced polymer, and 6061 aluminum alloy were considered. To select the most durable hinge material, tensile strength and torque to failure tests were conducted.

#### **3.6.2.1 Tensile strength**

An electromechanical tensile testing machine (United Testing Systems Inc., USA) was used to evaluate the tensile strength of the hinges. During the experiment, the load-displacement and tensile strength were obtained. The sample was 80 mm in length and extended to a fixated elongation of 100% or until the hinge broke at a constant rate of 5 mm/min. Due to the high material cost, only one sample was tested for each material.

#### **3.6.2.2 Torque to failure**

The Bionix Servohydraulic test system (MTS System Corp., USA) was used to conduct the torque to failure testing. During the experiment, the torque/torsional angle and torque to failure were recorded. The sample was 80 mm in length and was twisted to an angle of 60 degrees or until the hinge broke at a constant rate of 4 degrees/sec. Due to the high material cost, only one sample was tested for each material.

#### **3.6.2.3 Effect of hinge material on vertebral movement**

Since a high strength hinge material might improve the durability of the hinge, it is important to investigate whether the performance in spinal correction would be affected by varying the hinge material. Thus, four FEMs with hinges of different material properties were constructed. The results of the stress distribution of the functional intimate apparel and skeleton and the spinal curvature were compared among these four models.

### **3.6.3 Optimization of corrective padding**

To investigate the optimum load of the padding and further study the relationship between the corrective loading and vertebral movement, fifteen FEMs with different levels of thoracic and

lumbar loading were constructed. Three changes were examined with the loading, which are the changes with both thoracic and lumbar loading, and changes with only thoracic loading and only lumbar loading. The spinal curvature reduction of the models was investigated by comparing the vertebral movement.

### **3.7 Summary**

In this chapter, the research method for designing and developing the functional intimate apparel for AIS has been described in detail. The entire process consists of four components: 1) a clinical study of the posture correction girdle in Liu et al. (2014) as the background study, 2) design and development of the proposed functional intimate apparel, 3) a clinical study of the functional intimate apparel, and 4) formulation of a biomechanical model and design optimization of the functional intimate apparel.

First, to better understand the limitations of an existing flexible brace in Liu et al. (2014), a 6-9 month clinical study was conducted. The subjects underwent a radiographic examination, 3D body scanning and interface pressure measurement to investigate the effectiveness of the brace in Liu et al. (2014) on controlling the progression of spinal curvature and shoulder asymmetry as well as its biomechanics.

In the second phase, a framework for the design process was applied to construct the functional intimate apparel. The functional intimate apparel emphasizes spinal curvature reduction but is comfortable to wear and flexible. The elastic textile materials were sourced from the local market and their mechanical, thermal, sensorial and durability properties were evaluated and compared to choose the most suitable materials for the functional intimate apparel. Also, 3D body scanning was conducted to obtain the body measurements of the target group to construct the pattern of the functional intimate apparel.

A two-part clinical study was conducted to evaluate the efficacy of the functional intimate apparel. The first is a 2-hour study followed by a 3-month study. The former investigated the initial in-brace reduction, initial changes in the asymmetry of the body contours, psychological and physiological comfort and the biomechanics of the functional intimate apparel. The subject who shows more than 80% in-brace reduction of her spinal curvature participated in the 3-month clinical study. She was required to wear the functional intimate apparel at least 8 hours every day. After three months, the initial degree of spinal curvature reduction, changes in the asymmetry of the body contours, and views and comments about the functional intimate

apparel were obtained.

Finally, an FEM was formulated to simulate the performance of proposed functional intimate apparel. The FEM was found to well simulate the loading of the functional intimate apparel on the body. The changes in the spinal curvature after donning the functional intimate apparel were predicted. To validate the results obtained from the numerical model, a subject underwent an in-brace radiographic examination. The Cobb's angle and spinal curvature in the coronal plane were used as the parameters for comparison. After that, several FEMs with different material properties and amount of loading were constructed for the design optimization and biomechanical study of the functional intimate apparel.

## Chapter 4 Clinical study of posture correction girdle

### 4.1 Introduction

As mentioned in Chapter 2, the effectiveness of an existing posture correction girdle was ambiguous. To address this issue, a 6-month quasi-experimental pre-test-post-test clinical study of the posture correction girdle was carried out in this study. The aim of this clinical study is to obtain background information on the current design of the girdle and thus determine the possible modifications towards the proposed functional intimate apparel. The spinal deformity of the subjects was examined through x-rays. The effects of wearing the girdle on shoulder obliquity and rotation were assessed through 3D body images. Also, the interface pressure of the posture correction girdle was measured.

### 4.2 Subject recruitment

From 2015 to 2016, 883 students between the ages of 11 to 16 years old were screened for idiopathic scoliosis at 5 local secondary schools in Hong Kong and 182 (20.6%) participants showed signs of scoliosis; see

Table 4-1. Participants who have signs of scoliosis ( $ATR \geq 3^\circ$ ) were invited to undergo a radiographic examination to further assess the amount of spinal deformity. A total of 40 participants participated in the radiographic examination and 16 were diagnosed with scoliosis which is defined as individuals with a lateral curvature that is equal to or greater than 10 degrees (Hresko, 2013). The 16 participants were recruited as the human subjects in this study. Table 4-2 shows the demographics of the recruited subjects.

Table 4-1 Results of school screening

School name	Screening date	No. of participants	No. of students with signs of scoliosis ( $ATR > 3$ )
True Light Girls' College	17/09/2015	117	27
	23/09/2016	151	28
Belilios Public School	25/09/2015	125	24
	20/09/2016	114	18



Pope Paul VI College	21/03/2015	71	22
St Francis' Canossian College	25/05/2016	74	19
Holy Trinity College	28/06/2016	122	27
	14/10/2016	109	17
Total		883	182
Percentage of participants with signs of scoliosis			20.6%

Table 4-2 Demographics of recruited subjects

Lenke type	Subject code	Age	Height (cm)	Weight (kg)	BMI	Risser grade	Date of the pre-intervention x-ray	Cobb's angle in thoracic region (°)	Cobb's angle in lumbar region (°)
Lenke 1	16007	12	154	43.2	18.2	0	15/1/2016	13	-
	16009	13	148	37.3	17	2	16/1/2016	11.9	-
	16035	13	157	51	20.7	3	12/8/2016	12.1	-
	Mean	12.7	153.0	43.8	18.6	1.7	-	12.3	-
	SD	0.6	4.6	6.9	1.9	1.5	-	0.6	-
Lenke 3	16033	13	143	31.8	15.6	3	11/7/2016	16.1	14.5
	M1601	15	173	53.6	17.9	4.5	14/7/2016	28	25
	Mean	14.0	158.0	42.7	16.8	3.8	-	22.1	19.8
	SD	1.4	21.2	15.4	1.6	1.1	-	8.4	7.4

Lenke 5	16004	13	148	43	19.6	2	19/12/2015	-	23.8
	16010	12	154	52.9	22.3	3	18/1/2016	-	23.1
	16024	13	145.5	33.1	15.6	3.5	9/4/2016	-	14.4
	16030	12	162	69.3	26.4	3	12/7/2016	-	10.8
	16031	13	152	42	18.2	2	5/7/2016	-	10.5
	Mean	12.6	152.3	48.1	20.4	2.7	-	-	16.5
	SD	0.5	6.4	13.8	4.1	0.7	-	-	6.5
Lenke 6	15001	15	176	47.5	15.3	4	16/10/2015	21	18
	16013	14	155	38	15.8	3.5	27/2/2016	23.6	25.5
	16017	13	165	53.6	19.6	3.5	2/4/2016	16.2	18
	16019	13	156	38.4	15.8	2	2/4/2016	16.1	22.5
	16036	12	162	45.6	17.4	3	5/11/2016	20.4	22
	M1602	16	170	54	18.6	4	6/8/2016	16	20.4
	Mean	13.8	164.0	46.2	17.1	3.3	-	18.9	21.1
	SD	1.5	8.1	7.0	1.7	0.8	-	3.2	2.9
Total mean		13.3	157.5	45.9	18.4	2.9	-	17.7	19.1
SD		1.2	9.8	9.6	2.9	1.1	-	5.1	5.2

### 4.3 Fitting of the girdle

During the fitting session of the girdle, a professional prosthetist and orthoptist (P&O) was recruited to insert semi-rigid pads into the girdle. The aim of adding the pads is to exert corrective pressure onto the torso through the three-point pressure system. The location of the pads that were added to the girdle for each subject and its corresponding radiograph are shown in Figure 4-1 to 4-4.

For the three subjects with a Lenke 1 curve, a corrective pad was inserted into the 2<sup>nd</sup> or 3<sup>rd</sup> pocket to exert pressure onto the upper thoracic curve. Pads to counter the corrective force at the upper part of the curve were inserted into the 1<sup>st</sup> pocket for subject 16007 and into the 2<sup>nd</sup> pocket for subject 16035 and pads to counter the corrective force at the lower part of the curve were inserted into the 3<sup>rd</sup>, 4<sup>th</sup> and 5<sup>th</sup> pockets for subjects 16007, 16009 and 16035.

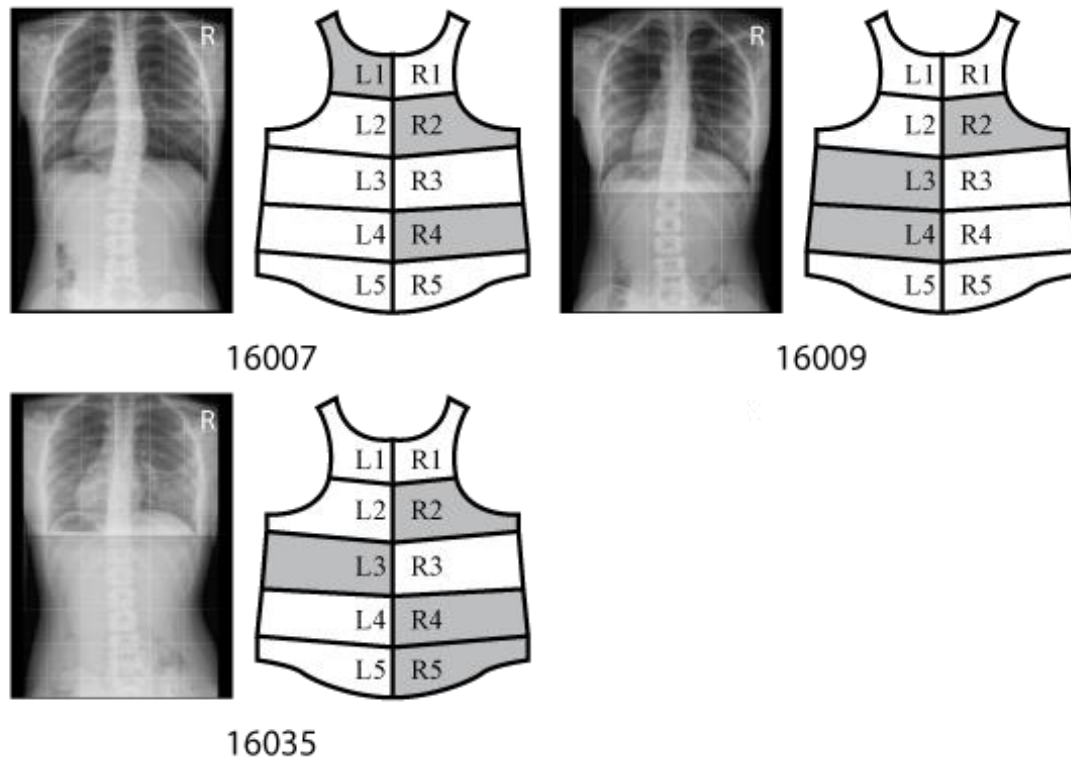


Figure 4-1 Radiographic images and location of inserted pads: Lenke 1 curve

There were no subjects with a Lenke 2 curve.

There were two subjects with a Lenke 3 curve. For Subject 16033, the P&O tightened the right shoulder strap to provide corrective pressure onto the thoracic curve and inserted lumbar pads into the 3<sup>rd</sup> and 4<sup>th</sup> pockets to correct the lumbar curve. For Subject M1601, due to the large thoracic curvature, instead of tightening the shoulder strap, a pad to correct the thoracic curve was inserted into the 1<sup>st</sup> and 2<sup>nd</sup> pockets of the girdle and a pad to correct the lumbar curve was inserted into the 4<sup>th</sup> pocket.

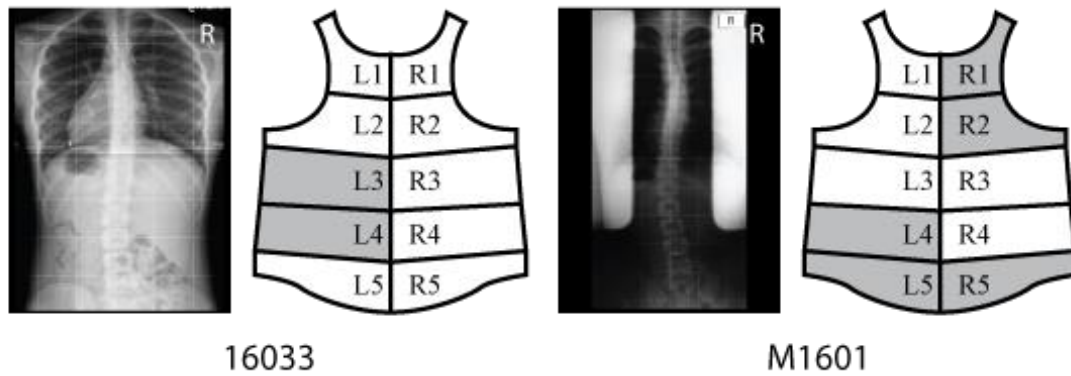


Figure 4-2 Radiographic images and location of inserted pads: Lenke 3 curve

There were no subjects with a Lenke 4 curve.

There were however, five subjects with a Lenke 5 curve. A corrective pad was inserted into the 3<sup>rd</sup> and/or 4<sup>th</sup> pocket of their girdle to correct the lumbar curve for all of them and counter pads were inserted into the 2<sup>nd</sup> and/or 5<sup>th</sup> pocket depending if the subject has an tilted pelvis.

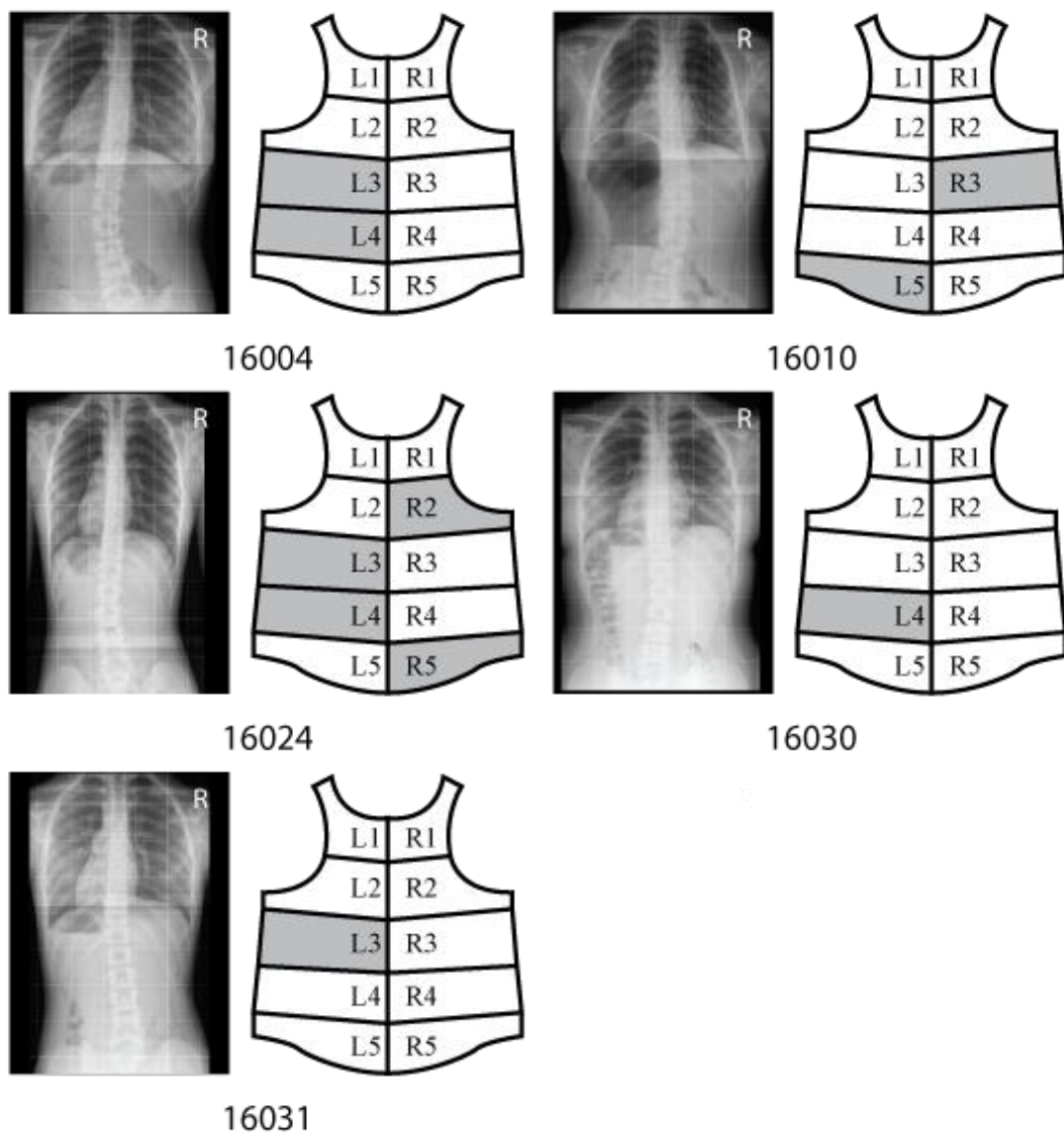


Figure 4-3 Radiographic images and location of inserted pads: Lenke 5 curve

There were six subjects with a Lenke 6 curve. In general, a corrective pad was inserted into the 2<sup>nd</sup> pocket for the thoracic curve and another corrective pad was inserted into the 3<sup>rd</sup> or 4<sup>th</sup> pocket for the lumbar curve. A counter pad was inserted into the 5<sup>th</sup> pocket depending if the subject has a tilted pelvis. For subject 16017, since her spine has a high flexibility, two pads were inserted in both sides of the 5<sup>th</sup> pocket to enhance the end-point control of scoliotic spine.

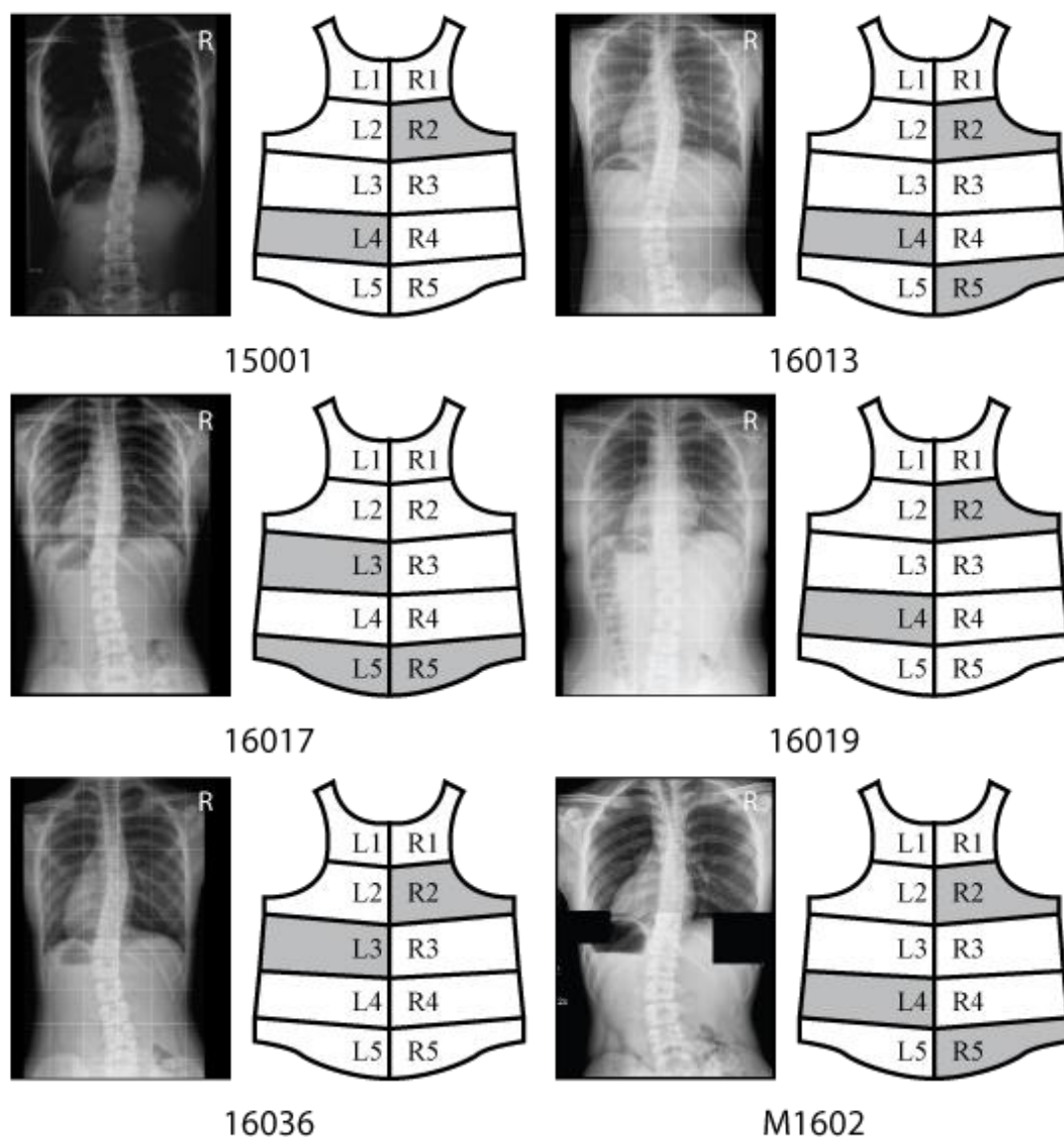


Figure 4-4 Radiographic images and location of inserted pads: Lenke 6 curve

In summary, a corrective pad was generally inserted into the 2<sup>nd</sup> pocket of the girdle if the patient had a thoracic curve, which is a Lenke 1, 3, or 6 curve(s). However, if the thoracic curve was not too severe, the P&O attempted to straighten the thoracic curve by tightening the shoulder strap instead of inserting a pad to exert a corrective force. This was the case for one of the patients with a Lenke 3 curve. Apart from the thoracic curve, the P&O would insert a corrective pad into the 3<sup>rd</sup> and/or 4<sup>th</sup> pocket to control the lumbar curve, which is a Lenke 3, 5, or 6 curve(s). If the patient had a tilted pelvis, then a counter pad was inserted to enhance the corrective effect; that is, the three-point pressure system would be used. Moreover, note that two pads were inserted into both the left and right 5<sup>th</sup> pockets for a patient with a high spinal

flexibility.

#### 4.4 Effects on spinal control

The in-brace and post-intervention radiographic examinations took place on the sixth month of the clinical study. Of the 16 subjects, 6 subjects withdrew from the study after the first visit, while the remaining 10 completed the 6-month clinical study. The percentage of those who left the study was therefore 37.5%. Table 4-3 presents the in-brace and out-brace Cobb's angle at the sixth month.

Table 4-3 Cobb's angle: in-brace and no brace at initial visit vs. six months of girdle wear

Lenke type	Subject code	Date of pre-intervention x-ray	Cobb's angle: Out brace at pre-intervention (°)	Date of out-brace x-ray at the 6 <sup>th</sup> month	Cobb's angle: Out-brace at 6 <sup>th</sup> month (°)	Date of in-brace x-ray at the 6 <sup>th</sup> month	Cobb's angle: In-brace at 6 <sup>th</sup> month (°)
Lenke 1	16007	15/1/2016	13.0	9/2/2017	12.0	31/8/2016	12.7
	16009	16/1/2016	11.9	11/3/2017	11.0	29/8/2016	11.1
	16035	12/8/2016	12.1	5/7/2017	7.8	23/6/2017	5.2
	Mean		12.3		10.3		9.7
	SD		0.6		2.2		4.0
Lenke 3	M1601	14/7/2016	28.0	17/11/2016	25.0	17/11/2016	25.0
	Mean		28.0		25.0		25.0
	SD		-		-		-
Lenke 5	16004	19/12/2015	23.8	25/1/2017	19.8	30/8/2016	17.6
	16010	18/1/2016	23.1	24/1/2017	28.4	31/8/2016	24.7
	16030	12/7/2016	10.8	19/5/2017	10.4	12/5/2017	8.1
	Mean		19.2		19.5		16.8
	SD		7.3		9.0		8.3
Lenke 6	15001	16/10/2015	18.0	16/10/2016	16.0	7/5/2016	12.0
	16013	27/2/2016	25.5	18/11/2016	26.8	18/11/2016	28.0

	M1602	6/8/2016	20.4	11/8/2017	17.2	27/7/2017	15.3
	Mean		21.3		20.0		18.4
	SD		3.8		5.9		8.4
	Overall mean		18.7		17.4		16.0
	SD		6.4		7.3		7.7

#### 4.4.1 Curvature reduction/increase after 6 months

Table 4-4 presents the rate of reduction/increase of Cobb's angle after the 6-month clinical study (Fok et al., 2018). The results showed that among the 10 subjects, 1 subject with a Lenke curve 5 experienced a spinal curve increase  $>5^\circ$ , 1 subject with a Lenke curve 6 experienced a spinal curve increase  $<5^\circ$ , while the remaining subjects (80%) experienced a spinal curve reduction that is  $<5^\circ$  but none had a reduction that is  $>5^\circ$ . The survival rate (those who did not experience a spinal curve progression of  $5^\circ$ ) over the 6 months was 90%.

The mean of the Cobb's angle at pre-intervention and post-intervention was  $18.7^\circ$  and  $17.4^\circ$  respectively. A Wilcoxon signed rank test indicated that there was no significant difference between pre-intervention and post-intervention; that is,  $Z = -1.4$  and  $p = 0.17$ . This result indicated that the girdle provided a short-term positive effect in term of controlling the progression of the spinal curve.

However, Wong et al. (2008) conducted a study on the effectiveness of the SpineCor flexible brace versus a rigid brace. Their result showed that the survival rate at the sixth month of use of the SpineCor and rigid braces was 95% and 100% respectively. Therefore, when the efficacy of the posture correction girdle was compared to that of the SpineCor and rigid brace, the ability of the posture correction girdle to reduce the progression of the spinal curve was still lacking.

Table 4-4 Spinal curvature reduction/increase after 6 months with posture correction girdle

Lenke type	Subject code	Reduction/ increase of Cobb's angle ( $^\circ$ )	Rate of reduction/ increase of Cobb's angle
Lenke 1	16007	-1.0	-8%
	16009	-1.0	-8%



	16035	-4.3	-36%
	Mean	-2.1	-17%
	SD	1.9	0.2
Lenke 3	M1601	-3.0	-11%
	Mean	3.0	11%
	SD	-	-
Lenke 5	16004	-4.1	-17%
	16010	+5.3	+23%
	16030	-0.4	-4%
	Mean	-0.3	-1%
	SD	4.7	0.2
Lenke 6	15001	-2.0	-11%
	16013	+1.3	+5%
	M1602	-3.2	-16%
	Mean	-1.3	-7%
	SD	2.3	0.1
Overall mean		-1.2	-8%
SD		2.9	0.2

#### 4.4.2 In-brace reduction/increase of spinal curvature

Table 4-5 presents the in-brace reduction/increase of spinal curvature after six months of wearing the posture correction girdle. Among the 10 subjects, 3 experienced an increase in their spinal curvature  $<5^\circ$ , 7 subjects reduced their spinal curvature  $<5^\circ$  and none reduced their spinal curvature  $>5^\circ$ . A Wilcoxon signed rank test indicated that there was no significant difference between the in-brace and out-brace conditions; that was,  $Z = -2.0$  and  $p = 0.051$ . Indeed, the measurement error of the Cobb's angle is generally about  $5^\circ$  (Malfair et al., 2010). Since none of the subjects demonstrated a reduction in their spinal curvature  $>5^\circ$  for the in-brace and out-

brace conditions, this could imply that the girdle did not provide a corrective effect.

Again, using the study results of Wong et al. (2008) who conducted a clinical study to compare the effectiveness of the SpineCor and rigid braces, the immediate in-brace reduction of spinal curvature of both braces was 21.5% and 18.1% respectively. Even if measurement error was neglected, the in-brace spinal curvature reduction rate of the posture correction girdle was still unsatisfactory in comparison to the SpineCor and rigid braces.

Table 4-5 In-brace reduction/increase of spinal curvature after six months of girdle wear

Lenke type	Subject code	In-brace reduction/ increase of Cobb's angle (°)	Rate of in-brace reduction/ increase of Cobb's angle
Lenke 1	16007	+0.7	+6%
	16009	+0.2	+1%
	16035	-2.6	-33%
	Mean	-0.6	-9%
	SD	1.8	0.2
Lenke 3	M1601	0.0	0%
	Mean	0.0	0%
	SD	-	-
Lenke 5	16004	-2.2	-11%
	16010	-3.7	-13%
	16030	-2.3	-22%
	Mean	-2.7	-15%
	SD	0.8	0.1
Lenke 6	15001	-4.0	-25%
	16013	+1.3	+5%
	M1602	-1.9	-11%

	Mean	-1.6	-10%
	SD	2.6	0.1
Overall mean		-1.5	-10%
SD		1.8	0.1

## 4.5 Effects on standing posture

### 4.5.1 Shoulder obliquity

Shoulder obliquity was measured for both the in-brace and out-brace conditions at the initial visit of the subjects. Of the 16 subjects, there was one who did not have any data due to technical issues with the equipment. The mean of the shoulder obliquity when the girdle was worn was 1.41° (SD: 1.34) but when the girdle was not worn, it was 2.26° (SD: 1.39). Figure 4-5 presents the shoulder obliquity of each subject for both the in-brace and out-brace conditions.

The Wilcoxon signed ranks test showed that shoulder obliquity was significantly reduced when the girdle was worn; that was,  $Z = -2.84$  and  $p = 0.05$ . This result was in agreement with that of a previous study by Liu et al. (2015). This result further proved that the posture correction girdle provided immediate reduction in the shoulder obliquity of AIS patients.

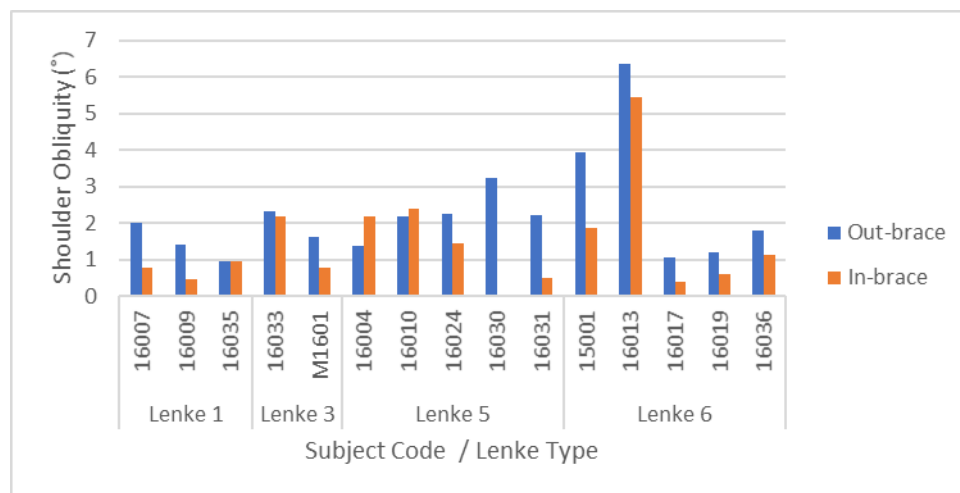


Figure 4-5 Shoulder obliquity of subjects: in-brace vs. out-brace

### 4.5.2 Shoulder rotation

Shoulder rotation was measured for both the in-brace and out-brace conditions at the initial

visit of the subjects. Of the 16 subjects, there was one who did not have any data due to technical issues with the equipment. The mean of the shoulder rotation when the girdle was worn was 2.26° (SD: 1.77) versus when the girdle was not worn of 3.32° (SD: 2.23). Figure 4-6 presents the shoulder rotation values of each subject for both the in-brace and out-brace conditions.

The Wilcoxon signed ranks test showed that shoulder rotation was significantly reduced when the girdle was worn; that was,  $Z = -2.27$  and  $p = 0.023$ . However, the result in this study differed from that in previous work conducted by Liu et al. (2015). Their result showed that patients generally had a substantial increase in shoulder rotation when they wore the girdle at their initial visit. According to the fitting process in the clinical study here, the shoulder rotation might be influenced by the difference in tension between the left and right shoulder straps. Since the shoulder straps have a free-end elastic design, wearers might not be able to balance the tension of the two shoulder straps well. When the tension of the right shoulder strap is greater than the left one, the shoulders may tend to rotate in a clockwise direction. When the tension of the left shoulder strap is greater than the right one, the shoulders may tend to rotate in an anti-clockwise direction. Thus, controlling the tension of the shoulder strap is important for this free-end shoulder strap design since the tension readily influences shoulder rotation. Further studies on the relationship between the tension of the shoulder straps and shoulder rotation are therefore recommended.

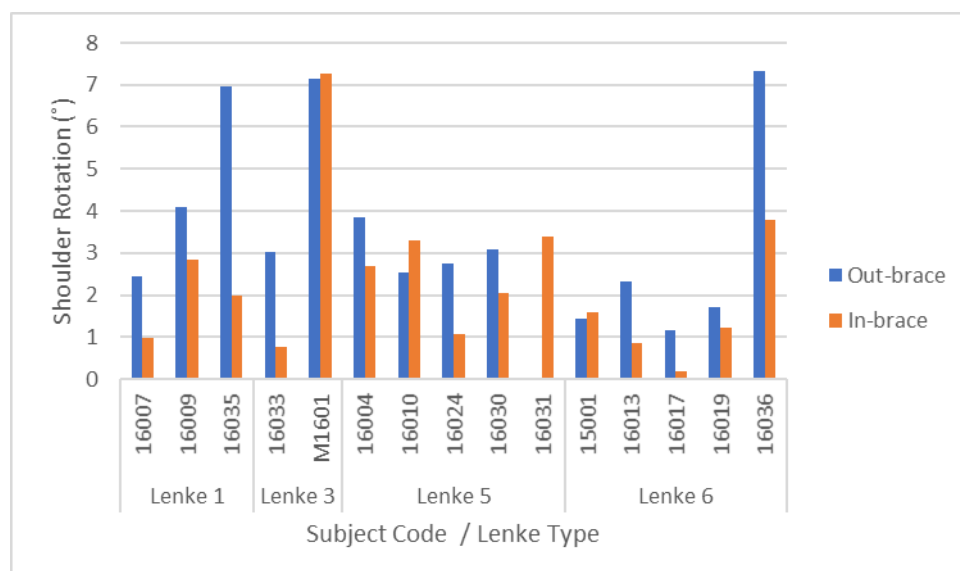


Figure 4-6 Shoulder rotation of subjects: in-brace vs. out-brace

## 4.6 Interface pressure

The pressure at the interface between different body parts and the posture correction girdle was measured at the initial visit. Of the 16 subjects, there were two who did not have any data due to technical issues with the equipment. The pressure at the interface between the under-bust area and girdle ranged between 0.66 kPa and 4.78 kPa; waist area and girdle ranged between 1.18 kPa and 4.73 kPa; and pelvis area and girdle ranged between 0.94 kPa and 6.37 kPa. The pressure at the interface between the under-bust, waist and pelvis areas and the girdle is presented in Figure 4-7, Figure 4-8 and Figure 4-9, respectively.

A study by Wong et al. (2000) was used for comparison purposes. They investigated the biomechanics of a rigid AIS brace and reported that the pressure ranged between 4.95 kPa and 9.34 kPa. Therefore, the amount of the interface pressure exerted by the posture correction girdle was much lower than the rigid brace. This implied that the corrective force of the girdle was inadequate. The low interface pressure might be also a possible reason for the poor results of spinal curvature correction when the girdle was worn.

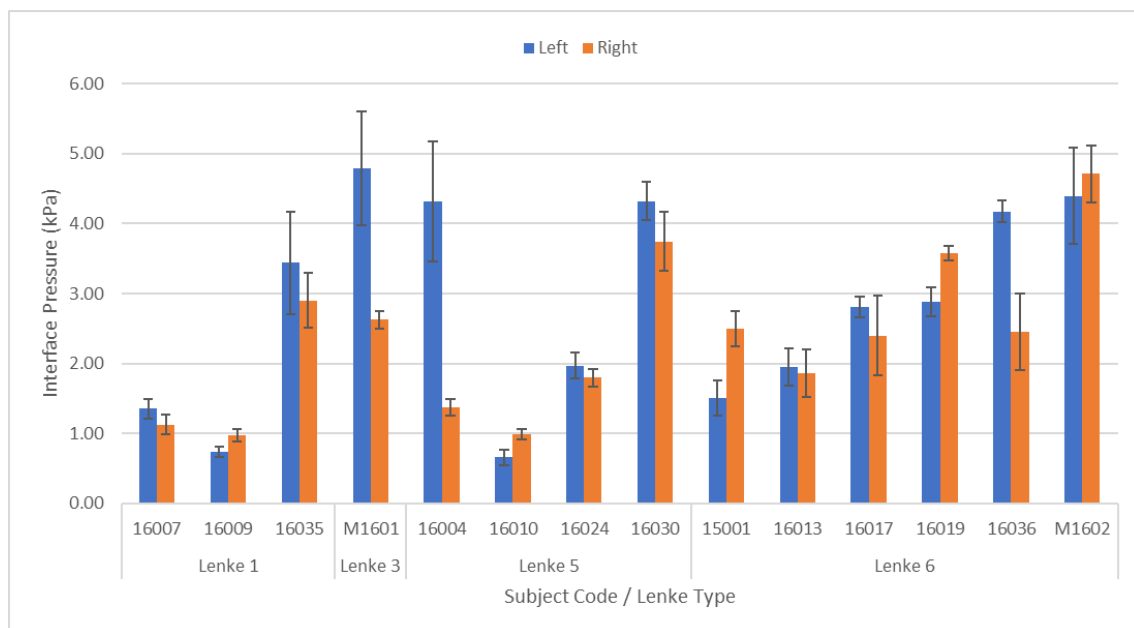


Figure 4-7 Interface pressure between under-bust and girdle

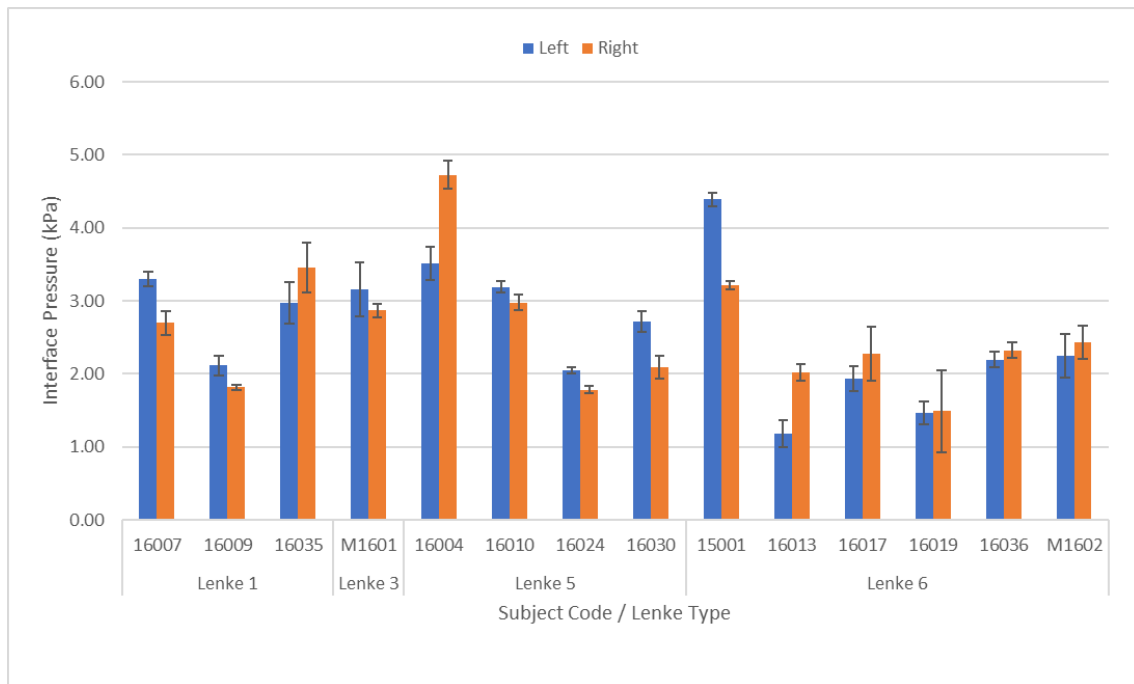


Figure 4-8 Interface pressure between waist and girdle

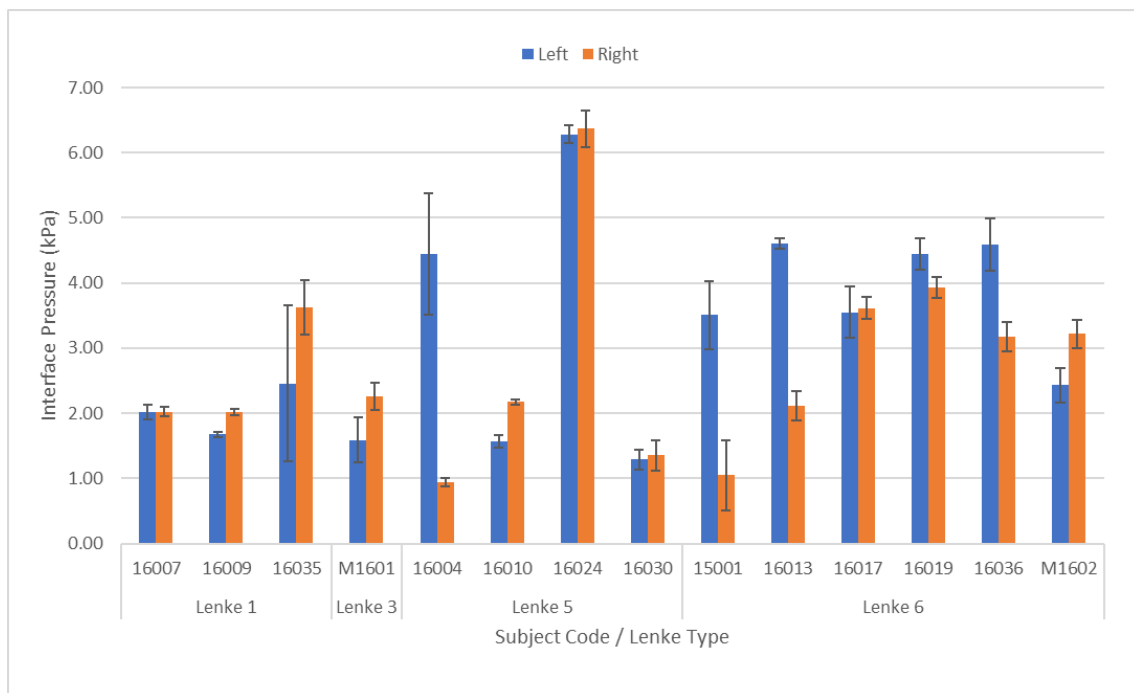


Figure 4-9 Interface pressure between pelvis and girdle

#### 4.6.1 Influence of pads on interface pressure

Liu (2015) stated that the reason for adding pads to the posture correction girdle was to induce pressure onto the spinal convexity and thus correct the spinal deformity. However, the result in this study did not agree with her corrective principles. The pads did not appear to have the

ability to effectively exert adequate corrective forces in the right direction. Sometimes, adding a pad might enhance the pressure to the counter side especially in the waist and pelvis areas.

It can be observed in Figure 4-7, Figure 4-8 and Figure 4-9 that even in the same areas, the pressure at the interface between the left and right sides differs for the three parts of the body measured; that is, the under bust, waist and pelvis. To further investigate the pressure distribution, the interface pressure was then analysed with reference to the intervention of the padding at each measured area. Figure 4-1, Figure 4-2, Figure 4-3 and Figure 4-4 show the position of the pads for each subject. In general, the 3<sup>rd</sup>, 4<sup>th</sup> and 5<sup>th</sup> pockets were located at the under-bust, waist and pelvis respectively.

Of the 14 subjects who had relevant data, a pad was inserted into the 3<sup>rd</sup> pocket for 7 of the subjects, which is at the under-bust because these subjects had a curvature in thoracolumbar region. Figure 4-10 shows the amount of interface pressure at the under-bust for these 7 subjects. It can be seen that most of the higher interface pressure was found at the side with a pad as opposed to its counter side. However, the difference was not significant. A Wilcoxon signed rank test indicated that there was no significant difference in the pressure at the interface between the under-bust and girdle for the side with a pad and its counter side; that was,  $Z = -1.35$  and  $p = 0.17$ . This showed that inserting a pad into the 3<sup>rd</sup> pocket only slightly exerted a corrective force onto the convexity.

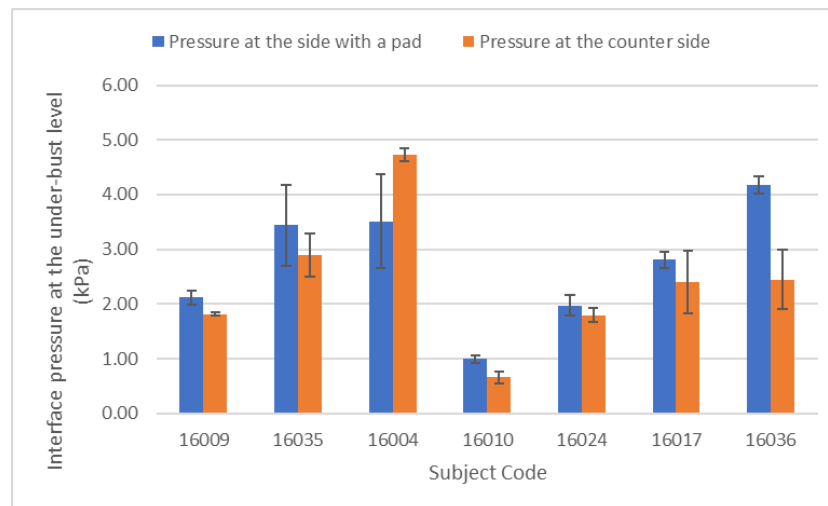


Figure 4-10 Pressure at interface between under-bust and girdle with pad inserted into 3<sup>rd</sup> pocket

Of the 14 subjects, a pad was inserted into the 4<sup>th</sup> pocket of the girdle for 11 of the subjects, which is in the waist area because these subjects had a curvature in lumbar region. Figure 4-11

shows the pressure at the interface between the waist area and girdle for these 11 cases. It was interesting to see that four of them showed a higher interface pressure to the counter side of the pads. Furthermore, a Wilcoxon signed rank test indicated that there was no significant difference in the pressure at the interface between the waist area and the girdle with respect to both padded and counter sides; that was,  $Z = -0.8$  and  $p = 0.42$ . This indicated that inserting a pad into the 4<sup>th</sup> pocket could not provide a corrective force onto the convexity. A possible explanation for the greater amount of pressure to the counter side is shape conformity. As the pad is sitting on a semi-rigid flat plate, there may be the lack of conformation with the body contours especially the convex shape of the waist. Thus, the non-conforming pad may create a gap between the brace and surface of the body. As a result, the counter side might be subjected to an unexpected higher pressure.

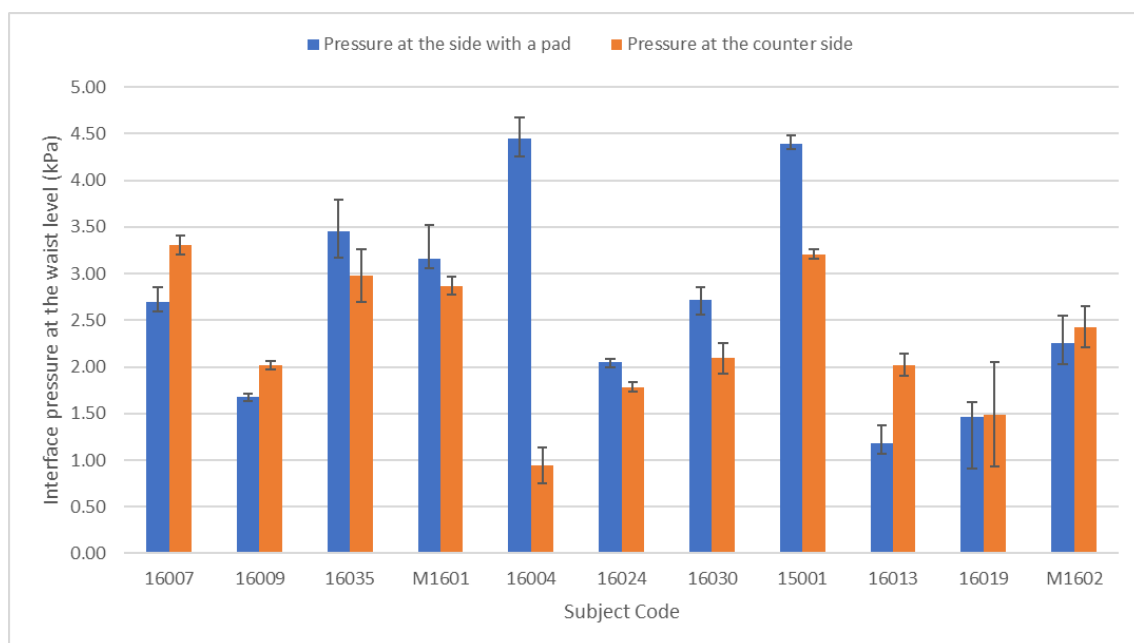


Figure 4-11 Pressure at interface between waist and girdle with pad inserted into 4<sup>th</sup> pocket

As for the pad at the pelvis, a pad was inserted into the 5<sup>th</sup> pocket of the girdle worn by 5 of the 14 subjects, which is in line with the pelvis because these subjects had a tilted pelvis. Figure 4-12 shows the pressure at the interface between the pelvis and girdle for these 5 cases. It can be seen that two of the cases showed a higher pressure to the counter side. A Wilcoxon signed rank test indicated that there was no significant difference in the pressure to the interface between the pelvis and girdle for both the side with a pad and its counter side; that was,  $Z = -0.14$  and  $p = 0.89$ . Similar to the findings for the pressure at the interface between the waist area and girdle, the effect of the pad on the interface pressure at the pelvis was ambiguous.



Nevertheless, the conformity of the pad to the body contours may be a possible reason for the greater pressure to the counter side.

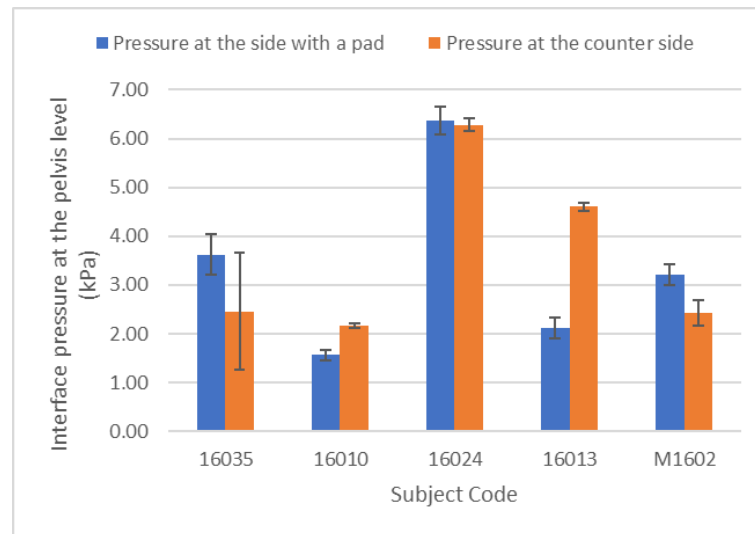


Figure 4-12 Pressure at interface between pelvis and girdle with pad inserted into 5<sup>th</sup> pocket

D. Périé et al. (2004) examined the biomechanics of a rigid brace by using a finite element model. They reported that there was no pressure found at the counter side. However, due to the symmetric design of the waist band of the girdle examined here, there was pressure exerted onto the entire trunk including both the convexity and concavity of the trunk. Therefore, an asymmetric design could possibly create a similar pressure distribution as that of a rigid brace.

#### 4.7 Summary

A flexible brace provides the benefits of mobility, comfort and aesthetics for scoliotic patients. Liu et al. (2014) developed a flexible brace for AIS called the posture correction girdle. However, its effectiveness was still ambiguous and there was a lack of studies on its biomechanics. Therefore, a 6-month clinical study has been conducted in this thesis to investigate its effectiveness in controlling spinal curvature and asymmetric body contours and its interface pressure.

In this study, a total of 16 patients were recruited to test the posture correction girdle. Of the 16 patients, 10 completed the study and 6 subjects withdrew from the study after the first visit. The percentage of those who left the study was therefore 37.5%. During the fitting session, a professional P&O helped to insert pads into the pockets of the girdle and the pad allocation effects were then subsequently studied. The results showed that the girdle had a positive effect in preventing the progression of spinal curvature. However, the brace could not reduce the

spinal curvature.

As for controlling asymmetric body contours, the initial corrective effects of the girdle in terms of shoulder obliquity and shoulder rotation were studied. The results indicated that shoulder obliquity and shoulder rotation were both significantly reduced, which implied that the girdle had a positive effect in reducing the asymmetry of the body contours.

In order to gain a better understanding of the biomechanics of the girdle, the interface pressure was also studied. The results showed that the interface pressure of the girdle was inferior compared to rigid braces. More importantly, the relationship between pad installation and interface pressure was also studied. It was surprising to find that adding a pad might sometimes increase the pressure to the counter side instead of the padded side. The conformity of the pad to the body contours might be a possible factor which caused greater pressure to the counter side. Also, the symmetrical waist band of the girdle might be a possible factor that had inhibited the effectiveness of the spinal correction.

A 6-month clinical study of the posture correction girdle has been completed in this thesis. The results showed that the subjects who wore the posture correction girdle for 6 months showed no significant difference in their Cobb's angles as compared to the initial stage. However, the results also showed that there was no significant difference in the Cobb's angle between the in-brace and out-brace conditions. Furthermore, the pressure distribution might not correspond to that of the three-point pressure system. The design of the girdle therefore needs to be modified in order to enhance its effectiveness for spinal correction.

## **Chapter 5 Design and development of functional intimate apparel for AIS**

### **5.1 Introduction**

Rigid bracing was discussed in Chapter 2 along with its effectiveness in controlling AIS. However, discomfort and mobility restriction are usually the limitations of rigid braces, which reduce treatment compliance as well as the quality of life of AIS patients. In response, flexible braces such as SpineCor and the posture correction girdle in Liu et al. (2014) have been developed. While these flexible braces are more comfortable and flexible than their rigid counterparts, their effectiveness in controlling spinal deformity was still debatable. In Chapter 3, a clinical study of the posture correction girdle in Liu et al. (2014) was discussed. The results showed that the in-brace correction of this girdle is unsatisfactory.

Therefore, the objective of this chapter is to elaborate on the design and development of a functional intimate apparel for AIS which not only aims to provide comfort and allow mobility, but also provide in-brace spinal correction. The design and development of the functional intimate apparel for AIS were first presented which include the design criteria and concept, development of the prototype, revamping of the design, and material selection.

### **5.2 Design criteria**

The objective of the proposed functional intimate apparel is to maximise the corrective effects of a flexible brace for spinal deformity and minimise the negative impacts, such as mobility restriction and discomfort of rigid braces. The design criteria (Table 5-1) are discussed based on functional, expressive, and aesthetics considerations.

Table 5-1 Design criteria of the proposed functional intimate apparel

Dimension	Design criterion	Details
Functional	Spinal control	Provides adequate in-brace correction.
	Mobility	Does not restrict body movement.
	Comfort	Breathable.

Expressive	Light in weight	Lighter than rigid braces.
	Flexible	Like a garment.
Aesthetic	Simple	Suitable for schoolchildren.
	White	Can be worn under school uniform.

The main functional consideration was spinal control. With reference to the 2011 Guidelines of the International Scientific Society on Scoliosis Orthopaedic and Rehabilitation Treatment (SOSORT), in-brace correction is the initial criterion for evaluating the quality of a new brace (Negrini et al., 2012). Thus, providing in-brace correction was the first goal of the proposed design in this study.

Other functional considerations were mobility and comfort. As mentioned in Chapter 2, mobility restriction and discomfort are usually the drawbacks of rigid braces which might influence treatment compliance and reduce the quality of life of AIS patients. Therefore, comfort and mobility were considered as goals.

As for the expressive criteria, the proposed design should be light in weight and appear to be like a functional garment instead of a rigid orthotic instrument. Danielsson et al. (2001) conducted a study on the quality of life for AIS patients after bracing treatment and reported that bracing reduces their psychological well-being. Thus, in order to reduce the psychological impacts, the proposed design would be one that resembles a garment instead of rigid orthotic instrument.

As for the aesthetic criteria, a simple design with a white colour was used since the target user would be AIS patients who are usually schoolchildren. The proposed design can be worn under their school uniform or outerwear, and thus remains obscure.

### 5.3 Preliminary idea

A bra top with a derotation strap was proposed. Figure 5-1 shows the first prototype, which was a long bra top that opened at the back with a crossed back design. The idea behind this design was derived from the corrective mechanism of the posture correction girdle in Liu et al. (2014) and SpineCor, which was to directly induce forces onto the spinal area by using their corrective movement principle. The correction pads could be inserted inside the elastic band to

create a direct force that pushes onto the convex part of the spine. Moreover, the derotation strap was used to derotate the thorax in a clockwise or counter-clockwise direction relative to the shoulders based on the corrective movement principle. In addition, some of the supporting resin bones were inserted around the trunk to reinforce the vertical support. Apart from these corrective components, there were some design elements that were used to cope with the expressive and aesthetic criteria. A high neckline design was used to provide a higher level of coverage and security. The soft bra cups were used to allow for breast development. The soft resin underwire was used to retain the shape of the breasts and was comfortable to wear. The hook and eye openings were used to accommodate different body circumferences.

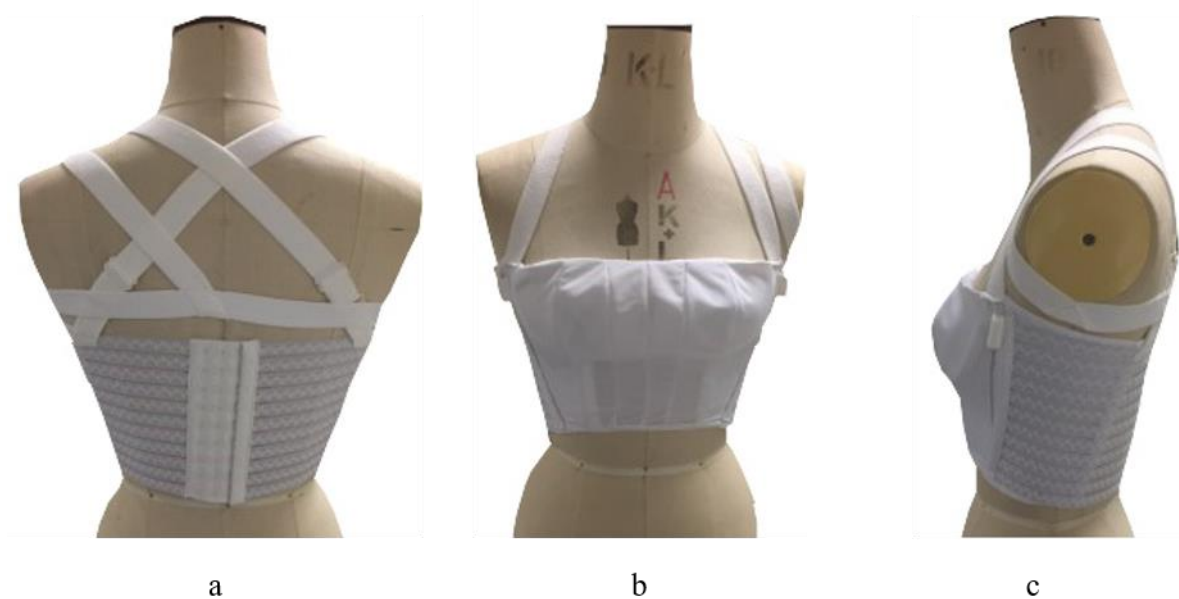


Figure 5-1 First prototype of bra top for AIS: (a) back, (b) front and (c) side views

### 5.3.1 Preliminary review of first prototype of bra top

A scoliotic subject (Subject Code: R17002) was invited to don the first prototype (Figure 5-2). The demographics of the subject are listed in Table 5-2. Due to the concerns of radiation and other ethical issues, only 3D body scanning and interface pressure measurements were conducted in this preliminary stage to study the first prototype for modifications.

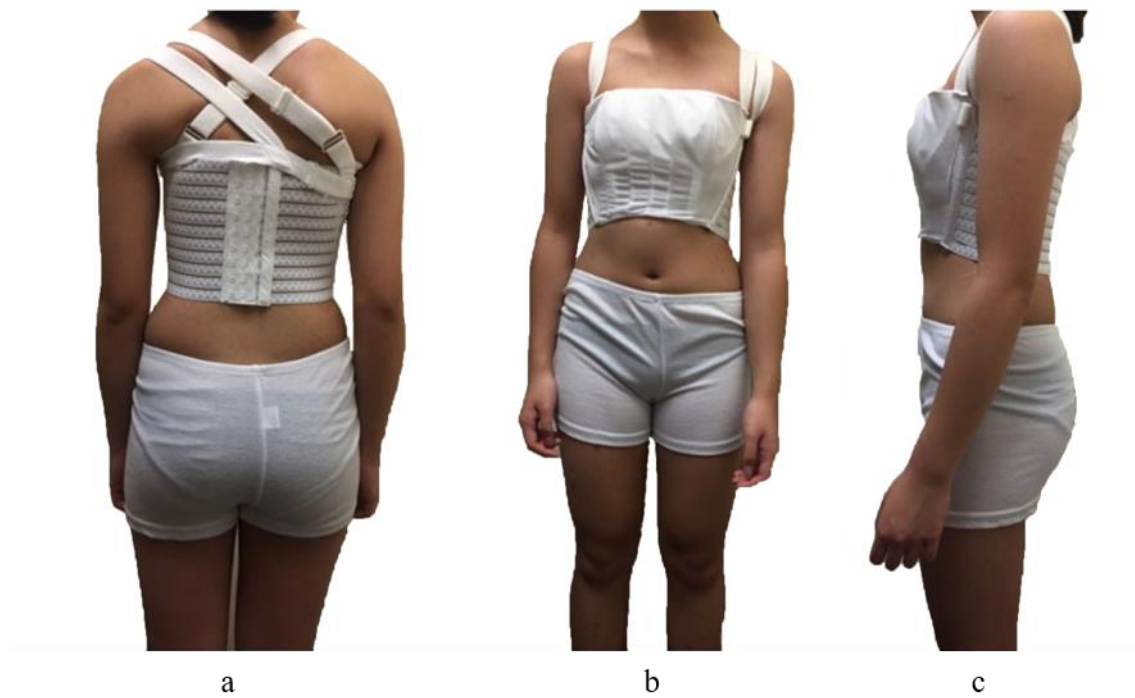


Figure 5-2 First prototype of bra top on Subject R17002: (a) back, (b) front and (c) side views

Table 5-2 Demographics of Subject R17002

Subject Code	Age (years old)	Height (cm)	Weight (kg)	BMI	Cobb's angle (degrees)
R17002	14	150	49.3	21.9 (normal)	45°(T4-T8) 27°(T8-L3)

### 5.3.1.1 Contour changes

The subject underwent 3D body scanning both in-brace and without the brace. Her physical contour changes such as body symmetry, shoulder obliquity and shoulder rotation were investigated. Figure 5-3 presents the measurements of the shoulder obliquity and shoulder rotation of the subject for both in-brace and without the brace. The degree of shoulder rotation was reduced after wearing the prototype. However, it was surprising that the prototype had a negative effect on shoulder obliquity. Since the derotation strap was used for the left underarm, the strap might lift up the left shoulder and thus caused a more oblique shoulder. Therefore, the design of the derotation strap for the shoulders was reconsidered.

Figure 5-4 presents the symmetry analysis along the z-axis for both in-brace and without the brace. The blue colour represents the convex part of the body while the red colour represents the concave part of the body of the subject. It was observed that the symmetry of the subject was slightly increased in the scapular region. This finding was in agreement with the measurement of the shoulder rotation. However, the prototype did not appear to have the ability to increase the symmetry in the lower thoracic region.

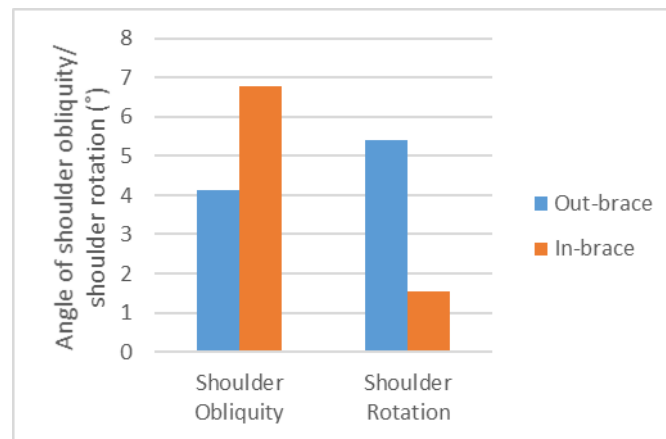


Figure 5-3 Shoulder obliquity and shoulder rotation results for in-brace and without brace:  
Subject R17001

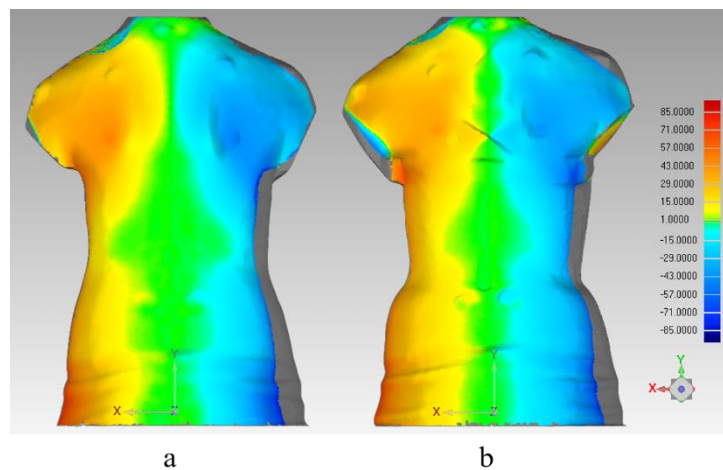


Figure 5-4 Symmetry analysis in 3D: (a) prototype not worn, and (b) prototype worn

### 5.3.2 Interface pressure

The interface pressure was measured at the thoracic pad and its counter side (Figure 5-5). The pressure range was 0.39-1.33 kPa for the padded side and 1.07-1.59 kPa for its counter side. However, the pressure at the counter side was higher than the padded side. A possible explanation could be that aside from the symmetric elastic band, the pad did not conform to

the curvature of the body very well which lead to some gapping between the interface of the body and brace. This meant that the pad did not induce a very large force. Therefore, the counter side of the body was subjected to a higher amount of pressure, which meant that there was an undesirable pressure distribution.

Apart from the pressure distribution, the magnitude of the interface pressure was insufficient. The interface pressure of rigid braces ranged between 4.95 and 30 kPa (Mac-Thiong et al., 2004; Wong et al., 2000). However, the interface pressure of the prototype was far lower (0.9 kPa). Since the interface pressure might be correlated to spinal correction, the amount of corrective force exerted needed to be examined more in depth in the proposed design.

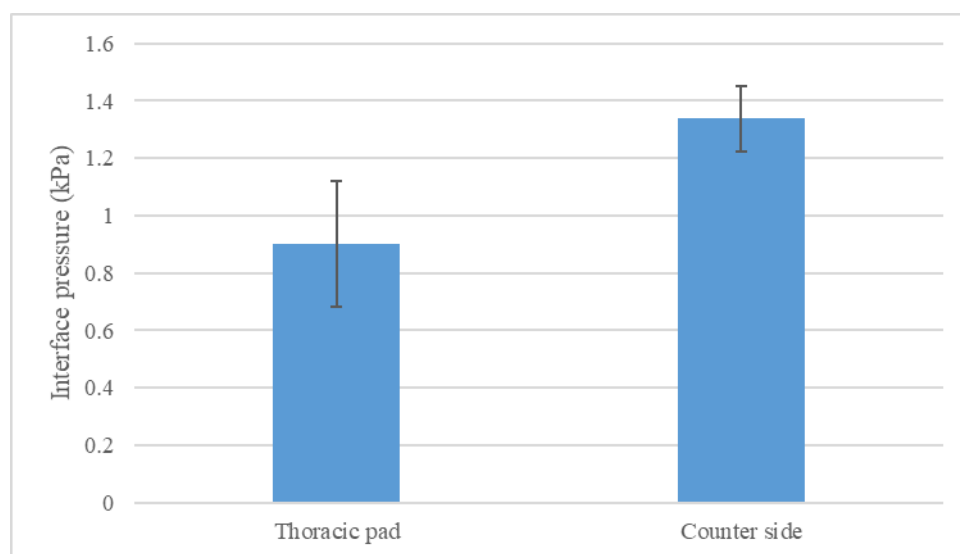


Figure 5-5 Interface pressure at thoracic pad and its counter side: Subject R17002

#### 5.4 Bra top modifications

After the preliminary review of the prototype, some modifications were made to the design. First, the problems with the design of the derotation strap at the shoulders and uneven pressure distribution were addressed. To prevent the unintended increase in shoulder obliquity, the derotation strap was removed. Moreover, in order to ensure a proper pressure distribution, an asymmetric design was instead used. The modified design continued to use the elastic band as the corrective component for the convex part of the body and a pad could be inserted to increase the level of exerted pressure. More importantly, an open design was adopted for the counter side to ensure a proper pressure distribution and allow shifting of the scoliotic spine.



### 5.4.1 Second prototype of bra top

Figure 5-6 shows the design of the second prototype of the bra top. The main design feature was the open design in the concave part of the body. The elastic band provided the pressure in the convex part of the body while no pressure was exerted on the concave side due to the open design. Moreover, a front opening was used to improve the ease of donning and doffing.

However, some problems with the fit were found in this design. The main problem was the distortion of the elastic band in the centre of the back. Due to the open design, there was an uneven pressure distribution between the convex and concave parts of the body when the elastic band stretched along with the wearer, which lead to the distortion of the elastic band when the body bend. To eliminate this problem, a rigid material was placed at the centre of the back which provided a fixed boundary for the corrective component.

The second problem was that the upper bust band is too tight. This resulted in double-breasts. Due to the open bra cup design, the pressure distribution at the bra cups was concentrated at the upper bust band when the wearer stretched the wide elastic band of the corrective component and ultimately caused double-breasts. To minimise this problem, a shell fabric was needed at the bra cups to evenly distribute the interface pressure. These issues were addressed in a third prototype.

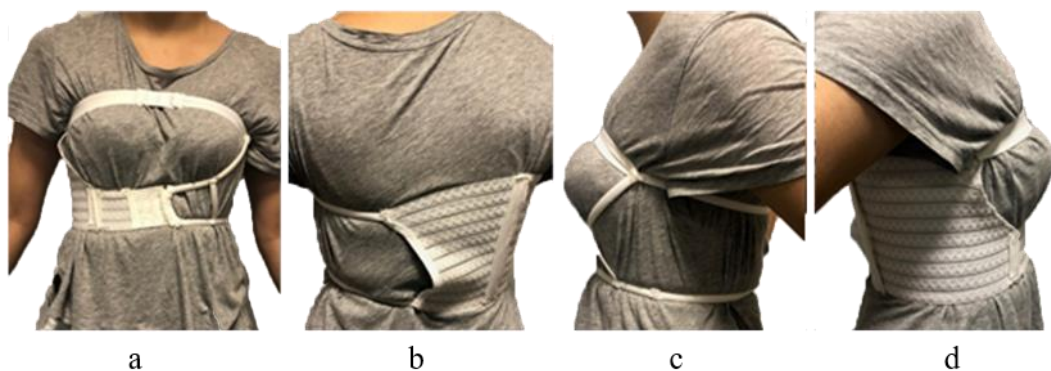


Figure 5-6 Second prototype of bra top: (a) front, (b) back, (c) left and (d) right views

### 5.4.2 Third prototype of bra top

Some of the fitting problems in the second prototype were addressed in the third prototype, which is shown in Figure 5-7. The third prototype had two parts: a frame bra top and a corrective component. The frame bra top provided the base of the brace and contributed to the stabilisation of the corrective component. The corrective component had the important role of

exerting direct corrective forces onto the convex part of the body to correct the spinal deformity. A pad could be inserted in the corrective component to enhance the exerted amount of pressure. Unlike the second prototype, shoulder straps, a full-bra cup design and an artificial back bone were added to the third prototype. The shoulder straps secured the bra top into a proper position. The full-bra cup design allowed even pressure distribution in the breast region. The artificial back bone acted as the base to stabilise the corrective component which prevented the distortion of the corrective component at the centre of the back.



Figure 5-7 Third prototype of frame bra top: (a) front, (b) back and (c) side views, and after attaching corrective component: (d) front, (e) back and (f) side views

## 5.5 Development of pants of prototype

As the pelvis was the basis for body alignment, fixation of the pelvis was important for spinal correction. Therefore, in addition to the bra top, pants with a pelvis belt to fix the pelvis and contribute to effective spinal alignment were fabricated for the prototype.

### 5.5.1 First prototype of pants

Figure 5-8 presents the first prototype of the bottom part of the functional intimate apparel. The gusset pants opened in the front and had a high-waist. The idea of using pants was to prevent the functional intimate apparel from riding up. Hooks and eyes were attached onto the centre of the front of the pants for opening and closing them. An elastic band was attached from the centre of the back to the centre of the front as a lumbar correction component.



Figure 5-8 First prototype of pants: (a) front, (b) back, (c) right and (d) left views

A scoliotic subject (Subject Code:18001) was invited to don the first prototype of the pants. Table 5-3 lists her demographics. Problems were observed during the fitting session. The end of the artificial back bone could not be secured during movement. Thus, the prototype could not effectively fix the pelvis in place. Moreover, it was found that the hook and eye opening was difficult to use.



Figure 5-9 First prototype of pants on Subject 18001: (a) front and (b) back views

Table 5-3 Demographics of Subject 18001

Subject Code	Age (years old)	Height (cm)	Weight (kg)	BMI (normal)	Cobb's angle (degrees)
18001	12	148	45.5	20.8 (normal)	21.6°(T4-T11) 17.3°(T11-L4)

### 5.5.2 Second prototype of pants

To address the problems of the first prototype of the pants, including that the end of the artificial back bone could not be secured during movement, and the difficulties of using hooks and eyes for the opening, a pelvis belt was attached from the end of artificial back bone to the front of the pants, and Velcro was used instead of the hooks and eyes, respectively.



Figure 5-10 Second prototype of pants on Subject 18001: (a) front and (b) back views

## 5.6 Development of artificial back bone

The function of the artificial back bone was intended to stabilise the corrective component that addressed lateral asymmetry, to provide space at the counter side of the corrective component for effective body alignment and to concur with body movements.

### 5.6.1 First prototype of artificial back bone

Figure 5-11 presents the schematic of the first artificial back bone prototype. The prototype was produced by using 3D jet printing. The back bones had obround slots. The bra top, corrective component and pelvis belt could be attached to the artificial back bone with straps through these slots.

The back bones were 3D printed with three different levels of hardness: a rigid resin with a hardness of Shore D86 was used for the body part and a soft resin with a hardness of Shore A40 and A70 was used for the joints. The soft resin joints allowed 3D movement of the body (Figure 5-12) which effectively stabilised the corrective component for body asymmetry yet did not restrict spinal movement. However, due to the weak bonding between the two different types of resins, the joints of the prototype easily broke off with large movement.

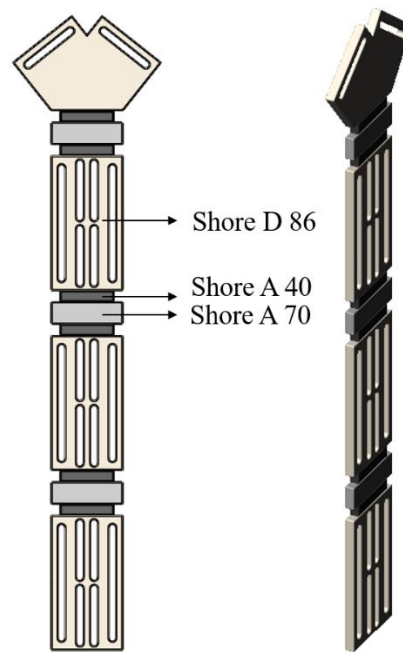


Figure 5-11 Illustration of first prototype of artificial back bone



Figure 5-12 Soft resin joints allow 3D movement of body



Figure 5-13 Broken off resin joint

### 5.6.2 Second prototype of artificial back bone

As the resin joints of the first prototype easily break off, hinges were used to replace the resin joints. The hinges were made of a rigid material which inhibited the rotation and loss of suspension of the brace and allowed forward bending. Similar to the first prototype, the obround slots on the leaf allowed attachment of the bra top, corrective component and pelvis belt. The prototype was produced with polyurethane (PU) by using 3D jet printing.

The second prototype consisted of 4 components, including the V-leaf, hinge pin and middle and end leaves. The leaves were joined with a hinge pin and the combination of each hinge couldn't be adjusted according to the required function and dimension. The V-leaf had one forked end and two obround slots to attach the shoulder straps that would stabilize the bra top onto the shoulders. The middle leaf had two forked ends and some obround slots for stabilising the corrective component. The end leaf had some obround slots, one forked end and one flat end for stabilising the pelvis belt. The function of the hinge pin was to lock into place the coupling of the forked ends of the leaves.

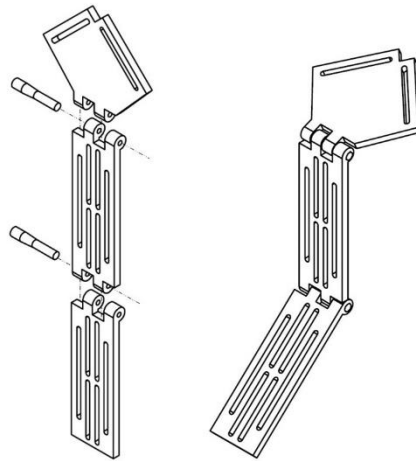


Figure 5-14 Schematic of artificial back bone with hinged joint



Figure 5-15 Second prototype of artificial back bone

### 5.6.3 Cushioning pad for artificial back bone

A scoliotic subject (Subject Code:18001) was invited to don the prototype with the artificial back bone with hinges. Her demographics are listed in Table 5-3. A short interview with the scoliotic subject on the comfort level of the artificial back bone with hinges was conducted. She said:

*The rigid material of the artificial back bone with hinges is uncomfortable. When I bend backwards, the hinges poke into my back and irritate my skin.*

To minimise the discomfort caused by the artificial back bone with hinges, a cushioning pad was inserted at the back of the hinges (Figure 5-16). The cushioning pad was made of EVA foam wrapped with fabric.



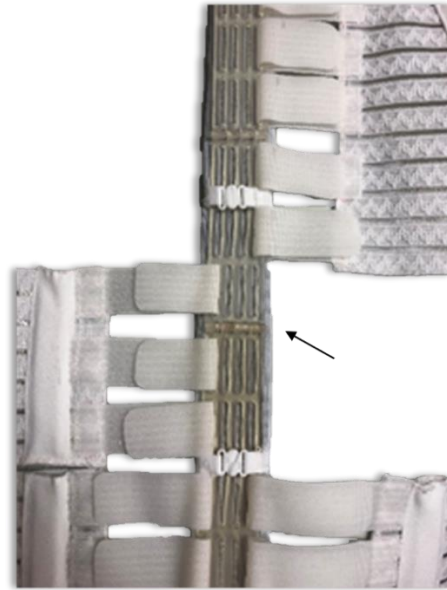


Figure 5-16 Cushioning pad inserted at back of hinge

### 5.7 Development of correction pad

The function of the correction pad is to enhance the exerted corrective pressure to correct spinal deformity. As mentioned in Chapter 4, flattening EVA foam caused the problem of conformity. Therefore, a semi convex pad was used. Figure 5-17 shows the mould of the correction pad. Due to its advantages of having a moderate hardness, a translucent appearance, small density, higher tear strength and high elongation at break, a silicone rubber, KE-1310ST, was used to mould the pad. Table 5-4 presents the specifications of KE-1310ST.

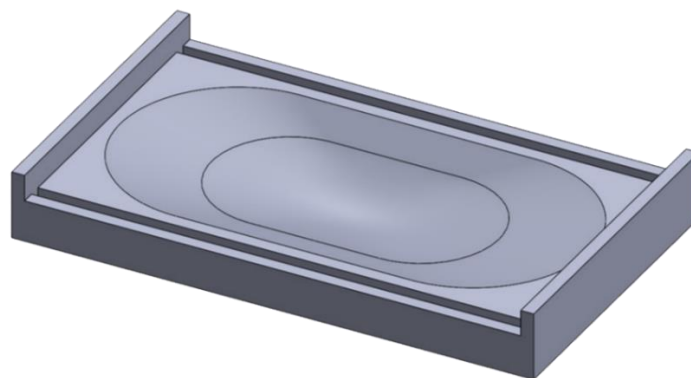


Figure 5-17 Schematic of mould of correction pad

Table 5-4 Specifications of KE-1310ST

Manufacturer	Shin-Etsu Chemical Co.
Code no.	KE-1310ST/CAT-1310
Cure type	Addition cure
Appearance	Translucent
Density at 23°C (g/cm <sup>3</sup> )	1.07
Viscosity (Pa·s)	75
Mix ratio by weight	100:10
Curing conditions	24 hours at 23°C
Working time	2 hours
Shore A hardness	40
Tensile strength (MPa)	5.9
Tear strength (kN/m)	23
% Elongation	380
Usable temperature range (°C)	-40 to +175

## 5.8 Fabric selection

The physical properties of the applied materials greatly affect the performance of the design in this study. Each component of the proposed design provided different functions and therefore involved different selection criteria. The mechanical performance, durability, thermal comfort, and sensorial comfort of the different materials were tested. As for the overall design, weft knitted fabric was used as the main fabric, elastic bands were used as the shoulder straps, upper and under bands, and corrective component. Besides the fabric structure, synthetic materials such as nylon spandex were used as they had high elasticity and good recovery, and were quick

to dry, and light in weight. As for the material selection for the proposed prototype, 4 types of knitted fabrics, 1 type of elastic for the strap and 4 types of elastics for the bands were pre-selected for material testing. The details of these materials are listed in Table 5-5.

Table 5-5 Specifications of tested material

Material	Code	Supplier	Structure	Composition	Fabric width	Weight (g/m <sup>2</sup> )
Fabric	DN64013S	Guangdong Derun Textile Co., Ltd.	Weft knit spacer	25% Spandex, 75% Micro Nylon	52"	320
	DXN873S	Guangdong Derun Textile Co., Ltd.	Weft knit interlock	36% Xtra Life Lycra, 64% Nylon	55"	225
	DN818SM	Guangdong Derun Textile Co., Ltd.	Weft knit interlock	38% Spandex, 62% Micro Nylon	60"	175
	DXN72001S	Guangdong Derun Textile Co., Ltd.	Weft knit interlock	34% Xtra Life Lycra, 66% Nylon	60"	190
Elastic band	R153132_166	Pioneer Elastic	Woven	N/A	166mm	-
Elastic strap	1280914_25	Pioneer Elastic	Woven	88% Stretch nylon, 2% bright yarn and 10% Spandex	25mm	-
	1280761_25	Pioneer Elastic	Woven	10% Nylon66, 80% Stretch nylon and 10% Spandex	25mm	-
	4443_25	Pioneer Elastic	Woven	90% Stretch nylon and 10% Spandex	25mm	-

	4246_25	Pioneer Elastic	Woven	90% Stretch nylon and 10% Spandex	25mm	-
--	---------	--------------------	-------	--------------------------------------	------	---

### 5.8.1 Stretch and recovery testing

The stretchability and recoverability of fabric are the most important considerations for a compression garment since such garments have to exert continuous pressure onto the body. The elastic properties are a significant factor that influences the actual amount of compression (Xiong & Tao, 2018).

The modulus is also an important criterion in selecting the material for the corrective component, main fabric and elastic straps. It is directly related to the interface pressure between the body and garment during stretching and determines the amount of resistance against deformity under intensive load. Due to the rigidity of the elastic band and elastic straps and their application, these materials were only subjected to stretch and recovery testing in the warp direction. Figure 5-18, Figure 5-19 and Figure 5-20 present the stress-strain curves of the four types of fabric and one elastic band in the warp direction, four types of fabric in the weft direction and four elastic straps in the weft direction respectively.

Figure 5-18 shows that Elastic Band R153132\_166 had an outstanding modulus followed by Fabrics DXNB873S, DNX64013S, DN818SM and then DXN72001S. Elastic Band R153132\_166 had a complex structure with a monofilament inlay, so it had the highest modulus. The elastic behaviour of a fabric was usually influenced by its structure. Therefore, in considering Fabrics DXNB873S, DN818SM and DXN72001S which had a similar fibre content and knit structure, it was found that the fabric weight was positively related to the modulus. This finding was in agreement with the findings of the structure and mechanics of knitted fabric in Schwartz and Textile (2008). In general, the fabric weight is related to the fabric density. A denser material implies that there are more fibres that resist the forces from stretching and a high modulus would be the result.

Figure 5-19 shows an interesting finding. The modulus of Fabric DN64013S was very high in the weft direction while the other three types of fabrics had a low modulus. A possible explanation was that Fabric DN64013S had a 3D spacer structure which enabled it to withstand stress in both the warp and weft directions.

Among the four types of elastic straps, Elastic Straps 4443\_25 and 4246\_25 had a relatively high modulus. Some parameters such as the ratios of the warp to weft yarn length per crossing

yarn , yarn diameter to yarn modular length, yarn compression rigidity to bending rigidity, yarn extension rigidity to bending rigidity, yarn compression index, and woven structure might affect the tensile properties of a woven material (Hu, 2004).

Moreover, it was also interesting to observe in Figure 5-18 that the curve pattern of Elastic Band R153132\_166 was different from the other four types of elastic bands. At the beginning of the stretching, the slope of Elastic Band R153132\_166 was very steep and gradually declined until about 40 mm which indicated a high moment of inertia. Then, the slope started to gradually increase. This pattern was similar to the stretching of the elastic straps plotted in Figure 5-20. It showed the elastic behaviour of typical elastic webbing. On the other hand, Figure 5-18 and Figure 5-19 show that the curves of the weft knitted fabric were relatively simple. Their slope was initially low and then gradually increased until the fabrics were 100% stretched. A possible explanation of the low slope at the initial stage of stretching was the presence of de-crimping and crimp-interchange of the fibre and yarn (Hu, 2004).

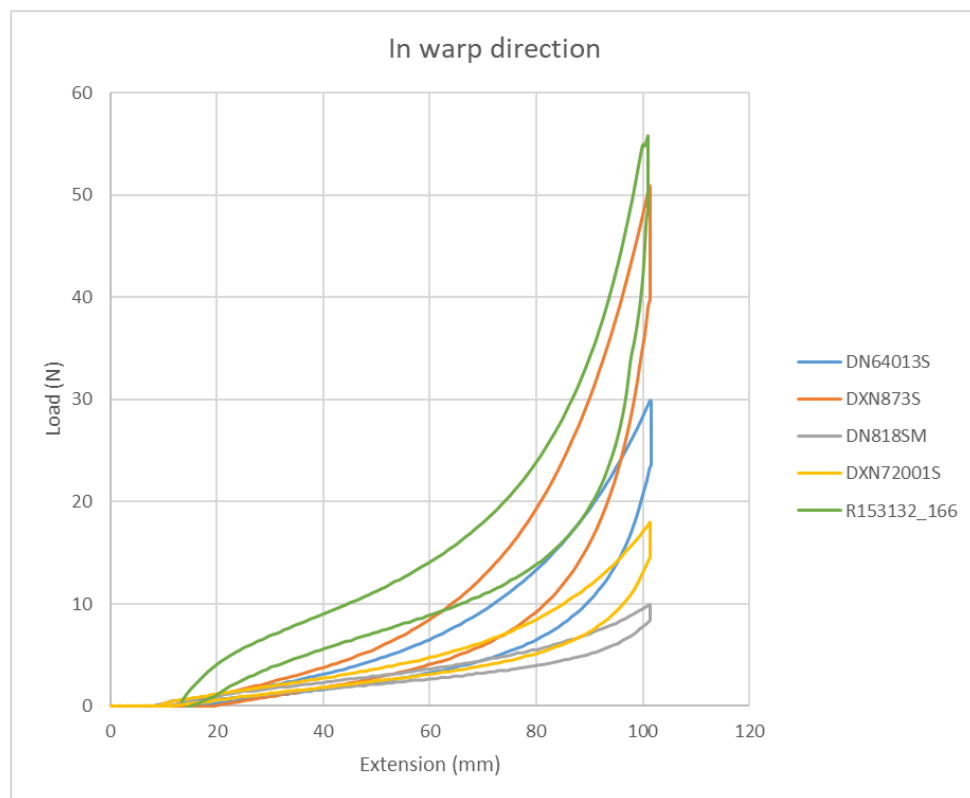


Figure 5-18 Stress-strain curves for 5<sup>th</sup> cycle of stretching four types of fabric in warp direction

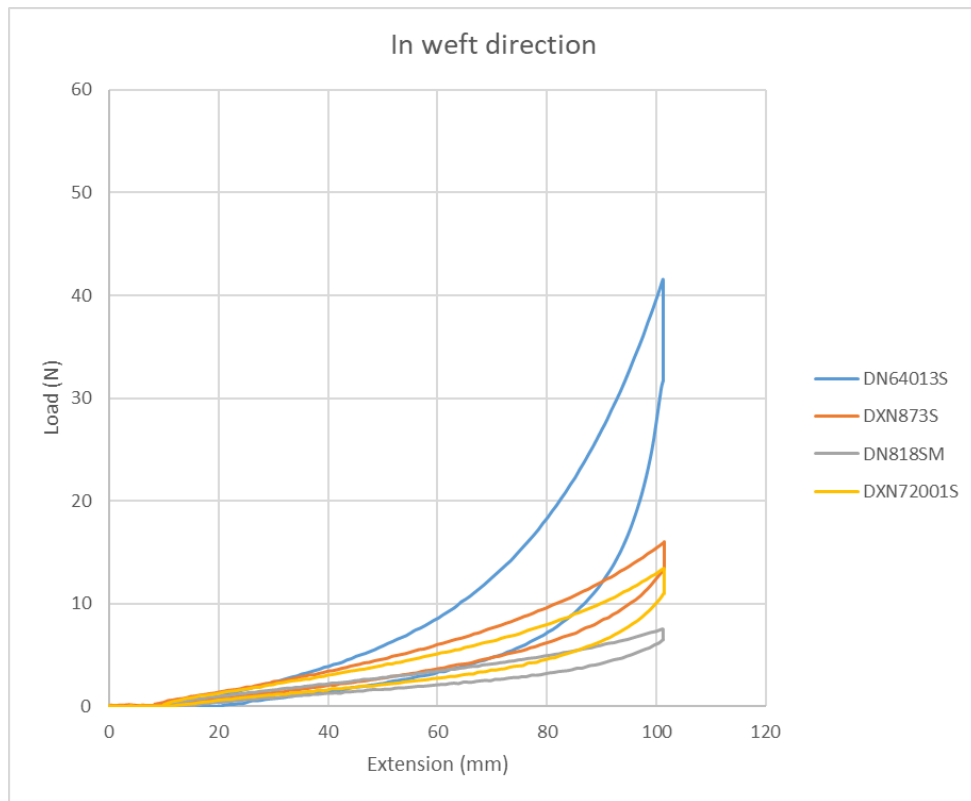


Figure 5-19 Stress-strain curves at 5<sup>th</sup> cycle of stretching four types of fabric in weft direction

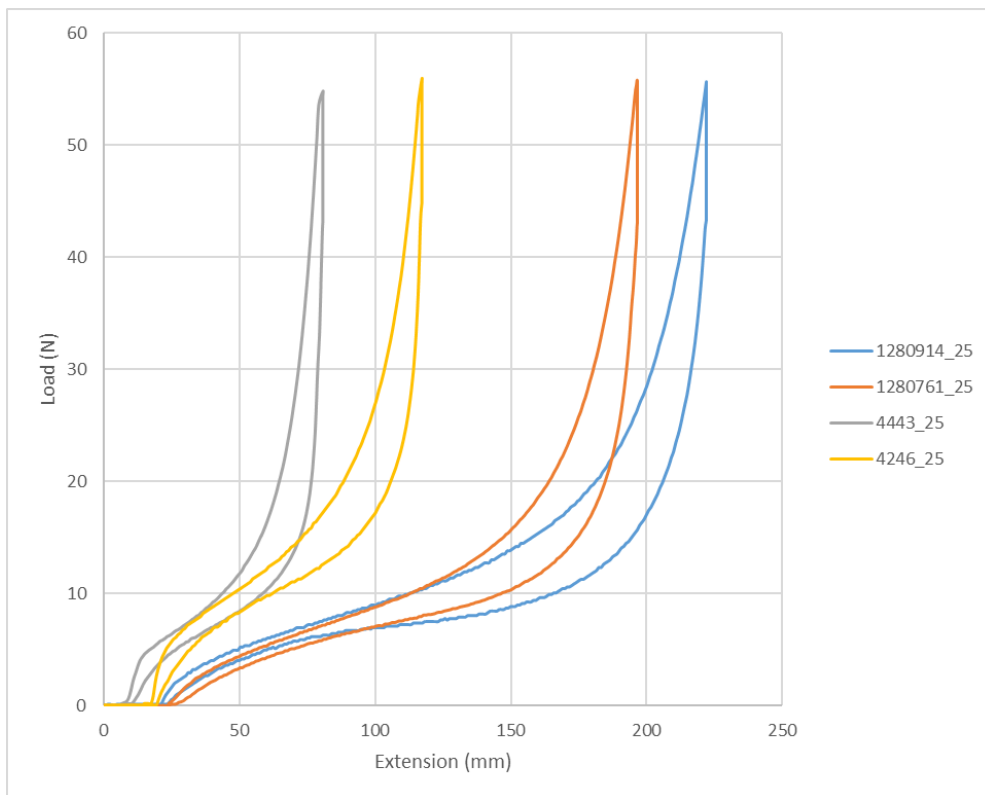


Figure 5-20 Stress-strain curves at 5<sup>th</sup> cycle of stretching five types of elastic bands in warp direction

Apart from the stress-strain curves, the force decay due to time and repeated exercise and recoverability also influence whether a consistent pressure is exerted and the ability to resist deformation under intensive load. When a fabric is under tension for over a period of time and subjected to repeated stretching, some of its stress is lost. This loss of stress would be considered as force decay over time and force decay over repeated exercise. Moreover, repeated stretching that results in high extension, yarn slippage or fibre extension might occur which causes irreversible elongation called plastic deformation (Hu, 2004; Postle, 1988). Thus, the force decay and elongation would reduce the interface pressure between the skin and garment. To provide consistent fit and compression control, the ideal material should have a low force decay and unrecoverable elongation.

Figure 5-21 and Figure 5-22 show the results of testing for force decay and unrecoverable elongation. Figure 5-21 shows that Elastic Band R153132\_166 had an extraordinarily low force decay due to exercise and good recoverability. This showed that Elastic Band R153132\_166 provided a relatively consistent amount of pressure on the body after repeated stretching.

Among the four different types of fabrics, Fabric DN818SM had a relatively low force decay and good recoverability. It was interesting to see that the force decay and unrecoverable elongation were positively related to the modulus. Since the fabric sample was extended to 100% during the experiment, the high modulus fabric would experience a large stretching force. Thus, the high modulus fabric resulted in a high force decay and unrecoverable elongation.

Among the four types of elastic straps in Figure 5-22, Elastic Strap 1280914\_25 showed a relatively low force decay. As mentioned above, a higher modulus material showed a higher force decay in the experiment. The results of the elastic straps were in agreement with this statement. Surprisingly, Elastic Strap 4443\_25 had the best recoverability. The shoulder strap was a narrow fabric and thus the sample was stretched to 53 N instead of 100% during the experiment. Elastic Strap 4443\_25 was extended to about 80 mm while the rest of the straps were extended to more than 120 mm, which might have exceeded the elastic limits and resulted in plastic deformation.

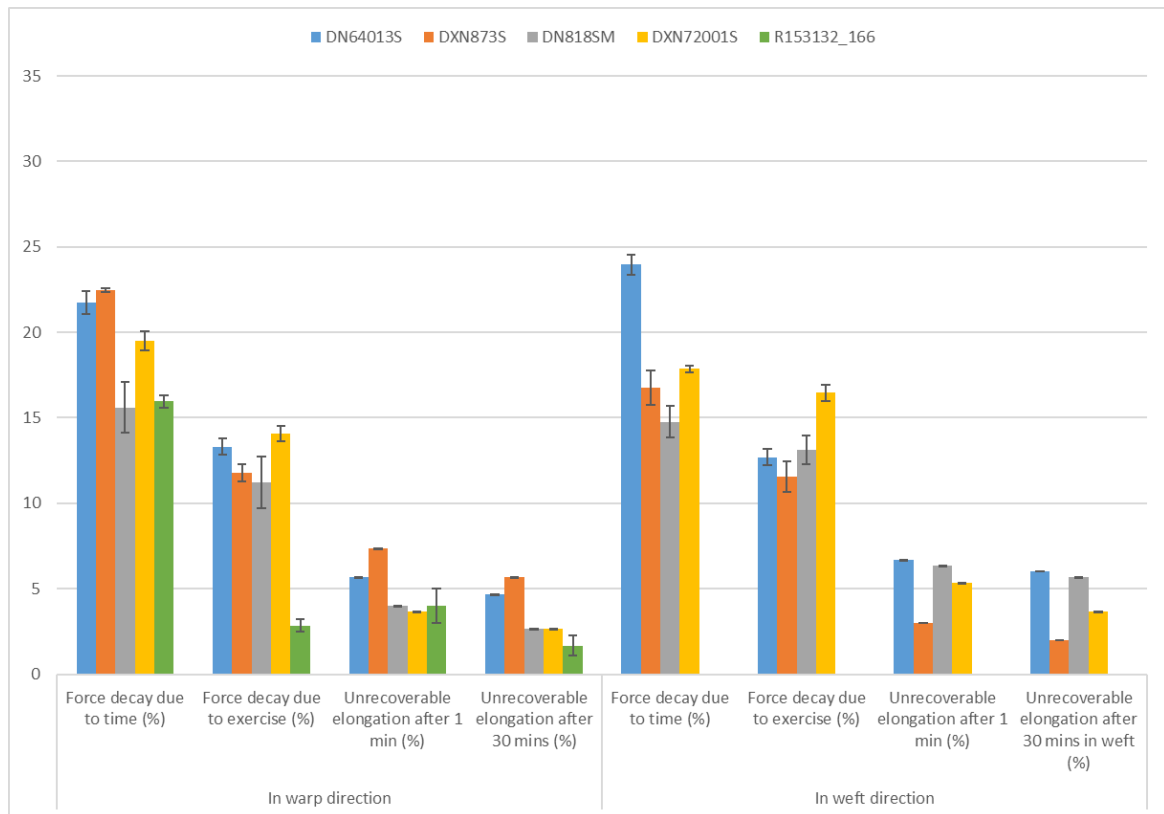


Figure 5-21 Bar chart of stretch and recovery test results of four types of fabric and one elastic band

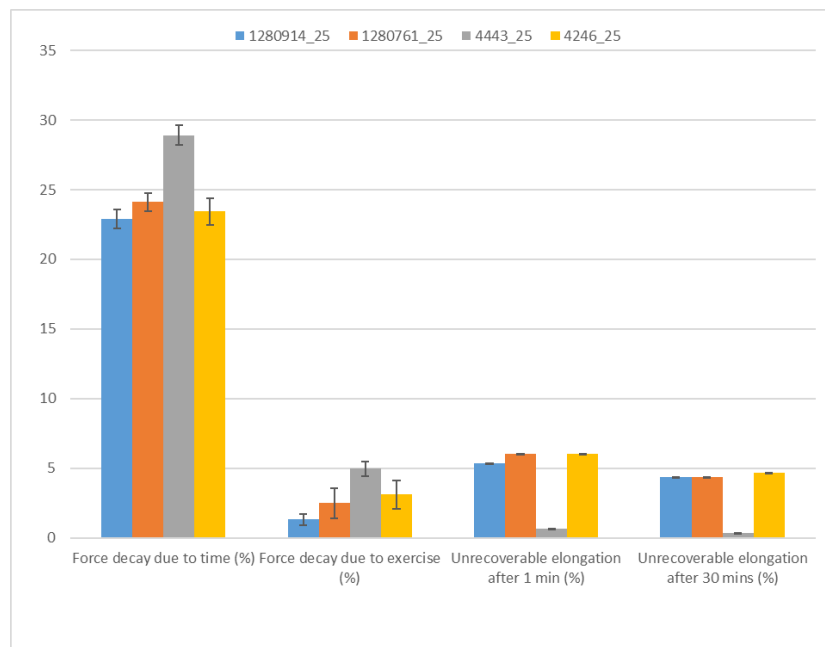


Figure 5-22 Bar chart of stretch and recovery test results of four types of elastic straps

## 5.8.2 Water vapor permeability test

Water vapor permeability is related to fabric comfort and regarded as one of the criteria for



comfort with intimate apparel as it allows ventilation of the skin surface by transferring sweat away into the surroundings. Therefore, the water vapor permeability of the four types of fabric was assessed for selecting the fabric for the functional intimate apparel in this study. The water vapor permeability test examines the amount of water vapor that passes from the skin to the surroundings through fabric. Thus, fabric with a large water vapor permeability value would provide a more comfortable wear experience. In Figure 5-23, Fabrics DN64013S and DXN72001S provided outstanding water vapor permeability. Thus, these two fabrics allowed for good wear comfort. The water vapor permeability is usually related to the fibre content, and yarn and fabric structures. In general, hydrophilic and hollow fibres, fibres with a special cross-section for wrinkling and mesh material promote water vapor permeability.

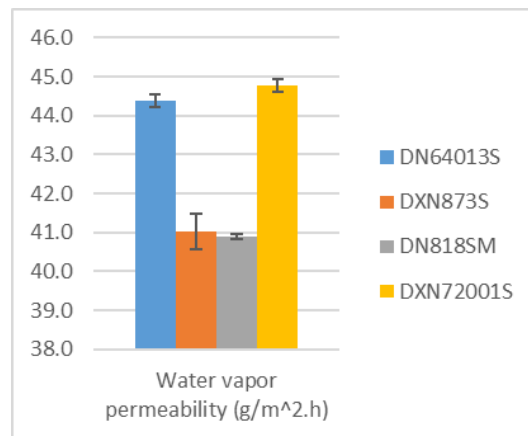


Figure 5-23 Bar chart of water vapor permeability test results of four type of fabric

### 5.8.3 Air permeability test

Apart from water permeability, air permeability also influences the wear comfort of a fabric. Air permeability testing measures the resistance of air flowing from one side to the other side of a textile material. The air resistant value is negatively proportion to the air permeability. In other words, a high air resistance value indicates poor air permeability. Figure 5-24 shows that Fabrics DN828SM and DXN72001S have good air permeability.

According to Yip and Ng (2008), there were several factors that affect air permeability, for example, fabric structure, density, thickness, surface and characteristics of the yarn. In considering Fabrics DXN873S, DN818SM and DXN72001S, the result showed that air permeability was related to the fabric weight. A denser fabric had a larger amount of fibre which blocked air and thus resulted in low air permeability. However, in comparing Fabrics DN64013S and DXN873S, even if the former had a lower weight, it still had good air

permeability due to its unique 3D spacer structure. This showed that aside from fabric density, the knit structure also influenced the air permeability.

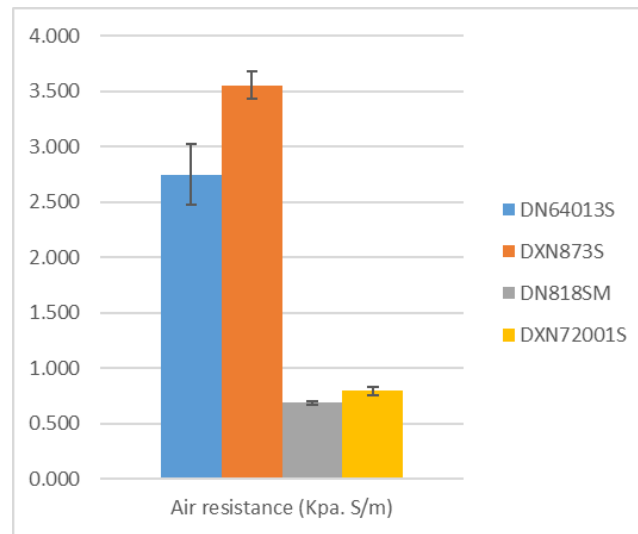


Figure 5-24 Bar chart of air permeability test results of four types of fabric

#### 5.8.4 Thermal conductivity test

Thermal conductivity is critical for intimate apparel, as it is related to determining the thermal microclimate of the skin surface. Thermal conductivity testing measures the amount of heat transferred from the skin surface to the surroundings through the fabric. A high thermal conductivity value implies that the fabric has good ability to dissipate body heat away from the skin. Figure 5-25 shows that Fabric DN64013S had the highest thermal conductivity value and thus would provide relatively good thermal comfort to the wearer. Fabric structure, thickness, density and the thermal conductivity of yarn were other possible influential factors of thermal conductivity (Yip & Ng, 2008). The result here showed that the spacer knit structure provided better thermal conductivity than the weft knit interlock structure. Moreover, the result showed that thermal conductivity was positively related to fabric thickness.

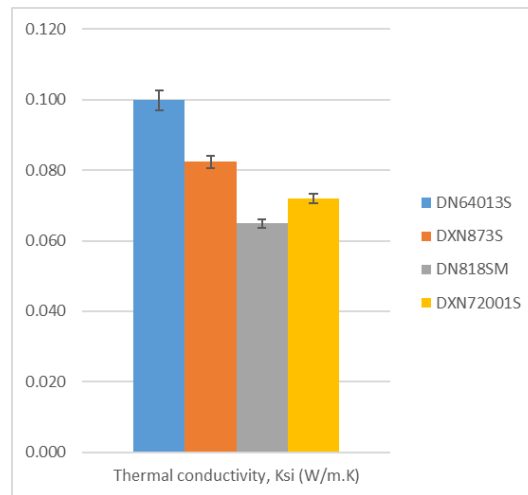


Figure 5-25 Bar chart of thermal conductivity test results of four types of fabric

### 5.8.5 Tensile test

To further evaluate the sensorial comfort of the fabric samples, their tensile properties at low stress were also considered. Tensile testing measures the tensile rigidity, energy and recoverability. A tensile rigidity value that approximates 1 indicates a higher tensile strength. The tensile recoverability reflects the stretchability of a material. A tensile recoverability value closer to 100 points means good recoverability. Table 5-6 shows that all of the fabrics had a similar tensile rigidity. Fabrics DN818SM and DXN72001S had a relatively higher stretchability and good recoverability at low stress. The tensile properties at low stress were related to the composition of the fibre content. The result in this study showed that a high percentage of spandex enhanced stretchability and recoverability.

Table 5-6 Results of tensile testing of four types of fabric

Fabric Sample	Tensile Rigidity, LT				Tensile Energy, WT				Tensile Recoverability, RT			
	Warp		Weft		Warp		Weft		Warp		Weft	
	Mean	SD	Mean	SD	Mean	SD	Mean	SD	Mean	SD	Mean	SD
DN64013S	1.04	0.02	1.04	0.02	4.68	0.09	3.49	0.11	75.00	0.45	65.76	1.41
DXN873S	1.00	0.00	1.04	0.01	2.67	0.03	4.22	0.11	79.22	0.69	75.71	0.97
DN818SM	1.10	0.01	1.10	0.01	8.12	0.30	6.96	0.26	82.24	1.20	69.70	0.37
DXN72001S	1.07	0.00	1.04	0.01	5.56	0.07	3.81	0.03	82.59	0.41	71.70	0.30

### 5.8.6 Shearing test

The shear properties reflect the hand feel of a fabric, which is very much related to sensorial comfort (Barker, 2002). A shearing test measures the shear rigidity, elasticity for minute shear and elasticity for large shear. A large shear rigidity value means a stiff fabric. A large elasticity for minute shear value indicates poor recoverability from the initial shear deformation. A large elasticity for large shear value means poor recovery. Thus, an ideal fabric should have low shear rigidity, low elasticity for minute shear and low elasticity for large shear. Table 5-7 shows that Fabric DN828SM had relatively low shear rigidity, elasticity for minute shear and elasticity for large shear values, which indicated a good shear property. The results showed that the shear properties were related to the material thickness and material weight. In general, a thicker or denser material is usually more rigid and has poor recoverability after the initial shear deformation and poor recovery.

Table 5-7 Results of shearing testing of four types of fabric

Fabric Sample	Shear Rigidity, G				Elasticity for Minute Shear, 2HG				Elasticity for Large Shear, 2HG5			
	Warp		Weft		Warp		Weft		Warp		Weft	
	Mean	SD	Mean	SD	Mean	SD	Mean	SD	Mean	SD	Mean	SD
DN64013S	1.09	0.03	1.21	0.01	1.71	0.10	1.77	0.06	1.95	0.08	2.25	0.07
DXN873S	1.37	0.01	1.38	0.03	1.69	0.03	1.64	0.02	1.44	0.02	1.59	0.02
DN818SM	0.68	0.04	0.72	0.02	1.02	0.08	1.07	0.05	1.20	0.06	1.40	0.04
DXN72001S	0.97	0.04	1.08	0.02	1.13	0.06	1.39	0.10	1.31	0.01	1.62	0.05

### 5.8.7 Bending test

The bending properties are related to the fabric softness which is also a factor of hand feel. A bending test measures the bending rigidity and bending hysteresis. A high bending rigidity value indicates more rigid bending while a high bending hysteresis value reflects poor recoverability. Table 5-8 shows that Fabric DN818SM had a low bending rigidity and good bending recoverability. The results showed that the bending rigidity and recoverability were related to the material weight. In general, a denser fabric is more difficult to bend and has less recoverability. Since a denser fabric usually consists of a large amount of fibres, more force is required to bend the material and thus a greater moment of inertia to return to its original position.

Table 5-8 Results of bending test for four types of fabric

Fabric Sample	Bending Rigidity, B				Bending Hysteresis, 2HB			
	Warp		Weft		Warp		Weft	
	Mean	SD	Mean	SD	Mean	SD	Mean	SD
DN64013S	0.10	0.00	0.06	0.00	0.08	0.00	0.04	0.00
DXN873S	0.05	0.00	0.00	0.00	0.03	0.01	0.02	0.00
DN818SM	0.02	0.01	0.01	0.00	0.02	0.01	0.02	0.00
DXN72001S	0.04	0.00	0.02	0.00	0.03	0.01	0.02	0.01

### 5.8.8 Compression test

The compression properties determine the fabric fullness, softness, smoothness and anti-drape stiffness which also are one of the parameters of sensorial comfort. Compression testing measures the compressional linearity, energy and recoverability. A compression linearity value closer to 1 indicates that the material is firm under compression. A high compressional energy value means high susceptibility to compression. A compressional recoverability that approximates 100 means that the material has good recoverability. Table 5-9 shows that all of the fabrics had similar compression, compression susceptibility and compression ability.

Table 5-9 Results of compression testing of four types of fabric

Fabric Sample	Compressional Linearity, LC		Compressional Energy, WC		Compressional Recoverability, RC	
	Mean	SD	Mean	SD	Mean	SD
DN64013S	0.5	0.01	0.1	0	39.9	1.06
DXN873S	0.6	0.02	0.1	0	54.1	2.56
DN818SM	0.4	0.01	0.2	0.01	43.6	0.6
DXN72001S	0.4	0.01	0.1	0.01	51	2.49

### 5.8.9 Surface test

Testing the surface properties allow the fullness, softness, smoothness and crispness of fabrics to be determined, which are also related to sensorial comfort. Surface tests measure the mean friction coefficient, fluctuation of the mean friction coefficient and surface roughness. A high mean friction coefficient value denotes less tendency to slip. A high fluctuation of mean friction

coefficient value means less smoothness and more roughness. A high surface roughness value indicates more surface unevenness. Table 5-10 shows that Fabric DN64013S had a relatively smoother and even surface and Fabric DN818SM was relatively less prone to slipping.

Table 5-10 Results of surface testing of four types of fabric

Fabric sample	Mean Friction Coefficient, MIU				Fluctuation of Mean Friction Coefficient, MMD				Surface Roughness, SMD			
	Warp		Weft		Warp		Weft		Warp		Weft	
	Mean	SD	Mean	SD	Mean	SD	Mean	SD	Mean	SD	Mean	SD
DN64013S	0.19	0.00	0.18	0.00	0.00	0.00	0.00	0.00	0.67	0.06	1.13	0.06
DXN873S	0.15	0.00	0.16	0.01	0.00	0.00	0.01	0.00	0.66	0.04	3.40	0.06
DN818SM	0.21	0.01	0.21	0.00	0.00	0.00	0.01	0.00	1.04	0.12	1.44	0.05
DXN72001S	0.14	0.00	0.19	0.00	0.00	0.00	0.01	0.00	0.80	0.02	4.27	0.04

#### 5.8.10 Dimensional changes to laundering test

Testing dimensional stability to laundering is important for material selection since it is related to material durability, fit and mechanical performance. According to ASTM D7019-14 Standard Performance Specification for Brassiere, Slip, Lingerie and Underwear Fabrics, the tolerance of dimensional changes of elastic fabric to laundering should be a maximum of 5%. Figure 5-26 and Figure 5-27 present the results of the laundering test. The results in general showed that all of the samples had good dimensional stability to laundering and all of the dimensional changes were within 3.5%. Moreover, it was surprising that all of the elastic band and elastic strap samples did not show dimensional changes in the weft direction after laundering. A possible explanation for this phenomenon could be due to their rigid weft yarns and densely woven structure.

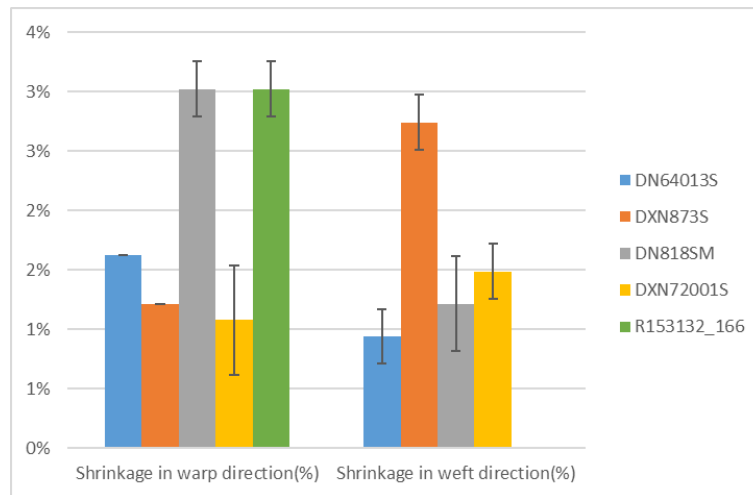


Figure 5-26 Bar chart of dimensional changes to laundering results of four types of fabric and one elastic type of band

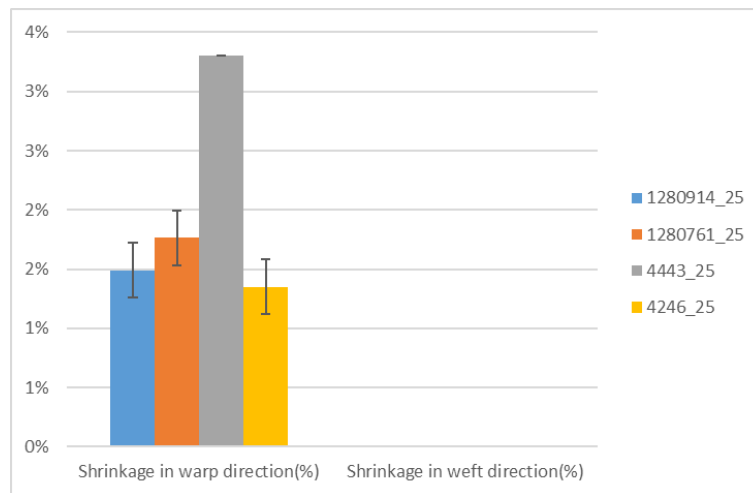


Figure 5-27 Bar chart of dimensional changes to laundering results of four types of elastic strap material

## 5.8.11 Overall evaluation based on test results

### 5.8.11.1 Material for corrective component

Regarding the material selection for the corrective component, only four types of fabric and one type of elastic band were considered due to the limitation of the size of the component. The function of the corrective component was to provide a constant amount of interface pressure between the body and garment. Thus, the mechanical performance was the main criterion for its material selection. Figure 5-18 shows that Elastic Band R153132\_166 had the highest modulus, which meant that this material could exert the largest amount of pressure onto the body under the same amount of extension. Moreover, Figure 5-21 shows that Elastic Band

R153132\_166 had a low force decay with time and exercise and low unrecoverable elongation. These implied that Elastic Band R153132\_166 could provide relatively consistent pressure. In addition, the laundering test to determine durability showed that the dimensional stability of Elastic Band R153132\_166 was good and met the specification requirement for underwear. Therefore, Elastic Band R153132\_166 was selected for use as the corrective component.

#### **5.8.11.2 Main fabric**

Regarding the material selection for the main fabric used for the garment, the mechanical properties, thermal comfort, sensorial comfort and durability were all considered. The fabric used should have a high modulus in order to withstand the intensive pressure and resist deformation during stretching and compression. Figure 5-18 and Figure 5-19 show that Fabric DXN873S had the highest modulus in the warp direction. However, its modulus in the weft direction was much lower. Therefore, this fabric sample might not be able to withstand intensive pressure exerted by a 3D body. On the other hand, Fabric DN6013S had a relatively high modulus in both the warp and weft directions. Thus, Fabric DN6013S was relatively able to resist deformation after the corrective component was attached.

Regarding the thermal comfort, the water vapor and air permeability tests and thermal conductivity test suggested that Fabric DN64013S followed by Fabric DXN873S provided outstanding thermal comfort and thus offered good microclimate control between the skin surface and the fabric.

Regarding the sensorial comfort, the ideal material of the main fabric should have a low tensile rigidity, high tensile stretchability, good tensile recoverability, low bending rigidity, high bending recoverability, easily compressible, high compression susceptibility, high compression recoverability, low shearing rigidity, high shearing recoverability, less tendency to slip, more smoothness, less roughness and more surface evenness. Considering the tensile behaviour, Figure 5-28 shows that Fabric DN818SM had a relatively low tensile rigidity, but outstanding stretchability and good recoverability. In considering the bending behaviour, Figure 5-28 shows that Fabric DN818SM had a low bending rigidity but good recoverability. In considering the shear behaviour, Figure 5-28 shows that Fabric DN818SM had low shearing rigidity, but good recoverability. In considering the compression behaviour, Figure 5-28 shows that Fabric DN818SM had good compression susceptibility yet moderate compression recoverability. In considering the surface behaviour, Figure 5-28 shows that Fabric DN64013S had outstanding surface evenness, good surface smoothness and moderate tendency to slip. In summary, Fabric



DN818SM had the highest sensorial comfort followed by Fabric DN64013S.

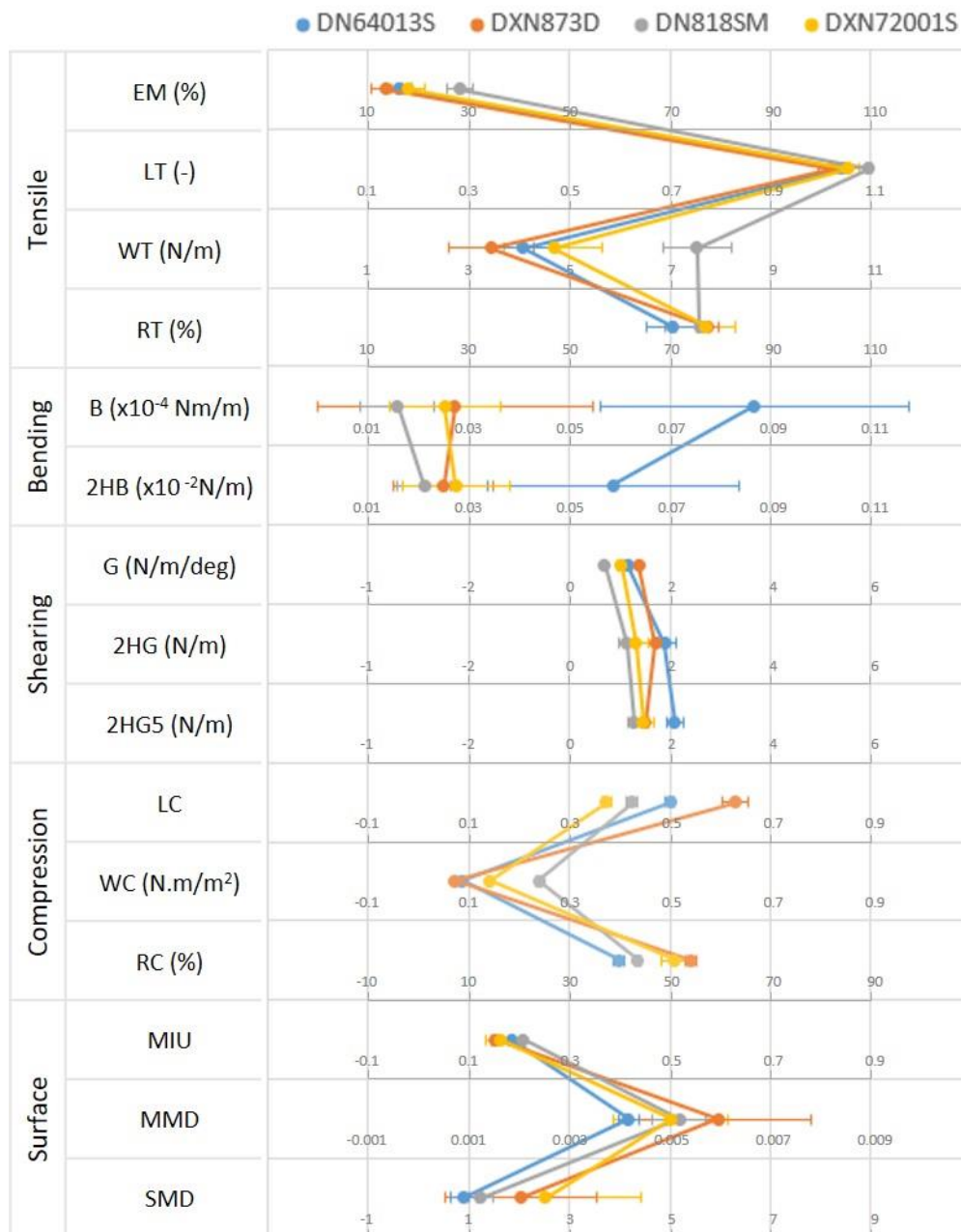


Figure 5-28 Overall sensorial comfort result of four types of fabric

As for durability, the ideal material should be able to withstand dimensional changes during laundering. Figure 5-26 shows that Fabric DN64013S had the least amount of shrinkage overall in terms of dimensional changes during laundering.

Taking into consideration the overall performance, Fabric DN64013S was selected as the main fabric due to its outstanding tensile behaviour, excellent thermal comfort, moderate sensorial comfort, and good dimensional stability during laundering.

### **5.8.11.3 Material for elastic webbing of bra top and pants**

Based on the stress-strain curves for the 5<sup>th</sup> cycle of stretching of the five types of elastic straps in the warp direction as shown in Figure 5-20, Elastic Strap 4443\_25 had the most outstanding modulus which was the ability to greatly resist deformation under tension. More importantly, the result implied that under the same amount of stretching, this elastic strap could still exert a relatively high compressive force which resulted in a higher interface pressure. As such, a corrective component with a higher modulus of elasticity could exert higher corrective forces onto the body. Furthermore, Elastic Strap 4443\_25 showed excellent recoverability after the tensile testing which indicated good dimensional stability after repeated use. As for durability, the laundering test showed that the dimensional stability of all of the elastic straps was good and therefore met the specification requirement for underwear. However, due to its outstanding modulus, excellent recoverability and good dimensional stability during laundering, Elastic Strap 4443\_25 was selected as the elastic webbing of the bra top and pants.

## **5.9 Pattern development process**

The pattern was derived from a basic block pattern in Shin (2015). The pattern of the proposed functional intimate apparel consists of five parts which included the bra top, pants, corrective component, pelvis belt, and cushioning pad for the hinges on the artificial back bone. The bra top included the bra cups, cradle, Velcro opening, hook and eye opening, Velcro for attaching the corrective component to the side of the bra top and upper abdominal, upper band, under band, abdominal band and shoulder straps. The pants included the front, side and back panels, Velcro for attaching the corrective component to the lower abdominal and pelvis belt, and a waist band. The corrective component consisted of two layers which were an outer layer of elastic band and a lining layer of the main fabric. The pelvis belt was a piece of elastic that covers the circumference of the pelvis with Velcro ends. The cushioning pad for the hinge of the artificial back bone had a shell panel constructed from the main fabric and cushioning pad made of EVA foam.

### **5.9.1 3D scanning measurements**

Body measurements are essential to this functional intimate apparel. To obtain the measurements, twenty-one female scoliotic subjects underwent body measurements with a 3D scanner to develop the pattern of the garment. Of 21 subjects, there were 11 (52.4%) subjects with a Lenke 1 curve, 3 (14.3%) with a Lenke 3 curve, and 7 (33.3%) with a Lenke 6 curve.

Table 5-11 lists their demographics. Table 5-12 shows the results of the body measurements.

The results of the body measurements in Table 5-13 show that BMI was positively correlated to all of the circumferential measurements. A Kendall's Tau-b correlation was run to determine the relationship between the BMI and all of the circumferential measurements among the 21 subjects. It was found that there was a highly positive correlation between the BMI and upper breast, under breast, under band, pelvis, and hip circumferences, which were statistically significant at  $r = .415$ ,  $p=.009$ ,  $r= .478$ ,  $p=.003$ ,  $r= .498$ ,  $p=.002$ ,  $r= .478$ ,  $p=.003$ , and  $r= .612$ ,  $p=.000$ , respectively. There was also a highly positive correlation between the BMI and leg hole, which was statistically significant at  $r= .679$ ,  $p=.000$ .

Furthermore, there was a positive correlation among all of the circumferential measurements. A Kendall's Tau-b correlation was run to determine the relationships among all of the circumferential measurements. There was a statistically significant positive correlation among the circumferential measurements of the upper breast, under breast, under band, pelvis, hip, and leg hole. Table 5-13 presents the correlation coefficient and p values among these circumferential measurements after conducting the Kendall's Tau-b correlation test.

Moreover, Table 5-12 shows that the standard deviation of some of the measurements was quite large. Since the proposed design was a tightly fitting garment, it was difficult to develop a one size prototype that would fit each subject well. The above findings therefore might be useful for clustering body size in pattern development.

Table 5-11 Demographics of 21 scoliotic subjects for 3D scanning measurements

n=21	Age (years old)	Height (cm)	Weight (kg)	BMI	Cobb's angle (°)
Mean	12.4	153.5	44.5	18.9	17.2
S.D.	0.7	4.1	5.2	2.3	4.3

Table 5-12 Results of body measurements

	a	b	c	d	e	f	g	j	i	j
n=21	Upper breast CIR (mm)	Under breast CIR (mm)	Under band CIR (mm)	Pelvis CIR (mm)	Hip CIR (mm)	Leg hole (mm)	Waist to gusset (mm)	Under band to pelvis (mm)	Upper breast to pelvis (mm)	Shoulder strap length (mm)
Mean	772	681	675	802	871	513	195	78	359	385

S.D.	35	39	61	49	50	40	25	26	31	24
Max.	834	760	838	916	974	594	260	146	439	427
Min.	700	608	583	717	766	444	154	42	311	343

Note: CIR denotes circumference

Table 5-13 Kendall's Tau-b correlation results

n=21		Upper breast	Under breast	Under band	Pelvis	Hip	Leg hole
Upper breast	Correlation coefficient	-	.539	.654	.415	.453	.453
	Sig.		.001	.000	.009	.004	.004
Under breast	Correlation coefficient	-	-	.488	.450	.536	.632
	Sig.			.002	.004	.001	.000
Under band	Correlation coefficient	-	-	-	.526	.612	.498
	Sig.				.001	.000	.002
Pelvis	Correlation coefficient	-	-	-	-	.545	.488
	Sig.					.001	.002
Hip	Correlation coefficient	-	-	-	-	-	.699
	Sig.						.000

### 5.9.2 Prototype size

Table 5-12 shows that there was a substantial difference between the smallest and largest measurements. Therefore, it was difficult to create a one-size prototype that would fit all of the subjects. On the other hand, tailor made prototypes for each subject would be time consuming and inefficient. Therefore, the prototype was created in two sizes (small and medium). As the BMI was statistically correlated to all of the circumferential dimensions and all of the circumferential dimensions are statistically correlated, the prototype size was clustered according to the BMI.

Patients with a BMI below 18.5 were considered underweight and therefore prescribed the small sized prototype, while patients with a BMI between 18.5 and 24.5 were considered to have a normal weight and recommended to use the medium sized prototype. See allocation of prototype based on BMI in Table 5-14.

Table 5-14 Allocation of prototype based on BMI

Size		a	b	c	d	e	f	g	j	i	j
		Upper breast CIR (mm)	Under breast CIR (mm)	Under band CIR (mm)	Pelvis CIR (mm)	Hip CIR (mm)	Leg hole (mm)	Waist to gusset (mm)	Under band to pelvis (mm)	Upper breast to pelvis (mm)	Shoul-der strap length (mm)
S n=7	Mean	744	650	620	764	822	208	90	368	473	375
	S.D.	28	32	27	38	30	33	34	41	17	23
M n=14	Mean	785	697	703	821	895	188	72	354	533	390
	S.D.	30	32	54	43	39	17	19	24	33	24

Note: CIR denotes circumference

### 5.9.3 Prototype pattern

The pattern for each prototype was made by referring to the measurements in Table 5-14. In order to provide a tight-fit, 25% shrinkage of the circumferential measurements was applied when drafting the pattern. In total, 35 pieces were constructed for the proposed functional intimate apparel prototypes, including one thoracic and one lumbar corrective component. Figure 5-29, Figure 5-30, Figure 5-31, Figure 5-32 and Figure 5-33 are the patterns of the bra top, pants, cushioning pad, pelvis belt and corrective components, respectively.

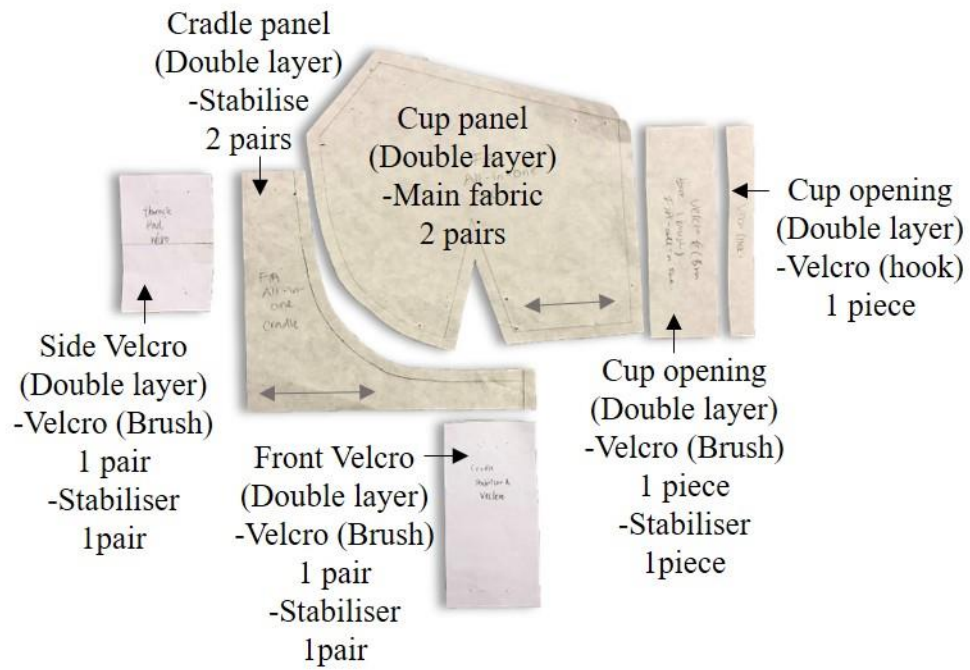


Figure 5-29 Bra top pattern

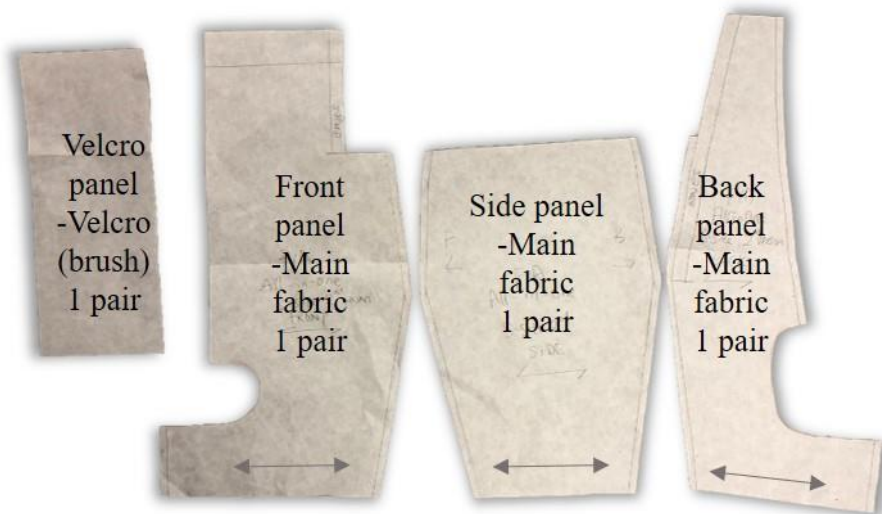


Figure 5-30 Pants pattern

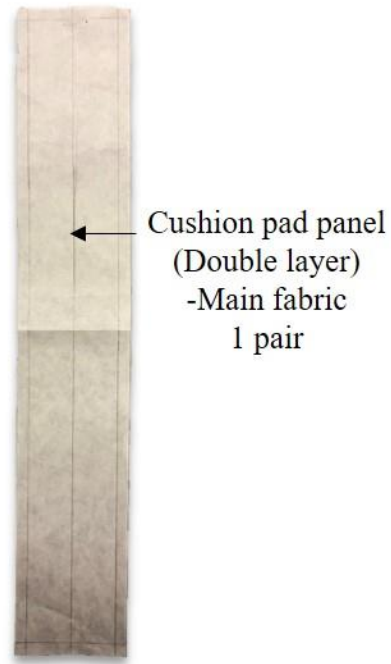


Figure 5-31 Cushioning pad pattern

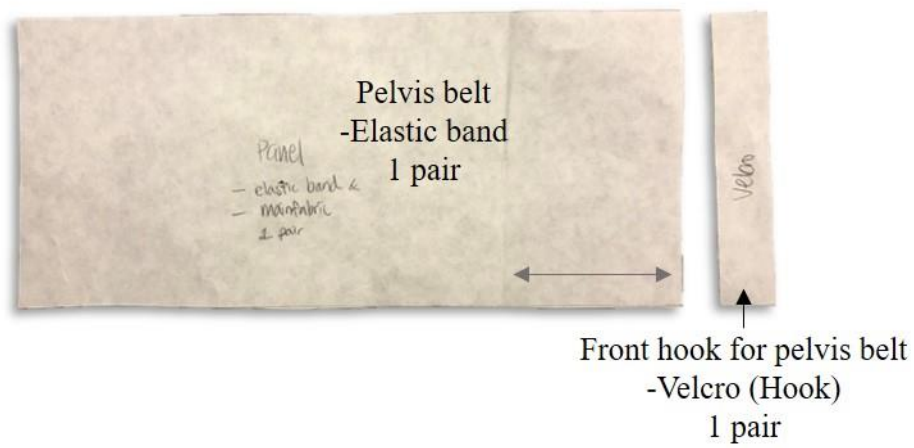


Figure 5-32 Pelvis belt pattern

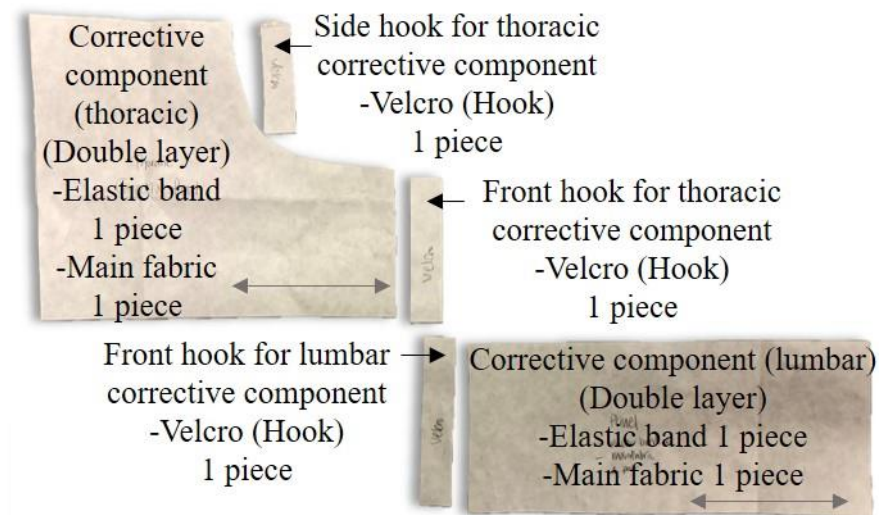


Figure 5-33 Thoracic and lumbar corrective component patterns

### 5.10 Prototype for clinical study

Figure 5-34 and Figure 5-35 show the prototypes for the clinical study. There were 5 main parts: a bra top, pants, a pelvis belt, the hinge of the artificial back bone with a cushioning pad and the corrective components. The bra top and underpants acted as the frame for attaching the corrective components. The use of bands instead of fabric for the construction of the bra top and underpants provided free space for the concave areas of the body to expand, which promoted the efficacy of the spinal correction. The pelvis belt that was attached from the artificial back bone to the front of underpants provides end-point control of the pelvis. The corrective components provided external forces to push the body surface in the perpendicular direction against the spinal curvature. High modulus elastic bands that were attached from the artificial back bone to the front of the bra top or underpants create external corrective forces that push against the spinal curvature. A semi-rigid convex pad made with silicone was inserted under the elastic band to enhance the corrective force.



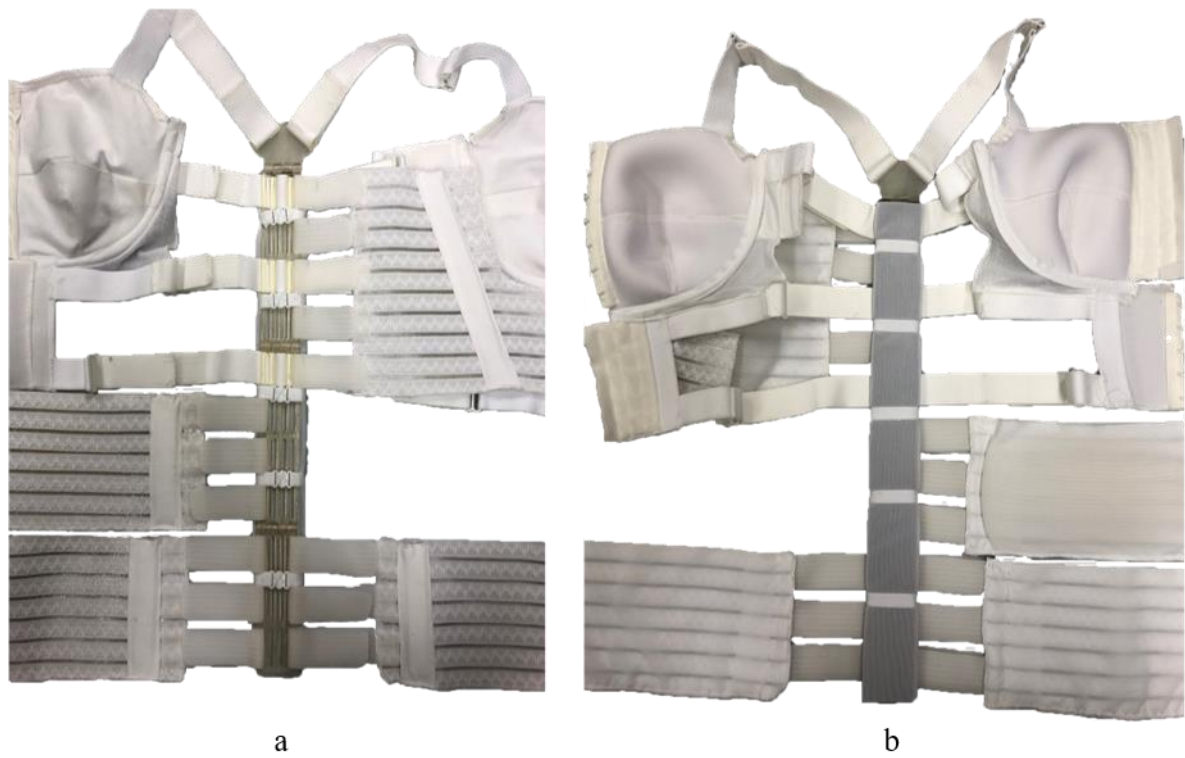


Figure 5-34 Prototype for clinical study: (a) front and (b) back views



Figure 5-35 Prototype worn by subject: (a) front and (b) back views

## 5.11 Summary

A functional intimate apparel that comprised a bra top, pants, a pelvis belt, an artificial back bone with hinges that were cushioned with padding and corrective components has been designed and developed to maximise the corrective effect of flexible bracing and minimise the negative impacts of rigid bracing, such as mobility restrictions and discomfort. The corrective component with a semi-rigid silicone pad is the key to providing direct corrective forces that push against the convex part of the body for spinal correction. The open design of the concave part of the brace allows for expansion of the body to promote the corrective performance.

The textile materials for the functional intimate apparel are also selected based on the fabric testing results and the criteria required of the individual components. Elastic band R153132\_166 was selected for the corrective component due to its high modulus and low force decay with time and repeated exercise movement. Fabric DN64013S was selected for the main fabric due to its outstanding tensile behaviour, excellent thermal comfort, moderate sensorial comfort, and good dimensional stability during laundering. Elastic Strap 4443\_25 was selected as the elastic webbing of the bra top and pants due to its outstanding modulus, excellent recoverability and good dimensional stability during laundering.

As for the development of the garment pattern, 21 AIS subjects were recruited to undergo 3D body scanning to obtain their measurements. Their upper breast, under breast, under band, pelvis, and hip circumferences, leg hold, waist to gusset, under band to pelvis, upper breast to pelvis and shoulder strap lengths were measured. In order to achieve a better fit through mass production of the prototype, two prototype sizes were developed - small and medium, according to the BMI results. In total, 35 pieces were used to construct the proposed functional intimate apparel for AIS including one thoracic and one lumbar corrective component. The result and evaluation of the functional intimate apparel prototype were discussed in Chapter 6.

## Chapter 6 Clinical study of functional intimate apparel for AIS

### 6.1 Introduction

The design and development process of a functional intimate apparel for AIS has been described in Chapter 5. In this chapter, a clinical study of the proposed functional intimate apparel for AIS was discussed in detail. The aim of this clinical study is to investigate the efficacy of the proposed brace design. The clinical study involves two phases. The first phase is a 2-hour clinical study to investigate the initial performance of the functional intimate apparel, including variables such as the initial in-brace performance, initial changes in the body contours, psychological and physiological comfort on the wearers and effect of the biomechanics of the brace on the interface pressure. The second phase is a 3-month clinical study that investigated the short-term effects of the proposed brace design, including evaluation of the changes in spinal deformity, body contours and quality of life.

### 6.2 Subject recruitment

Between March 2018 and January 2019, five female subjects were recruited for a clinical trial study of the functional intimate apparel for AIS through a school screening programme for scoliosis in local secondary schools or at The Duchess of Kent Children's Hospital at Sandy Bay. The demographics of the recruited subjects are provided in Table 6-1. All of the subjects participated in the first phase which was the 2-hour clinical study. Among these subjects, only Subject 19002 participated in the second phase which was the 3-month clinical study.

Table 6-1 Demographics of clinical study subjects

Subject code	Age	Weight (kg)	Height (cm)	BMI	Risser grade	Lenke type	Type of spinal curve	Curve level	Apex	Cobb's angle
18001	12	45.5	148	20.8	2	Lenke 3	Right thoracic	T4-T11	T8	21.6
							Left lumbar	T11-L4	L2	17.3
18002	12	43.7	153	18.7	2	Lenke	Right thoracic	T5-T11	T8	14.6

						6	Left lumbar	T11-L4	L2	21.8
18003	12	45.4	150	20.2	2	Lenke 3	Right thoracic	T5-T11	T8-9	25.3
							Left lumbar	T11-L3	L1	21.8
19001	12	35.8	148	16.8	2	Lenke 6	Right thoracic	T2-T11	T8	17.8
							Left lumbar	T12-L4	L2	20.0
19002	13	37.9	149	17.1	0	Lenke 5	Left thoracolumbar	T8-L3	T12	23.0
Average	12.2	41.7	149.6	18.7	1.6	-	-	-	-	22.3 (primary curve)
S.D.	0.4	4.5	2.1	1.8	0.9	-	-	-	-	2.0

### 6.3 Fitting of the functional intimate apparel for AIS

During the fitting session, corrective components with a semi-rigid silicon pad were attached to the artificial back bone. The corrective component was meant to create a direct force that pushed onto the convex part of the spine to correct the curvature. Figure 6-1 shows the corrective components and pad location and the corresponding radiograph image.

Subject 18002 was the first subject to take part in the clinical study. The corrective components with silicon pads were applied to the right side of the upper thoracic spine and the left side of the lumbar spine. Moreover, a silicon pad was inserted at the right side of the pelvis belt. The purpose of applying these three pads was to replicate the three-point pressure system and correct the lumbar curve effectively. Figure 6-2 shows the radiograph images of Subject 18002 with and without the brace. However, the in-brace radiograph image showed that the pelvis pad was tilted which caused the over-rotation of the pelvis. Unlike the thermoplastic material of rigid resin braces, the insertion of a silicon pad might cause the elastic pelvis belt to tilt which resulted in the displacement of the pelvis padding due to leg movement. This might be attributed to the use of an elastic pelvis belt with a pad and thus was a design limitation. Furthermore, the pelvis pad also affected the equilibrium of the artificial back bone. Thus, the

pelvis pad was not used for any of the other subjects.

Furthermore, Subjects 18001, 18003 and 19001 also had right thoracic and left lumbar curves. However, the problems with the pelvis pad meant that it was not used for these three subjects. The corrective components with silicon pads were applied on the right side of the upper thoracic curve and the left side of the lumbar curve.

Subject 19002 had a single left thoracolumbar curve and thus a corrective component with a silicon pad was applied to the thoracolumbar region.

To summarize the location of the pads, the corrective components were attached at three levels, which are the upper thoracic, thoracolumbar and lumbar spines. The placement of the pads depended on the level of the apex of the scoliotic spine.

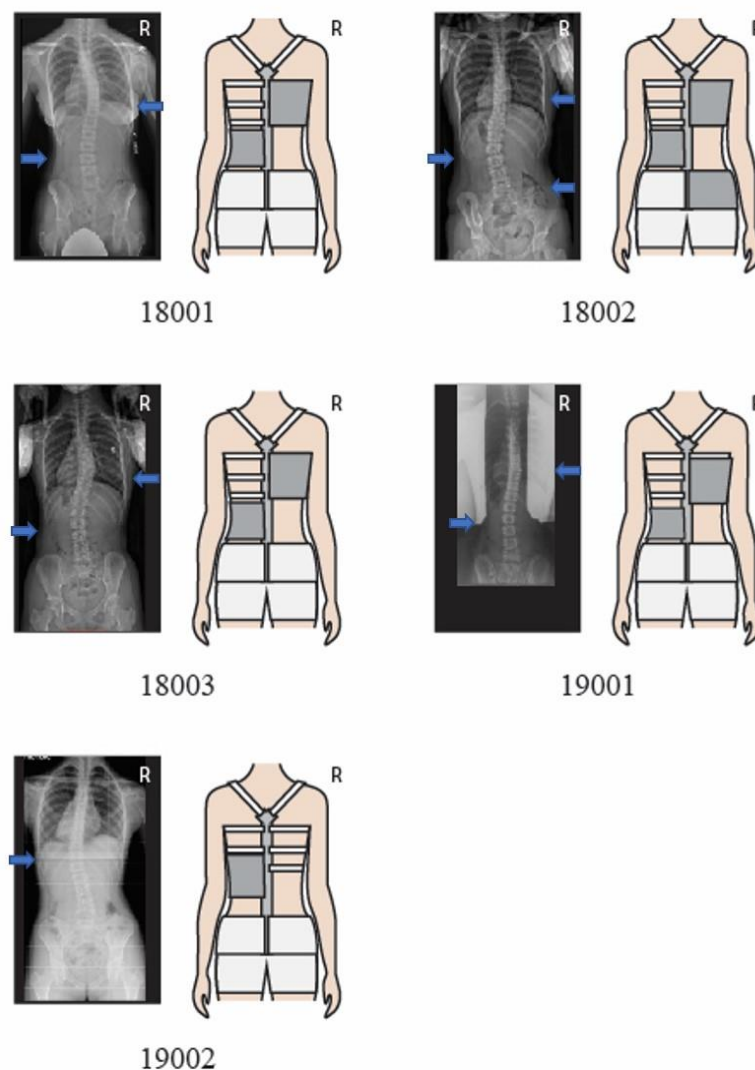


Figure 6-1 Radiograph images and placement of corrective components



Figure 6-2 Radiograph image of Subject 18002: (a) without brace, and (b) in-brace

#### 6.4 Two-hour clinical study

All of the subjects were invited to take part in a 2-hour clinical study, during which the in-brace radiograph images, 3D scanned images of the body, survey on psychological and physiological comfort and interface pressure were examined.

##### 6.4.1 Effects on the initial in-brace reduction of spinal curvature

Radiographic imaging was carried out after the subjects had worn the functional intimate apparel for two hours. Figure 6-2 shows the results of the initial effect of the garment on the spine. Out of the 5 subjects, 3 had more than a  $5^\circ$  reduction in their primary curvature, 1 within  $5^\circ$  and 1 had a  $5^\circ$  increase in her primary curvature. The rate of reduction in spinal curvature in the in-brace condition ranged between 9.7% and 88.7%. Subject 19002 who had a single thoracolumbar curve showed the highest rate of in-brace reduction of her spinal curvature with the functional intimate apparel.

The placement of the pads influenced the in-brace results (Clin, Aubin, Parent, et al., 2010). As for Subject 18002 who had three pads inserted at the right thoracic and left lumbar curves and

right pelvis, respectively, the intention was to correct the lumbar spine curvature by replicating the three-point pressure system. However, the pelvis pad shifted due to the leg movement and hence, she experienced an increase in her spinal curvature. Therefore, a pad applied to the pelvis was not recommended. Moreover, this showed that the placement of the pad impacted the bracing results.

As mentioned above, the fitting problems of Subject 18002 meant that her result was atypical and did not reflect the efficacy of the proposed design. Thus, her results were omitted and the functional intimate apparel showed an average rate of reduction of about 39% in the spinal curvature.

Among the 4 other subjects, the rate of in-brace reduction of the spinal curvature ranged between 9.7% and 88.7% so the variation was substantial. Cheung et al. (2017) suggested that the success of the in-brace reduction of the curvature depended on the inherent flexibility of the spine. However, in this study, supine x-rays were not done due to concerns around exposure to radiation, and thus information about the inherent flexibility of the patients could not be obtained, which also constituted as one of the limitations of this study.

In addition to the inherent flexibility of the spine, Lang et al. (2019) performed a retrospective analysis with 112 AIS subjects who were undergoing rigid brace treatment and found that the Cobb's angle, sagittal and coronal balance (CD) and lumbar-pelvis relationship (LPR) influenced the in-brace reduction of the curvature. Figure 6-3 shows that there was a negative relationship between the rate of in-brace reduction of the curvature and CD and the rate of in-brace reduction of the curvature and LPR. Based on the results of a Kendall's Tau test, there was a significantly negative correlation between the rate of in-brace reduction of the curvature and LPR;  $\tau = -1$ , and  $p < 0.01$ . The rate of in-brace reduction of the curvature was significantly and negatively correlated with the CD;  $\tau = -1$ , and  $p < 0.01$ . Briefly speaking, the patient with a good LPR and coronal balance had the highest percentage of in-brace reduction of the curvature while the patient with a relatively poor LPR and coronal balance had the lowest percentage of in-brace reduction of the curvature. This preliminary finding agreed with Lang et al. (2019) who concluded that the LPR was negatively correlated with the in-brace reduction of the curvature and also patients with coronal balance would experience a higher rate of in-brace reduction of the curvature. Nevertheless, the data in this study showed that there was no relationship between in-brace reduction of the curvature and the Cobb's angle.

This study had conducted initial case studies to investigate the possibility of using flexible

materials to achieve spinal correction. In-brace reduction of the curvature was the initial step for assessing the quality of new braces (Negrini et al., 2012). Guo et al. (2014) conducted a randomised controlled study with scoliotic subjects who have a Cobb's angle between 20°-30° to examine the effectiveness of a rigid brace and the SpineCor flexible brace, and reported that the initial rate of in-brace reduction of the spinal curvature was 15.9% and 21.3% respectively. Karol (2001) examined the effectiveness of several types of rigid braces in male scoliotic subjects with a Cobb's angle between 18°-45° and found that the initial rate of in-brace reduction of the curvature with the Milwaukee, Boston and Charleston braces was 17.4%, 35.6% and 62.2% respectively. Here, the initial case studies showed a similar in-brace result as some of the currently available rigid and flexible braces. This initial finding implied the potential of using textile materials to control spinal deformity.

Furthermore, the results discussed in Chapter 4 indicated that the posture correction girdle developed by Liu et al. (2014) only offered an average of a 1.5° reduction in the spinal curve when worn, while the functional intimate apparel in this study provided an average of 6.1° reduction in the spinal curve. A Mann-Whitney test indicated that the functional intimate apparel provided a higher in-brace reduction of the curvature in comparison to the posture correction girdle;  $U=5.0$ , and  $p=.034$ . This showed that the functional intimate apparel in this study had a higher in-brace corrective effect compared to an available flexible brace – the posture correction girdle developed by Liu et al. (2014).

Table 6-2 Measured Cobb's angle with different conditions

Subject code	Date of pre-intervention x-ray	Date of in-brace x-ray	Curve level	Pre-intervention Cobb's angle (°)	In-brace Cobb's angle (°)	In-brace reduction/increase of Cobb's angle (°)
18001	16/7/2018	4/10/2018	T4-T11	21.6	19.5	-2.1
			T11-L4	17.3	21.1	+3.8
18002	15/5/2017	18/7/2018	T5-T11	14.6	17.6	+3.0
			T11-L4	21.8	26.7	+4.9
18003	12/2/2018	26/7/2018	T5-T11	25.3	18.7	-6.6



			T11-L3	21.8	18.8	-3.0
19001	3/7/2018	23/2/2019	T2-T11	18.8	1.1	-17.7
			T12-L4	20.0	13.7	-6.3
19002	27/12/2018	9/2/2019	T8-L3	23.0	2.6	-20.4

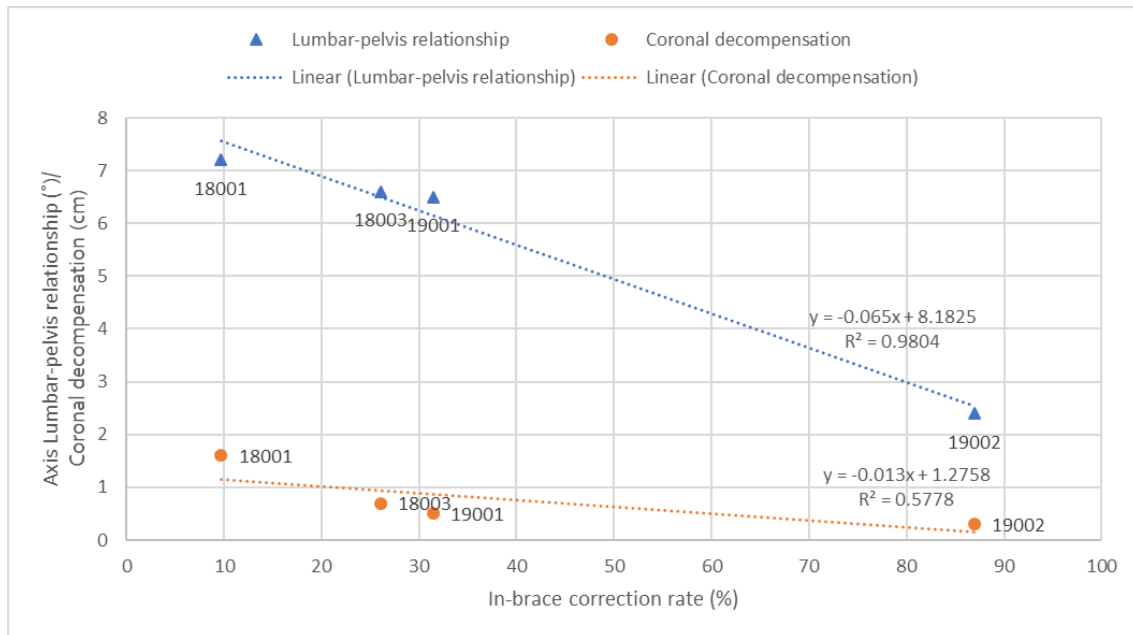


Figure 6-3 Relationship between in-brace rate of correction and lumbar-pelvis relationship and in-brace rate of correction and coronal decompensation

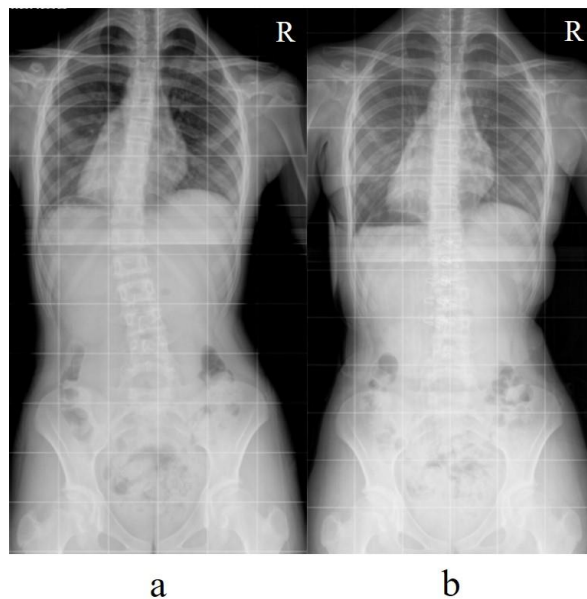


Figure 6-4 Radiograph images of Subject 19002: (a) without brace, and (b) with brace

## 6.4.2 Effects on initial changes in body contours

### 6.4.2.1 Shoulder obliquity

The shoulder obliquity was measured both with the brace donned and without the brace. Of the 5 subjects, only 2 of them had a reduction in the obliquity by more than 1° while 2 of them had more oblique shoulders. Figure 6-5 shows the obliquity of the shoulders of each subject both with the brace donned and without the brace. The figure shows that surprisingly, Subject 19002 had more oblique shoulders even though her Cobb's angle was reduced by 20.4°. This might imply that there was no positive correlation between physical contour control and spinal control with the proposed functional intimate apparel. This result also reinforced that the involuntary imbalance of the shoulders or waist line was commonly caused by bracing in order to realize a higher rate of curvature correction (Kotwicki et al., 2007).

Furthermore, when the shoulder obliquity results of the posture correction girdle developed by Liu et al. (2014) were compared with those of the proposed functional intimate apparel, it was apparent that the former had a better performance.

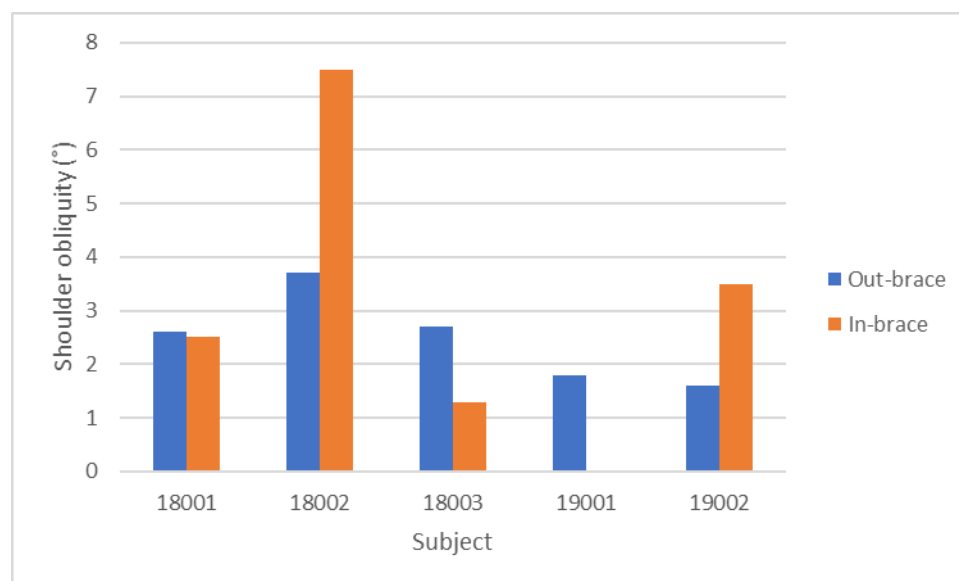


Figure 6-5 Shoulder obliquity results

### 6.4.2.2 Shoulder rotation

The shoulder rotation was measured both with the brace donned and without the brace. Of the 5 subjects, 3 of them showed less shoulder rotation while the other 2 subjects showed more shoulder rotation. Figure 6-6 shows the shoulder rotation results of each subject both with the brace donned and without the brace. The figure shows that surprisingly, Subject 19002

experienced more shoulder rotation even though her spinal curvature was substantially reduced. This implicated that there was no positive correlation between physical contour control and spinal control. Moreover, the involuntary imbalance of the shoulders was a common negative effect of bracing treatment in order to realize a higher rate of curvature correction (Kotwicki et al., 2007).

When the results of the posture correction girdle developed by Liu et al. (2014) were compared with those of the proposed functional intimate apparel, it was apparent that the former was able to better reduce the amount of shoulder rotation.

Besides, there was also an interesting finding in terms of the correlation between the change in shoulder rotation and shoulder obliquity. A Kendall's tau-b test suggested that there was a positive correlation between the two factors;  $r=0.8$ , and  $p=0.05$ . This could imply that changes in the physical contours in the coronal and transverse planes were correlated.

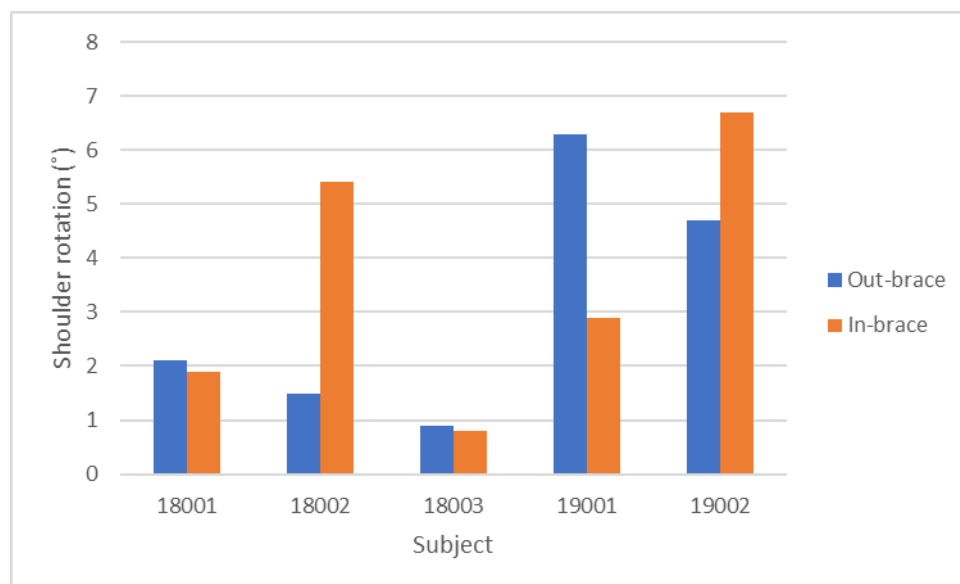


Figure 6-6 Shoulder rotation results

#### 6.4.2.3 Posterior trunk symmetry index

Apart from the shoulder asymmetry, the symmetry of the posterior trunk both with the brace donned and without the brace was also studied. Figure 6-7 shows the posterior trunk symmetry index (POSTI) of each subject both with the brace donned and without the brace. The value of POSTI is positively related to the asymmetry of the posterior trunk. Of the 5 subjects, 4 of them reduced the asymmetry of their posterior trunk when wearing the functional intimate apparel. The POSTI without the brace ranged between 22.1 and 38.6 while that with the brace donned

ranged between 15.0 and 33.2. The rate of reduction of the posterior trunk asymmetry in terms of the POTSI ranged from 14.1% to 43.2%. This suggested that the functional intimate apparel could have had a positive effect on the body contour symmetry. Nevertheless, after reviewing Table 6-2 and Figure 6-8, there did not appear to be a strong correlation between in-brace reduction of the curvature and body contour changes. This finding concurred with Durmala et al. (2015) who reported that there was no correlation between the POTSI value and spinal curvature angle.

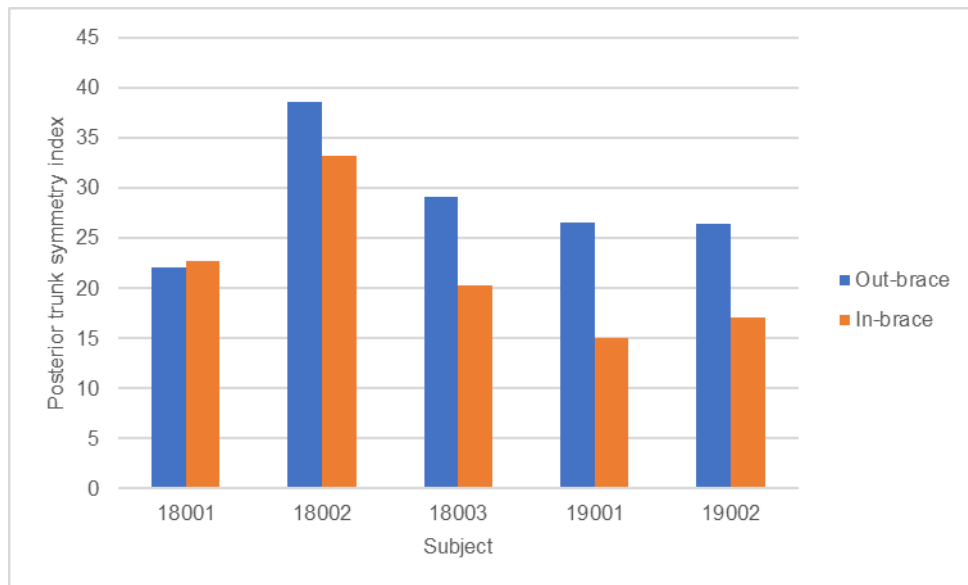


Figure 6-7 Posterior trunk symmetry index results

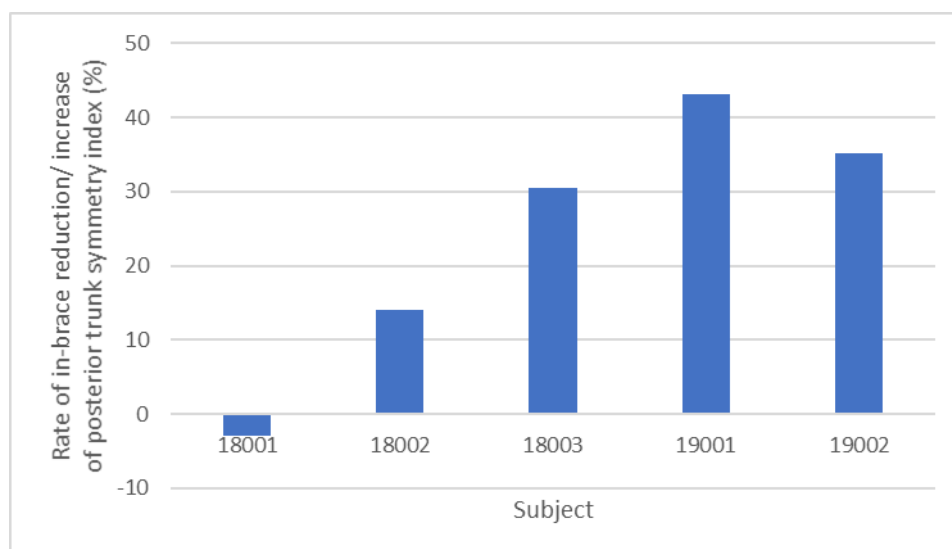


Figure 6-8 Rate of in-brace reduction/ increase: posterior trunk symmetry index

### 6.4.3 Wear comfort

After the subjects wore the functional intimate apparel for 2 hours, they were asked to complete two questionnaires: the Bad Sobernheim Stress Questionnaire (BSSQ) - Brace and Brace Questionnaire (BrQ) to assess the psychological and physiological comfort.

#### 6.4.3.1 Bad Sobernheim Stress Questionnaire - Brace

Figure 6-9 shows the BSSQ-Brace score of each subject. Botens-Helmus et al. (2006) proposed the categorisation of the BSSQ-Brace scores into three levels of stress. A score of 0-8 indicates a high level of stress, 9-16 indicates a moderate level of stress and 17-24 means a low level of stress. Of the 5 subjects, 2 of them obtained a BSSQ-Brace score higher than 16 which signified low stress levels while the other 3 obtained a score between 9 and 16 which pointed to moderate stress levels.

Weiss et al. (2007) examined the quality of life of AIS patients who were undergoing treatment with a Cheneau brace and reported that their average BSSQ-Brace score was 11.04. In comparison to the score of 14.0 in this study, the mean score here was higher. This could be interpreted that the proposed design reduces the stress of AIS patients compared to the available rigid braces.

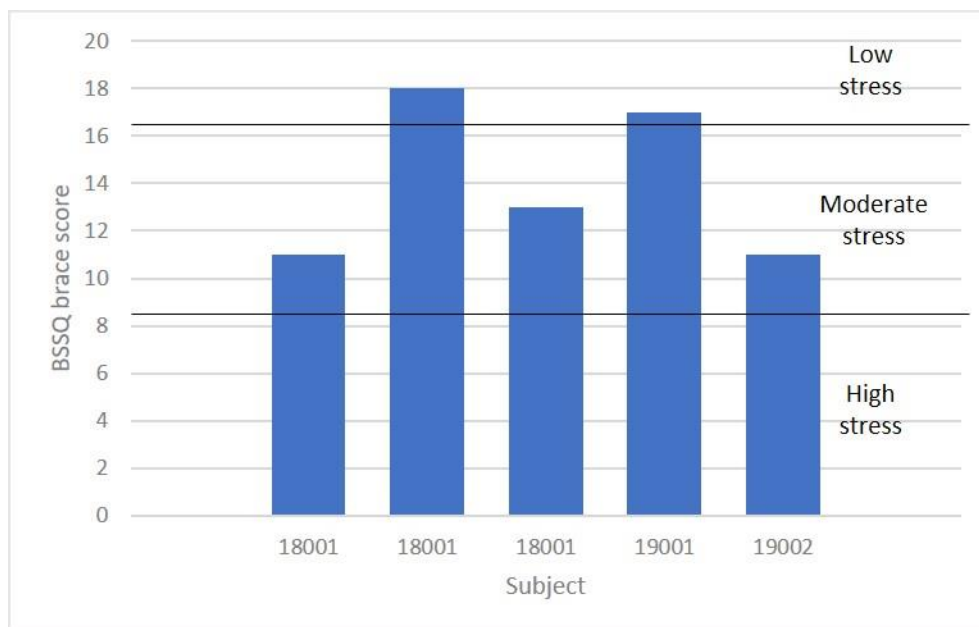


Figure 6-9 BSSQ-Brace scores

#### 6.4.3.2 Brace questionnaire

The BrQ was used to assess the perceived general health, physical and emotional functioning,

body pain and social functioning based on the functional intimate apparel. Figure 6-10 shows the score for each question.

In terms of the perceived general health, Figure 6-10 shows that the subjects indicated that the brace sometimes made them feel ill. However, they also indicated that they were almost never afraid that their spinal curvature would increase in severity.

As for the physical functioning, the subjects responded that when wearing the brace, they almost never felt tired during walking, almost never were not eating well, almost never could not sleep well and almost never could not breathe. Also, they mentioned that when wearing the brace, most of the time they were able to run and manage the brace without any help. These responses showed that the proposed functional intimate apparel would not have severe physical impacts on their daily activities, such as running, eating, sleeping and breathing.

As for emotional functioning, the subjects responded that they almost never felt nervous and worried by the brace and almost never thought that their life would be better if they were not wearing the brace. Moreover, most of the time, they felt that the treatment was beneficial. These responses may imply that the proposed functional intimate apparel would not have severe negative emotional impacts on the subjects.

In terms of body pain, the subjects mentioned that while wearing the brace, they almost never experienced pain while walking, sitting or climbing stairs, and never felt pins and needles in their arms and legs. The result showed that the proposed functional intimate would not cause pain during daily movement.

With respect to social functioning, the subjects indicated that they almost never felt different from their peers and did not believe that their relationship with their family or friends would be better if they were not wearing the brace. The results implied that the proposed intimate apparel would not cause serious social barriers.

To conclude, the results implied that the proposed functional intimate apparel almost never caused negative impacts or problems around perceived general health, physical functioning, body pain and social functioning.

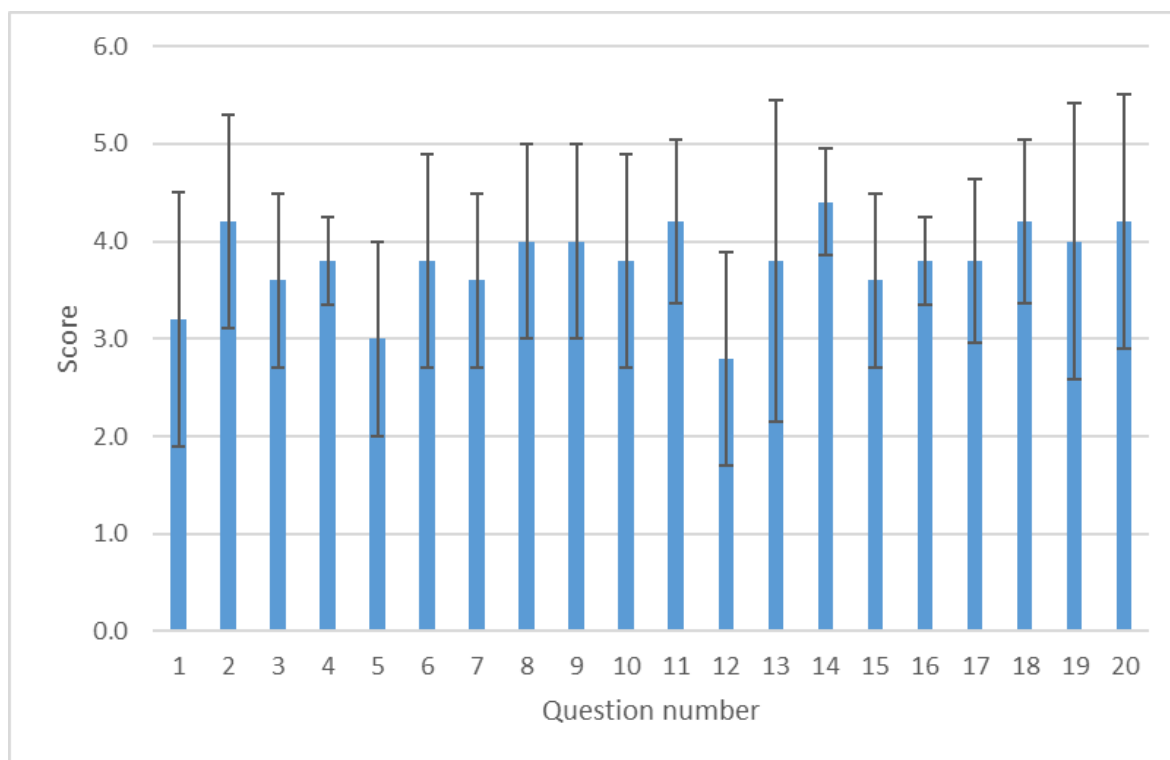


Figure 6-10 Scores for individual BrQ questions

#### 6.4.4 Interface pressure

The interface pressure of the functional intimate apparel was measured at the initial visit. The interface pressure values are shown in Figure 6-11. The interface pressure of the thoracic corrective pad ranged between 6.0 kPa and 24.4 kPa. The interface pressure of lumbar/thoracolumbar corrective pad ranged between 6.1 kPa and 9.7 kPa.

Apart from the corrective pads, the interface pressure between the pelvis belt and body was also recorded. Subject 18002 inserted a corrective pad on the right side of the pelvis belt. The interface pressure of the right and left sides of the pelvis belt of Subject 18002 was 25.2 kPa and 0.62 kPa respectively. The interface pressure of the padded pelvis belt was far more higher than the unpadded side. This finding further showed that the use of a semi-rigid pad enhanced the interface pressure. Moreover, the use of a pelvis pad might influence the pressure distribution of the corrective components for the thoracic and lumbar curvatures since it was related to the equilibrium of the artificial back bone. According the equilibrium principle, the sum of forces and the bending moments created must be zero to maintain stability. In such a case, the corrective component for the pressure of right thoracic curve might be lowered to maintain the balance of the artificial back bone since pressure was increased to the right side of the pelvis.

The unfortunate experience of Subject 18002 meant that the other four subjects did not insert any pads in their pelvis belt. Therefore, the pressure of the interface between their pelvis belt and body ranged from 1.8 kPa to 16.0 kPa. There was an interesting finding of uneven pressure distribution between the right and left sides of the pelvis belt. Figure 6-11 shows that the interface pressure on the right side of the pelvis belt was greater than that on the left side of the pelvis belt. The range of the pressure on the right and left sides of the pelvis belt was between 7.7-16.0 kPa and 1.8-9.8kPa respectively. Figure 6-1 shows that a corrective component was placed onto the left lumbar/ thoracolumbar curve of all of the subjects. The position of the lumbar/thoracolumbar curve may influence the pressure distribution of the pelvis belt depending if the corrective component was placed on the right or left side. All of the corrective components and the pelvis belt were attached to the artificial back bone at the back of the patient. The pelvis belt provided end-point control of the pelvis. After the corrective component was placed onto the left lumbar/ thoracolumbar curve, the pelvis belt might exert a larger amount of tension on the artificial back bone as opposed to the left side of the pelvis belt in order to create equilibrium with the artificial back bone. Even if no pad was inserted on the right side of the pelvis belt, the right side of the pelvis belt would also exert a higher amount of pressure than the left side of the pelvis belt when a corrective component was used on the left lumbar/ thoracolumbar curve. The results here showed that a three-point pressure system was possible with the proposed functional intimate apparel.

There were no previous studies that have focused on the biomechanics of flexible braces; however, there has been related work on rigid braces. Wong et al. (2000) investigated the biomechanics of rigid braces and reported that the pressure exerted by rigid braces ranged from 4.9 kPa to 9.34 kPa. Mac-Thiong et al. (2004) also experimentally conducted pressure measurements with rigid braces and showed that the pressure of the Boston brace ranged between 10 kPa and 30 kPa. In this study, the interface pressure exerted by the functional intimate apparel ranged between 6.0 kPa and 24.4 kPa, which was very similar to the pressure exerted by rigid braces. This showed that flexible materials could also enable exert forces against the torso, as seen with rigid braces. These results created the possibility of using flexible materials such as elastic straps, semi-rigid padding and artificial hinges to provide adequate corrective pressure.

Another interesting finding was that the pressure from the thoracic pad was higher than that from the lumbar pad. This finding was consistent with that of a previous biomechanics study on rigid braces by Wong et al. (2000). A possible explanation might involve the ribcage. The



ribcage could directly withstand the pressure from the thoracic pad while the fat in the waist region might diffuse the pressure from the lumbar pad.

According to the law of mechanics, it might be expected that a larger force results in more in-brace reduction of the curvature. A certain amount of corrective force was undoubtedly necessary for spinal correction. However, the preliminary results in this study showed that there was no significant correlation between the interface pressure and the rate of in-brace reduction of the curvature. This finding might imply that after a certain amount of corrective force was exerted onto the body, increasing the amount of force might not provide further corrective effects. Therefore, further studies on the relationship between spinal curvature correction and interface pressure were recommended.

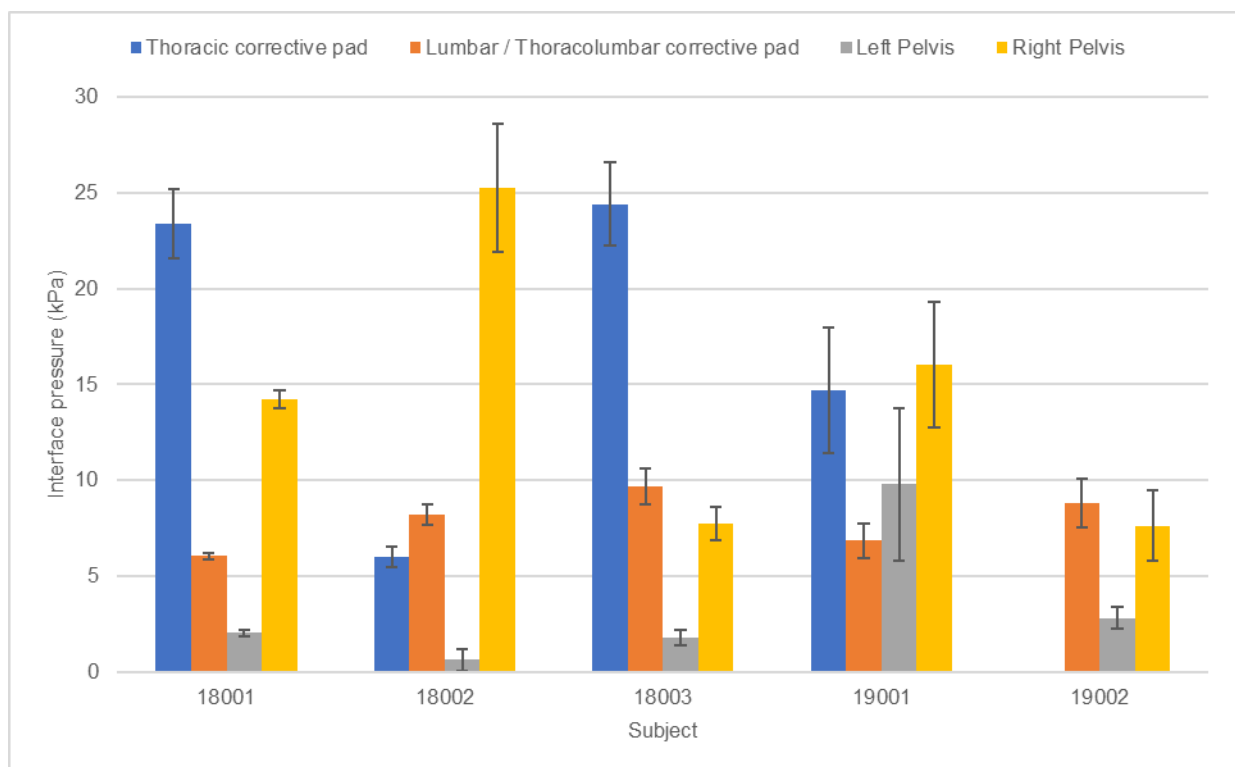


Figure 6-11 Interface pressure of the functional intimate apparel

## 6.5 Three-month clinical study

One of the subjects (Subject 19002) was invited and agreed to participate in the 3-month clinical study. The objective of this 3-month clinical study is to investigate the short-term effects of the functional intimate apparel. The subject underwent an ultrasound examination of her spine and 3D body scanning as well as completed a survey on the quality of her life with the brace.

### **6.5.1 Effects on spinal curvature progression**

The ultrasound examination of the spine of the subject (Scolioscan™) was carried out at pre-intervention and on the 3<sup>rd</sup> month of intervention. The Cobb's angle as determined by Scolioscan™ at pre-intervention and on the 3<sup>rd</sup> month of intervention was 28.1° and 13.3° respectively (Figure 6-12). The initial rate of correction was therefore 52.7%.

Xu et al. (2017) investigated the initial rate of correction and the success rate of bracing and reported that the group who experienced a 40-50% initial rate of correction showed a 100% success rate of bracing. Since the case in this study experienced an initial rate of correction that was higher than 50%, it may be hypothesized that there would be successful bracing outcomes with this treatment.

According to Wong et al. (2008), the SpineCor and rigid brace only showed an in-brace reduction of 17.4% and 12.3% after 3 months of intervention. In comparison, the functional intimate apparel here demonstrated a good short-term spinal corrective effect of 52.7 %.

Hawary et al. (2019) conducted a review on the progression factors of bracing treatment. They concluded that poor bracing treatment compliance, low skeletal maturity, large Cobb's angle, presence of spinal rotation, low in-brace reduction of the curvature and a main thoracic curve were the risk factors of curve progression.

In this study, the subject showed an initial in-brace reduction of the spinal curvature of 89% and a reduction of the spinal curvature of 52.7% in the 3<sup>rd</sup> month of intervention. This result was in agreement with a previous study (Clin, Aubin, Sangole, et al., 2010) which suggested that immediate in-brace reduction of the curvature could be used to predict the long-term outcome of the bracing treatment. As the case in this study showed a very large in-brace reduction of the spinal curvature, it was reasonable to hypothesize that most likely a very low rate of curvature progression will be the result, or even permanent spinal correction.

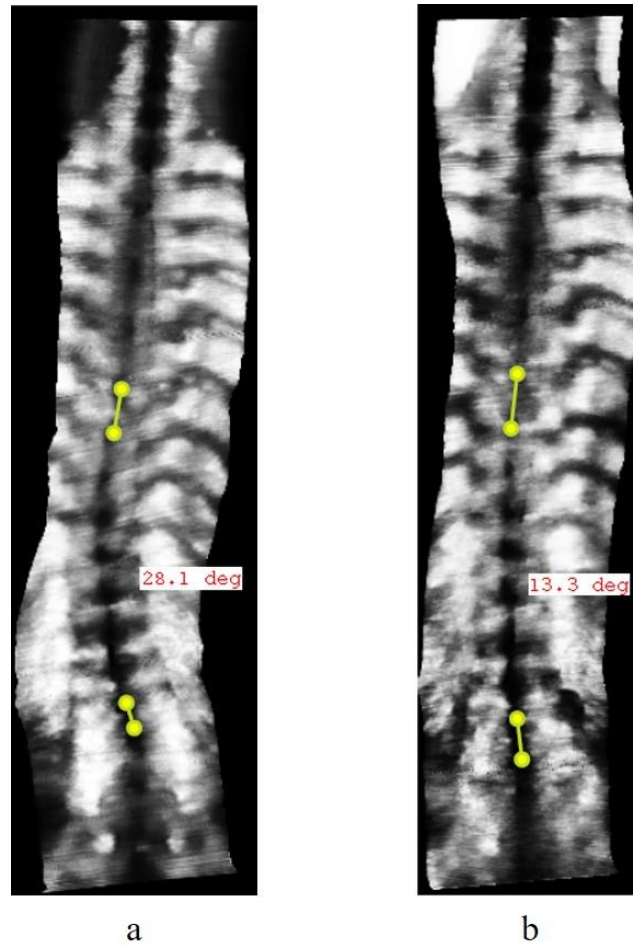


Figure 6-12 Ultrasound images of Subject 19002: (a) pre-intervention and (b) 3<sup>rd</sup> month of intervention

### 6.5.2 Effects on body contour changes

The subject underwent 3D body scanning without donning the brace at pre-intervention and on the 3<sup>rd</sup> month of intervention. The shoulder obliquity, shoulder rotation and POSTSI were examined. Figure 6-13 shows the results of the degree of obliquity for the shoulders, degree of rotation in the shoulders and the POSTI at pre-intervention and on the 3<sup>rd</sup> month of intervention.

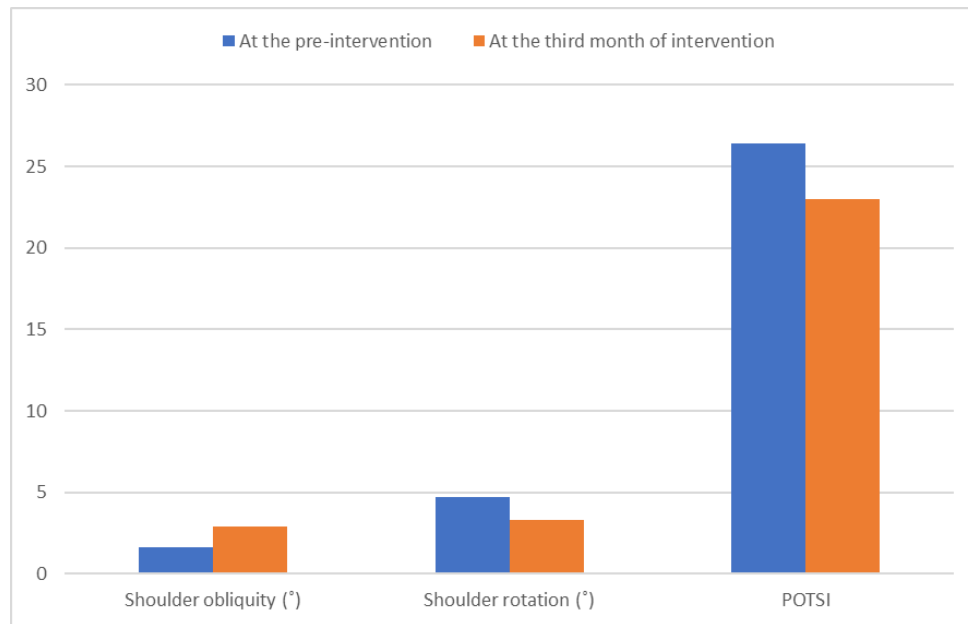


Figure 6-13 Degree of obliquity (shoulders), degree of rotation (shoulders) and POSTI at pre-intervention and on 3rd month of intervention

#### 6.5.2.1 Shoulder obliquity

Figure 6-13 shows that the shoulder obliquity increased by  $1.3^{\circ}$  after 3 months of intervention. Recall that Figure 6-5 also shows that the shoulder obliquity was increased with the brace donned in the 2-hour clinical study. This might imply that the proposed functional intimate apparel caused shoulder obliquity. Recall Figure 6-1 which shows a corrective pad inserted at the left thoracolumbar curve. This pad might cause sensory feedback and resulted in a reflective response which involved lifting of the left shoulder. Thus, shoulder obliquity might be a possible negative effect of the proposed functional intimate apparel.

#### 6.5.2.2 Shoulder rotation

In terms of the shoulder rotation, the subject showed a reduction of  $1.4^{\circ}$  (Figure 6-13). Liu et al. (2015) conducted a 3-month clinical study of their posture correction girdle and reported that the posture correction girdle reduced shoulder rotation by  $0.31^{\circ}$ . In comparing the posture correction girdle developed by Liu et al. (2014) and the proposed functional intimate apparel, the latter might reduce the shoulder rotation to a greater extent.

#### 6.5.2.3 Posterior trunk symmetry index

Apart from the shoulder asymmetry, the POSTI was reduced from 26.4 to 23.0 after 3 months of bracing intervention. This result showed that the proposed functional intimate apparel

reduced trunk asymmetry. Durmala et al. (2015) studied the relationship between self-esteem and trunk asymmetry and pointed out that trunk asymmetry in the coronal plane had a negative effect on self appraised self-esteem. Thus, reducing the trunk asymmetry might have a positive effect on self-esteem.

### **6.5.3 Effects on quality of life**

The quality of life was determined with the Scoliosis Research Society-22 (SRS-22) Questionnaire. The subject completed the SRS-22 Questionnaire at pre-intervention and on the 3<sup>rd</sup> month of intervention, with a total SRS-22 Questionnaire score of 99 and 96, respectively. Both scores were similar, which implied that her quality of life was not very much affected after wearing the functional intimate apparel.

Apart from the total score, the SRS-22 Questionnaire investigates the quality of life in 5 domains which include function, pain, self-image, mental health and satisfaction with management. Figure 6-14 shows the score of each domain at pre-intervention and on the 3<sup>rd</sup> month of intervention. Rainoldi et al. (2015) conducted a cross-sectional study to investigate the reference value of the SRS-22 Questionnaire. They reported a score of function, pain, self-image, mental health and total score for subjects with a Cobb's angle between 11°-20° to be 4.5, 4.7, 3.6, 4.3 and 94.6 respectively. In comparing the reference value and the results in this study, the function, pain, mental health and total scores were still higher than the reference value after wearing the proposed functional intimate apparel for 3 months. However, the score for self-image was less than the reference value. This might imply that the proposed design was unable to make any difference to self-image and could also be a limitation of the proposed brace.

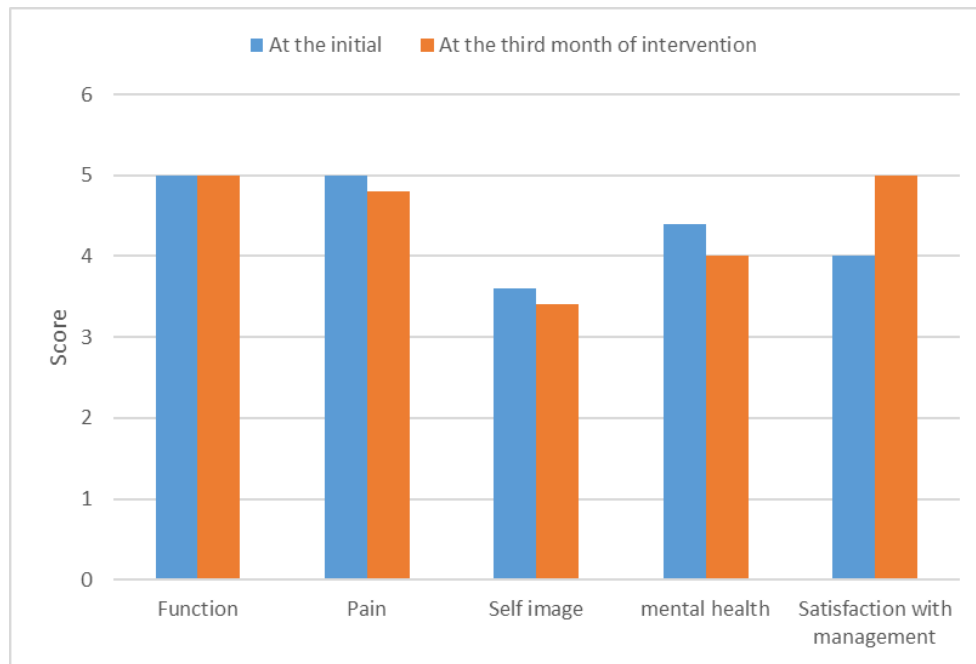


Figure 6-14 Scoring of five domains in SRS-22 Questionnaire at pre-intervention and on 3<sup>rd</sup> month of intervention

#### 6.5.4 Feedback from subject

Apart from the quantitative measurement, a short interview (qualitative assessment) with the subject was conducted to further investigate the limitations of the proposed design. The subject stated that:

*The hinges (of the artificial back bone) break when I move.*

During the 3-month clinical study, it was found that the hinges (Figure 6-15) broke after the brace was used a few times and required a new replacement. The hinge prototype was produced by using 3D jet printing which offered rapid production and was a cost effective method. However, the production method resulted in a weak material. As a result, the hinges easily break. To address this issue, more rigid materials such as carbon fibre and metal were recommended. More importantly, milling was recommended for constructing the prototype instead of 3D printing.

Apart from the durability of the hinges of the artificial back bone, the subject mentioned that:

*The Velcro on the under-band and upper-band feels a little bit prickly.*

The function of the Velcro was to allow for fitting adjustments. Thus, the Velcro was a critical element in the design which could not be eliminated. To address the problem of a prickly hand

feel, a layer of lining was recommended to prevent direct contact between the Velcro and skin.

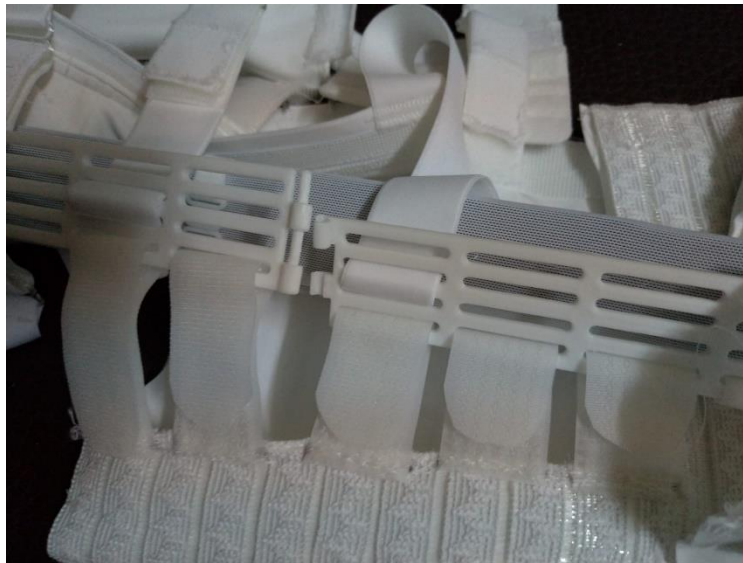


Figure 6-15 Broken hinge of artificial back bone due to large body movements

## 6.6 Summary

Five subjects were recruited in this study to participate in a 2-hour clinical study to determine the initial effect of the proposed functional intimate apparel on the reduction of their spinal curvature, changes in their body contours and wear comfort. The biomechanics of the brace on the interface pressure were also studied. Of these 5 subjects, one of them was a participant in a subsequent 3-month clinical study to investigate the short-term effects of the functional intimate garment on spinal deformity, asymmetry control and quality of life.

In the two-hour clinical study, 3 of the 5 subjects showed an in-brace reduction of more than 5° in their spinal curvature, 1 about 5° and 1 showed an in-brace increase in curvature of about 5°. For the latter, a review of the x-ray film images, and interface pressure data showed that the pelvis pad was displaced due to movement and unnecessary pressure was distributed by the pelvis pad. Thus, the pelvis pad was not recommended for use in the garment.

The initial rate of the in-brace reduction of the spinal curvature ranged between 9.7% and 88.7%. The subject with a single thoracolumbar curve and Risser grade 0 had the highest rate of in-brace reduction. A strong negative correlation of the rate of in-brace reduction of the spinal curvature with the LPR and CD was found. In comparing the results of Chapter 4, the rate of the in-brace reduction of the proposed functional intimate apparel was significantly higher than that of the posture correction girdle, which implied that the proposed design exceeded the in-brace reduction of the curvature of available flexible brace. The result of this preliminary

study might be potentially comparable with those of some of the rigid braces in the literature.

As for the changes in the initial asymmetry of the contours, the results showed that there was no correlation between shoulder asymmetry and in-brace reduction of the spinal curvature. Nevertheless, 4 of the 5 subjects showed a reduction in body asymmetry and the in-brace rate of reduction of POTSI ranged between 13.1% and 43.2%.

To assess the wear comfort of functional intimate apparel, the subjects answered the BSSQ-Brace and BRQ questionnaires. The average BSSQL-Brace score among the 5 subjects was  $14.0 \pm 3.3$  which meant that the subjects experienced a moderate level of stress when they wore the garment. Also, the results of the BrQ showed that the proposed brace almost never caused negative impacts or problems in terms of their perceived general health, physical functioning, body pain and social functioning.

As for the biomechanics, the interface pressure of the thoracic corrective pad and lumbar/thoracolumbar corrective pad ranged between 6.0 kPa-24.4 kPa and 6.1 kPa-9.7 kPa respectively. Compared to the results in the literature, the interface pressure of the proposed brace was similar to that of the rigid braces. This implied that textile materials might be possible to exert a similar amount of corrective force as rigid braces.

One of the subjects consented to participation in a three-month clinical study. Her Cobb's angle was found to be reduced from  $28.1^\circ$  to  $13.3^\circ$  as a result of the treatment with the brace. Her initial rate of reduction in spinal curvature after 3 months was 52.7%.

After wearing the brace for 3 months, the shoulder rotation of this subject was reduced by 29.8% and her posterior trunk symmetry was increased by 13.1%. However, her shoulder obliquity increased by  $1.3^\circ$ .

In terms of changes in quality of life, her SRS-22 Questionnaire score at pre-intervention and after 3 months of brace wear was similar, which implied that her quality of life was not substantially affected after wearing the proposed brace.

In summary, the proposed functional intimate apparel enhances spinal curvature correction compared to available flexible braces such as SpineCor and the posture correction girdle developed by Liu et al. (2014). Moreover, the in-brace reduction of the curvature and initial amount of reduction in spinal curvature after 3 months of intervention might be comparable with some of the available rigid braces. This chapter therefore shown the potential of the proposed design to treat scoliosis.



## **Chapter 7 Biomechanical simulation model for functional intimate apparel to treat AIS**

### **7.1 Introduction**

Finite element (FE) analysis is a numerical method that is used to solve problems in engineering and physics. However, it is now being extended to other fields. For instance, FE analysis is now commonly used to simulate the effectiveness of scoliosis braces and optimise brace designs. In this chapter, a biomechanical model for a functional intimate apparel (FIA) to treat AIS was discussed. The aim of this model is to simulate the effectiveness of the FIA on the initial in-brace spinal correction. In this model, the geometry of the torso body, skeletal structure and FIA, and the mechanical properties of the tissues and FIA were incorporated into a numerical stress analysis. The model then simulated the wear process of the FIA. The corresponding pressure distribution on the skeletal model and the displacement of each vertebral body could thus be calculated and more importantly, the degree of spinal deformity which was determined by the Cobb's angle could be estimated. By changing the material properties or the design of the FIA, the effectiveness of the in-brace spinal correction and the pressure distribution on the skeletal model could be accurately predicted. The biomechanical model in this study was a radiation-free method that also eliminated the difficulties of human wear trials in investigating the efficacy of the FIA and optimising its design.

### **7.2 FE model building**

The stress simulation model in this study mainly consisted of three parts, which were the torso body, skeletal structure and FIA. To build the FE model, first, geometric models of the torso body, skeleton and FIA were created. Secondly, the material properties and element type were defined. After meshing, numerical simulation of the donning of the FIA on the torso was conducted by defining the initial and boundary conditions, displacement conditions of the FIA and the loading conditions of the torso surface to obtain the numerical solution. Then, the results were post-processed and validated.

#### **7.2.1 Geometric modelling of scoliotic torso and FIA to treat AIS**

A scoliotic female subject (Subject code: 18003) was recruited for the development of the FE model and her parents provided consent for her participation in the study. The demographics of this subject are listed in Table 7-1. The subject underwent a radiographic examination, and

then 3D body scanning to extract the geometric details of her skeletal frame and torso.

Table 7-1 Demographics of scoliotic subject

Subject code	Age	Weight (kg)	Height (cm)	BMI	Risser grade	Curve type	Curve level	Apex	Cobb angle
18003	12	45.4	150	20.2	2	Right thoracic	T5-T11	T8-9	25.3 °
						Left lumbar	T12-L3	L1	21.8°

### 7.2.1.1 Construction of torso body

The torso contours were obtained by using point cloud data which were obtained with a Vitus Smart XXL 3D body scanner (Human Solutions GmbH, Germany). Geomagic Studio 2012 (Geomagic Inc., USA) was used to reconstruct the 3D scanned images into a geometric model of the torso body. To compensate for the scanning errors, which are also called scanning noise, the points were moved to statistically correct locations to produce a smooth arrangement of the points. After reducing the noise and making the points uniform, they were transformed into a polygon object by wrapping a mesh around a point cloud. Then, the polygon object was further processed by filling the holes and flattening the spikes for single points. After smoothing the polygon object, it was converted into an object that can be described exactly by the polygon function. Thus, contour lines were drawn on the surface of the object. After that, a patch boundary structure from the contour and boundary lines were generated and an ordered u-v grid in every patch was created. Finally, a non-uniform rational B-spline (NURBS) surface which is a function of two parameters mapped to a surface in three-dimensional space was generated on the surface of the object. Figure 7-1 shows the development of the geometric model of the torso body. Figure 7-2 shows the final geometric model of the torso body.

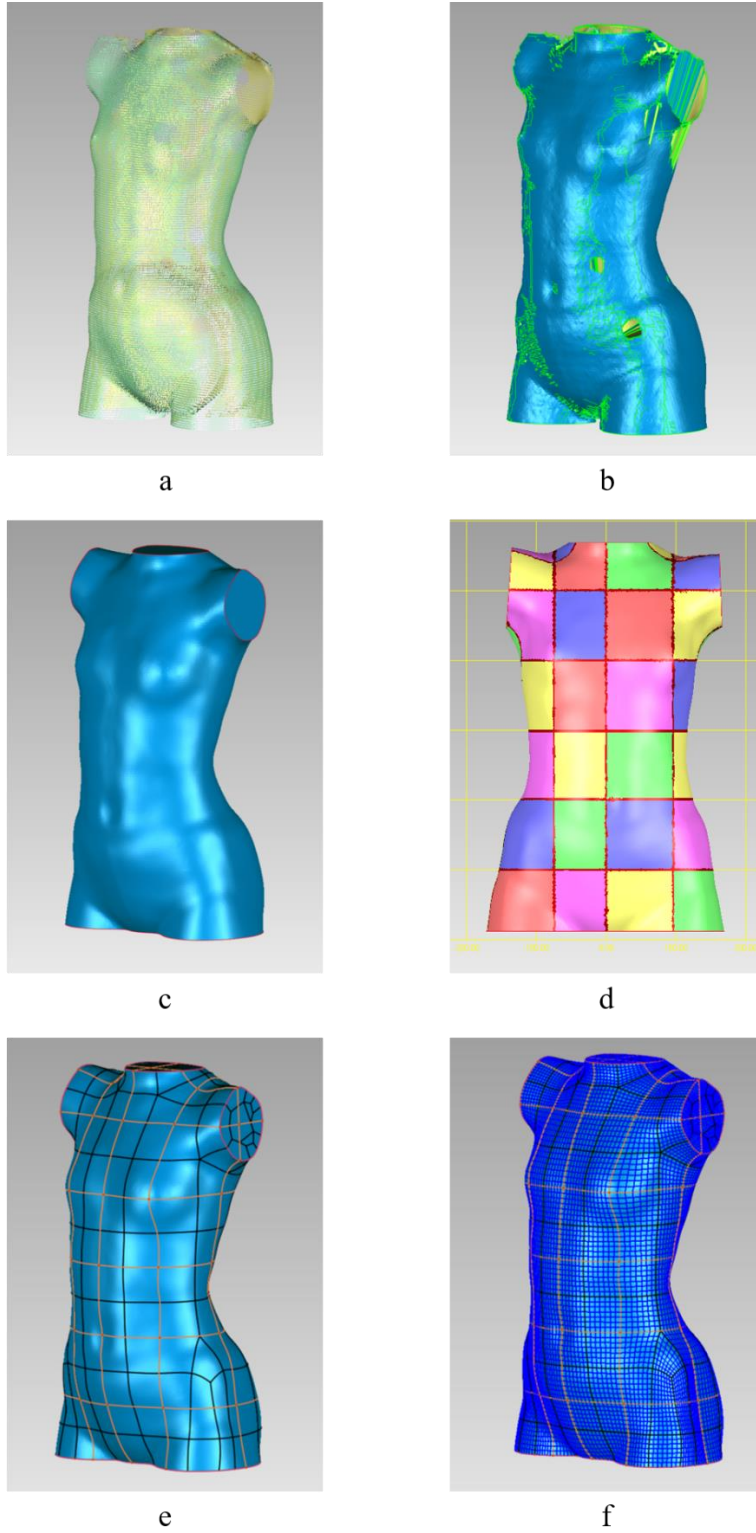


Figure 7-1 Construction of torso body model: (a) point cloud of 3D scanned image, (b) polygon object before processing, (c) polygon object after processing, (d) divided regions to identify contours, (e) polygon object with patch boundary structure, and (f) polygon object with ordered u-v grid in every patch

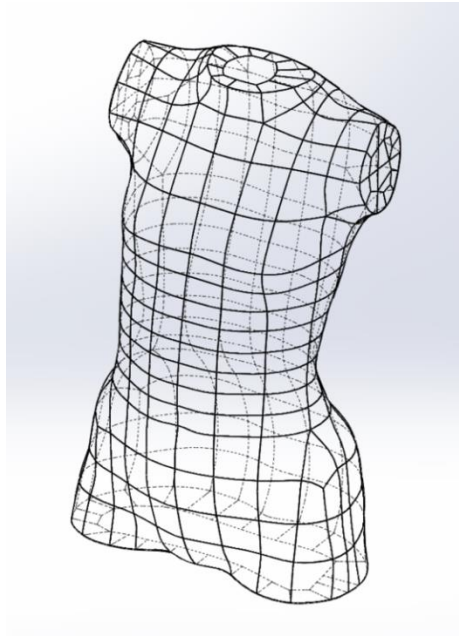


Figure 7-2 Final geometric model of torso body

#### **7.2.1.2 Construction of skeletal model**

SolidWorks 2012 x64 Edition (Dassault Systèmes SolidWorks Corp., USA) was used to develop the skeletal model. The skeletal model was built according to the bi-planar radiographic images of Subject 18003 as shown in Figure 7-3. The bone tissues were developed from a standard skeletal model as shown in Figure 7-4. The thoracic and lumbar vertebrae, sacrum, pelvis, ribs and sternum from a standard skeletal model were rotated, deformed and resized by referring to the bi-planar radiographic images as shown in Figure 7-5. In addition to the bone tissues, an intervertebral disc was built between two successive vertebrae by using subtraction (Figure 7-6).

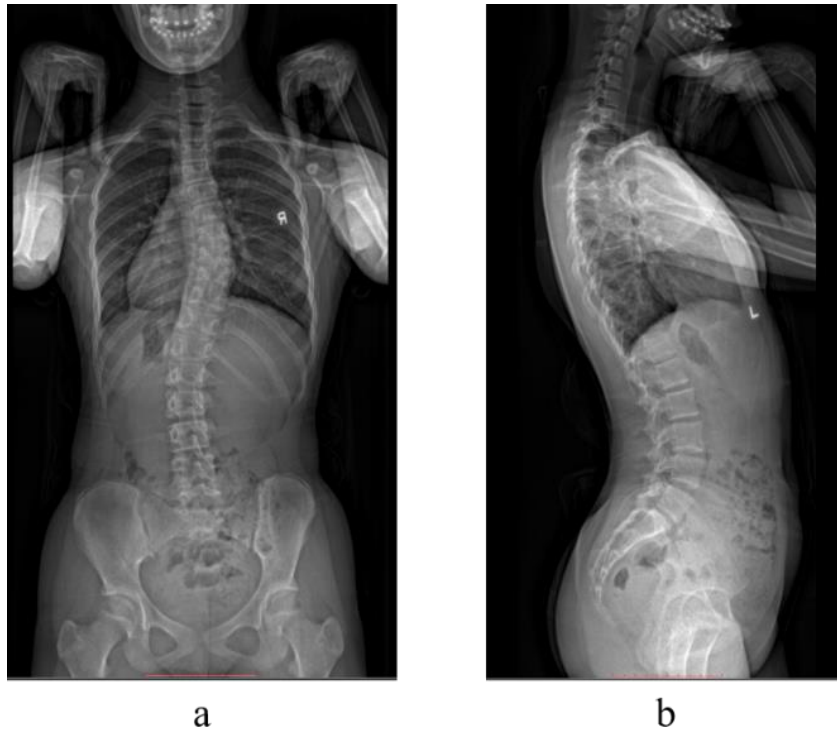


Figure 7-3 Radiographic images of Subject 18003: (a) frontal plane and (b) sagittal plane



Figure 7-4 Standard skeletal model

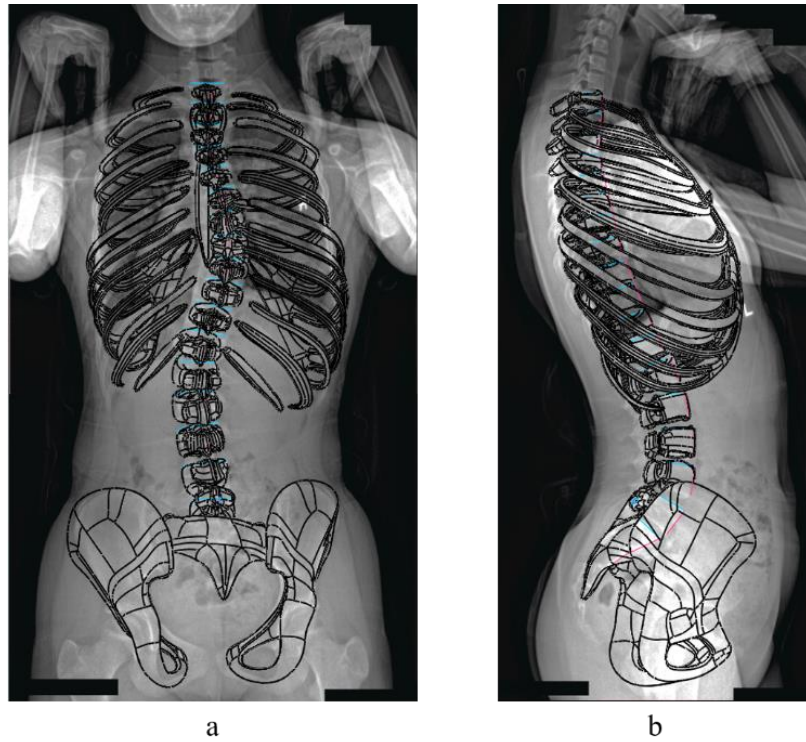


Figure 7-5 Bone tissues of first skeletal model in: (a) frontal plane and (b) sagittal plane

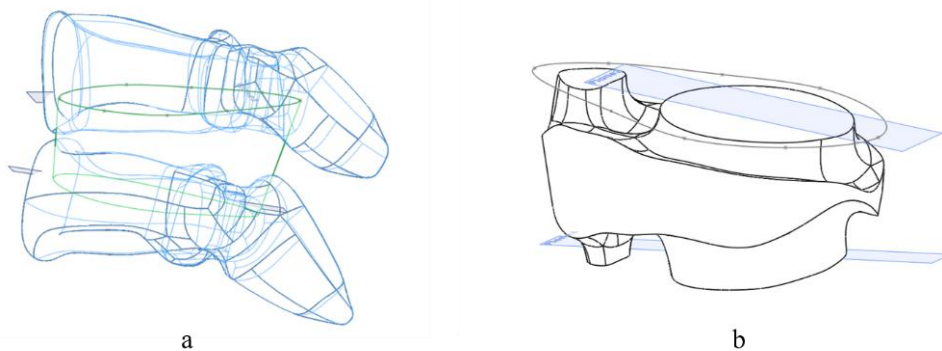


Figure 7-6 (a) Intervertebral disc built between two successive vertebrae, and (b) intervertebral disc

However, due to the complex geometry of the standard skeletal model and its large file size, a skeletal model developed by using the standard model could not be imported into Abaqus/CAE 6.14-4 (Dassault Systèmes Simulia Corp., USA) for numerical processing. Therefore, a second skeletal model was developed and to do so, the vertebrae were built by extruding an oval surface, the ribs were built by sweeping an oval profile along a 3D path which created a solid feature and the intervertebral discs were built by extruding the top and bottom surfaces of the vertebrae (Figure 7-7). All of the sketches and sweeping paths were drawn by referring to the bi-planar radiographic images.



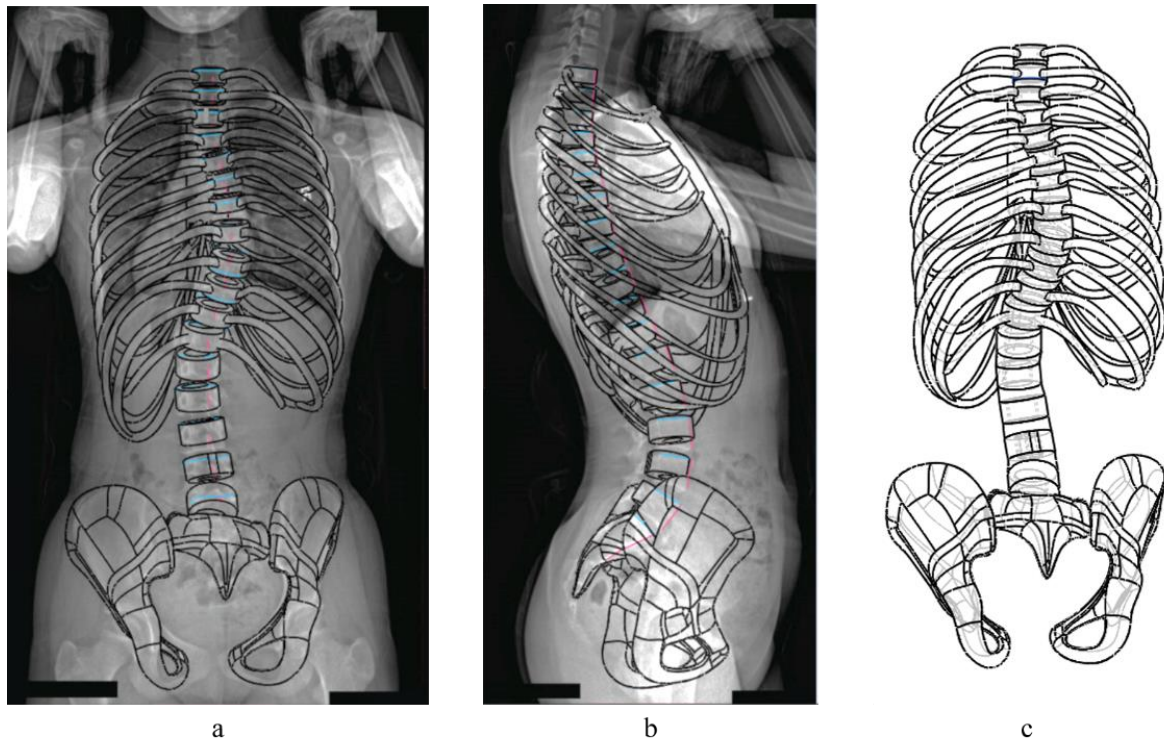


Figure 7-7 Bone tissues of second skeletal model in the (a) frontal plane and (b) sagittal plane, and (c) second geometric model of skeletal structure

The second geometric model of the skeletal structure was successfully imported into Abaqus/CAE 6.14-4 (Dassault Systèmes Simulia Corp., USA). Nevertheless, when discretizing the geometric model into meshing elements for numerical simulation, it was found that a large volume of mesh was required to simulate the organic shape of the ribs, sacrum and pelvis and thus would incur an extremely long calculation time in the numerical simulation process. For efficiency purposes, a simplified skeletal model was used instead. In the final skeletal model, the vertebral bodies from the first thoracic to fifth lumbar, sacrum, pelvis, intervertebral discs and sternum were built as a regular geometric shape instead of organic shape by extruding the sketches built (Figure 7-8). All sketches were drawn by referring to the bi-planar radiographic images.

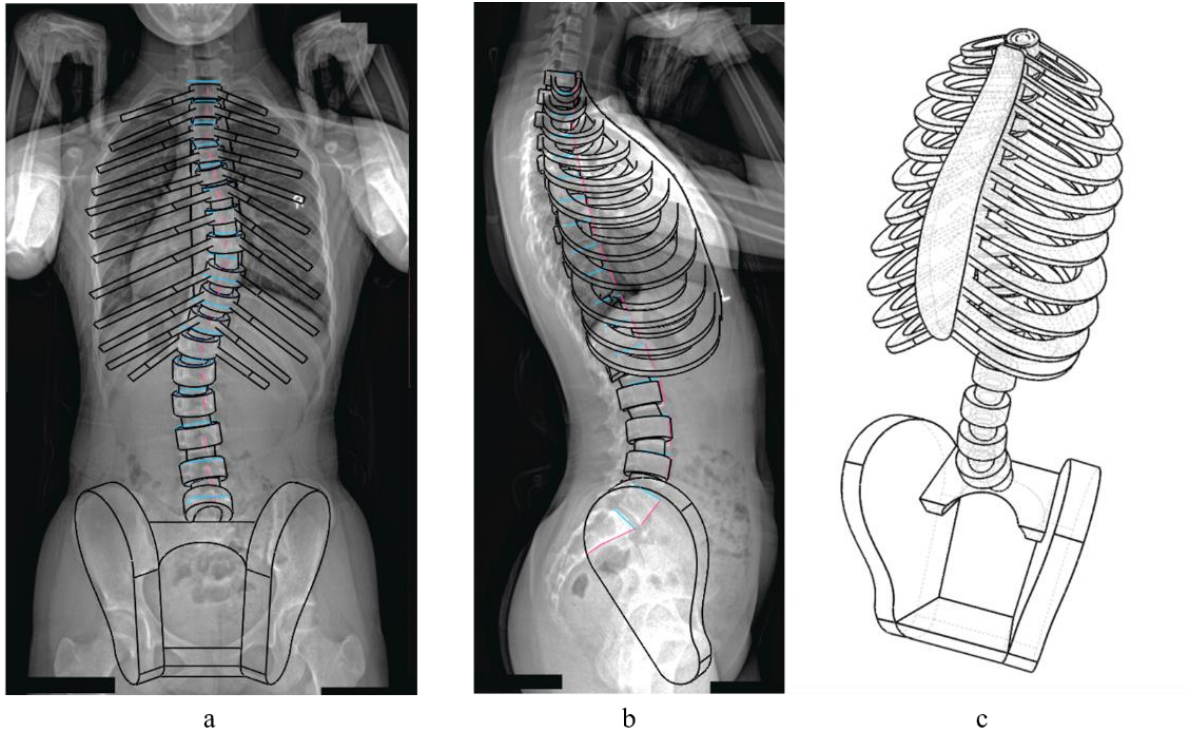


Figure 7-8 Bone tissues of final skeletal model in the (a) frontal plane and (b) sagittal plane, and (c) third geometric model of skeletal structure

### 7.2.1.3 Construction of FIA for AIS

SolidWorks 2012 x64 Edition (Dassault Systèmes SolidWorks Corp., USA) was used to develop the model of the FIA. The geometric model of the FIA was built from the geometric model of the torso body. To build the model of the FIA, a thin walled feature was created by removing the inner material of the torso body in the solid geometric model. After creating the thin walled feature, the model of the FIA was created by removing the unnecessary parts. The model was then segmented into four components.



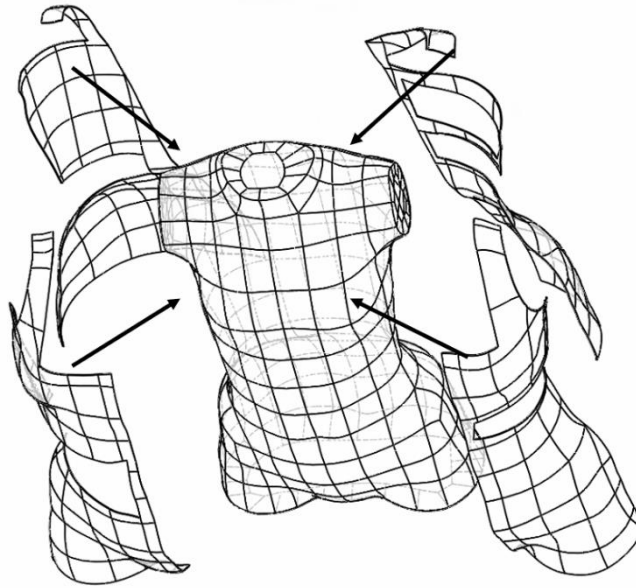


Figure 7-9 Segmentation of FIA into 4 components

The advantage of segmenting the FIA into 4 components was to prevent the shear of the contact elements between the surface of the torso and the inside surface of the FIA which made it easy to numerically simulate the wear process. However, this model of the FIA could not accurately reflect the wear process. To further improve the model, the final model of the FIA had only one opening which was placed at the centre of the model front which simulated the process of closing a front opening bra top and tightening the corrective component and pelvis belt (Figure 7-10).

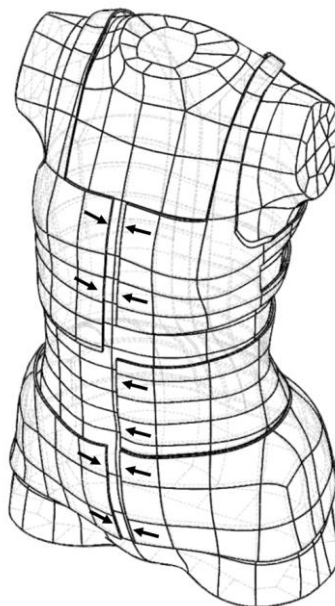


Figure 7-10 Final model of FIA which has only one opening

### 7.2.2 Defining material properties

The geometric models of the torso body, skeletal structure including the bone and intervertebral tissues, and FIA were imported into Abaqus/CAE 6.14-4 (Dassault Systèmes Simulia Corp., USA) and subsequently assembled. Previous works on the mechanical properties of the torso body, bone and intervertebral disc tissues defined the Young's modulus ( $E$ ) and Poisson's ratio ( $\nu$ ) of the torso body tissues as 0.01-1 MPa and 0.2-0.45 respectively, bone tissues as 5000-12,000 MPa and 0.2-0.3 respectively, and intervertebral disc tissues as 1-3.59 MPa and 0.3-0.45 respectively (Cahill et al., 2012; Cheng et al., 2010; D. Périé et al., 2004).

The Young's modulus ( $E$ ) of the FIA was determined from the stress-strain curve of its textile material while the Poisson's ratio ( $\nu$ ) was defined based on previous research (Zhou et al., 2010). Figure 7-11 shows the tensile stress-strain curve for the warp direction of the fabric material of the FIA. The Young's modulus ( $E$ ) and Poisson's ratio ( $\nu$ ) of the textile material were 0.59 MPa and 0.4 (Zhou et al., 2010), respectively.

As for the hinge material of the FIA, which was polyurethane thermoplastic, the Cambridge University Engineering Department (2003) has defined the physical and mechanical properties as follows: the Young's Modulus ( $E$ ) and Poisson's ratio ( $\nu$ ) were 2070 MPa and 0.33 respectively. The material properties used for the model of the torso body, skeletal structure and FIA are shown in Table 7-2.

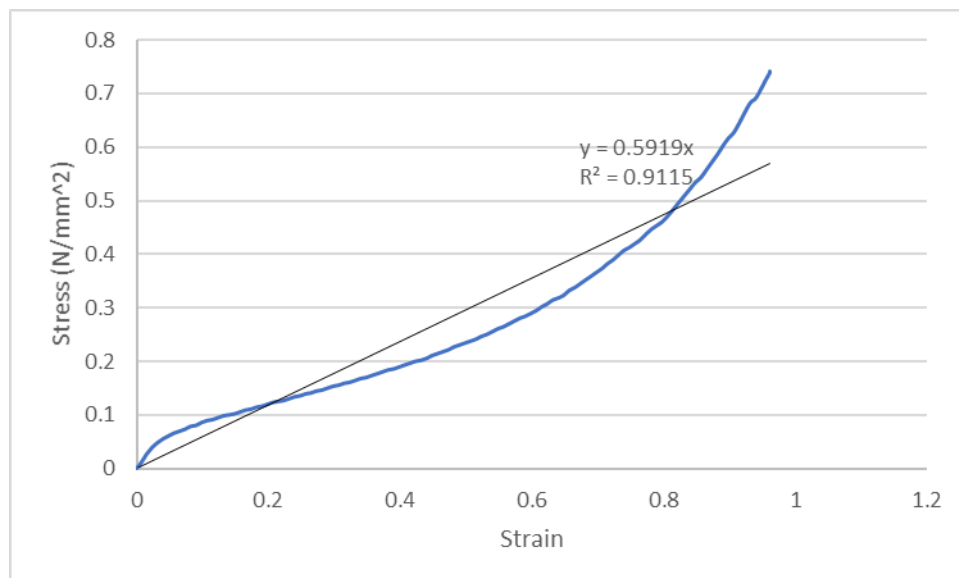


Figure 7-11 Tensile stress-strain curves for warp direction of FIA material

Table 7-2 Material properties of models of scoliotic torso and FIA

	Young's modulus (MPa)	Poisson's ratio
Torso body	0.05	0.4
Bones	10,000	0.3
Intervertebral disc	1	0.3
Textile material of FIA	0.59	0.4
Hinge material of FIA	2070	0.3

### 7.2.3 Defining type of mesh element

The mesh elements used for the scoliotic torso model were 10-node linear quadratic tetrahedral elements with three degrees of freedom at each node (C3D10) (Figure 7-12). The minimum mesh size was 40 mm. The scoliotic torso model consisted of 36,976 elements in total including 4345 elements for the intervertebral disc, 8827 elements for the bones and 23,804 elements for the torso body. Figure 7-13 shows the meshed model of the scoliotic torso.

The mesh elements used for the model of the FIA were also 10-node linear quadratic tetrahedral elements with three degrees of freedom at each node (C3D10) (Figure 7-12). The minimum mesh size was 46 mm. The model of the FIA consisted of 2314 elements in total including 2041 elements for the textile material and 273 elements for the hinge material. Figure 7-14 presents the meshed model of the FIA.

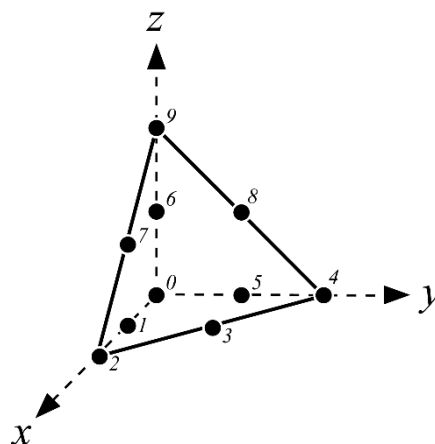


Figure 7-12 10-node quadratic tetrahedral element

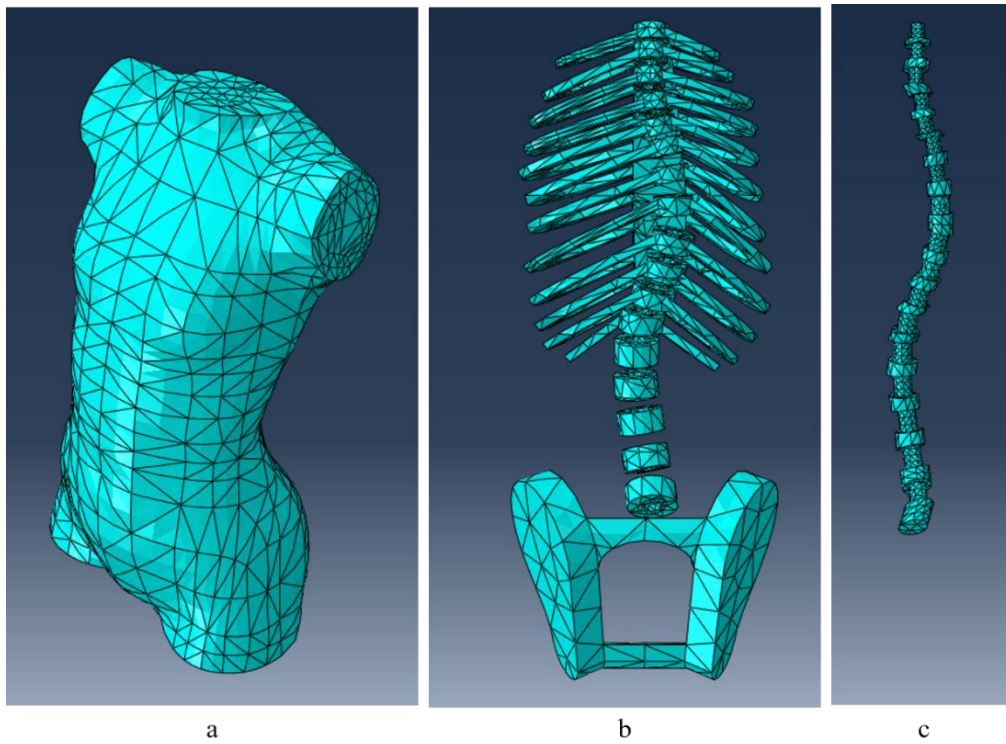


Figure 7-13 Meshed model of (a) scoliotic torso, (b) skeletal structure, and (c) intervertebral disc

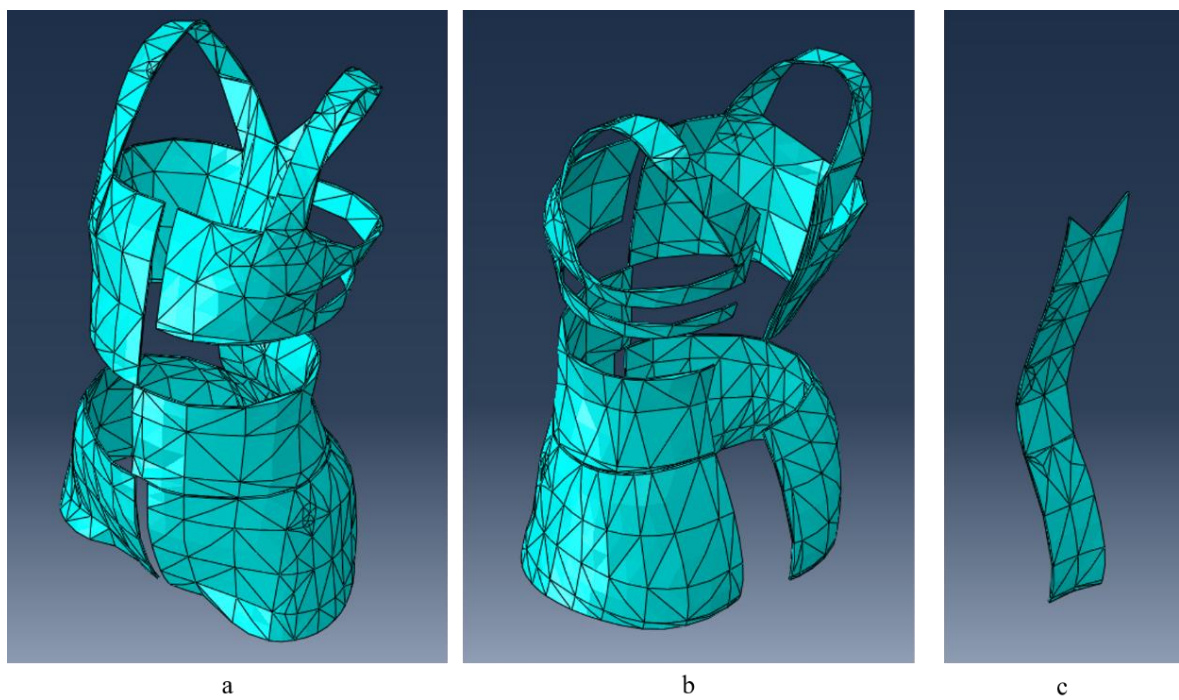


Figure 7-14 Meshed model of (a) FIA, (b) textile material, and (c) hinge

#### **7.2.4 Simulating brace wear in model**

To don the FIA, first, the bra top was applied to the shoulders, placed onto the breasts and closed with a front Velcro. Pants were placed onto the thighs, passed through the hips and closed with a front Velcro. The second step was to insert a pad into the corrective component. Then, the corrective component was attached to the artificial hinge. Convexity was applied and then the corrective component was secured at the front with a Velcro panel. Finally, the pelvis belt was attached to the artificial hinge, placed around the pelvis and closed with a front Velcro.

To simulate this process and the corrective forces exerted by the FIA onto the torso, the textile material of the FIA was stretched until fully enclosed around the torso and loading was applied on the surface of the torso under the corrective component to simulate in-brace spinal correction (Figure 7-15). Boundary conditions in the form of translational displacement were applied on the edge of the textile material of the FIA to simulate the tightening force of the corrective components and pelvis belt. During the analysis, the front edges of the right of the thoracic corrective component and left of the bra top were moved towards the midline of the body. The front edge of the left of the lumbar corrective component was moved towards the right of the lumbar corrective component. Both edges of the pelvis belt were moved towards the midline of the body. After tightening the corrective components and pelvis belt, loading was applied on the surface of the torso under the right of the thoracic corrective component and left of the lumbar corrective components. The magnitude of the loading was applied based on the measured pressure on the subject. The subject was asked to don the FIA and the interface pressure of the thoracic and lumbar pads was measured. In this model, the loading of the thoracic and lumbar pads was 24.4 kPa and 9.6 kPa respectively based on the pressure data obtained from the subject.

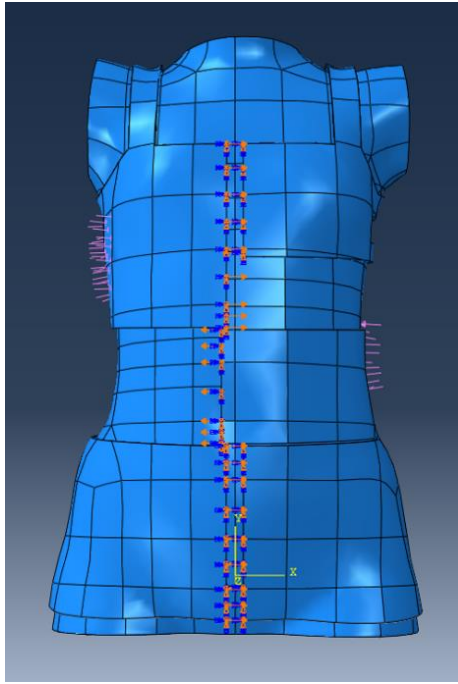


Figure 7-15 Tightening corrective components and pelvis belt and adding load on surface of torso under corrective component

In the simulation of the initial stage of the wear process, the model of the scoliotic torso and FIA were aligned by using the same relative coordinate system without any contact between the two models. Surface-to-surface contact was used to simulate the interactions between the surface of the two components. When one object forcibly came into contact with the other, the rigid body was set as the master surface while the deformable body as the slave surface to avoid penetration. Thus, the internal surface of the model of the FIA was set as the master surface while the surface of the torso model was set as the slave surface (Figure 7-16).

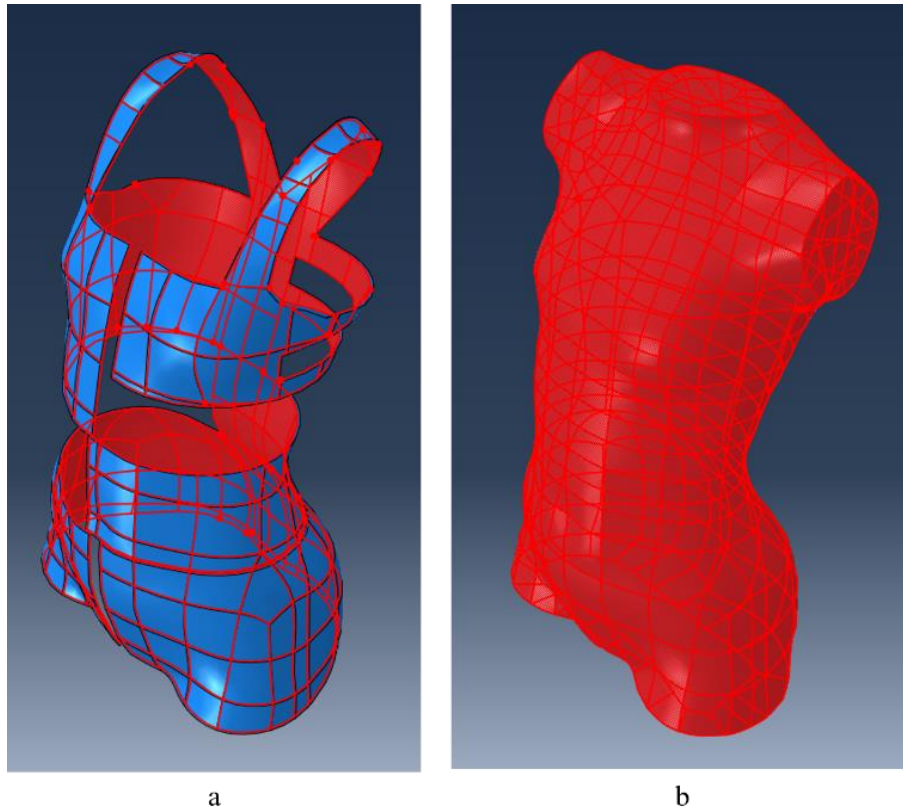


Figure 7-16 (a) Master and (b) slave surface for surface to surface interaction

The boundary conditions for this FE model were defined based on real-life situations. The aim of this model is to investigate the in-brace spinal effects. Thus, this model only included the torso of the body and the skeletal structure of the thoracic and lumbar vertebrae, sacrum, pelvis, ribs and sternum. It was assumed that the forces applied onto the torso by the FIA did not cause any displacement of the head and legs. Therefore, the top surface of the T1 vertebra and the bottom surface of the torso body were fixed by restricting all degrees of freedom which are U1 translation (heaving- up and down), U2 translation (swaying- left and right), U3 translation (surging- forward and backward), UR1 rotation (pitching-tilt forward and backward), UR2 rotation (yawing-swivel left and right) and UR3 rotation (rolling-pivot side to side) (Figure 7-17).



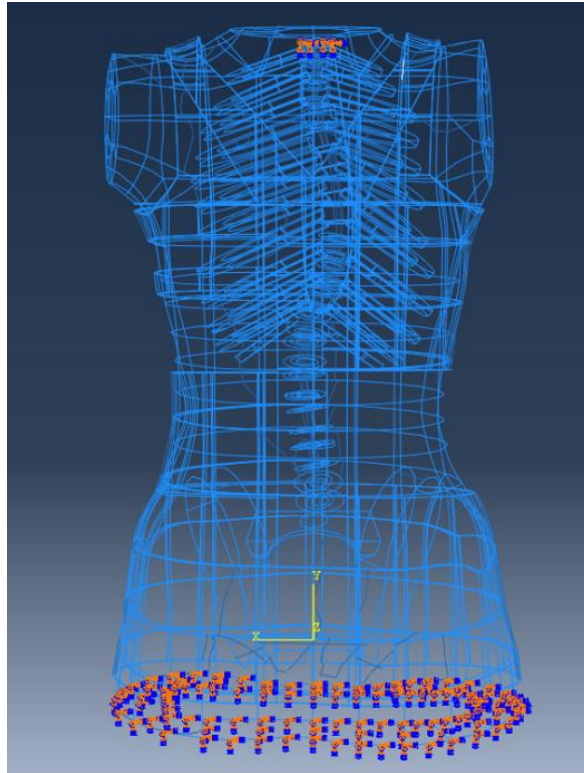


Figure 7-17 Boundary conditions of scoliotic torso model

### 7.2.5 Validation

Validation is essential in simulation work as it verifies whether the simulation results reflect the real situation and the accuracy of the simulation model. To validate the displacement of the scoliotic spine predicted by the simulation process, the radiographic images of two conditions, in-brace and without the brace, were measured and compared with the results of the FE model.

The Cobb's angle and spinal curve in the coronal plane were used as the parameters for comparison. To plot the spinal curve, the position of each vertebral body was defined by the horizontal distance between the vertebral body and central sacral vertical line. SolidWorks 2012 x64 Edition (Dassault Systèmes SolidWorks Corp., USA) was used to measure the Cobb's angle and the horizontal distance between the vertebral body and central sacral vertical line.

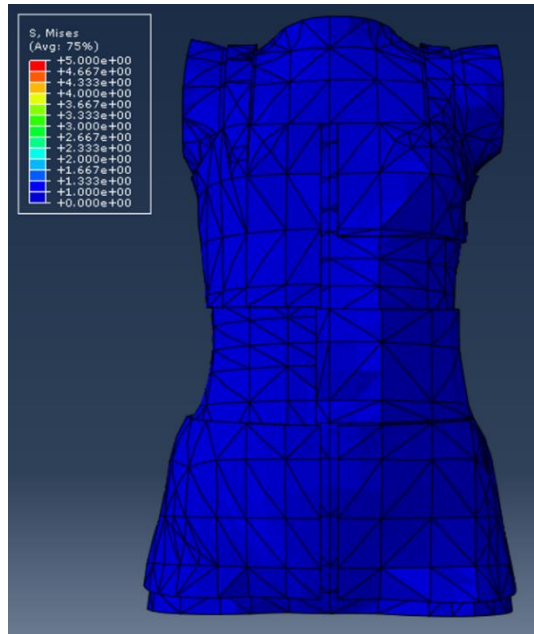
The predicted Cobb's angle and the spinal curve were then compared with the measurements of the radiographic images. Moreover, the predicted Cobb's angle and position of each vertebral body in the coronal spinal curve were then compared with the experimentally obtained results.

## 7.3 Results and discussion

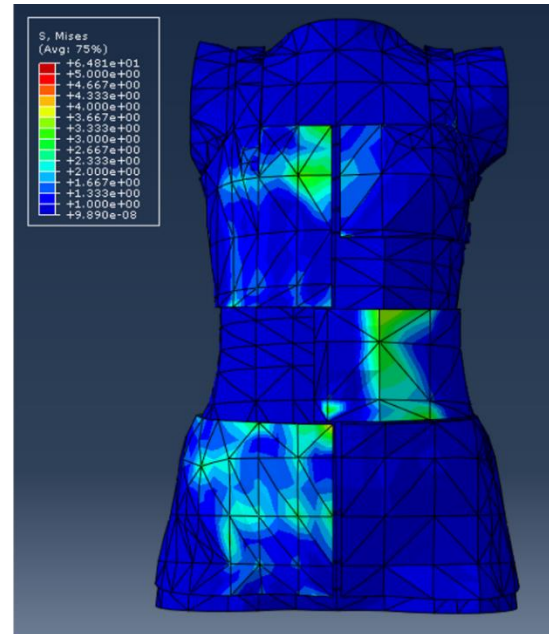
Figure 7-18 shows the shape deformation and the stress distribution of the FE model in the



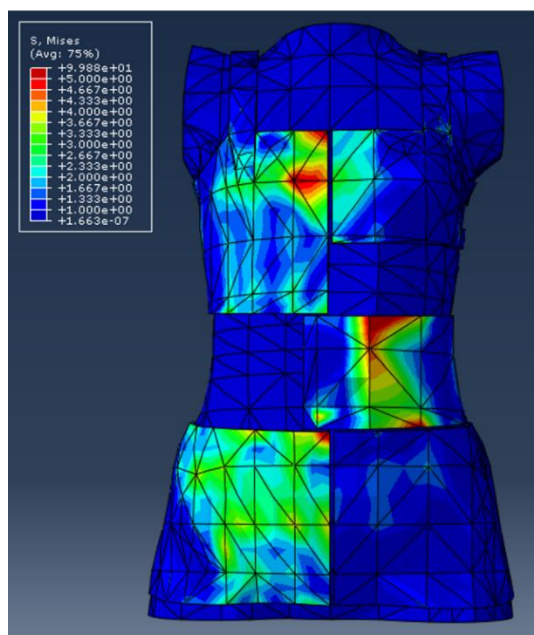
initial stage during and after the analysis. High stress levels are presented in red colour, whereas lower stress levels are shown in blue colour. The stress distribution plot showed that when stretching the corrective components and pelvis belt, there were relatively higher stress levels on the centre of the right front of the bra, left of the lumbar corrective component and right of the pelvis belt. The results reflected the influence of the body contours on pressure distribution in which the pressure was mainly distributed on the convex parts of the body, such as the abdomen.



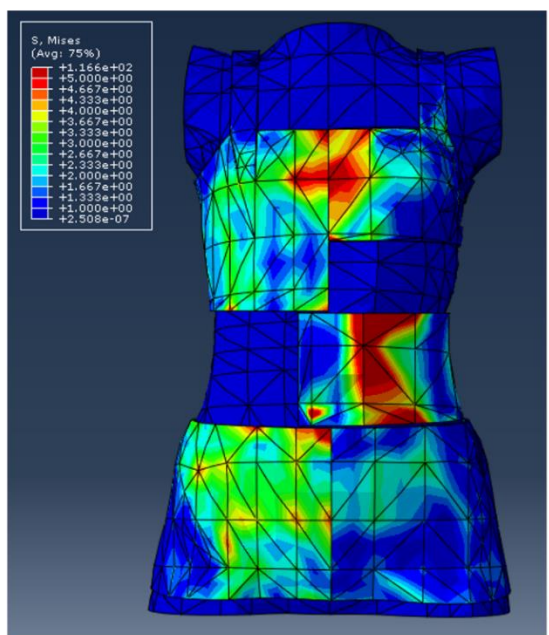
a



b



c



d

Figure 7-18 FE model (a) initial stage, (b) - (c) during analysis and (d) after analysis

Apart from the stress distribution of the FIA, Figure 7-19 shows the pressure distribution of the torso body. It was observed that a relatively high level of stress was found on the right thoracic, left lumbar and left pelvic regions. The distribution of stress accorded with the position of the corrective components and pelvis belt. Moreover, the stress was concentrated on the lateral side of body which might be due to the convexity of the body and the loading of the pads. In addition, it was surprising to see a high level of stress exerted onto the lateral of the lower left lumbar region. A possible explanation was that there was a gap between the edge of the lumbar corrective component and pelvis belt.

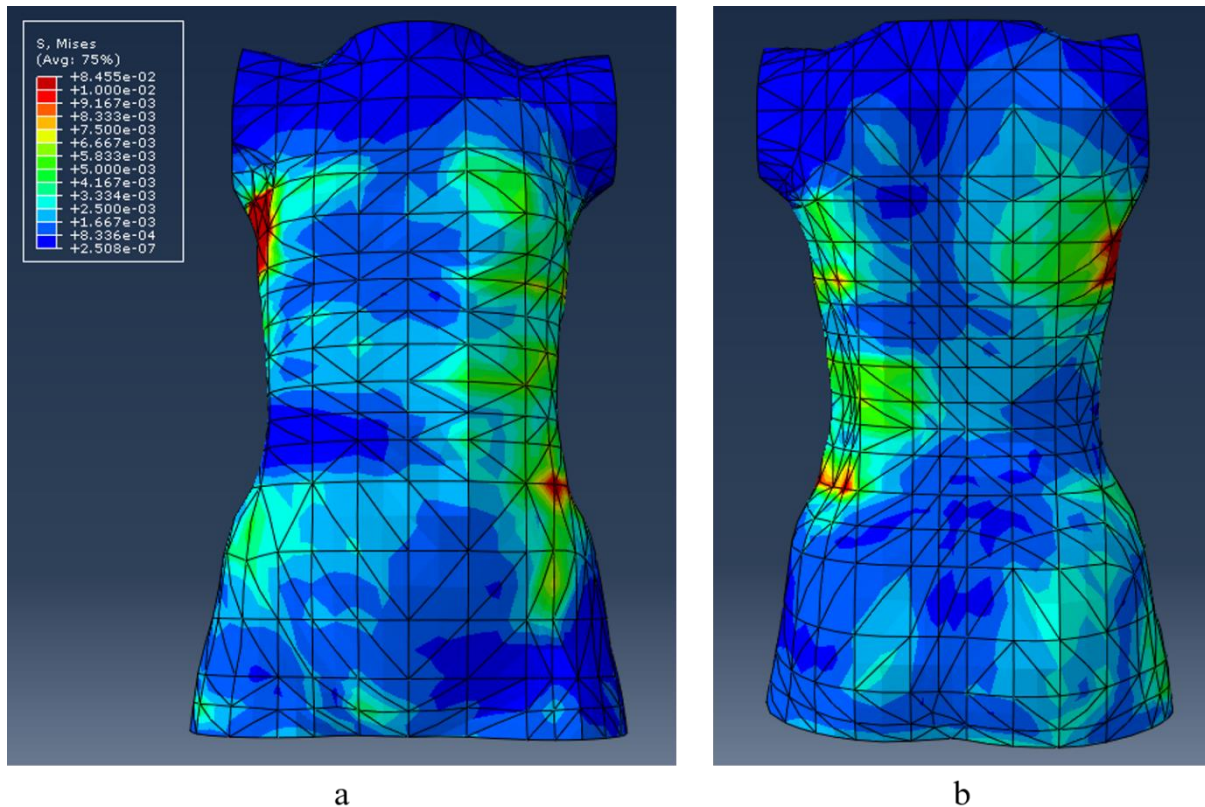


Figure 7-19 Stress distribution of torso body: (a) front and (b) back views

Figure 7-20 shows the stress distribution of the skeletal model after the analysis. It could be observed that the highest stress was found on the first rib. A possible explanation was that there was the constraint of boundary conditions in the first vertebral body. Besides, a high level of stress was also found on the seventh and eighth ribs on the right side of the body due to the thoracic pad. Moreover, it was interesting to see that the stress on the vertebral bodies was

relatively low while the stress on the ribs was relatively high. This pressure distribution might be due to the medial position of the vertebral bodies. In the law of physics, the magnitude of the diffused pressure was negatively related to the distance. The pressure induced by the FIA was diffused from the skin surface towards the body. Thus, a higher level of stress was exerted onto the ribs rather than the vertebral bodies.

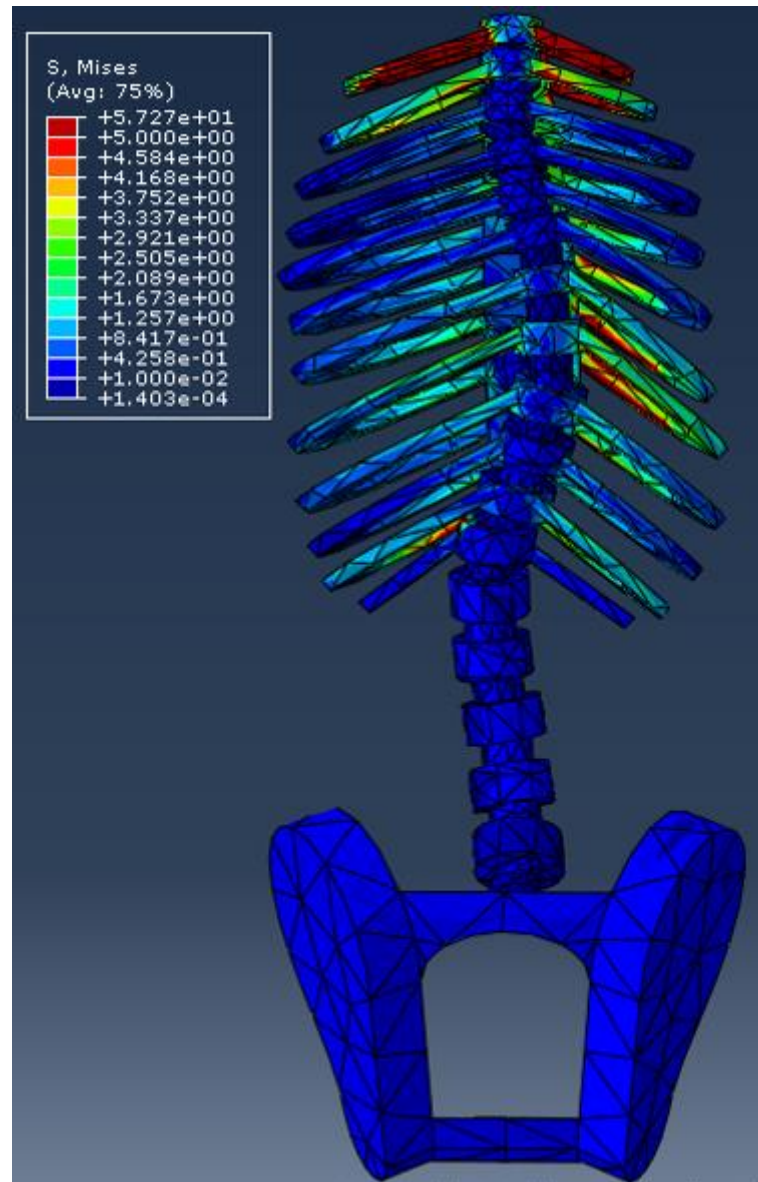


Figure 7-20 Stress distribution on skeletal system after analysis

Figure 7-21 shows that the displacement of the skeletal model after the analysis. The red arrow shows large deformations while the blue arrow indicates a small amount of displacement. The figure shows that the thoracic vertebra shifted to the left and the lumbar vertebra to the right. The largest amount of displacement was found at the 8<sup>th</sup> and 9<sup>th</sup> thoracic vertebrae which



comprised the apex of the thoracic curve. This implied that the severity of the thoracic curvature tended to be lower. Apart from the movement of the thoracic vertebrae, the lumbar vertebrae shifted towards the right. From the analysis results, the scoliotic spine tended to be straightened while the movement of vertebrae was correlated with the stress distribution of the torso body.

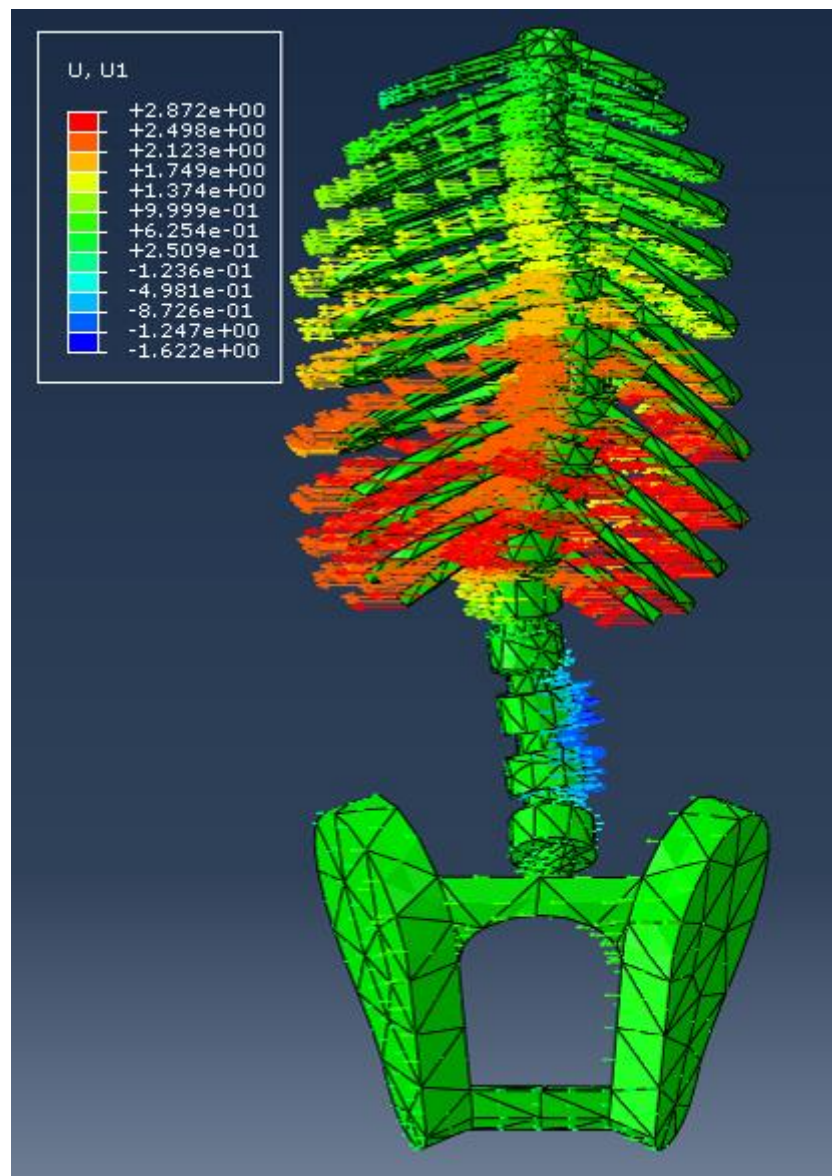


Figure 7-21 Displacement of skeletal model

In order to validate the FE model in this study, the predicted spinal curve was compared with the actual curvature obtained through the radiographic images. Figure 7-22 illustrates the spinal curves obtained from the simulation and radiographic images of the subject when the brace was donned or not worn. The movement of the simulated spinal curve obtained with the FE model showed a similar trend as the in-brace image. Considering the movement obtained from the in-brace image and result estimated by the FE model, the first thoracic to second lumbar

vertebral bodies (T1-L2) of both the in-brace and estimated spinal curves shifted towards the left while the third and fourth lumbar vertebral bodies (L3-L4) of both curves shifted towards the right.

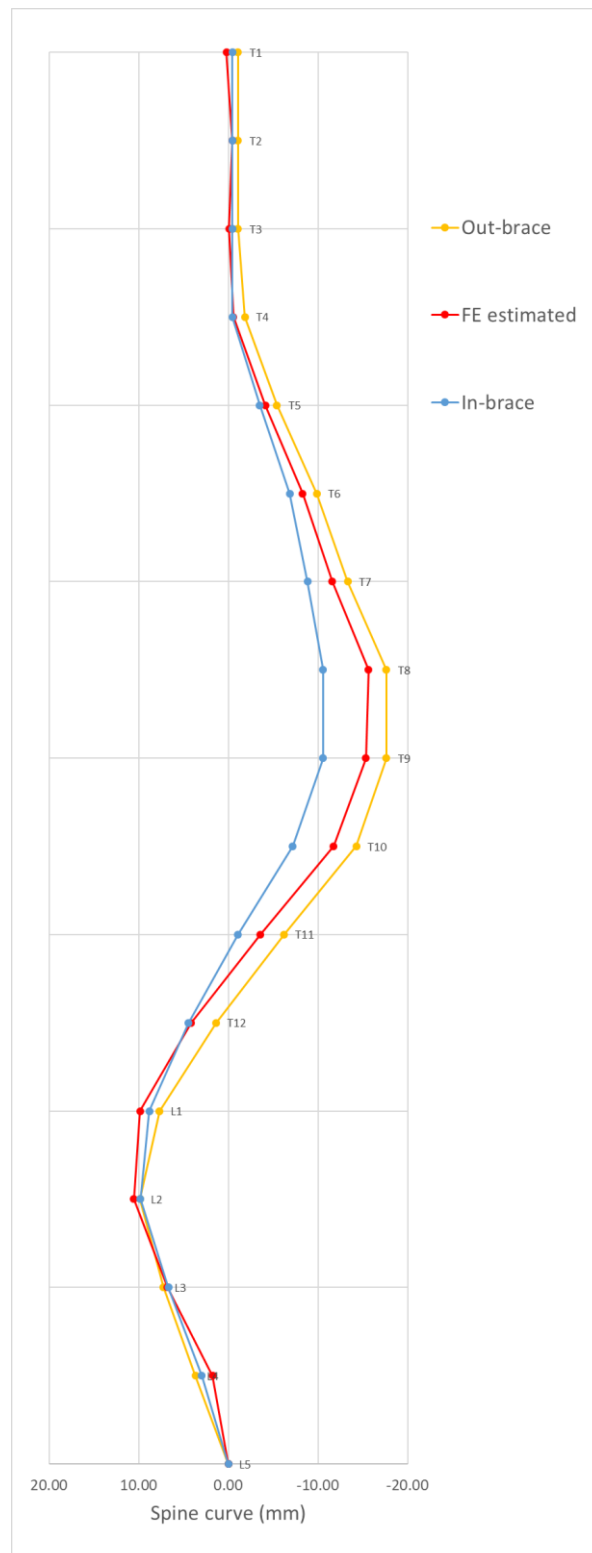


Figure 7-22 Spinal curves of subject based on radiographic images vs. FE model

The magnitude of displacement of the vertebral body obtained from the FE model was partially correct when compared with the results from the in-brace correction. The correlation coefficient of the vertebral body displacement was 0.74. The FE model underestimated the amount of movement of the seventh to eleventh thoracic vertebral bodies (T7-T11).

In addition to the spinal curve, the Cobb's angle of the geometric model of the skeletal system was compared with the in-brace radiographic image to further validate the model. Table 7-3 shows the Cobb's angle based on radiographic measurement and the FE model. The FE model showed a reduction of the Cobb's angles in both the thoracic and lumbar curves which was the same in the in-brace radiographic image. In comparing the Cobb's angle between the in-brace radiographic images and FE model, the value obtained by the latter or through measurements of the in-brace radiographic images of both the thoracic and lumbar curves was slightly larger than that by the former. This result was in agreement with the results of the displacement of the vertebral bodies.

Table 7-3 Cobb's angle: with and without brace and FE model

	In-brace	Without brace	Estimation
Cobb's angle in thoracic curve	18.7°	25.3°	20.8°
Cobb's angle in lumbar curve	18.8°	21.8°	19.4°

Both the displacement of the vertebral bodies and the Cobb's angle indicated that the FE model underestimated the spinal corrective effect. This implied that the corrective forces induced by the pads were not enough to provide the expected amount of thoracic correction. This result was in agreement with a previous finding in D. Périé et al. (2004) on the discrepancies of FE estimation models and real in-brace radiography. This result was in agreement with other mechanisms such as muscle control to shift the trunk away from the areas of pressure, which is also called proprioception, and could also be used in spinal correction as suggested by Périé et al. (2003). Moreover, another possible explanation was the mechanical properties of the model. The flexibility of the spine might influence in-brace correction (Cheung et al., 2017) and the current study was a patient specific model. However, the mechanical properties of this torso model were taken from other studies in the literature. Thus, the mechanical properties might not be the same as those in this study which could result in some errors. Furthermore, as mentioned above, the geometric model of the skeletal system was simplified for efficiency of

simulation, and the scoliotic torso model only included three different material properties of the torso body, bones, and intervertebral disc. Some elements such as ligaments, muscles, internal organs, blood vessels, and skin were neglected. They might very well be possible factors that caused errors in this FE model.

#### **7.4 Modification of hinge**

As mentioned above, the FE model allowed the biomechanics and in-brace performance of the FIA to be investigated based on the design and materials of the FIA and spinal conditions of the patients for design optimisation.

In Chapter 6, the clinical study subject was challenged by the durability of the hinge which broke easily. As mentioned in Chapter 5, 3D jet printing was used to produce the hinge prototype because it was both time and cost effective. However, the bonding of the printed material was poor, which compromised the durability of the hinge. To address this issue, milling was suggested to produce the hinge prototype instead of 3D printing.

In the following section, five prototypes produced by milling of different materials were given an introduction. Physical testing was conducted to select the most suitable material for optimising the durability of the hinge. Moreover, the hinge samples were further analysed by using an FE model to investigate their spinal performance by changing their material properties.

##### **7.4.1 Prototypes of modified hinge**

Five prototypes were produced by milling with different materials to improve the durability of the hinge. Cast acrylic (polymethyl methacrylate (PMMA)), polyoxymethylene (POM), carbon fibre and aluminium were used as the materials. PMMA was used due to its advantages of being light in weight and a translucent appearance. POM had excellent elasticity. Carbon fibre was light in weight and high in strength. Aluminium was also light in weight compared to other metals such as iron, steel, copper or zinc and high in strength. Apart from the leaf materials, iron and steel pins were also used.

In Chapter 6, it was observed that the knuckles and pins broke during body movement. Thus, it was believed that the leaf joints were the weak areas of the proposed hinge prototype. Due to a limited research budget, the testing specimen only had 2 leaves with 1 pin (Figure 7-23) and each hinge was tested with only one sample. Table 7-4 shows the specifications of each hinge.

Table 7-4 Specifications of hinges

Hinge	#1	#2	#3	#4	#5
Material of leaf	Cast acrylic (PMMA)	Polyoxymethylene (POM)	Carbon fibre reinforced polymer	6061 Aluminium alloy	6061 Aluminium alloy
Material of pin	Iron	Iron	Iron	Iron	Steel
Density (g/cm <sup>3</sup> )	1.19	1.41	2.0	2.7	2.7

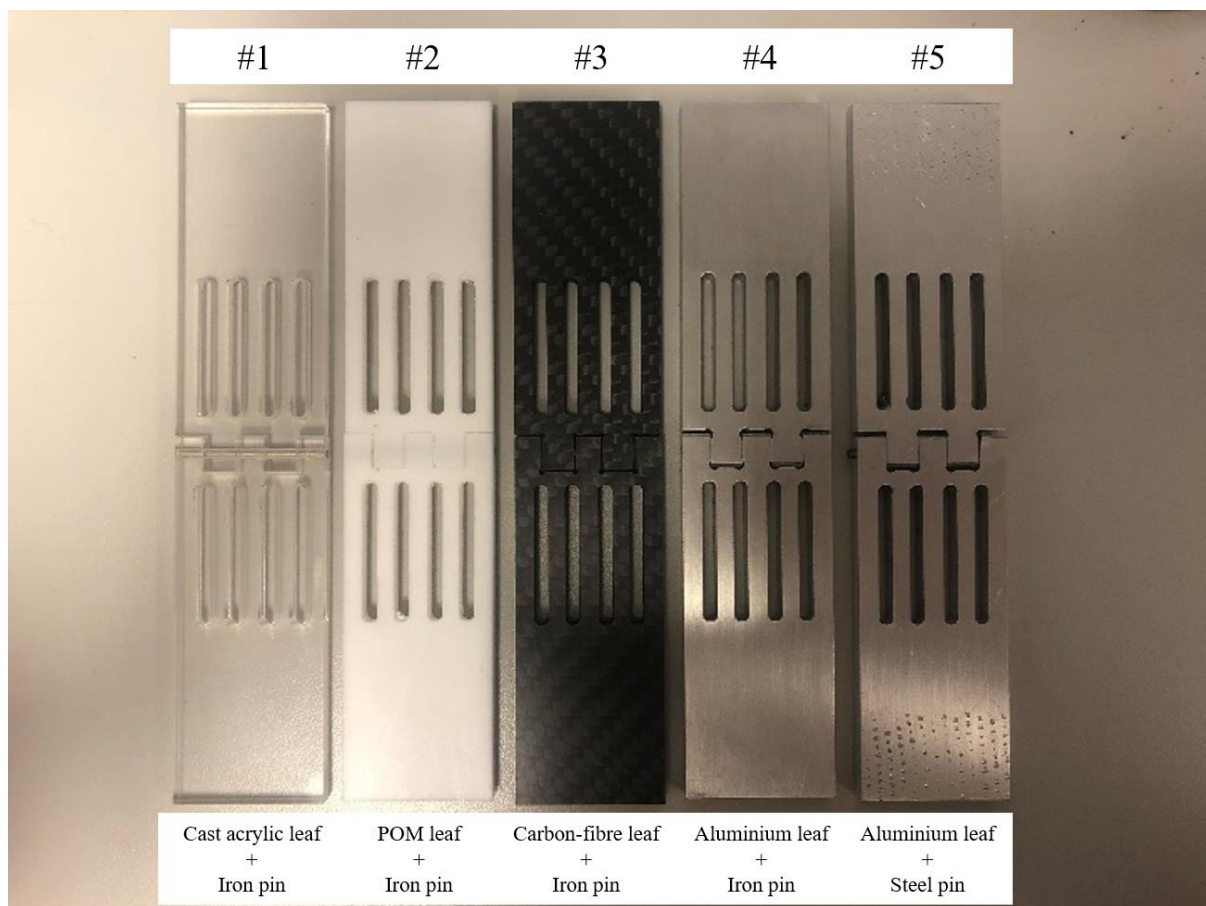


Figure 7-23 Five test specimens



### 7.4.2 Tensile strength

An ideal hinge should have a high tensile strength which implies good durability. Figure 7-24 shows that Hinge #5 had the highest tensile strength which meant that using an aluminium leaf with steel pins could withstand the highest amount of force along the longitudinal axis. Thus, in considering the tensile strength, Hinge #5 would have the best durability performance.

To further examine the weak points of each type of hinge material, the broken specimen and its load-displacement curve were studied. Figure 7-25 shows the specimens after tensile testing. The figure shows that the leaf of Hinges #1, #2 and #3 was broken while the pins of Hinges #3 and #4 were broken but not the leaf itself. This implied that the iron pins had a higher tensile strength than PMMA, POM and carbon-fibre. However, the aluminium leaf had a higher tensile strength than both the iron and steel pins.

In comparing the tensile strengths of the different leaves, the aluminium leaf had the highest tensile strength followed by the carbon-fibre, POM and PMMA leaves, see Figure 7-24.

On the other hand, when the results of Hinges #4 and #5 were compared, the tensile strength of Hinge #5 was much higher than that of Hinge #4. This implied that the material of the pin also influenced the tensile strength of the hinge. Figure 7-24 also shows that the steel pins increased the tensile strength by 90% in comparison to the iron pins. Thus, steel pins were recommended due to their high tensile strength.

Apart from the tensile strength, there was an interesting finding in the load-displacement curves (Figure 7-26 to Figure 7-30). The plotted load vs. displacement of Hinges #1, #3, #4 and #5 was typically linear before reaching the breaking point. This linear curve showed the brittleness of the materials. Moreover, there were clear breaking points and a hinge that did not deform, which further confirmed the brittleness of PMMA, carbon-fibre, iron and steel in Figure 7-26 and 28-30. On the other hand, a gradual slope could be observed in the load-displacement curve of Hinge #2 in Figure 7-27. This indicated that the POM was subjected to a large amount of deformation before breaking. This gradual slope showed the ductility of POM. Also, Figure 7-25 shows deformed POM knuckles which further confirmed its ductile behaviour.

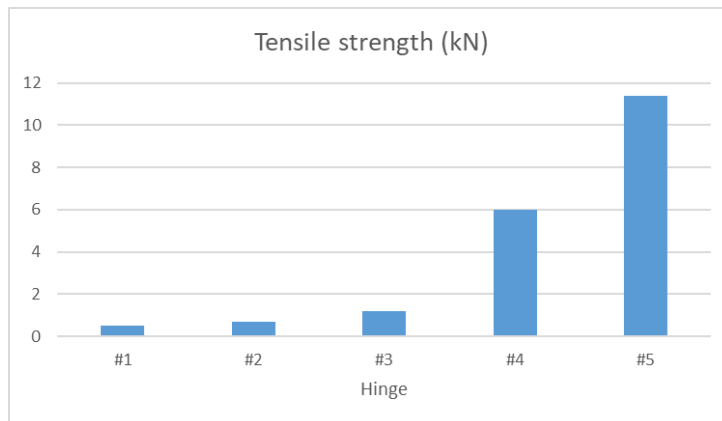


Figure 7-24 Tensile strength of five hinges

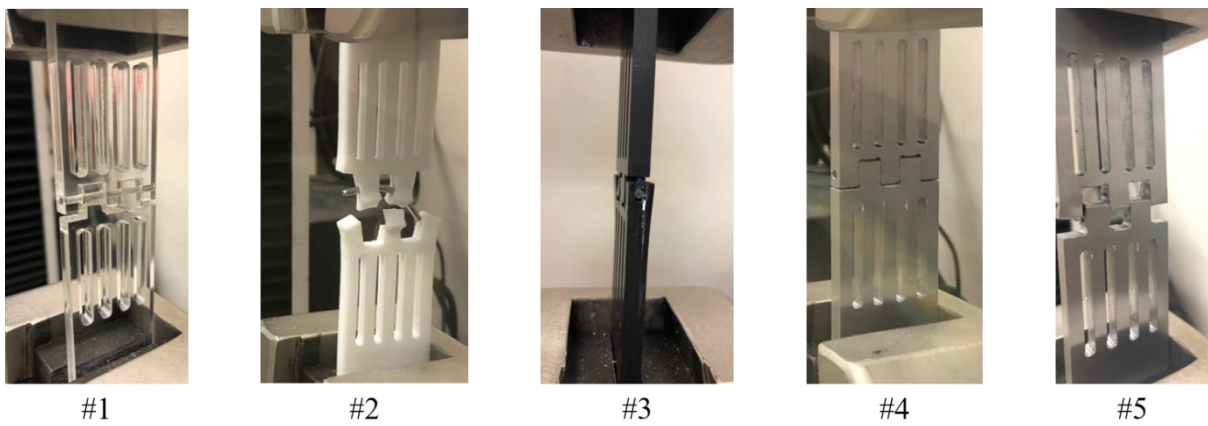


Figure 7-25 Five specimens after tensile test

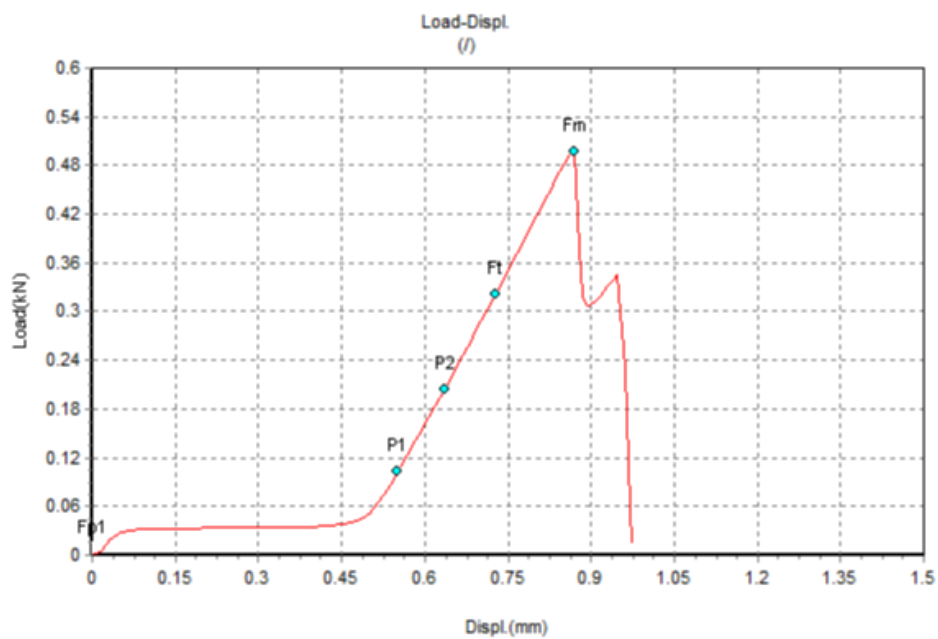


Figure 7-26 Load-displacement curve of Hinge #1

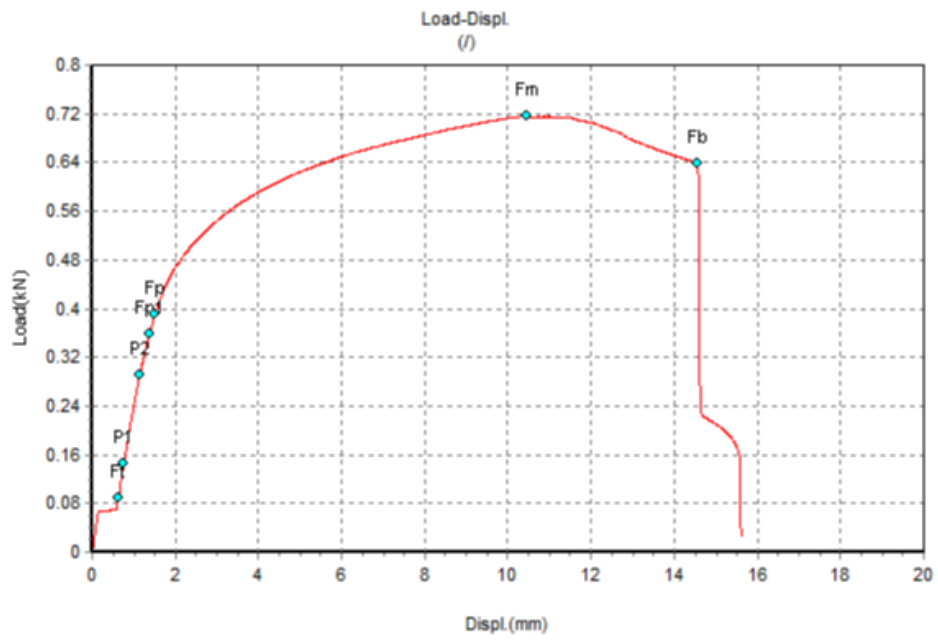


Figure 7-27 Load-displacement curve of Hinge #2

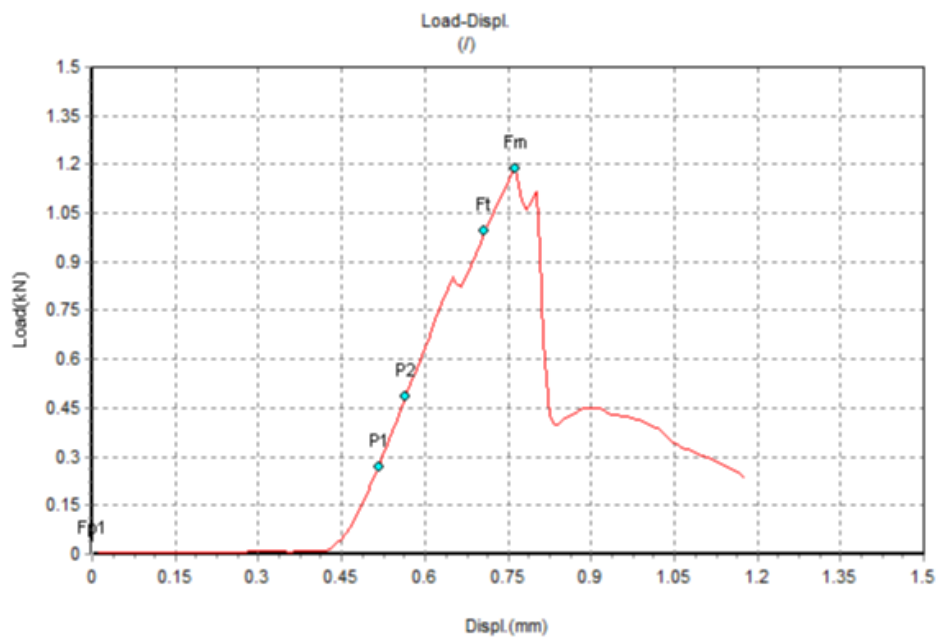


Figure 7-28 Load-displacement curve of Hinge #3

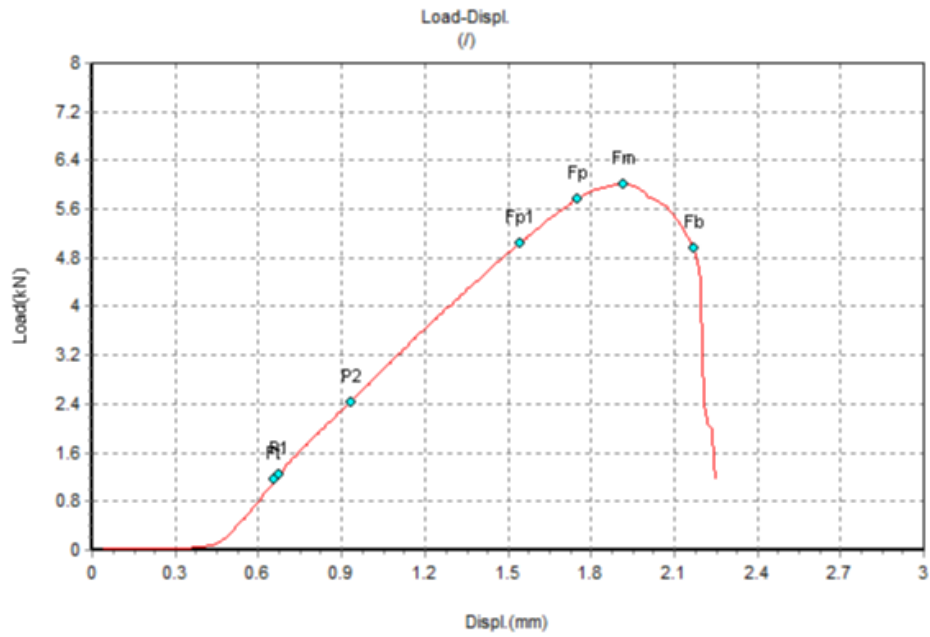


Figure 7-29 Load-displacement curve of Hinge #4

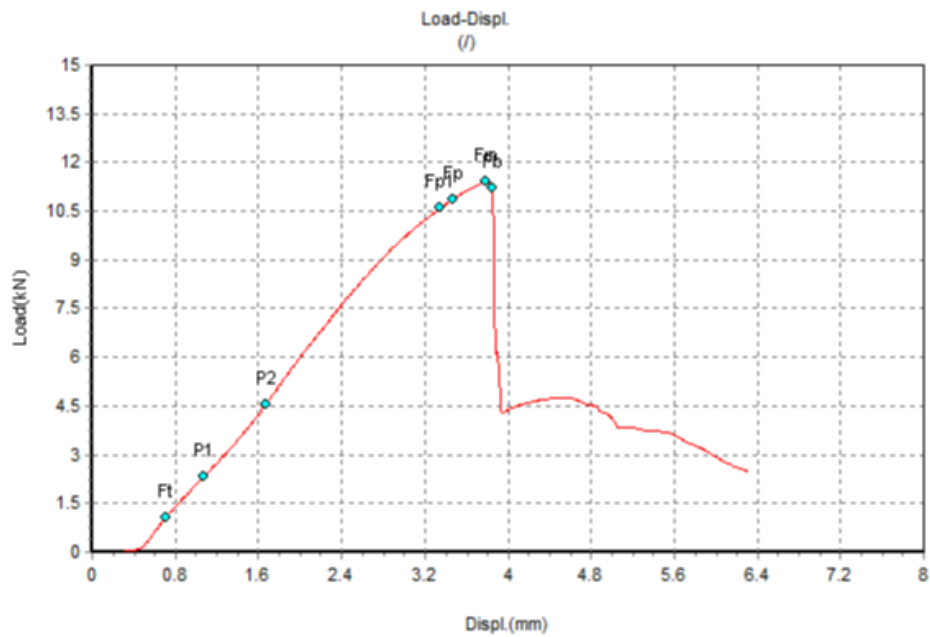


Figure 7-30 Load-displacement curve of Hinge #5

### 7.4.3 Torque to failure

Apart from the tensile strength, torque to failure is also a critical indicator of the durability of the hinge. An ideal hinge should withstand a high torque to failure. Figure 7-31 shows that Hinge #1 broke when twisted to an angle of about 18 degrees and the torque to failure was 1.7 N-m, which was the lowest torque to failure. Hinge #2 did not break when twisted to an angle

of 60 degrees and the torsional torque to 60 degrees was 1.0 N-m. This showed the high elasticity of POM. Furthermore, Figure 7-32 showed that Hinge #2 had good recoverability after twisting. Hinge #3 broke when twisted to an angle of 26 degrees and the torque to failure was 7.2 N-m. Figure 7-32 also shows that the groove of Hinge #3 delaminated and there was typical failure of the laminated structure of the carbon reinforced fibre plate. Hinge #4 broke when twisted to an angle of 15 degrees and the torque to failure was 20.4 N-m. Unlike Hinges #1 and #3, the pin of Hinge #4 broke instead of the leaf as shown in Figure 7-32 which implied that the aluminium leaf could withstand a higher torque to failure than the iron pin. Hinge #5 never broke even when twisted to an angle of 60 degrees and the torsional torque to 60 degrees was 32.3 N-m. Similar to Hinge #2, it was observed that Hinge #5 had good recoverability after twisting; see Figure 7-32.

In comparing Hinges #4 and #5, it was found that the steel pins resisted a higher torque under torsion than the iron pins. In comparing Hinges #1, #2, #3 and #4, it was found that the aluminium leaf had the greatest amount of torsional torque, followed by the carbon reinforced fibre, PMMA and POM leaves. Moreover, the torsion tests showed that the POM and aluminium leaves did not break after subjected to a torsion of 60 degrees.

Therefore, Hinge #5 had the greatest amount of torsional torque among all of the hinges. This meant that using an aluminium leaf with steel pins could resist the greatest amount of torsional torque when twisted to an angle of 60 degrees. Thus, in considering the torsional torque, Hinge #5 had the best durability.

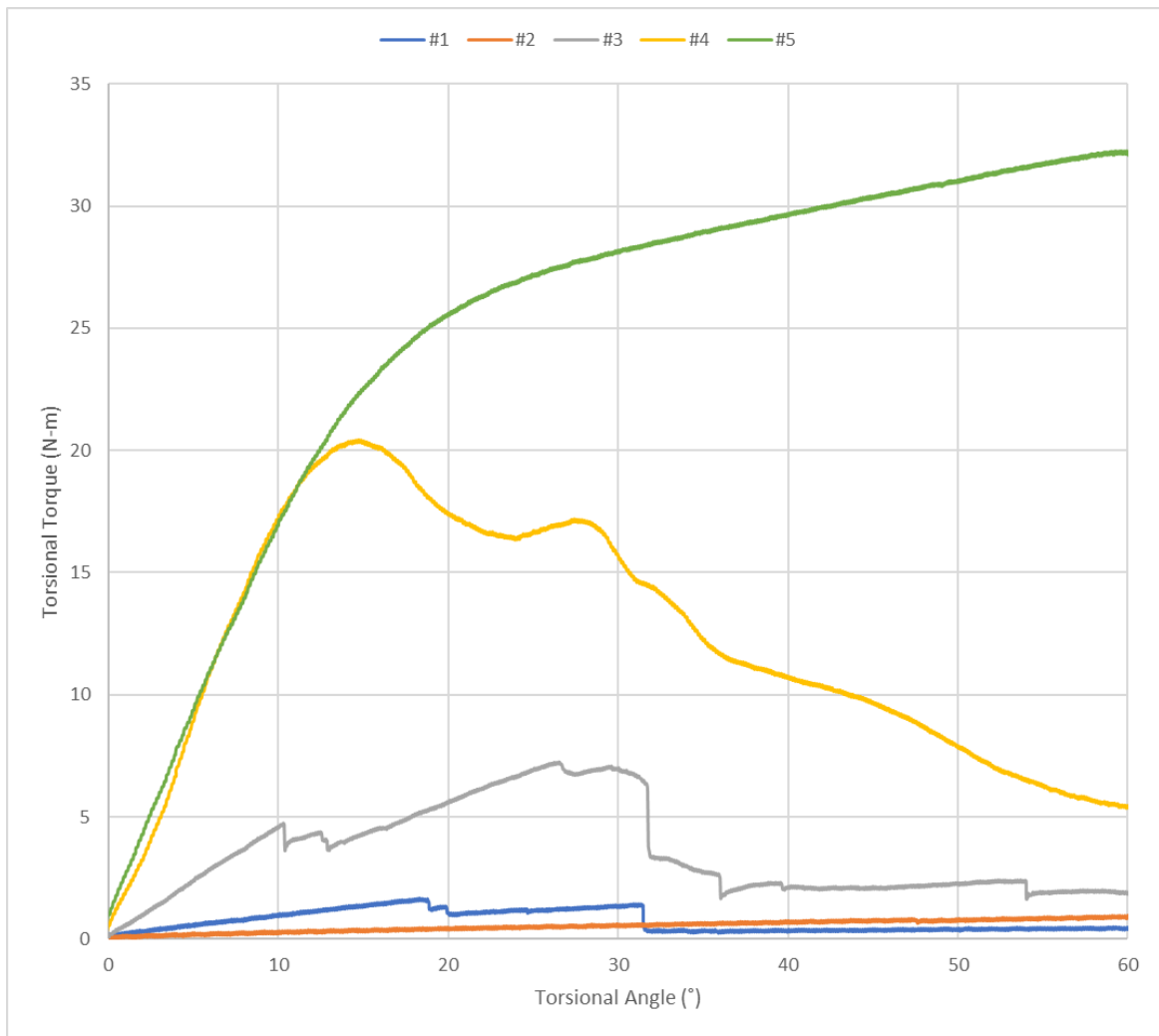


Figure 7-31 Torsional torque vs. torsional angle for hinges

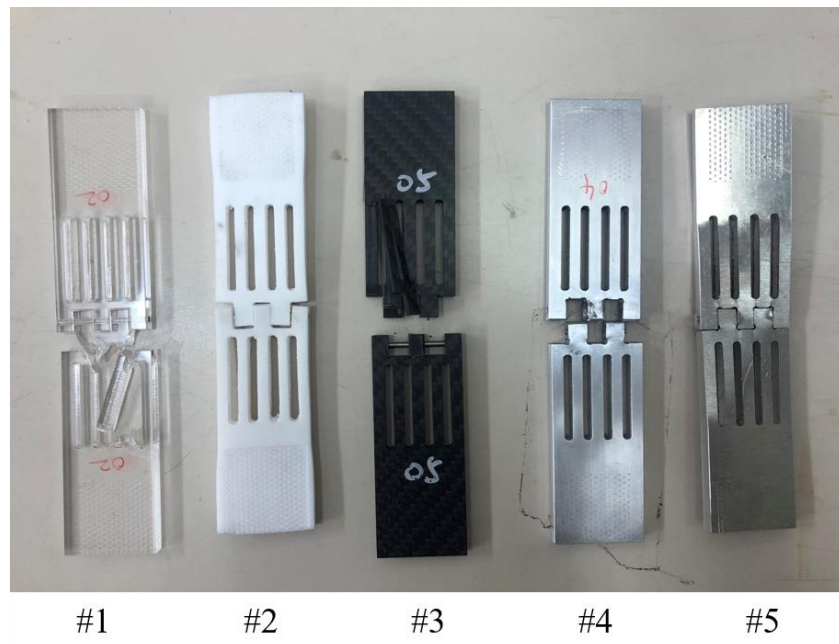


Figure 7-32 Five specimens after torsion test

#### 7.4.4 Effect of hinge materials on vertebral movement

The validated FE model in this study was used to further investigate the effect of the hinges of different materials on vertebral movement. Four FE models with hinges of different material properties were constructed. In considering the efficiency of the models, the material properties of the hinges were determined by examining the material properties of the leaf only which had already been defined in the literature (Brandrup et al., 1999; Cambridge University Engineering Department, 2003; Fukada, 2017) and the material properties of the pins were neglected. The material properties of the hinges used in the FE models are shown in Table 7-5.

Table 7-5 Material properties of hinges

Model code	PMMA hinge	POM hinge	Carbon fiber hinge	Aluminium hinge
Hinge material	Cast acrylic (PMMA)	Polyoxymethylene (POM)	Carbon fiber reinforced polymer	6061 Aluminium alloy
Modulus of hinge (MPa)	3020	3750	100,000	75,000

Poisson's ratio of hinge	0.36	0.44	0.21	0.32
-----------------------------	------	------	------	------

Figure 7-33 shows the stress distribution of the FIA by each model. It was observed that the FIA with the carbon fiber hinge exerted the largest amount of stress especially in the lumbar corrective panel and pelvis belt followed by the aluminium, POM and PMMA hinges. The results of all of the models showed that the stress of the FIA was positively correlated with the modulus of the hinge. High modulus material had the ability to greatly resist deformation under force. Since the textile panels and hinge were attached, the material properties of the hinge would influence the behaviour of the textile panels during stretching. Thus, stretching a textile panel attached to a hinge with a higher modulus usually requires a higher force.



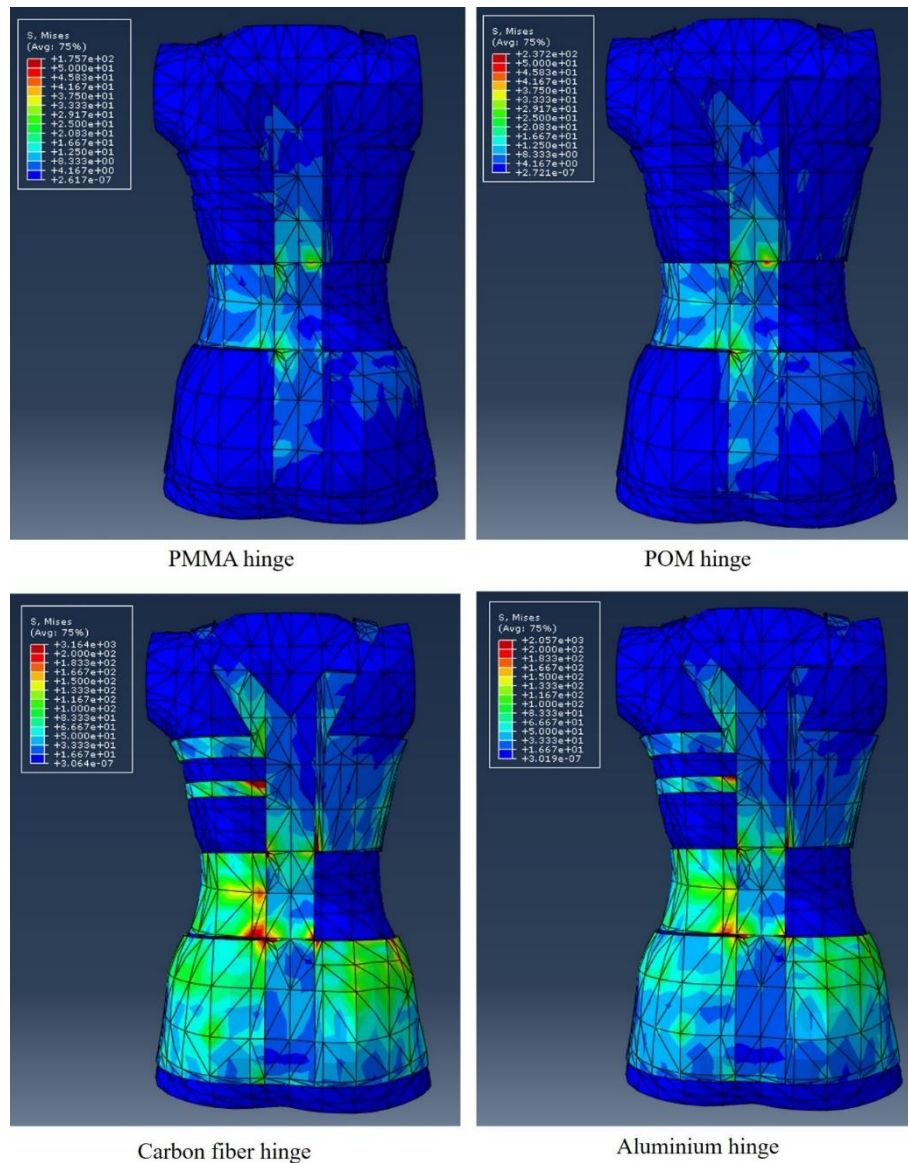
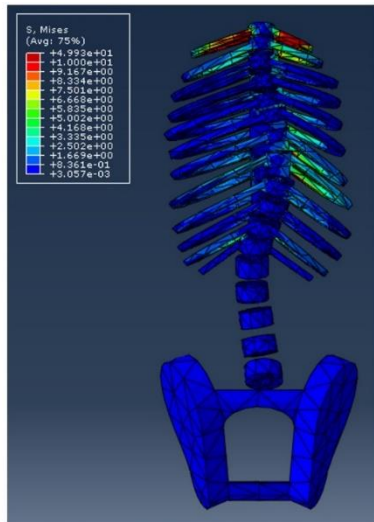


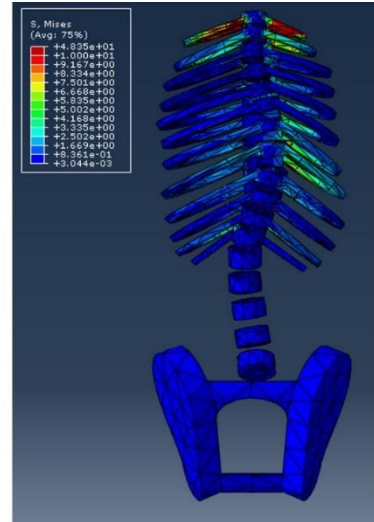
Figure 7-33 Stress distribution on FIA with different hinges

Figure 7-34 shows the stress distribution on the scoliotic spine with different hinges. There was no obvious difference in the stress distribution among the four models. This implied that there was no obvious correlation between the stress distribution on the FIA and scoliotic spine. There was minimal influence of the material properties of the hinges on the scoliotic spine. The spinal curve of these models (Figure 7-35) further confirmed that the material properties of the hinges were not the critical factor that influenced spinal correction.

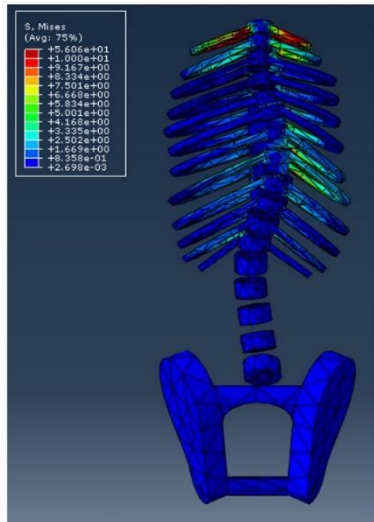
As a result, among the PMMA, POM, carbon fibre and aluminium hinges, Hinge #5 which had an aluminium leaf and steel pins was recommended when considering both the durability and effect on spinal correction.



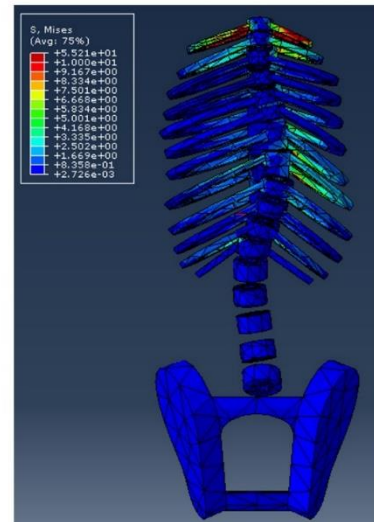
PMMA hinge



POM hinge



Carbon fiber hinge



Aluminium hinge

Figure 7-34 Stress distribution on scoliotic spine with different hinges

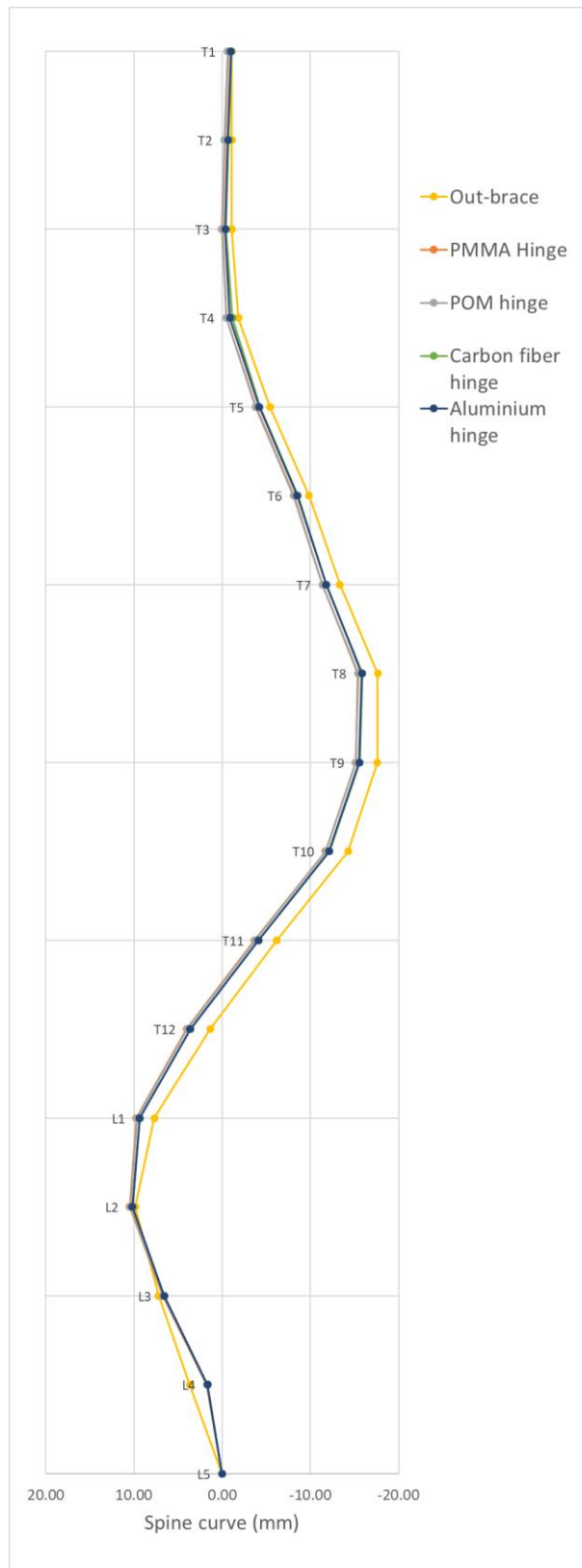


Figure 7-35 Spinal curves: PMMA, POM, carbon fibre and aluminium hinges

## 7.5 Effect of corrective pads on vertebral movement

As mentioned in Chapter 6, no correlation between the interface pressure of the FIA and in-brace correction was found due to the limited sample size in this study. To further investigate the biomechanics of the brace and optimise the design of the brace, the effect of loading which was applied on the torso surface on the vertebrae was studied.

Fifteen models with thoracic and lumbar loading which increased from 20% to 140% and decreased from 20% to 80% were created to investigate the effect of the spinal curve on the magnitude of loading. Table 7-6 shows the magnitude of loading of each model.

Table 7-6 Magnitude of thoracic and lumbar loading in each model.

Model	Details	Magnitude of thoracic loading (kPa)	Magnitude of lumbar loading (kPa)
#L0	Original loading	24.4	9.6
#L1	20% increment of both thoracic and lumbar loadings	29.3	11.5
#L2	50% Increment of both thoracic and lumbar loadings	36.6	14.4
#L3	20% Decrement of both thoracic and lumbar loadings	19.5	7.7
#L4	50% Decrement of both thoracic and lumbar loadings	12.2	4.8
#L5	20% Increment of thoracic loading	29.3	9.6
#L6	20% Decrement of thoracic loading	19.5	9.6
#L7	40% Decrement of thoracic loading	14.6	9.6
#L8	60% Decrement of thoracic loading	9.6	9.6

#L9	80% Decrement of thoracic loading	4.9	9.6
#L10	40% Increment of lumbar loading	24.4	13.4
#L11	60% Increment of lumbar loading	24.4	15.4
#L12	100% Increment of lumbar loading	24.4	19.2
#L13	140% Increment of lumbar loading	24.4	23.0
#L14	40% Decrement of lumbar loading	24.4	5.8
#L15	60% Decrement of lumbar loading	24.4	3.8

### 7.5.1 Effect of change in thoracic and lumbar loading

Figure 7-36 shows that increasing the same percentage of both the thoracic and lumbar loading reduced the thoracic curvature but increased the lumbar curvature. When both types of loading were reduced, there was less increase in the lumbar curvature but the correction of the thoracic curve was reduced. Thus, increasing the amount of both thoracic and lumbar loading lead to the problem of deterioration of the lumbar curve which might be due to the substantial thoracic loading. As the original amount of thoracic loading was much greater than that of lumbar loading, the difference between the two types of loading increased with the same percentage of change of both types of loading. In this situation, lumbar loading could not counter the thoracic loading and deterioration of the lumbar curve results.

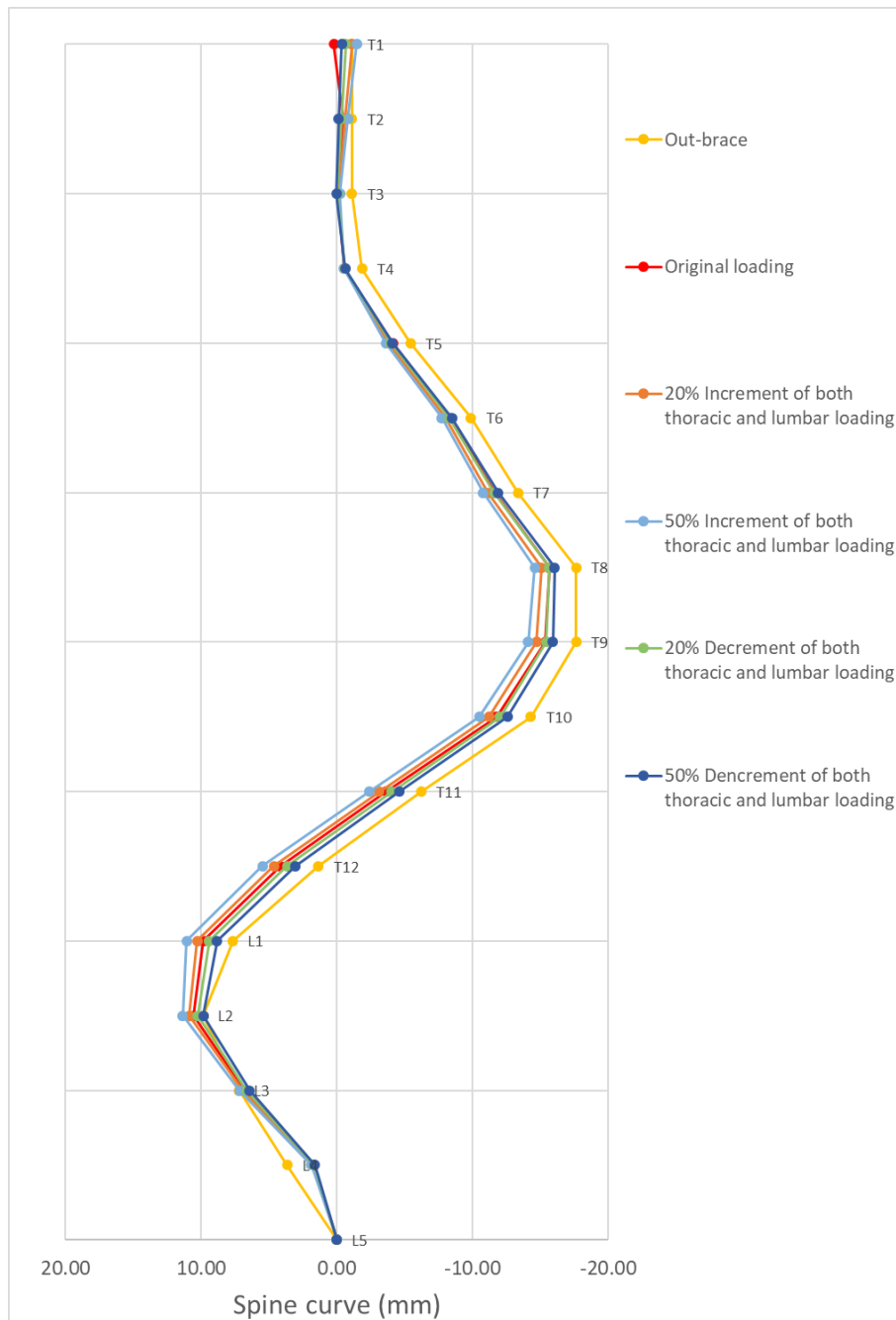


Figure 7-36 Spinal curves: Models #L0-#L4

### 7.5.2 Effect of change of thoracic loading

Figure 7-37 shows the effect of thoracic loading on the spinal curve. The figure shows that the correction of the thoracic curve and deterioration of the lumbar curve were positively correlated with the amount of thoracic loading. As the thoracic loading was increased, the lumbar could not withstand the counter force of the thoracic loading and thus deterioration of the lumbar curve was the result. The current results implied that excessive thoracic loading would lead to the deterioration of the lumbar curve while an insufficient amount of lumbar loading might

inhibit the correction of the thoracic curve. This showed that managing the counter force in spinal correction was critical.

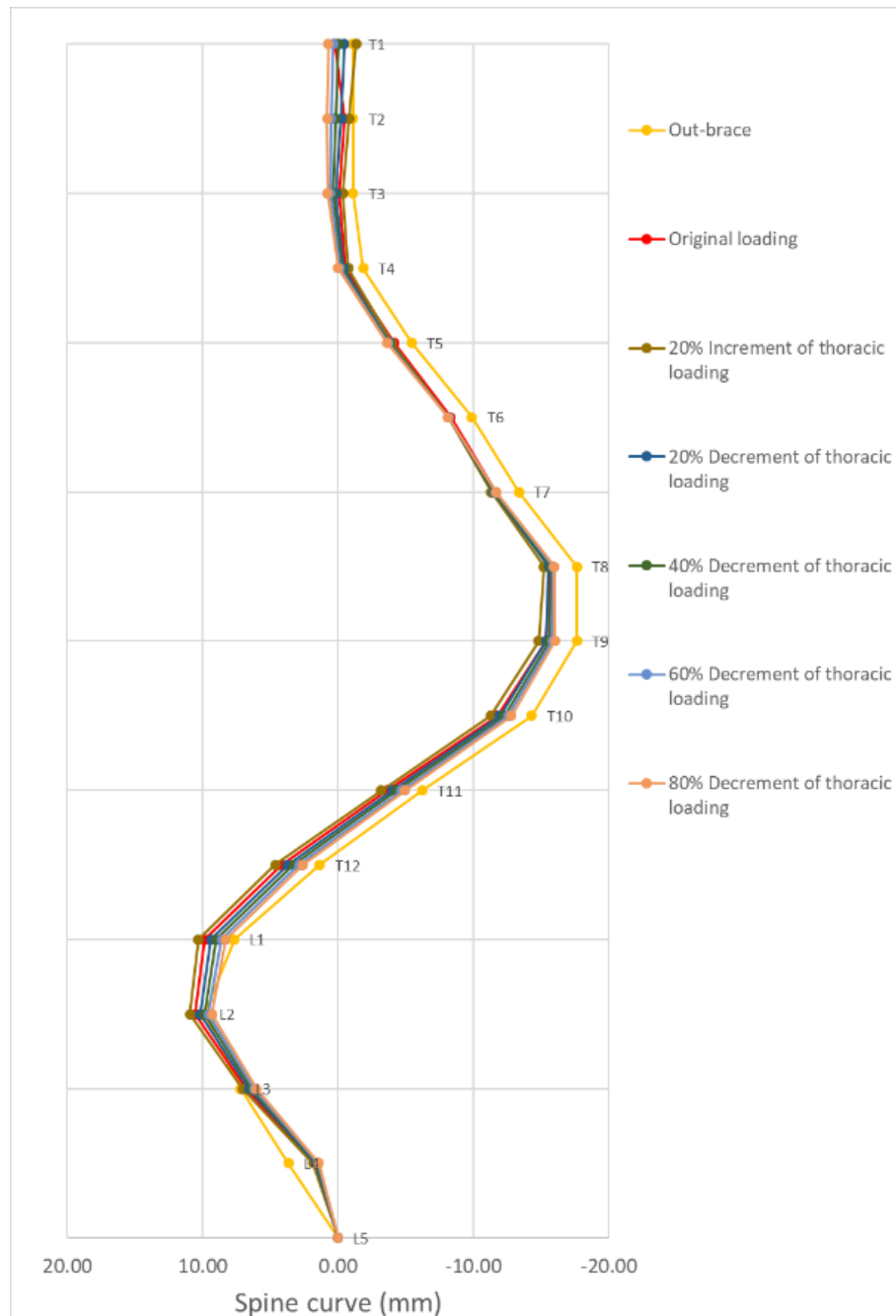


Figure 7-37 Spinal curves: Models #0, #5-9

### 7.5.3 Effect of the change of lumbar loading

Figure 7-38 shows the effect of lumbar loading on the spinal curve. It was surprising to see that the amount of lumbar loading was positively correlated with the extent of the thoracic correction. Increasing lumbar loading promoted thoracic correction. In contrast, when the

amount of lumbar loading was reduced, the extent of the thoracic correction was also reduced, and the lumbar curves progressively increased in severity. This further confirmed that the counter forces were important for spinal correction. Lumbar loading as a counter force to thoracic loading influenced the extent of thoracic correction. More importantly, the result indicated that insufficient lumbar loading would lead to the progression of the lumbar curve. The results in this study showed that it was important to increase the corrective forces of the lumbar pad to increase spinal correction.



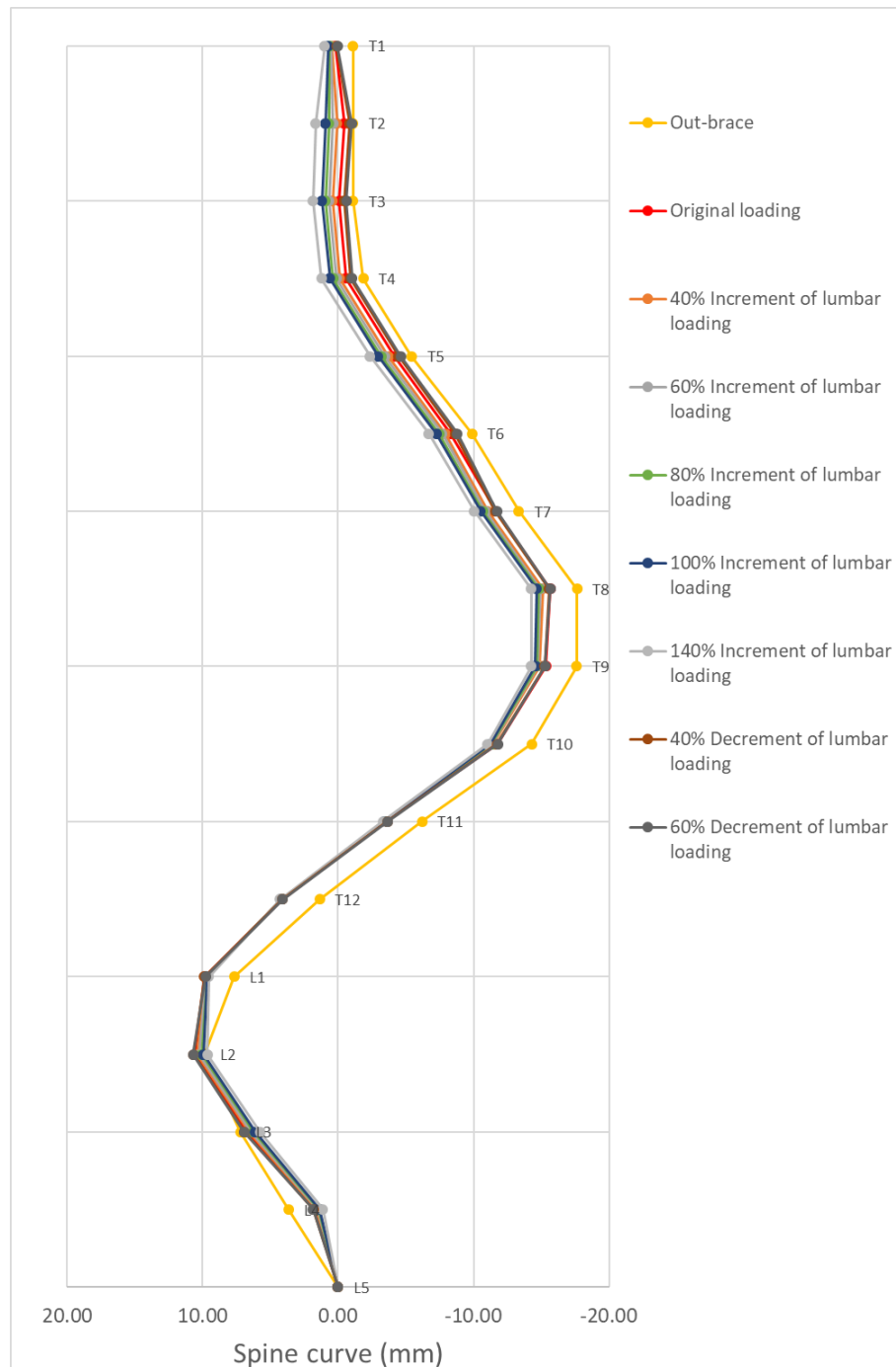


Figure 7-38 Spinal curves: Models #0, #10-15

## 7.6 Summary

In this chapter, a simulation model was constructed which simulated the loading of the FIA onto the body, showed the biomechanics of the FIA and predicted spinal movement after using the FIA. The FE model consisted of a scoliotic torso, skeletal structure, and FIA models. The FE model showed that after donning the FIA, there were relatively high levels of stress on the right thoracic, left lumbar and left pelvis regions of the torso. As for the effect on the spine, the

FE model showed that a relatively high level of stress was exerted onto the 7<sup>th</sup> and 8<sup>th</sup> ribs on the right side of the body due to the thoracic pad. After using the FIA, the thoracic vertebra shifted to the left side of the body and the lumbar vertebra shifted to the right side. This showed that the thoracic curvature was reduced after wearing the FIA.

To validate this FE model, a scoliotic patient was recruited and an in-brace radiographic examination was conducted. The measured and simulated spinal curves showed a similar trend. The FE model results were comparable to the results obtained experimentally.

To improve the durability of the current 3D printed hinge, five hinges milled by using different material including PMMA, POM, carbon reinforced fiber and aluminium were proposed. The results of the physical testing suggested that the hinge with aluminium leaves and steel pins had the highest tensile strength and torsional torque to failure. In addition, five FE models were built to investigate the effect of the hinge material on vertebral movement. The results indicated that the influence of the material properties of the hinge on the scoliotic spine was minimal, and there was no obvious difference among the five FE modelled spinal curves.

Apart from hinge modification, fifteen FE models with different thoracic and lumbar loadings were created to further investigate the biomechanics of the FIA and optimise the loading of the pads. It was found that thoracic loading increments contributed to a greater extent of thoracic correction but deteriorated the correction of the lumbar curve. On the other hand, increased lumbar loading contributed to a greater extent of the thoracic correction as well as the lumbar correction. The results show that managing lumbar loading was essential since it was a counter force to the thoracic loading and influenced the movement of the thoracic and lumbar vertebrae. The models in this study showed that a 140% increase in lumbar loading provided the optimum amount of spinal correction.

## **Chapter 8 Conclusion and recommendations for future work**

### **8.1 Conclusion**

Scoliosis is a spinal deformity that is found in patients with a Cobb's angle that is equal or greater than 10 degrees. Scoliosis not only affects the physical profile such as spinal asymmetry, trunk deformity, shoulder obliquity, scapular asymmetry, and increased pelvis inclination, but also causes spinal pain, restricts body movement, affects cardiac and pulmonary functions or even leads to death (Hresko, 2013; McElvenny, 1953).

The universal non-invasive means of treating scoliosis is bracing. There are two types of braces - rigid and flexible braces. The former is the conventional type of brace proven to be effective for reducing or inhibiting the progression of the spinal curvature (Weinstein et al., 2013b). However, movement restriction, discomfort and skin irritation are usually the shortcomings of wearing rigid braces (Bunge et al., 2010; Wong et al., 2008). To address these issues, flexible braces such as SpineCor (Coillard et al., 2008) and a posture correction girdle (Liu et al., 2014) have been developed. Nevertheless, their correction mechanism and effectiveness are still questionable.

Therefore, a flexible brace called a functional intimate apparel for AIS has been developed in this study to improve the corrective effects of existing flexible braces and address the shortcomings of rigid braces. The objectives of this study are to: 1) research the background information on AIS and the treatment methods, and review the different corrective mechanisms of functional intimate apparel in order to design and develop a suitable functional intimate apparel for adolescents with scoliosis; 2) further investigate the performance of an existing posture correction girdle developed by Liu et al. (2014) and study the biomechanics and spinal correction process of the girdle; 3) design an innovative functional intimate apparel which will: a) offer compression and pulling forces through a tightly fitting garment pattern, b) prevent lumbar flexion with a supporting belt, c) exert transverse forces through the 3-point pressure system, d) prevent axial rotation or address simultaneous movement of the body regions due to uneven pressure distribution from the use of different types of straps, and e) provide corrective forces that shift the trunk away from areas of pressure to reduce the spinal curvature and enhance the posture of individuals with AIS; 4) conduct wear trials of the proposed innovative functional intimate apparel, evaluate its effectiveness in terms of the degree of spinal curvature reduction through radiography and measure the amount of pressure exerted onto the torso; and

5) formulate a model that simulates the biomechanical effect of the proposed functional intimate apparel for AIS. These objectives have been realised and the results of the research work are summarised as follows.

1) After the literature review was conducted, background information on scoliosis including the methods for diagnosis and classification of AIS as well as non-invasive treatment methods for AIS treatment including rigid and flexible bracing and specific physiotherapy exercises for scoliosis has been obtained. Furthermore, the design and mechanisms of bracing treatment were obtained, and the limitations of currently available braces were identified. Information on some of the currently available functional intimate apparel for medical use was collected and details on the use of elastic fabrics, straps and supporting components to provide support, compressive forces and pulling forces to the body were obtained. Furthermore, the findings of previous studies on finite element analyses of bracing and pressure garments were gathered which facilitated a better understanding of the methodology for formulating and validating numerical simulation models.

2) A 6-month clinical study of the posture correction girdle developed by Liu et al. (2014) was conducted to investigate its efficacy in controlling spinal curvature and body contour asymmetry, as well as the amount of interface pressure distribution. The results allowed a better understanding of the current designs of girdles and thus determined the optimal modifications for the novel functional intimate apparel. It was found that the posture correction girdle could prevent the progression of the spinal curvature and reduce shoulder obliquity and rotation. However, the posture correction girdle could not provide in-brace correction. The relationship between the location of the padding and interface pressure was then studied and it was surprising to find that adding a pad might increase the pressure to the counter side instead of the padded side. That is, the conformity of the pad to the body contours and the symmetric waist band of the girdle might be possible factors that inhibited the effectiveness of the girdle. Therefore, modifications of the padding and an asymmetric design might potentially enhance in-brace spinal correction.

3) A novel flexible brace was designed, which was the functional intimate apparel in this study. It was a tightly fitting pressure garment that covered the body from the shoulders through the entire torso to the thighs, and composed of a bra top, pants, a pelvis belt, an artificial back bone with hinges that were cushioned with padding and corrective components. The aim of this flexible brace is to provide the highest possible corrective effect to remedy spinal deformity,

and address the shortcomings of rigid braces, such as mobility restrictions and discomfort. Preliminary fittings with human subjects were conducted to optimise the design. Laboratory tests were carried out to determine the most suitable types of textile materials to construct the brace. Following that, 3D body scanning with AIS patients was conducted and their body measurements were collected to construct the brace pattern. After analysing the data of the body measurements, two sizes of prototype were developed.

4) A two-phase clinical study, which comprised a 2-hour clinical study and a 3-month clinical study of the novel functional intimate apparel showed the effectiveness of the functional intimate apparel on reducing the spinal curvature and asymmetric parts of the body with enhanced psychological comfort. The biomechanics information of the functional intimate apparel was also obtained. The 2-hour clinical study showed that the novel functional intimate apparel provided a certain degree of in-brace correction and adequate interface pressure. After wearing the brace for 3 months, some initial reduction in spinal curvature was found. In comparison to the results of the posture correction girdle, the novel functional intimate apparel contributed to spinal correction. This study demonstrated the possibility of using textile in the proposed design to treat scoliosis.

5) A biomechanical simulation model was formulated to simulate the loading of the novel functional intimate apparel onto the body and predict spinal movement. The FEM was composed of models of a scoliotic torso, skeletal structure, and brace. A scoliotic patient was recruited and undergone a radiographic examination to validate the model. The measured and simulated spinal curvatures showed the same trend. Therefore, the results of the FEM were comparable to those obtained experimentally. Several models with different pad loadings were constructed to further examine the biomechanics of the novel functional intimate apparel and optimise the loading of the pads. The results showed that managing the pad was critical since insufficient loading might reduce the corrective effects while excessive loading might cause the progression of the counter curve. The models in this study showed that a 140% increase in the lumbar load was the optimum load for spinal correction.

## **8.2 Limitations of the study**

As with all studies, there were limitations that prevent the generalisation of the results. Those of this study are as follows.

1) With regard to the clinical study of the posture correction girdle, compliance of the subjects

with the treatment was not considered due to limited resources. However, to fully investigate the performance of the girdle, the relationship between compliance and efficacy were needed to be studied. In addition, this study did not have a control group. Due to lack of information on the rate of the progression of the spinal curvature of the control subjects who would constitute as the observation group, this study could not effectively investigate the effectiveness of the functional intimate apparel on preventing the progression of scoliosis.

2) With regard to the development of the novel functional intimate apparel, ethical concerns of radiation exposure meant that only assessments of the fit, changes in the body contours through 3D scanned images, and interface pressure were used in the preliminary review of the initial prototypes. A better result could be obtained if radiographic examination was carried out and the results were used to modify the initial design. Moreover, due to limited resources, only one type of silicone which was used for the corrective pad was purchased from the market. The correlation among the material properties of the silicone, interface pressure and in-brace spinal correction were not taken into consideration.

3) As for the clinical study on the functional intimate apparel, the sample size was very small. In addition, there was no control group. Compliance with the bracing treatment were not taken into account. Furthermore, it was assumed that the textile material was more flexible compared to thermoplastic material. However, due to limited resources, no comparison was carried out on the difference in movement of the subjects when the functional intimate apparel and rigid brace were worn. More importantly, due to the concerns of repeated radiation exposure, the assessment of spinal inherent flexibility was not conducted. Thus, the amount of correction achievable of each subject was unknown and it was difficult to investigate the efficacy of proposed brace.

5) In terms of the formulation of the biomechanical simulation model, limitations of the equipment and the issue of a large file size resulted in the use of a simplified skeletal model instead of a more complex geometric model. The model of the torso was constructed as a single component which neglected some of the components such as the skin, blood vessels, muscles, tendons, ligaments and organs. The model of the brace was constructed as a single textile and a hinge component only and the material properties of some of the components such as the bra cup, seams, v-fold elastic, hooks and eyes, and pin of the hinge are neglected. Moreover, some of the material properties in this study were based on those in the previous literature which might be different from the characteristics of the subjects and brace in this study. These were

also the reasons why the trend of the predicted spinal curve was similar to the experimental result but had a different magnitude of vertebral displacement.

### **8.3 Recommendations for future work**

Based on the established research findings, the following are some recommendations for future work.

- 1) In order to obtain a better understanding of the effects of corrective pad, different material properties of the pads with different geometries should be investigated and compared. As such, the optimum pad design could be determined to enhance the corrective effects of the flexible brace. Moreover, it is recommended that a review is carried out on the biomechanics of flexible braces for correcting spinal deformity
- 2) To obtain results based on robust evidence, a randomised control trial with a large sample size is recommended. A comparison of the effectiveness of the functional intimate apparel and rigid brace should also be conducted. Apart from the effectiveness in reducing spinal curvature and asymmetric body contours, enhancing quality of life and optimizing the interface pressure, body movement was suggested as a factor for study which could be obtained through motion capture. Moreover, a temperature logger was recommended for determining treatment compliance. More importantly, a supine radiographic examination was suggested for determining the amount of correction achievable with brace-wear.
- 3) A precise model of the torso with components that included the skin, blood vessels, muscles, tendons, ligaments and organs, and a detailed model of the brace should be developed in the future. More importantly, different material properties of the model of the brace and different positions and magnitude of loading should be further investigated by using finite element modelling to obtain the optimum design of a flexible brace.

## **Appendix I. Information sheet for participant in clinical study of posture correction girdle**

(English version)

### **INFORMATION SHEET**

#### **Posture Correction Girdle for Adolescents with Early Scoliosis**

This research study is supervised by Dr. YIP Yiu Wan, Joanne of Institute of Textiles and Clothing, The Hong Kong Polytechnic University and her team members. Please take time to read the following information carefully and discuss it with your parents, relatives and your family doctor if you wish. Ask us if there is anything that is not clear or if you would like to have more information. Take time to decide whether or not you wish to take part.

#### **Purpose of the study**

The purpose of this study is to gain the clinical information necessary for the design of posture correction girdle for adolescents with early scoliosis. The posture correction girdle is designed to control the curve progression and poor posture of adolescent.

#### **Who will be invited to participate in this study?**

Adolescents are screened from local primary/secondary schools, students with signs of scoliosis will be invited to undergo an ultrasound scan in the Hong Kong Polytechnic University to examine the curve patterns and angle. The inclusion criteria are: i) Cobb's angle 10°-20°, ii) Risser grade ≤ 2, iii) aged 10-13, iv) female, and v) no prior treatment.

#### **What will happen if you decide to take part?**

Participants will be invited to undergo a fitting session of posture correction girdle in the Hong Kong Polytechnic University. After the fitting, participants will join a 6-month wear trial of the posture correction girdle. Participants are required to wear the girdle for 8 hours a day and the compliance will be recorded by a logbook daily. Participants will be invited to undergo assessments before the wear trial, after the trial of 3 months, and after the trial of 6 months. The measure outcomes of the assessment include 1) ultrasound scanning image, 2) 3D body scan, 3) electromyography signal, 4) garment pressure, and 5) questionnaire. All assessments are conducted in the Hong Kong Polytechnic University, and each assessment will be hold about 2 hours.

#### **Do you have to take part?**

It is up to you to decide whether or not to take part. If you do decide to take part you will be given this information sheet to keep and be asked to sign a consent form. If you decide to take part you are still free to withdraw at any time without giving a reason. The choice of participation in the study would not affect the standard of care you receive in the clinic. During the study, if you failed to turn up at appointments, your participation in this study will be immediately terminated without further notice.

#### **What is the posture correction girdle being tested?**

Adolescent idiopathic scoliosis (AIS) is a prevalent chronic condition that gradually leads to the three dimensional deformity of the spine. Spine curvature increases in youths as puberty progresses. Generally, only observation is suggested for adolescents with early scoliosis



(Cobb's angle  $\leq 20^\circ$ ). Rigid brace treatment is too draconian for them due to the high corrective force which nearly constrains all movements. Flexible brace treatment is an alternative option; however, its efficacy is still controversial. Posture correction girdle with a specialized design for teenagers with scoliosis is limited and most part of them can only provide some improvement for bad postures, such as hunchback. A scientific approach should be used to design and develop posture correction girdle as a treatment option for adolescents with early scoliosis.

The design of posture correction girdle will incorporate different mechanisms, such as a) compression and pulling forces through a close fit of the intimate apparel, b) lumbar flexion by using a supporting belt, c) transverse forces applied by inserting pads inside the pocket lining by using the principle of the 3-point pressure system, d) axial rotation or coupled motion by using a system with uneven straps, and e) an active mechanism that aims to shift the trunk away from areas of pressure.

As early management of spinal deformity may prevent the need to prescribe orthotic bracing and surgery, this project aims to develop functional intimate apparel (made of comfortable textile, fabrication materials) that can control curve progression and poor posture of adolescents with early signs of scoliosis.

#### **What are the disadvantages and risks of taking part?**

Ultrasound scan, 3D body scan, muscle electromyography examinations, measurement of garment pressure and questionnaire: no risk.

Posture correction girdle: materials and design of the new functional intimate apparel are safe and comfortable. As compared with the rigid orthotic brace and/or posture correction vests presently being used, it may probably cause skin allergy and/or discomfort. However, this garment has been tested in human subjects for short durations during its design and production periods. In such, there are no special compensation arrangements in this study.

#### **What are the benefits of taking part?**

The potential benefit is to provide an option of a less intrusive orthotic treatment with better design, fitting and comfort for patients with early signs of scoliosis to control progression curvature in lieu of observation, bracing and surgery, and thus preserve growth of children and their quality of life.

#### **What if something goes wrong?**

There are no special compensation arrangements in this study. If you wish to complain about any aspect of the way you have been approached or treated during the course of this study, you can also contact The Secretary of the Human Subjects Ethics Sub-Committee of The Hong Kong Polytechnic University in person or in writing (c/o M1303, Human Resources Office of the University).

#### **Will my taking part in this study be kept confidential?**

If you agree to take part in this study, the measurement results will only be reviewed by the research team to obtain essential information. All information collected will be kept confidential.

#### **What will happen to the results of the research study?**

The results will be published in referred journal.

**Who is organizing and funding the research?**

The research is organized by Institute of Textiles and Clothing, The Hong Kong Polytechnic University.

**Who has reviewed the study?**

The study has been reviewed by Departmental Research Committee of Institute of Textiles and Clothing, The Hong Kong Polytechnic University.

Please keep this information sheet for your reference, together with a signed consent form.

If you have any query, please do not hesitate to contact Dr. YIP Yiu Wan at 2766 4848. Thank you very much in helping us to improve our patients' care.

Updates of this study will only be informed, if necessary.

Dr. YIP Yiu Wan, Joanne

Principle Investigator/Chief Supervisor

Tel: 27664848

Email: tcjyip@

## 資料篇

### 發展適用於早期脊柱側彎的青少年的姿勢矯正束身衣

我們誠意邀請閣下參與一項研究，這項研究由香港理工大學紡織及製衣學系教職員葉曉雲博士及其成員籌劃。請詳細閱讀以下資料，亦可與親友或醫護人員商量。若有任何不清晰的地方或需要更多資料，請隨便向我們提出。

#### 研究主旨

這項研究的目的是根據臨床資料，發展適用於輕微脊柱側彎學童的束身衣，以支撐及托提供矯正力，防止脊柱持續變形及改善學童的坐姿及站姿。

#### 誰會被邀請參與這項研究？

此研究會在小學或中學進行篩選，並邀請被診斷患有輕微的脊柱（脊柱側彎的角度需 $10^{\circ}$ - $20^{\circ}$ ），及很大機會有脊柱持續變形可能的女童進行徹底的評估，被邀參與的女童年齡需介乎 10 至 13 歲。

#### 決定參加後，你需要做什麼？

首先，你的子女會被邀請到香港理工大學接受超聲波掃描，量度脊柱形狀。接著參加者會被邀請到醫療中心接受 X 光診斷，深入了解參加者脊柱側彎的完整情況及有關資料。

之後，參加者會被邀請到香港理工大學，研究人員會使用直接量度的方法取得學童準確的體型資料。所得的量度資料均會用於製造矯形束身衣之用。

參加者將被邀請量度肌動電流圖，由紅外線相機量度體溫分佈，作記錄姿勢矯正過程之用。

當矯形束身衣造好後，您的子女將被邀請進行骨科檢查及參加一個為期六個月的矯形束身衣的進度監測，參加者須每三個月回到香港理工大學，評估治療進度。參加者日常活動時使用束身衣的情況及變化會由姿勢監測器記錄。

除了骨科檢查外，參加者的姿勢亦會被檢查及拍照用作記錄參加者的姿勢變化。

#### 你是否必定要參加？

這完全由你決定。如果你決定參加, 請保留這資料篇, 我們會給你簽署一張同意書。你參與後有權隨時退出而不需要作任何解釋。你是否參加亦不會影響你在診所內接受的診斷服務。參與研究期間, 若你沒有按時出席覆診, 對你的研究亦會立刻終止, 雙方不須另行通知。

### **測試的「姿勢矯正束身衣」究竟是怎樣的?**

根據香港衛生署於二零零五的資料, 香港約有百分之十七的中學生被診斷為脊柱側彎(或脊柱變形)。雖然病患原因未明, 但大部份病例均在發育期間持續及快速變形。若彎度少於二十度之輕微脊柱側彎學童, 現時的處理方法只限於定期觀察。若彎度增加至二十至四十五度之中度脊柱側彎學童, 便必須配置硬而龐大的矯形模具, 以支撐及準確控制脊柱壓力, 防止脊柱持續變形, 然而矯形模具須每天使用不少於二十三小時至完成發育(若 4-6 年)。若脊柱持續變彎, 便須進行矯形手術。現時的矯形模具一般選用硬膠物質製造, 其設計, 貼身度, 舒適度及外觀均不易被病者接納, 直接影響病者使用量及治療效用。

在脊柱側彎病例中, 及早進行適當治療十分重要, 可減少日後配置矯形模具, 或進行手術的需要, 因此, 我們希望能以舒適的紡織物料, 配合新設計, 發展適用於輕微脊柱側彎學童的束身衣, 準確控制脊柱彎度及改善學童的坐姿及站姿。

### **參與此研究有風險嗎?**

脊骨狀況檢查, 立體素描及動作記錄系統, 溫度及壓力的感應器材, 和單次性的 X 光檢查均無危險性。

束身衣的選料及設計亦安全, 舒適。和硬的矯形模具或現有的姿勢矯形背心比較, 個別受試者或有輕微皮膚敏感或因物料壓力造成不適, 然而, 於束身衣的設計及生產過程中, 該物料已於人類中使用及研究了一段短時間。故與此研究有關的創傷均沒有任何意外賠償。

### **參加此研究有什麼實際益處?**

與現有的定期觀察, 矯形模具及手術相比, 我們希望可以針對輕微脊柱側彎學童, 提供一項較少侵入性的矯形治療, 透過貼身舒適及較容易接納的治療方法去防止側彎惡化, 令學童健康成長。

### **參加此項研究, 你有什麼補償?**

本研究對受試者沒有提供補償安排。如果閣下對這項研究有任何人權問題, 你亦可親身或以書面形式聯絡香港理工大學人事倫理委員會秘書(地址: 香港理工大學人力資源辦公室 M1303 室轉交)。

**我參與這研究資料是否保密?**

如閣下同意參與此項研究,凡有關閣下的資料均會保密,一切量度結果只有研究人員知道,並用作研究用途。其他的資料一概保密。

**我們會怎樣處置研究結果?**

我們會把結果發報在醫學矯形和紡織設計刊物等。

**是誰統籌和資助此研究?**

是項研究是由香港理工大學紡織及製衣學系統籌。

**誰審核過此研究?**

是項研究經香港理工大學紡織及製衣學系研究委員會審核。

請保存這份資料和同意書作日後參考。

如有疑問,請至電 27664848 向葉曉雲博士查詢。特此再次多謝你的參與, 閣下的支持定能對將來改善醫院病人的服務有很大的幫助。

有關此研究的更新資料或資訊,有須要時,將會個別另行通知。

葉曉雲 博士

研究組組長

Tel: 27664848

Email: [tcjyip@](mailto:tcjyip@polyu.edu.hk)

## **Appendix II. Consent to participant in clinical study of posture correction girdle**

(English version)

### **PARTICIPANT CONSENT FORM**

#### **Title of Project: Functional Intimate Apparel for Adolescents with Early Scoliosis**

Name of Researchers:

Dr. YIP Yiu Wan, Dr. YICK Kit-lun, Dr. NG Sun-pui, Dr. CHEUNG Mei-chun

1. I confirmed that I have had the opportunity to ask questions.
2. I understand that my child's participation is voluntary and that I am free to withdraw at any time, without giving any reasons, without my legal rights being affected.
3. I understand that sections of any of my child's medical notes may be looked at by responsible individuals from the researcher's team or from regulatory authorities where it is relevant to my taking part in research. I give permission for these individuals to have access to my records.
4. The results will be published in referred journal. All information collected will be kept confidential.
5. I agree to take part in the above study.

_____	_____	_____
Name of parent/Legal guardian	Date	Signature
_____	_____	_____
Name of witness (if applicable)	Date	Signature
_____	_____	_____
Researcher	Date	Signature

Copies to:

- Parent/Legal guardian
- researcher's file

(Chinese version)

## 參與研究項目同意書

研究主題：發展適用於早期脊柱側彎的青少年的姿勢矯正束身衣

研究人員名稱：葉曉雲博士，易潔倫博士，吳新培博士，謝志勇先生，袁駿華教授及羅家明博士

1. 本人確定已詳細閱讀並了解於\_\_\_\_\_/\_\_\_\_\_/\_\_\_\_\_提供之資料單張,並已有足夠時間發問問題。
2. 本人明白是次參與全是自願性質, 本人有權隨時退出而不必提出任何理由, 而本人法律權利不會有改變。
3. 本人明白及同意本人子女之病歷記錄需要時給與研究員和有關人事作參考。
4. 研究結果將會發報在醫學矯形和紡織設計刊物內。其他收集的資料一概保密
5. 本人同意參與此項研究。

-----  
參加者家屬/監護人姓名

-----  
日期

-----  
簽名

-----  
見証人(如適用)

-----  
日期

-----  
簽名

-----  
研究員

-----  
日期

-----  
簽名

副本給與:

- 參加者家屬/監護人
- 研究員

### Appendix III. Data sheet for clinical study of posture correction girdle

研究主題：發展適用於早期脊柱側彎的青少年的姿勢矯正束身衣

#### 參加者資料

Subject Code: \_\_\_\_\_

中文姓名: \_\_\_\_\_

英文姓名: \_\_\_\_\_

出生日期: \_\_\_\_\_

地址: \_\_\_\_\_

聯絡電話: \_\_\_\_\_

身份証號碼: \_\_\_\_\_

試穿日期: \_\_\_\_\_

身高: \_\_\_\_\_

體重: \_\_\_\_\_

BMI: \_\_\_\_\_

X-ray report:

---

---

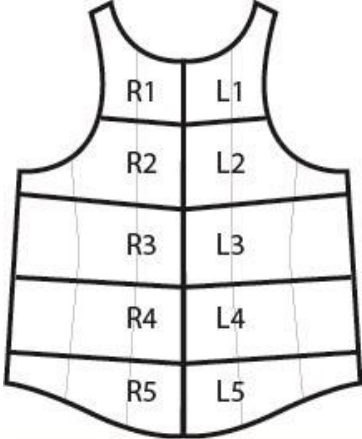
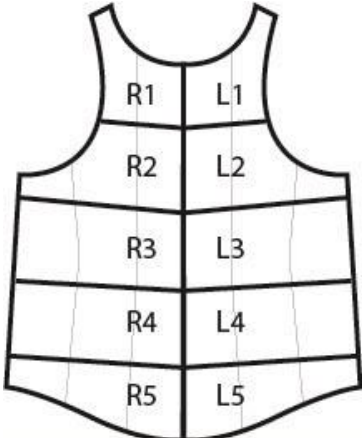
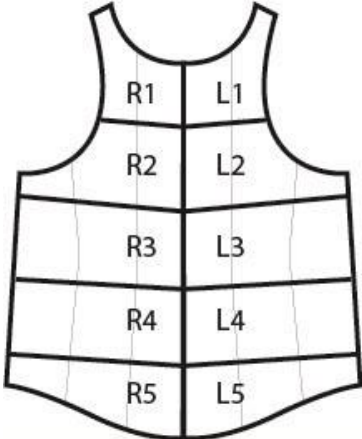
---



### Girdle fitting

Pelvis level: Left:   cm Right:   cm

Shoulder balance measurement

	Left (cm)	Right (cm)
Before wearing girdle		
1 <sup>st</sup> Fitting Without Padding		
2 <sup>nd</sup> Fitting 		
3 <sup>rd</sup> Fitting 		
4 <sup>th</sup> Fitting 		

## **Appendix IV. Information sheet for participant in clinical study of functional intimate apparel**

(Chinese version)

### **資料篇**

#### **發展適用於脊柱側彎的青少年的功能內衣**

我們誠意邀請閣下參與一項研究，這項研究由香港理工大學紡織及服裝學系教職員葉曉雲博士及其成員籌劃。請詳細閱讀以下資料，亦可與親友或醫護人員商量。若有任何不清晰的地方或需要更多資料，請隨便向我們提出。

#### **研究主旨**

這項研究的目的是根據臨床資料，發展適用於脊柱側彎學童的功能內衣，以支撐及托提供矯正力，防止脊柱持續變形及改善學童的坐姿及站姿。

#### **誰會被邀請參與這項研究？**

此研究會在小學或中學進行篩選，並邀請有脊柱側彎徵狀的學童到香港理工大學接受超聲波掃描，量度脊柱形狀及彎度。參加者須 i) 被診斷患有脊柱側彎（側彎角度  $15^{\circ}$ - $35^{\circ}$ ）、ii) 骨骼發育中（骨盆成熟度指數於 2 或以下程度）、iii) 年齡介乎 10 至 13 歲、iv) 女性 及 v) 過去沒有接受任何脊柱側彎治療。

#### **決定參加後,你需要做什麼？**

試身前，參加者會進行 X 光檢查。之後，參加者會被邀請到香港理工大學進行功能內衣試身。完成試身後，參加者會穿上功能內衣進行 X 光檢查。如 X 光報告顯示其功能內衣對參加者有正面效果，參加者將會參與一個為期六個月的束身衣試穿計劃，參加者須每天穿著功能內衣八小時，穿著計劃期間參加者須每天記錄當天穿著時數。參加者會接受合共三次評估。三次評估分別會在試穿前、試穿後三個月及試穿後六個月進行。每次評估包含 1) 進行超聲波掃描、2) 進行三維人體掃描、3) 量度肌電訊號、4) 量度功能內衣提供的壓力 及 5) 填寫問卷。評估須在理工大學進行，並需時約兩個小時。

### **你是否必定要參加？**

這完全由你決定。如果你決定參加，請保留這資料篇，我們會給你簽署一張同意書。你參與後有權隨時退出而不需要作任何解釋。參與研究期間，若你沒有按時出席覆診，對你的研究亦會立刻終止，雙方不須另行通知。

### **測試的「青少年脊柱側彎的功能內衣」究竟是怎樣的？**

根據香港衛生署於二零零五的資料，香港約有百分之十七的中學生被診斷為脊柱側彎(或脊柱變形)。雖然病患原因未明，但大部份病例均在發育期間持續及快速變形。若彎度少於二十度之輕微脊柱側彎學童，現時的處理方法只限於定期觀察。若彎度增加至二十至四十五度之中度脊柱側彎學童，便必須配置硬而龐大的矯形模具，以支撐及準確控制脊柱壓力，防止脊柱持續變形，然而矯形模具須每天使用不少於二十三小時至完成發育(若 4-6 年)。若脊柱持續變彎，便須進行矯形手術。現時的矯形模具一般選用硬膠物質製造，其設計，貼身度，舒適度及外觀均不易被病者接納，直接影響病者使用量及治療效用。

在脊柱側彎病例中，及早進行適當治療十分重要，可減少日後配置矯形模具，或進行手術的需要，因此，我們希望能以舒適的紡織物料，配合新設計，發展適用於脊柱側彎學童的功能內衣，準確控制脊柱彎度及改善學童的坐姿及站姿。

### **參與此研究有風險嗎？**

超聲波掃描、三維人體掃描、量度肌電訊號及量度功能內衣提供的壓力均無危險性。

功能內衣的選料及設計亦安全，舒適。個別受試者或有輕微皮膚敏感或因物料壓力造成不適，然而，於功能內衣的設計及生產過程中，該物料已於人類中使用及研究了一段短時間。故與此研究有關的創傷均沒有任何意外賠償。

### **參加此研究有什麼實際益處？**

與現有的定期觀察，矯形模具及手術相比，我們希望可以針對脊柱側彎學童，提供一項較少侵入性的矯形治療，透過貼身舒適及較容易接納的治療方法去防止側彎惡化，令學童健康成長。

### **參加此項研究，你有什麼補償？**

本研究對受試者沒有提供補償安排。如果閣下對這項研究有任何人權問題，你亦可親身或以書面形式聯絡香港理工大學人事倫理委員會秘書(地址：香港理工大學人力資源辦公室 M1303 室轉交)。

### **我參與這研究資料是否保密？**

如閣下同意參與此項研究，凡有關閣下的資料均會保密，一切量度結果只有研究人員知道，並用作研究用途。其他的資料一概保密。

### **我們會怎樣處置研究結果？**

我們會把結果發報在醫學矯形和紡織設計刊物等。

### **是誰統籌此研究？**

是項研究是由香港理工大學紡織及服裝學系統籌。

### **誰審核過此研究？**

是項研究經香港理工大學紡織及服裝學系研究委員會審核。

請保存這份資料和同意書作日後參考。

如有疑問，請至電 27664848 向葉曉雲博士查詢。特此再次多謝你的參與，閣下的支持定能對將來改善醫院病人的服務有很大的幫助。

有關此研究的更新資料或資訊，有須要時，將會個別另行通知。

葉曉雲博士

研究組組長

Tel: 27664848

Email: [tcjyip@](mailto:tcjyip@polyu.edu.hk)

## **Appendix V. Consent to participant in clinical study of functional intimate apparel**

(Chinese version)

### 參與研究同意書

**研究主題：發展適用於脊柱側彎的青少年的功能內衣**

本人\_\_\_\_\_同意參與由 葉曉雲博士，易潔倫博士，吳新培博士開展的上述研究。

本人知悉此研究所得的資料可能被用作日後的研究及發表，但本人的私隱權利將得以保留，即本人的個人資料不會被公開。

研究人員已向本人清楚解釋列在所附資料片上的研究程序，本人明瞭當中涉及的利益及風險；本人自願參與研究項目。

本人知悉本人有權就程序的任何部分提出疑問，並有權隨時退出而不受任何懲處。

參與者姓名

\_\_\_\_\_

參與者簽署

\_\_\_\_\_

家長或監護人姓名  
(如適用)

\_\_\_\_\_

家長或監護人簽署  
(如適用)

\_\_\_\_\_

研究人員姓名

\_\_\_\_\_

研究人員簽署

\_\_\_\_\_

日期

\_\_\_\_\_

## Appendix VI. Data sheet for clinical study of functional intimate apparel

研究主題：發展適用於脊柱側彎的青少年的功能性內衣

### 參加者資料

Subject Code: \_\_\_\_\_

中文姓名: \_\_\_\_\_

英文姓名: \_\_\_\_\_

出生日期: \_\_\_\_\_

地址: \_\_\_\_\_

聯絡電話: \_\_\_\_\_

身份証號碼: \_\_\_\_\_

身高: \_\_\_\_\_

體重: \_\_\_\_\_

BMI: \_\_\_\_\_

Cobb' s angle: \_\_\_\_\_

x-ray: \_\_\_\_\_

Scolioscan™: \_\_\_\_\_

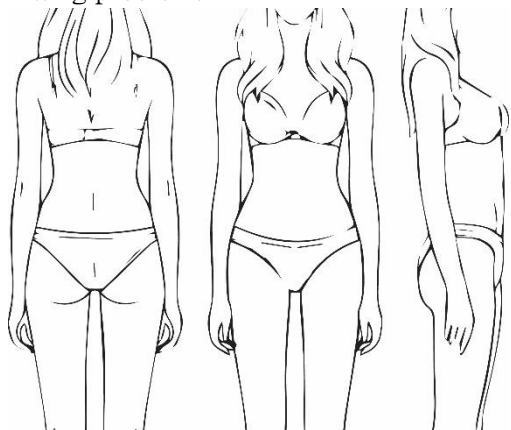
量身日期: \_\_\_\_\_

試穿日期: \_\_\_\_\_

Pressure data:

L1	R1
L2	R2
L3	R3

Fitting problem:



## Appendix VII. Bad Sobernheim Stress Questionnaire

(Chinese version)

### BSSQ-支具 問卷調查表

以下問題均與您戴矯形支具的感受有關，請認真閱讀問題並以真實的感受作答。以下問題的答案分析，將有助於我們評估出或識別出矯形支具帶給您在心理方面的壓力，在對您進一步的治療中將給予我們很好的建議或指導方向。

1. 我身體外觀在 AIS 功能內衣內，我覺得不舒適。

☐完全正確      ☐差不多正確      ☐幾乎不正確      ☐完全不正確

2. 對我來說，我脫下 AIS 功能內衣是很困難的。

☐完全正確      ☐差不多正確      ☐幾乎不正確      ☐完全不正確

3. 當別人能看到我佩戴的 AIS 功能內衣的情況下，我覺得不舒服。

☐完全正確      ☐差不多正確      ☐幾乎不正確      ☐完全不正確

4. 當別人看我佩戴的 AIS 功能內衣時我不會感到尷尬。

☐完全正確      ☐差不多正確      ☐幾乎不正確      ☐完全不正確

5. 我盡量避免身體接觸以至於沒人知道我佩戴 AIS 功能內衣。

☐完全正確      ☐差不多正確      ☐幾乎不正確      ☐完全不正確

6. 當決定穿什麼衣服時或戴假髮時，我試圖確保我的 AIS 功能內衣隱藏好。

☐完全正確      ☐差不多正確      ☐幾乎不正確      ☐完全不正確

7. 在我親近的人面前展現我佩戴的 AIS 功能內衣我不感到尷尬（例如：父母，朋友，同學）。

☐完全正確      ☐差不多正確      ☐幾乎不正確      ☐完全不正確

8. 由於佩戴脊椎側彎功能內衣，我避免活動/興趣愛好，即便這些活動是我以前愛做的。

☐完全正確      ☐差不多正確      ☐幾乎不正確      ☐完全不正確

## Appendix VIII. Brace Questionnaire

(Bilingual version)

Please tell us a few things about yourself:

You are: ☐ a girl ☐ a boy Age: ..... years old

You are wearing the brace since .....

You are wearing the brace for ..... hours /day

Date.....

<i>During the past 2 hours...</i>	Never (從不)	Almost never (幾乎從不)	Sometimes (有時)	Most of the time (大多數時候)	Always (經常)
1. The functional intimate apparel for AIS (FIA) made you feel ill (AIS功能內衣讓你感覺不舒服不舒服)					
2. You were afraid that your back will get worse (你擔心你的背部會變得更差)					
3. You felt tired when walking (你走路時感到疲倦)					
4. You were able to run (你可以跑步)					
5. You managed to wear the FIA without any help (你能在沒有任何幫助的情況下戴上AIS功能內衣)					
6. You managed to take out the FIA without any help (你能在沒有任何幫助的情況下脫下AIS功能內衣)					
7. You couldn't eat well (你不能舒適地進食)					
8. You couldn't sleep well (你不能舒適地睡覺)					



9. You couldn't breath well (你不能舒適地呼吸)					
10. The FIA made you feel nervous (AIS功能內衣讓你感到緊張)					
11. You felt worried because of the FIA (你因AIS功能內衣而感到擔憂)					
12. You felt happy (你感到高興)					
13. You believed that your life would be better if you were not on brace (你覺得如果你不穿AIS功能內衣，你的生活會更好)					
14. You believed that FIA treatment was beneficial (你相信AIS功能內衣治療是有益的)					
15. You felt proud of yourself (你為自己感到自豪)					
16. You were satisfied with your body (你對你的身體感到滿意)					
17. You felt strong and full of energy (你感到強壯而充滿活力)					
18. You felt tired and exhausted because of the brace (你因AIS功能內衣治療而感到疲倦和筋疲力盡)					
24. You had pain when walking (你走路時感到疼痛)					
25. You had pain when sitting (你坐著時感到疼痛)					
26. You had pain when climbing stairs					

(你爬樓梯時感到疼痛)					
27. You felt pins and needles to your arms or legs (你的手腳感到疼痛)					
30. You felt different from your peers (你感到你和同齡人有所不同)					
32. You believed that your relationship with your family or your friends would be better if you were not on FIA (你覺得如果你不用穿著 AIS 功能內衣，你和家人或朋友的關係會更好)					

## Appendix IX. SRS-22 Questionnaire

(Chinese version)

### SRS-22 病人問卷

姓名: 出生日期 (年/月/日): 性別: M/F

電話: 年齡:

指示: 我們正在小心評估你背部的情況，因此問卷上的每一條問題必須由你親自回答。

請在每一條問題所提供的選擇中，小心圈出你認為最正確的一個答案。

1. 以下哪一項最能夠準確描述你在過去六個月所感受到痛楚的程度？  
無痛楚／ 輕微／ 中等／ 中等至嚴重／ 嚴重
2. 以下哪一項最能夠準確描述你在過去一個月所感受到痛楚的程度？  
無痛楚／ 輕微／ 中等／ 中等至嚴重／ 嚴重
3. 整體來說，在過去六個月期間你有感到十分焦慮嗎？  
完全沒有／ 小部分時間／ 有時／ 大部分時間／ 全部時間
4. 如果你必須在背部維持現狀不變的情況下繼續生活，你會有甚麼感受？  
十分愉快／ 某程度上愉快／ 沒有愉快或不愉快／ 某程度上不愉快／ 十分不愉快
5. 你現時的活動能力如何？  
只限於床上／基本上不能活動／些微的運動及勞動／有限度的運動及勞動／活動不受限制
6. 你在穿上衣服後的外觀如何？  
很好／ 好／ 可以接受／ 差勁／ 十分差勁
7. 在過去六個月期間你曾感到十分沮喪以至於任何事物也不能讓你開懷嗎？  
經常／ 大多數時間／ 有時／ 很少數時間／ 完全沒有
8. 你在休息時背部有感到疼痛嗎？  
經常／ 大多數時間／ 有時／ 很少數時間／ 完全沒有
9. 你現時在工作/學校的活動能力為多少？  
正常的100％／ 正常的75％／ 正常的50％／ 正常的25％／ 正常的0％
10. 以下哪一項最能夠描述你軀幹的外觀？(軀幹的定義為人的身體除去頭部及四肢)  
很好／ 好／ 可以接受／ 差勁／ 十分差勁

11. 下例哪一項最能準確地描述你因背部疼痛而所需要服用的藥物？  
無／ 一般止痛藥(每星期服用一次或更少)／ 一般止痛藥(天天服用)／ 特效止痛藥(每星期服用一次或更少)／ 特效止痛藥(天天服用)／  
其他〔藥物名稱： 使用程度(每星期或更少或天天): 〕
12. 你的背部疼痛有否影響你做家務的能力？  
沒有／ 少許／ 某程度上有／ 很大程度上有／ 經常有
13. 整體來說，你在過去六個月期間有感到安寧和平靜嗎？  
經常／ 大多數時間／ 有時／ 很少數時間／ 完全沒有
14. 你有否感到你背部的狀況對你的人際關係構成影響？  
沒有／ 少許／ 某程度上有／ 很大程度上有／ 經常有
15. 你以及/或你的家人有否因為你背部的問題而在經濟方面遇到困難？  
極有／ 很大程度上有／ 某程度上有／ 少許／ 沒有
16. 整體來說，在過去六個月期間你有否感到失落和灰心？  
完全沒有／ 很少數時間／ 有時／ 大多數時間／ 經常
17. 在過去三個月期間你有否因背痛而向學校/公司請假？如有，共有多少天？  
零天／ 一天／ 兩天／ 三天／ 四天或以上
18. 你背部的狀況有否阻礙你和家人/朋友外出？  
從來沒有／ 很少數時間／ 有時／ 大多數時間／ 經常
19. 你現時背部的狀況會否讓你覺得自己仍有吸引力？  
會，很有吸引力／ 會，某程度上有吸引力／ 無影響／ 否， 沒有甚麼吸引力  
／ 否，完全沒有吸引力
20. 整體來說，你在過去的六個月裏感到愉快嗎？  
完全沒有／ 很少數時間／ 有時／ 大多數時間／ 經常
21. 你對你背部治療的成效感到滿意嗎？  
十分滿意／ 滿意／ 不是滿意也不是不滿意／ 不滿意／ 非常不滿意
22. 如果你的背部再次遇到同類的情況你會否接受同樣的治理？  
一定會／ 可能會／ 不清楚／ 可能不會／ 一定不會

多謝你的合作，如有任何意見請填寫在以下的空位上。

~問卷完~

## REFERENCES

- Adobor, R. D., Rimeslatten, S., Steen, H., & Brox, J. I. (2011). School screening and point prevalence of adolescent idiopathic scoliosis in 4000 Norwegian children aged 12 years. *Scoliosis*, 6, 23-23. <https://doi.org/10.1186/1748-7161-6-23>
- Alam, M., Newton, P. O., Yaszay, B., & Bastrom, T. P. (2013). Are Thoracic Curves With a Low Apex (T11 or T11/T12) Really Thoracic Curves? *Spine Deformity*, 1(2), 139-143. <https://doi.org/10.1016/j.jspd.2012.12.004>
- American Society for Testing and Materials International. (2014). *Standard Performance Specification for Brassiere, Slip, Lingerie and Underwear Fabrics* (Vol. ASTM D7019-14).
- Anderson, B. (2015). *Undergarment for masking scoliosis* [United States Patent]. <https://www.google.com.hk/patents/US20150101618>
- Anitha, H., & Prabhu, G. (2012). Identification of Apical Vertebra for Grading of Idiopathic Scoliosis using Image Processing. *The Journal of the Society for Computer Applications in Radiology*, 25(1), 155-161. <https://doi.org/10.1007/s10278-011-9394-x>
- Aulisa, A. G., Guzzanti, V., Falciglia, F., Giordano, M., Marzetti, E., & Aulisa, L. (2015). Lyon bracing in adolescent females with thoracic idiopathic scoliosis: a prospective study based on SRS and SOSORT criteria.(Research article)(Clinical report). *BMC Musculoskeletal Disorders*, 16, 316.
- Barker, R. L. (2002). From fabric hand to thermal comfort: the evolving role of objective measurements in explaining human comfort response to textiles. *International Journal of Clothing Science and Technology*, 14(3/4), 181-200. <https://doi.org/10.1108/09556220210437158>
- Berdishevsky, H., Lebel, V. A., Bettany-Saltikov, J., Rigo, M., Lebel, A., Hennes, A., Romano, M., BiaAek, M., M'Hango, A., Betts, T., de Mauroy, J. C., & Durmala, J. (2016). Physiotherapy scoliosis-specific exercises - a comprehensive review of seven major schools.(Report). *Scoliosis*, 11(1). <https://doi.org/10.1186/s13013-016-0076-9>
- Bernau, A. (1983). *Orthopaedic positioning in diagnostic radiology*. Urban & Schwarzenberg.
- Bettany-Saltikov, J., Campo, A., M'hango, A., Colliard, C., Durmala, J., De Mauroy, J. C., Rigo, M., Bialek, M., Romano, M., & Negrini, S. (2012). *Physical Therapy for Adolescents with Idiopathic Scoliosis*. INTECH Open Access Publisher.

- Botens-Helmus, C., Klein, R., & Stephan, C. (2006). The reliability of the Bad Sobernheim Stress Questionnaire (BSSQbrace) in adolescents with scoliosis during brace treatment. *Scoliosis*, 1(1), <xocs:firstpage xmlns:xocs=""/>. <https://doi.org/10.1186/1748-7161-1-22>
- Brandrup, J., Immergut, E. H., & Grulke, E. A. (1999). *Polymer handbook* (4th ed.. ed.). Wiley.
- Bunge, E. M., de Bekker-Grob, E. W., van Biezen, F. C., Essink-Bot, M.-L., & de Koning, H. J. (2010). Patients' preferences for scoliosis brace treatment: a discrete choice experiment. *Spine*, 35(1), 57. <https://doi.org/10.1097/BRS.0b013e3181bdeaa6>
- Burwell, R. G., Stokes Ian, A., & Dangerfield Peter, H. (2006). Biomechanical spinal growth modulation and progressive adolescent scoliosis – a test of the 'vicious cycle' pathogenetic hypothesis: Summary of an electronic focus group debate of the IBSE. *Scoliosis*, 1(1), 16. <https://doi.org/10.1186/1748-7161-1-16>
- Cahill, J. P., Wang, R. W., Asghar, R. J., Booker, R. R., Betz, R. R., Ramsey, R. C., & Baran, R. G. (2012). The Use of a Transition Rod May Prevent Proximal Junctional Kyphosis in the Thoracic Spine After Scoliosis Surgery: A Finite Element Analysis. *Spine*, 37(12), E687-E695. <https://doi.org/10.1097/BRS.0b013e318246d4f2>
- California Department of Education. (2007). *Standards for scoliosis screening in California public schools*
- Cambridge University Engineering Department, U. o. C. (2003). *Materials Data Book*.
- Cecen, G., Gulabi, D., Cecen, A., Oltulu, İ., & Guclu, B. (2016). Computerized tomography imaging in adolescent idiopathic scoliosis: prone versus supine. *European Spine Journal*, 25(2), 467-475. <https://doi.org/10.1007/s00586-015-3938-6>
- Chan, S. L. (2014). *A correlation study among the orthotic treatment effectiveness, compliance to spinal orthosis and health-related quality of life of the patients with adolescent idiopathic scoliosis (AIS) in the initial treatment period*. Faculty of Health and Social Sciences, The Hong Kong Polytechnic University.
- Chase, A. P., Bader, D. L., & Houghton, G. R. (1989). The biomechanical effectiveness of the Boston brace in the management of adolescent idiopathic scoliosis. *Spine*, 14(6), 636.

- Chassagne, F., Molimard, J., Convert, R., Giraux, P., & Badel, P. (2016). Numerical Approach for the Assessment of Pressure Generated by Elastic Compression Bandage. *Annals of Biomedical Engineering*, 44(10), 3096-3108. <https://doi.org/10.1007/s10439-016-1597-3>
- Cheh, G., Lenke, L., Kim, Y., Lehman, R., Daubs, M., Nunley, R., & Bridwell, K. (2006). Use of a Supine Radiograph to Accurately Predict Structural Curve in Operative Adolescent Idiopathic Scoliosis. *The Spine Journal*, 6(5), 67S-68S. <https://doi.org/10.1016/j.spinee.2006.06.170>
- Cheng, F.-H., Shih, S.-L., Chou, W.-K., Liu, C.-L., Sung, W.-H., & Chen, C.-S. (2010). Finite element analysis of the scoliotic spine under different loading conditions. *Bio-medical materials and engineering*, 20(5), 251. <https://doi.org/10.3233/BME-2010-0639>
- Cheung, K., Senkoylu, A., Alanay, A., Genc, Y., Lau, S., & Luk, K. (2007). Reliability and concurrent validity of the adapted Chinese version of scoliosis research society-22 (SRS-22) questionnaire. 32(10), 1141-1145.
- Cheung, Y. J. P., Yiu, L. K. K., Vidyadhara, Y. S., Chan, H. P. P., Cheung, C. P. W., & Mak, C. K. (2017). Predictability of Supine Radiographs for Determining In-brace Correction for Adolescent Idiopathic Scoliosis. *Spine*. <https://doi.org/10.1097/BRS.0000000000002503>
- Chou, W., Liu, C., Liao, Y., Cheng, F., Zhong, Z. C., & Chen, C. S. (2012). Using Finite Element Method to Determine Pad Positions in a Boston Brace for Enhancing Corrective Effect on Scoliotic Spine: A Preliminary Analysis. *J. Med. Biol. Eng.*, 32(1), 29-35. <https://doi.org/10.5405/jmbe.758>
- Clin, J., Aubin, C.-E., Parent, S., Sangole, A., & Labelle, H. (2010). Comparison of the biomechanical 3D efficiency of different brace designs for the treatment of scoliosis using a finite element model. *European Spine Journal*, 19(7), 1169-1178. <https://doi.org/10.1007/s00586-009-1268-2>
- Clin, J., Aubin, C.-É., Sangole, A., Labelle, H., & Parent, S. (2010). Correlation between immediate in-brace correction and biomechanical effectiveness of brace treatment in adolescent idiopathic scoliosis. *Spine*, 35(18), 1706. <https://doi.org/10.1097/BRS.0b013e3181cb46f6>
- Coillard, C., Circo, A., & Rivard, C. H. (2008). A new concept for the non-invasive treatment of Adolescent Idiopathic Scoliosis: The Corrective Movement © principle integrated in the SpineCor System. *Disability and Rehabilitation: Assistive Technology*, 3(3), 112-119. <https://doi.org/10.1080/17483100801903913>

- Coillard, C., Leroux, M., Zabjek, K., & Rivard, C. (2003). SpineCor – a non-rigid brace for the treatment of idiopathic scoliosis: post-treatment results. *European Spine Journal*, 12(2), 141-148. <https://doi.org/10.1007/s00586-002-0467-x>
- Cramer, G. D. (2014). *Clinical anatomy of the spine, spinal cord, and ANS* (3rd ed.). Elsevier/Mosby.
- Danielsson, A., Wiklund, I., Pehrsson, K., & Nachemson, A. (2001). Health-related quality of life in patients with adolescent idiopathic scoliosis: a matched follow-up at least 20 years after treatment with brace or surgery. *European Spine Journal*, 10(4), 278-288. <https://doi.org/10.1007/s005860100309>
- de Mauroy, J. C., Lecante, C., & Barral, F. (2011). "Brace Technology" Thematic Series - The Lyon approach to the conservative treatment of scoliosis [journal article]. *Scoliosis*, 6(1), 4. <https://doi.org/10.1186/1748-7161-6-4>
- Dewellton LLC. (2008). *Stitch guide*. Estonia, Wapductions Inc.
- Dimeglio, A. (2001). Growth in Pediatric Orthopaedics. *Journal of Pediatric Orthopaedics*, 21(4), 549-555.
- Dobosiewicz, K., Durmala, J., Czernicki, K., & Jendrzek, H. (2002). Pathomechanic basics of conservative treatment of progressive idiopathic scoliosis according to Dobosiewicz method based upon radiologic evaluation. *Stud Health Technol Inform*, 91, 336-341.
- Duong, L., Mac-Thiong, J.-M., & Labelle, H. (2009). Real time noninvasive assessment of external trunk geometry during surgical correction of adolescent idiopathic scoliosis.(Research)(Report). *Scoliosis*, 4, 5.
- Durmala, J., Blicharska, I., Droszol-Cop, A., & Skrzypulec-Plinta, V. (2015). The Level of Self-Esteem and Sexual Functioning in Women with Idiopathic Scoliosis: A Preliminary Study. *International Journal of Environmental Research and Public Health*, 12(8), 9444-9453. <https://doi.org/10.3390/ijerph120809444>
- Edgar, M. (2002). A new classification of adolescent idiopathic scoliosis. *The Lancet*, 360(9329), 270-271. [https://doi.org/10.1016/S0140-6736\(02\)09562-4](https://doi.org/10.1016/S0140-6736(02)09562-4)
- Federico, C., & André, K. (2011). Adolescent idiopathic scoliosis: Indications and efficacy of nonoperative treatment. *Indian Journal of Orthopaedics*, 45(1), 7-14.



<https://doi.org/10.4103/0019-5413.73655>

Fok, Q., Yip, J., Yick, K.-I., Ng, S.-P., & Tse, C.-Y. (2018). Effectiveness of Posture Correction Girdle as Conservative Treatment for Adolescent Idiopathic Scoliosis: a Preliminary Study. *Orthopedic Research Online Journal*, 1(5).

Fukada, Y. (2017). Stress redistribution as an effect of non-uniform in-plane laminate stresses in laminate composite plates. *Composite Structures*, 159, 505-516. <https://doi.org/10.1016/j.compstruct.2016.09.089>

Gignac, D., Aubin, C. É., Dansereau, J., & Labelle, H. (2000). Optimization method for 3D bracing correction of scoliosis using a finite element model. *E Spine J*, 9(3), 185-190. <https://doi.org/10.1007/s005860000135>

Giorgi, S., Piazzolla, A., Tafuri, S., Borracci, C., Martucci, A., & Giorgi, G. (2013). Chêneau brace for adolescent idiopathic scoliosis: long-term results. Can it prevent surgery? *European Spine Journal*, 22(6), 815-822. <https://doi.org/10.1007/s00586-013-3020-1>

Gomez, A. J., Hresko, T. M., & Glotzbecker, P. M. (2016). Nonsurgical Management of Adolescent Idiopathic Scoliosis. *Journal of the American Academy of Orthopaedic Surgeons*, 24(8), 555-564. <https://doi.org/10.5435/JAAOS-D-14-00416>

Grivas, T. B., Bountis, A., Vrasami, I., & Bardakos, N. V. (2010). Brace technology thematic series: the dynamic derotation brace. *Scoliosis*, 5, 20-20. <https://doi.org/10.1186/1748-7161-5-20>

Guo, J., Lam, T., Wong, M., Ng, B., Lee, K., Liu, K., Hung, L., Lau, A., Sin, S., Kwok, W., Yu, F., Qiu, Y., & Cheng, J. (2014). A prospective randomized controlled study on the treatment outcome of SpineCor brace versus rigid brace for adolescent idiopathic scoliosis with follow-up according to the SRS standardized criteria. *European Spine Journal*, 23(12), 2650-2657. <https://doi.org/10.1007/s00586-013-3146-1>

Hawary, R. E., Zaaroor-Regev, D., Floman, Y., Lonner, B. S., Alkhalife, Y. I., & Betz, R. R. (2019). Brace treatment in adolescent idiopathic scoliosis: risk factors for failure-a literature review. *The spine journal : official journal of the North American Spine Society*. <https://doi.org/10.1016/j.spinee.2019.07.008>

Horne, J. P., Flannery, R., & Usman, S. (2014). Adolescent idiopathic scoliosis: diagnosis and management. *American family physician*, 89(3), 193.

Hresko, M. T. (2013). Idiopathic Scoliosis in Adolescents. *The New England Journal of*

*Medicine*, 368(9), 834-841. <https://doi.org/10.1056/NEJMcp1209063>

Hu, J. (2004). *Structure and mechanics of woven fabrics*. Woodhead Publishing Limited.

Human Solutions GmbH. (2015). *The perfectly precise one for size & fit perfectionists*. Retrieved 9/3/2017 from [http://www.human-solutions.com/fashion/front\\_content.php?idcat=139&lang=7](http://www.human-solutions.com/fashion/front_content.php?idcat=139&lang=7)

Janicki, J. A., & Alman, B. (2007, Nov). Scoliosis: Review of diagnosis and treatment. *Paediatr Child Health*, 12(9), 771-776. <https://doi.org/10.1093/pch/12.9.771>

Karol, L. A. (2001). Effectiveness of bracing in male patients with idiopathic scoliosis. *Spine*, 26(18), 2001.

Kato Tech Co. Ltd. *KES-G5 Compression Tester* [website]. <https://english.keskato.co.jp/archives/products/kes-g5>

Katz, D. E., Herring, J. A., Browne, R. H., Kelly, D. M., & Birch, J. G. (2010). Brace wear control of curve progression in adolescent idiopathic scoliosis. *Journal of Bone and Joint Surgery*, 92(6), 1343. <https://doi.org/10.2106/JBJS.I.01142>

Katz, E. D., & Durrani, A. A. (2001). Factors That Influence Outcome in Bracing Large Curves in Patients With Adolescent Idiopathic Scoliosis. *Spine*, 26(21), 2354-2361. <https://doi.org/10.1097/00007632-200111010-00012>

Kawabata, S., Niwa, M., & Yamashita, Y. (2002). Recent developments in the evaluation technology of fiber and textiles: Toward the engineered design of textile performance. *Journal of Applied Polymer Science*, 83(3), 687-702. <https://doi.org/10.1002/app.2264>

Keenan, B. E., Izatt, M. T., Askin, G. N., Labrom, R. D., Percy, M. J., & Adam, C. J. (2014). Supine to standing Cobb angle change in idiopathic scoliosis: the effect of endplate pre-selection. *Scoliosis*, 9, 16. <https://doi.org/10.1186/1748-7161-9-16>

King, K. M., Tsuyuki, R., Faris, P., Currie, G., Maitland, A., & Collins-Nakai, R. L. (2006). A randomized controlled trial of women's early use of a novel undergarment following sternotomy: The Women's Recovery from Sternotomy Trial (WREST). *American Heart Journal*, 152(6), 1187-1193. <https://doi.org/10.1016/j.ahj.2006.07.026>

Klepps, S. J., Lenke, L. G., Bridwell, K. H., Bassett, G. S., & Whorton, J. (2001). Prospective comparison of flexibility radiographs in adolescent idiopathic scoliosis. *Spine*, 26(5),

- Konieczny, M., Senyurt, H., & Krauspe, R. (2013). Epidemiology of adolescent idiopathic scoliosis. *Official Journal of the European Paediatric Orthopaedic Society (EPOS)*, 7(1), 3-9. <https://doi.org/10.1007/s11832-012-0457-4>
- Kotwicki, T. (2008). Evaluation of scoliosis today: Examination, X-rays and beyond. *Disability & Rehabilitation*, 2008, Vol.30(10), p.742-751, 30(10), 742-751. <https://doi.org/10.1080/09638280801889519>
- Kotwicki, T., & Cheneau, J. (2008). Biomechanical action of a corrective brace on thoracic idiopathic scoliosis: Cheneau 2000 orthosis. *Disability & Rehabilitation: Assistive Technology*, 2008, Vol.3(3), p.146-153, 3(3), 146-153. <https://doi.org/10.1080/17483100801905744>
- Kotwicki, T., Kinel, E., Stryla, W., & Szulc, A. (2007). Discrepancy in clinical versus radiological parameters describing deformity due to brace treatment for moderate idiopathic scoliosis. *Scoliosis*, 2(1), 18-18. <https://doi.org/10.1186/1748-7161-2-18>
- Kotwicki, T., Negrini, S., Grivas, T. B., Rigo, M., Maruyama, T., Durmala, J., & Zaina, F. (2009). Methodology of evaluation of morphology of the spine and the trunk in idiopathic scoliosis and other spinal deformities - 6 th SOSORT consensus paper. *Scoliosis*, 4, 26-26. <https://doi.org/10.1186/1748-7161-4-26>
- Lamb, J. M., & Kallal, M. J. (1992). A Conceptual Framework for Apparel Design. *Clothing and Textiles Research Journal*, 10(2), 42-47. <https://doi.org/10.1177/0887302X9201000207>
- Lang, C., Huang, Z., Sui, W., Di, M., He, S., Fan, H., Deng, Y., & Yang, J. (2019). Factors That Influence In-Brace Correction in Patients with Adolescent Idiopathic Scoliosis. *World Neurosurgery*, 123, e597-e603. <https://doi.org/10.1016/j.wneu.2018.11.228>
- Laurnen, E. L., Tupper, J. W., & Mullen, M. P. (1983). The Boston brace in thoracic scoliosis. A preliminary report. *Spine*, 8(4), 388.
- Law, D., Cheung, M.-C., Yip, J., Yick, K.-L., & Wong, C. (2016). Scoliosis brace design: influence of visual aesthetics on user acceptance and compliance. *Ergonomics*, 1-11. <https://doi.org/10.1080/00140139.2016.1227093>
- Lee, M. C., Solomito, M., & Patel, A. (2013). Supine magnetic resonance imaging Cobb measurements for idiopathic scoliosis are linearly related to measurements from

standing plain radiographs. *Spine*, 38(11), E656.  
<https://doi.org/10.1097/BRS.0b013e31828d255d>

Lenke, L. G., Betz, R. R., Harms, J., Bridwell, K. H., Clements, D. H., Lowe, T. G., & Blanke, K. (2001). Adolescent idiopathic scoliosis: a new classification to determine extent of spinal arthrodesis. *The Journal of bone and joint surgery. American volume*, 83-A(8), 1169.

Leonisa Inc. (2017). *Posture Corrector Wireless Back Support Bra*  
<http://www.leonisa.com/en/products/posture-corrector-wireless-back-support-bra/>

Liu, H., Chen, D., Wei, Q., & Pan, R. (2011). A study of the relationship between clothing pressure and garment bust strain, and Young's modulus of fabric, based on a finite element model. *Textile Research Journal*, 81(13), 1307-1319.  
<https://doi.org/10.1177/0040517510399961>

Liu, P.-Y., Yip, J., Yick, K.-L., Yuen, C.-W. M., Ng, S.-P., Tse, C.-Y., & Lawa, D. (2014). An Ergonomic Flexible Girdle Design for Preteen and Teenage Girls with Early Scoliosis. *Journal of Fiber Bioengineering and Informatics*, 7(2), 233-246.  
<https://doi.org/10.3993/jfbi06201410>

Liu, P.-Y., Yip, J., Yick, K.-L., Yuen, C.-W. M., Tse, C.-Y., Ng, S.-P., & Law, D. (2015). Effects of a tailor-made girdle on posture of adolescents with early scoliosis. *Textile Research Journal*, 85(12), 1234-1246. <https://doi.org/10.1177/0040517514561928>

Liu, P. Y. (2015). *Development of posture correction girdle for adolescents with early scoliosis* [The Hong Kong Polytechnic University]. 2014.

Luk, K., Cheung, K., Yip, P., Fong, D., Lee, C., Cheng, J., Ng, B., Lam, T., & Mak, K. (2010). Clinical effectiveness of school screening for adolescent idiopathic scoliosis: A large population-based retrospective cohort study. 35(17), 1607-1614.

Lusardi, M. M. (2012). *Orthotics & prosthetics in rehabilitation* (3rd ed.. ed.). Elsevier Saunders.

Lusini, M., Donzelli, S., Minnella, S., Zaina, F., & Negrini, S. (2014). Brace treatment is effective in idiopathic scoliosis over 45[degrees]: an observational prospective cohort controlled study.(Clinical report). *The Spine Journal*, 14(9), 1951.

Mac-Thiong, J.-M., Petit, Y., Aubin, C.-E., Delorme, S., Dansereau, J., & Labelle, H. (2004). Biomechanical evaluation of the Boston brace system for the treatment of adolescent

- idiopathic scoliosis: relationship between strap tension and brace interface forces. *Spine*, 29(1), 26.
- Malfair, D., Flemming, A. K., Dvorak, M. F., Munk, P. L., Vertinsky, A. T., Heran, M. K., & Graeb, D. A. (2010). Radiographic evaluation of scoliosis: review. *AJR. American journal of roentgenology*, 194(3 Suppl), S8. <https://doi.org/10.2214/AJR.07.7145>
- Maruyama, T., Takeshita, K., & Kitagawa, T. (2008). Milwaukee brace today. *Disability & Rehabilitation: Assistive Technology*, 2008, Vol.3(3), p.136-138, 3(3), 136-138. <https://doi.org/10.1080/17483100801904036>
- McElvenny, R. T. (1953). Structural scoliosis. *Clinical orthopaedics*, 1, 87.
- McGhee, D. E., & Steele, J. R. (2010). Optimising breast support in female patients through correct bra fit. A cross-sectional study. *Journal of Science and Medicine in Sport*, 13(6), 568-572. <https://doi.org/10.1016/j.jsams.2010.03.003>
- Meccariello, L., Muzii, V. F., Falzarano, G., Medici, A., Carta, S., Fortina, M., & Ferrata, P. (2016). Dynamic corset versus three-point brace in the treatment of osteoporotic compression fractures of the thoracic and lumbar spine: a prospective, comparative study. *Aging Clinical and Experimental Research*. <https://doi.org/10.1007/s40520-016-0602-x>
- Medi GmbH & Co. KG. (2015). *Spinomed® active: Damen* [Catalog]. <https://www.medi.de/en/products/orthosesbraces/back-braces/spinomedr-active/>
- Mordecai, S. C., & Dabke, H. V. (2012). Efficacy of exercise therapy for the treatment of adolescent idiopathic scoliosis: a review of the literature. *Eur Spine J*, 21(3), 382-389. <https://doi.org/10.1007/s00586-011-2063-4>
- Mungo, T. A. (1952). *Posture-corrective brassiere* [United States Patents]. <https://www.google.com.hk/patents/US2591462>
- Naismith, C., & Street, A. (2005). Introducing the Cardibra: A randomised pilot study of a purpose designed support bra for women having cardiac surgery. *European Journal of Cardiovascular Nursing*, 4(3), 220-226. <https://doi.org/10.1016/j.ejcnurse.2005.03.008>
- Negrini, S., Aulisa, A. G., Aulisa, L., Circo, A. B., de Mauroy, J. C., Durmala, J., Grivas, T. B., Knott, P., Kotwicki, T., Maruyama, T., Minozzi, S., O'Brien, J. P., Papadopoulos, D., Rigo, M., Rivard, C. H., Romano, M., Wynne, J. H., Villagrasa, M., Weiss, H.-R., & Zaina, F. (2012). 2011 SOSORT guidelines: Orthopaedic and Rehabilitation treatment

of idiopathic scoliosis during growth. *Scoliosis*, 7, 3-3. <https://doi.org/10.1186/1748-7161-7-3>

- Negrini, S., Fusco, C., Minozzi, S., Atanasio, S., Zaina, F., & Romano, M. (2008). Exercises reduce the progression rate of adolescent idiopathic scoliosis: Results of a comprehensive systematic review of the literature. *Disabil Rehabil*, 30(10), 772-785. <https://doi.org/10.1080/09638280801889568>
- O'Brien, M. F., Kuklo, T. R., Blanke, K. M., & Lenke, L. G. (Eds.). (2008). *Radiographic Measurement Manual*. Medtronic Sofamor Danek USA, Inc.
- Otman, S., Kose, N., & Yakut, Y. (2005). The efficacy of Schroth's 3-dimensional exercise therapy in the treatment of adolescent idiopathic scoliosis in Turkey. *Saudi Med J*, 26(9), 1429.
- Park, J. H., Jeon, H. S., & Park, H. W. (2018, Jun). Effects of the Schroth exercise on idiopathic scoliosis: a meta-analysis. *Eur J Phys Rehabil Med*, 54(3), 440-449. <https://doi.org/10.23736/s1973-9087.17.04461-6>
- Patias, P., Grivas, T. B., Kaspiris, A., Aggouris, C., & Drakoutos, E. (2010). A review of the trunk surface metrics used as Scoliosis and other deformities evaluation indices. *Scoliosis*, 5, 12-12. <https://doi.org/10.1186/1748-7161-5-12>
- Pea, R., Dansereau, J., Caouette, C., Cobetto, N., & Aubin, C.-É. (2018, 2018/05/01/). Computer-assisted design and finite element simulation of braces for the treatment of adolescent idiopathic scoliosis using a coronal plane radiograph and surface topography. *Clinical Biomechanics*, 54, 86-91. <https://doi.org/https://doi.org/10.1016/j.clinbiomech.2018.03.005>
- Périé, D., Aubin, C. E., Lacroix, M., Lafon, Y., & Labelle, H. (2004, 2004/05/01). Biomechanical modelling of orthotic treatment of the scoliotic spine including a detailed representation of the brace-torso interface. *Medical and Biological Engineering and Computing*, 42(3), 339-344. <https://doi.org/10.1007/BF02344709>
- Périé, D., Aubin, C. E., Petit, Y., Beauséjour, M., Dansereau, J., & Labelle, H. (2003). Boston brace correction in idiopathic scoliosis: A biomechanical study [Article]. *Spine*, 28(15), 1672-1677. <https://doi.org/10.1097/00007632-200308010-00008>
- Périé, D., Aubin, C. E., Petit, Y., Labelle, H., & Dansereau, J. (2004). Personalized biomechanical simulations of orthotic treatment in idiopathic scoliosis. *Clin Biomech (Bristol, Avon)*, 19(2), 190-195. <https://doi.org/10.1016/j.clinbiomech.2003.11.003>

- Pham, V. M., Houilliez, A., Schill, A., Carpentier, A., Herbaux, B., & Thevenon, A. (2008). Study of the pressures applied by a Chêneau brace for correction of adolescent idiopathic scoliosis. *Prosthetics and Orthotics International*, 32(3), 345-355. <https://doi.org/10.1080/03093640802016092>
- Postle, R. (1988). *The mechanics of wool structure*. Ellis Horwood.
- Qian, B., Zhao, Q., Mao, S., Qiu, Y., Jiang, J., & Zhu, F. (2010). The influence of elastic orthotic belt on sagittal profile in adolescent idiopathic thoracic scoliosis: a comparative radiographic study with Milwaukee brace. *BMC Musculoskeletal Disorders*, 11(1), 219. <https://doi.org/10.1186/1471-2474-11-219>
- Rahman, M. F., Haque, E., & Islam, M. I. (2012). Identification of the ways of evaluating comfort and physical properties of textile materials. *Annals of the University of Oradea. Fascicle of Textiles, Leatherwork*, XIII(2), 139-145.
- Rainoldi, L., Zaina, F., Villafañe, J. H., Donzelli, S., & Negrini, S. (2015). Quality of life in normal and idiopathic scoliosis adolescents before diagnosis: reference values and discriminative validity of the SRS-22. A cross-sectional study of 1,205 pupils. *The Spine Journal*, 15(4), 662-667. <https://doi.org/10.1016/j.spinee.2014.12.004>
- Reamy, B. V., & Slakey, J. B. (2001). Adolescent idiopathic scoliosis: review and current concepts. *American family physician*, 64(1), 111.
- Rigo, M. (2011). Patient evaluation in idiopathic scoliosis: Radiographic assessment, trunk deformity and back asymmetry. *Physiotherapy Theory and Practice*, 2011, Vol.27(1), p.7-25, 27(1), 7-25. <https://doi.org/10.3109/09593985.2010.503990>
- Rigo, M. D., Villagrasa, M., & Gallo, D. (2010). A specific scoliosis classification correlating with brace treatment: description and reliability. *Scoliosis*, 5, 1-1. <https://doi.org/10.1186/1748-7161-5-1>
- Rohan, P.-Y., Badel, P., Lun, B., Rastel, D., & Avril, S. (2015). Prediction of the Biomechanical Effects of Compression Therapy on Deep Veins Using Finite Element Modelling. *Ann Biomed Eng*, 43(2), 314-324. <https://doi.org/10.1007/s10439-014-1121-6>
- Schwartz, P., & Textile, I. (2008). *Structure and mechanics of textile fibre assemblies*. Woodhead Pub. in association with the Textile Institute  
CRC Press.



- Seymour, R. (2002). *Prosthetics and orthotics : lower limb and spinal*. Lippincott Williams & Wilkins.
- Shin, K. (2010). *Patternmaking for underwear design*. Createspace.
- Shin, K. (2015). *Patternmaking for underwear design* (2nd edition.. ed.). [Createspace].
- Shivanna, K. H., Tadepalli, S. C., & Grosland, N. M. (2010). Feature-based multiblock finite element mesh generation. *Computer-Aided Design*, 42(12), 1108-1116. <https://doi.org/10.1016/j.cad.2010.07.005>
- Smith, M. K. (2002). Elastic Strapping Orthosis for Adolescent Idiopathic Scoliosis: A Preliminary Report and Initial Clinical Observations. *JPO Journal of Prosthetics and Orthotics*, 14(1), 13-18. <https://doi.org/10.1097/00008526-200203000-00005>
- Srirekhha, A., & Bashetty, K. (2010). Infinite to finite: An overview of finite element analysis. *Indian Journal of Dental Research*, 21(3), 425-432. <https://doi.org/10.4103/0970-9290.70813>
- Sun, X., Wu, T., Liu, Z., Zhu, Z., Qian, B., Zhu, F., Ma, W., Yu, Y., Wang, B., & Qiu, Y. (2013). Osteopenia Predicts Curve Progression of Adolescent Idiopathic Scoliosis in Girls Treated With Brace Treatment. *Journal of Pediatric Orthopaedics*, 33(4), 366-371. <https://doi.org/10.1097/BPO.0b013e31827b7b5f>
- Torell, G., Nachemson, A., Haderspeck-Grib, K., & Schultz, A. (1985). Standing and supine Cobb measures in girls with idiopathic scoliosis. *Spine*, 10(5), 425.
- Upadhyay, S. S., Nelson, I. W., Ho, E. K. W., Hsu, L. C. S., & Leong, J. C. Y. (1995). New Prognostic Factors to Predict the Final Outcome of Brace Treatment in Adolescent Idiopathic Scoliosis. *Spine*, 20(5), 537-545. <https://doi.org/10.1097/00007632-199503010-00006>
- van Loon Piet, J., Roukens, M., Kuit Joop, D., & Thunnissen Frederik, B. (2012). A new brace treatment similar for adolescent scoliosis and kyphosis based on restoration of thoracolumbar lordosis. Radiological and subjective clinical results after at least one year of treatment. *Scoliosis*, 7(1), 19. <https://doi.org/10.1186/1748-7161-7-19>
- Vasiliadis, E., Grivas, T., & Gkoltsiou, K. (2006). Development and preliminary validation of Brace Questionnaire (BrQ): a new instrument for measuring quality of life of brace



- treated scoliotics. *Scoliosis*, 1(1), 7. <https://doi.org/10.1186/1748-7161-1-7>
- Wang, H. J. (2013). *Posture-correcting garment* [China patent]. <https://www.google.com.hk/patents/CN203303208U?cl=en>
- Weinstein, S. L., Dolan, L. A., Wright, J. G., & Dobbs, M. B. (2013a). Design of the Bracing in Adolescent Idiopathic Scoliosis Trial (BrAIST). *Spine*, 38(21), 1832. <https://doi.org/10.1097/01.brs.0000435048.23726.3e>
- Weinstein, S. L., Dolan, L. A., Wright, J. G., & Dobbs, M. B. (2013b). Effects of Bracing in Adolescents with Idiopathic Scoliosis. *The New England Journal of Medicine*, 369(16), 1512-1521. <https://doi.org/10.1056/NEJMoa1307337>
- Weiss, H.-R., Negrini, S., Rigo, M., Kotwicki, T., Hawes, M. C., Grivas, T. B., Maruyama, T., & Landauer, F. (2006). Indications for conservative management of scoliosis (guidelines). *Scoliosis*, 1(1), 5-5. <https://doi.org/10.1186/1748-7161-1-5>
- Weiss, H.-R., Werkmann, M., & Stephan, C. (2007). Brace related stress in scoliosis patients – Comparison of different concepts of bracing. *Scoliosis*, 2(1), 10-10. <https://doi.org/10.1186/1748-7161-2-10>
- Weisz, I., Jefferson, R. J., Carr, A. J., Turner-Smith, A. R., McNerney, A., & Houghton, G. R. (1989). Back shape in brace treatment of idiopathic scoliosis. *Clinical orthopaedics and related research*(240), 157-163.
- Wills, B. P. D., Auerbach, J. D., Zhu, X., Caird, M. S., Horn, B. D., Flynn, J. M., Drummond, D. S., Dormans, J. P., & Ecker, M. L. (2007). Comparison of Cobb angle measurement of scoliosis radiographs with preselected end vertebrae: traditional versus digital acquisition. *Spine*, 32(1), 98.
- Wong, M. S., Cheng, J. C. Y., Lam, T. P., Ng, B. K. W., Sin, S. W., Lee-Shum, S. L. F., Chow, D. H. K., & Tam, S. Y. P. (2008). The effect of rigid versus flexible spinal orthosis on the clinical efficacy and acceptance of the patients with adolescent idiopathic scoliosis. *Spine*, 33(12), 1360. <https://doi.org/10.1097/BRS.0b013e31817329d9>
- Wong, M. S., Mak, A. F. T., Luk, K. D. K., Evans, J. H., & Brown, B. (2000, 2000/08/01). Effectiveness and biomechanics of spinal orthoses in the treatment of adolescent idiopathic scoliosis (AIS). *Prosthetics and Orthotics International*, 24(2), 148-162. <https://doi.org/10.1080/03093640008726538>
- Xiong, Y., & Tao, X. (2018). Compression Garments for Medical Therapy and Sports. *Polymers*,

10(6). <https://doi.org/10.3390/polym10060663>

- Xu, L., Qin, X., Qiu, Y., & Zhu, Z. (2017). Initial Correction Rate Can be Predictive of the Outcome of Brace Treatment in Patients With Adolescent Idiopathic Scoliosis. *Clinical Spine Surgery*, 30(4), E475-E479. <https://doi.org/10.1097/BSD.0000000000000343>
- Yazici, R. M., Acaroglu, R. E., Alanay, R. A., Deviren, R. V., Cila, R. A., & Surat, R. A. (2001). Measurement of Vertebral Rotation in Standing Versus Supine Position in Adolescent Idiopathic Scoliosis. *Journal of Pediatric Orthopaedics*, 21(2), 252-256.
- Yinglei, L., Choi, K.-F., Luximon, A., Lei, Y., Hu, J., & Li, Y. (2011). Finite element modeling of male leg and sportswear: contact pressure and clothing deformation. *Textile Research Journal*, 81(14), 1470-1476. <https://doi.org/10.1177/0040517510395997>
- Yip, J., & Ng, S.-P. (2008). Study of three-dimensional spacer fabrics:: Physical and mechanical properties. *Journal of Materials Processing Tech.*, 206(1-3), 359-364. <https://doi.org/10.1016/j.jmatprotec.2007.12.073>
- Yu, W. W.-M. (2006). *Innovation and technology of women's intimate apparel*. Woodhead Pub. CRC Press.
- Zaina, F., Negrini, S., Atanasio, S., Fusco, C., Romano, M., & Negrini, A. (2009, 2009/04/07). Specific exercises performed in the period of brace weaning can avoid loss of correction in Adolescent Idiopathic Scoliosis (AIS) patients: Winner of SOSORT's 2008 Award for Best Clinical Paper. *Scoliosis*, 4(1), 8. <https://doi.org/10.1186/1748-7161-4-8>
- Zapata, K., Parent, E. C., & Sucato, D. (2016). Immediate effects of scoliosis-specific corrective exercises on the Cobb angle after one week and after one year of practice. *Scoliosis Spinal Disord*, 11(Suppl 2), 36. <https://doi.org/10.1186/s13013-016-0101-z>
- Zhang, J., Shi, X., Liang, L., Wang, X., Zhang, Y., & Guo, F. (2013). *Computerized Lenke classification of scoliotic spine* 35th Annual International Conference of the IEEE EMBS, Japan.
- Zheng, R., Hill, D., Hedden, D., Moreau, M., Southon, S., & Lou, E. (2018). Assessment of curve progression on children with idiopathic scoliosis using ultrasound imaging method. *Eur Spine J*, 27(9), 2114-2119. <https://doi.org/10.1007/s00586-017-5457-0>
- Zheng, Y. P., Lee, T. T., Lai, K. K., Yip, B. H., Zhou, G. Q., Jiang, W. W., Cheung, J. C., Wong, M. S., Ng, B. K., Cheng, J. C., & Lam, T. P. (2016). A reliability and validity study for

Scolioscan: a radiation-free scoliosis assessment system using 3D ultrasound imaging. *Scoliosis Spinal Disord*, 11, 13. <https://doi.org/10.1186/s13013-016-0074-y>

Zhou, J., Li, Y., Lam, J., & Cao, X. (2010). The Poisson Ratio and Modulus of Elastic Knitted Fabrics. *Textile Research Journal*, 80(18), 1965-1969. <https://doi.org/10.1177/0040517510371864>